# Hyperspectral remote sensing of vegetation parameters using statistical and physical models

Roshanak Darvishzadeh

**Promotors:**
Prof. Dr. Andrew K. Skidmore
Professor of Vegetation and Agricultural Land Use Survey
International Institute for Geo-information Science and Earth Observation (ITC) and Wageningen University, the Netherlands

Prof. Dr. Herbert H. T. Prins
Professor of Resource Ecology
Wageningen University, the Netherlands

**Co-promotor:**
Dr. Clement Atzberger
Research Scientist, Joint Research Centre of the European Commission
Ispra, Italy

**Examining Committee:**
Prof. Dr. Ir. A. Veldkamp
Wageningen University, the Netherlands

Prof. Dr. S.M. de Jong
Utrecht University, the Netherlands

Prof. Dr. F.D. van der Meer
International Institute for Geo-information Science and Earth Observation (ITC) and Utrecht University, the Netherlands

Prof. Dr. M.D. Steven
University of Nottingham, United Kingdom

This research is carried out within the C.T. de Wit Graduate School for Production Ecology and Resource Conservation (PE&RC) in Wageningen University, the Netherlands.

# Hyperspectral remote sensing of vegetation parameters using statistical and physical models

Roshanak Darvishzadeh

**Thesis**

To fulfil the requirements for the degree of Doctor
on the authority of the Rector Magnificus of Wageningen University
Prof. Dr. M.J. Kropff
to be publicly defended on Friday 16th of May, 2008 at 15:00 hrs
in the auditorium at ITC, Enschede, The Netherlands

Hyperspectral remote sensing of vegetation parameters using statistical and physical models

ISBN: 978-90-8504-823-7
International Institute for Geo-information Science & Earth Observation, Enschede, the Netherlands (ITC)
ITC Dissertation Number: 152

# Content

## Summary

Accurate quantitative estimation of vegetation biochemical and biophysical characteristics is necessary for a large variety of agricultural, ecological, and meteorological applications. Remote sensing, because of its global coverage, repetitiveness, and non-destructive and relatively cheap characterization of land surfaces, has been recognized as a reliable method and a practical means of estimating various biophysical and biochemical vegetation variables. The advent of hyperspectral remote sensing has offered possibilities for measuring specific vegetation variables that were difficult to measure using conventional multi-spectral sensors.

Utilizing hyperspectral measurements, we examined the performance of different statistical techniques such as univariate versus multivariate techniques for predicting biophysical and biochemical vegetation characteristics such as leaf area index (LAI) and chlorophyll content. The study further investigated and compared the performance of the statistical approach with that of the physical approach for mapping and predicting these vegetation characteristics. From the laboratory up to airborne levels, the investigation involved structurally different vegetation canopies and heterogeneous fields with different vegetation communities.

It was concluded that the red edge inflection point (REIP) is not an appropriate variable to be considered for LAI estimations at canopy level, especially if several contrasting species are pooled together or a heterogeneous canopy is being investigated. However, it may be appropriate for single species. Throughout this study, the bands in the shortwave infrared (SWIR) region have appeared to make a sound contribution in terms of the strength of relationships between spectral reflectance and LAI. Considering that the SWIR bands were important in all three investigated levels and for most vegetation indices in this study, vegetation indices that do not include this spectral region may be less satisfactory for LAI estimation. The results suggest that, when using remote sensing vegetation indices for LAI estimation, not only is the choice of vegetation index of importance but also prior knowledge of plant architecture and soil background. Hence, some kind of landscape stratification is required before using hyperspectral imagery for large-scale mapping of biophysical vegetation variables. Furthermore, the study results highlight the significance of using multivariate techniques such as partial least squares regression rather than univariate methods such as vegetation indices for providing enhanced estimates of heterogeneous grass canopy characteristics. The newly introduced subset selection algorithm based on average absolute error (AAE) indicated that a carefully selected spectral subset contains adequate information for a successful model inversion. The results of the study demonstrated that, through the inversion of a radiative transfer model, grass canopy characteristics such as LAI and canopy chlorophyll content can be estimated with accuracies comparable to those of statistical approaches. Given that

the accuracies obtained through the inversion of a radiative transfer model were comparable to those of statistical approaches, and considering the lack of robustness and transferability of statistical models for varying environmental conditions (Asner et al., 2003; Gobron et al., 1997), the radiative transfer models may be considered proper alternatives.

In summary, the study contributes to the field of information extraction from hyperspectral measurements and enhances our understanding of vegetation biophysical and biochemical characteristics estimation. Several achievements have been registered in exploiting spectral information for the retrieval of vegetation biophysical and biochemical parameters using statistical and physical approaches. These involve the derivation of new vegetation indices and the successful implementation of a radiative transfer model inversion (with extensive validation), which comprised the development of a new method to subset the spectral data based on average absolute error.

# Samenvatting

Voor vele agrarische, ecologische, en meteorologische toepassingen is een nauwkeurige kwantitative meeting van de bio-chemische en bio-fysische karakteristieken van vegetatie van belang. Vanwege zijn wereldwijde dekking, frequente opnames, niet-destruktieve en relatief goedkope eigenschappen is 'Remote Sensing' erkend als een betrouwbare en praktische methode om diverse bio-fysische en bio-chemische variabelen in vegetatie te meten. Door het in gebruik nemen van hyper-spectrale Remote Sensing is het nu mogelijk specifieke vegetatie variabelen te meten, die voorheen met conventionele multi-spectrale sensoren niet waren te meten.

Met behulp van hyper-spectrale metingen hebben we verschillende statistische technieken, zoals univariate versus multivariate technieken, onderzocht voor het voorspellen van bio-fysische en bio-chemische vegetatie karakteristieken, zoals het blad oppervlak index (LAI) en het chlorofiel gehalte. Deze studie heeft verder onderzocht en vergeleken, hoe de statistische benadering zich gedroeg ten opzichte van de fysische benadering met betrekking tot het karteren en voorspellen van deze vegetatie karakteristieken. Het onderzoek betrof, van laboratoria niveau tot in het luchtruim, struktureel verschillende vegetatie lagen en heterogene velden met verschillende vegetatie groepen.

De conclusie was, dat de 'rode hoek inflektie punt' (REIP) geen geschikte variabele is voor het meten van het blad oppervlak index (LAI) op vegetatie lagen niveau, vooral niet wanneer diverse kontrasterende soorten samen voorkomen of wanneer een heterogene laag werd onderzocht. Des al niet te min, voor afzonderlijke soorten was het resultaat bevredigend. Gedurende deze studie bleken de banden in de korte golflengte infra-rood goede resultaten op te leveren met betrekking tot een sterke relatie tussen spectrale reflektie en LAI. In aanmerking nemende, dat de SWIR banden belangrijk waren in alle drie onderzochte niveau's en ook voor de meeste vegetatie indexen in deze studie, kan worden geconcludeerd dat vegetatie indexen die niet binnen deze spectrale regio vallen minder geschikt zijn voor het bepalen van de LAI. De resultaten suggereren dat, wanneer de Remote Sensing vegetatie index voor LAI berekeningen worden gebruikt, niet alleen de keuze van de vegetatie index belangrijk is, maar ook voorkennis van de bouw van de plant en van de bodem achtergrond. Daarom is enige voorkennis van de stratifiekatie van het landschap nodig, alvorens hyper-spectrale beelden voor het op grote schaal karteren van bio-fysische vegetatie variabelen toe te passen. Bovendien laten de onderzoeks resultaten duidelijk het belang zien van 'multi-variate' technieken zoals 'partial least squares regression' boven het gebruik van 'uni-variate' methodes zoals vegetatie index voor het gerekenen van heterogene gras bedekkings karakteristieken. Daarom is eerstgenoemde techniek aanbevolen wanneer gebruik makend van hyper-spectrale gegevens. De nieuw ontwikkelde 'subset selektie algoritme', die gebaseerd is op een gemiddelde absolute fout

(AAE), geeft aan dat een zorgvuldig gekozen spectrale subset genoeg informatie bevat voor een geslaagd model inversie. De resultaten van deze studie laten ook zien, dat via de inversie van een 'radiative transfer model', de grass bedekkings karakteristieken zoals LAI en chlorofiel gehalte van de bedekking gemeten kan worden met een nauwkeurigheid die vergelijkbaar is met die van statistische berekeningen. Daarom kunnen de 'radiative transfer modellen' als waardige alternatieven voor de statistische modellen worden beschouwd. Gezien het feit, dat de nauwkeurigheid, verkregen door de inversie van een 'radiative transfer model', vergelijkbaar waren met die via een statistische benadering, en gezien het gebrek aan robuustheid en overdraagbaarheid van statistische modellen voor diverse omgevings omstandigheden (Asner et al., 2003; Gobron et al., 1997), kan aangenomen worden, dat de 'radiative transfer model' een geschikt alternatief is.

Samenvattend, deze studie draagt bij in het veld van informatie vergaren met betrekking tot hyper-spectrale metingen en verbeterd onze inzicht in het bepalen van de biofysische- en biochemische eigenschappen van vegetatie. Diverse vooruitgangen zijn geboekt in het onderzoeken van spectrale informatie voor het bepalen van biofysische- en biochemische eigenschappen van vegetatie met behulp van statistische en fysische benaderingen. Deze omvatten produkten van nieuwe vegetatie indexen en het succesvol implementeren van een inversie van het 'radiative transfer model' (uitgebreid gevalideerd), inclusief de ontwikkeling van een nieuw ontwikkelde methode om spectrale data te partioneren, gebaseerd op een gemiddelde absolute fout.

## Acknowledgements

Gratitude is owed to many individuals who have helped me in one way or another over the past four years, often without knowing they were doing so.

My deepest appreciation goes to my first promotor, Prof. Andrew Skidmore, for his confidence, advice, encouragement, commitment and unsparing support during the period of my study. He taught me how to be an independent scientist by letting me make my own choices at decisive points along the way. Further, I would like to express my gratitude to my other promotor, Prof. Herbert Prins, for the continuous encouragement and generous support I received from him. This work would not have been possible without the invaluable contribution and help I received from my co-promotor, Dr. Clement Atzberger. He was always ready to assist me, promptly answering my emails and questions. I highly appreciate his significant support, criticisms, expertise and enthusiasm during the period of this work.

I deeply acknowledge the excellent advisory support of Dr. Martin Schlerf, my adviser, in many difficult situations, and am grateful for the many inspiring scientific discussions we shared. It was easy for me to communicate with him because of his friendly and sincere attitude. Special thanks go to Dr. Fabio Corsi, who substantially helped me in organizing and conducting the fieldwork and who devoted considerable time and support to my work during the phase of proposal writing. Many thanks go to Dr. Sip van Wieren for his support during my laboratory and field experiments. Whenever I needed to arrange something in Wageningen, he was there to assist me.

I would like to thank the whole NRS department for their support. I appreciated the friendly atmosphere and especially the pleasant chats over coffee on Monday mornings. To Eva Skidmore, I would like to say thank you for the hospitality, for the friendship, and for editing my first article, which is now in print in the International Journal of Remote Sensing. My sincere thanks go to Dr. Bert Toxopeus for his wonderful support and encouragement; it was always a pleasure to see his cheerful face. Thank you for translating my abstract into Dutch.

Talking to the PhD community, particularly on Friday afternoons, always seemed to lighten the workload. They were each special in their own way and some of them have become good friends. I thank you all! Special thanks go to my colleagues Dr. Moses Cho, Dr. Md Istiak Sobhan, Dr. Pieter Beck, Dr. Marleen Noomen, Dr. Jelle Ferwerda, Dr. Chudamani Joshi, Dr. Uday Bhaskar Nidumolu, Dr. Grace Nangendo, Dr. Martin Yemefack, Dr. Peter Minang, Dr. Jamshid Farifteh, Mr. Mohammad Abouali, Mr. Farhang Sargordi, Mr. Bahman Farhadi, Mrs. Nicky Knox, Mrs. Filiz Bektas, Mr. Wang Tiejun, Mrs. Jane Bemigisha and Mrs. Chiara Polce for the support, scientific discussions and sound advice.

Many people at ITC helped and supported me when it came to technical issues. I cannot possibly mention everybody, but a few people must be singled out: Willem Nieuwenhuis, Gerard Reinink, Boudewijn de Smeth, Jelger Kooistra, Ard Kosters, Andries Menning, Wim Bakker, Wan Bakx, Benno Masselink, Job Duim, Ronnie Geerdink, Harry Homrighausen, Rob Teekamp and Gerard Leppink. Thank you all!

I extend my gratitude to several people at ITC who assisted me in one way or another: Loes Colenbrander, David Rossiter, Patrick van Laake, Martin Hale, Alfred Stein, Paul van Dijk, Fred Paats, Esther Hondebrink, Eric Mol, Bettine Geerdink, Marie Chantal Metz, Theresa van den Boogaard, Marga Koelen, Carla Gerritsen, Petry Maas – Prijs, Saskia Tempelman, Saskia Groenendijk, Marion Pierik, Kim Velthuis, Bianca Haverkate, Adrie Scheggetman, André Klijnstra and former ITC staff: Professor Klaas Jan Beek, Wilma Grotenboer, Anneke Homan and Janice Collins. I appreciate all the help and support I received from you during the past years.

I am grateful to my former teachers and supervisors in the ITC cartography and UPM departments. They were all a great source of encouragement and support for me: Richard Sliuzas, Sherif Amer, Ben Gorte, Corné van Elzakker, Connie Blok, Sjef van der Steen, Ton Mank and Jeroen van den Worm, to name but a few.

I appreciate all the help and support received from my Iranian colleagues and acquaintances in the Netherlands, some of whom have become good friends: the Sharif family, the Sharifi family, the Farshad family, the Daftari family, the Farhadi family, and many more - I apologize for not mentioning you all by name. I appreciated your presence, particularly in difficult times, and wish you all good luck.

I extend my gratitude to my father and mother, brothers and sister, who went through a lot while I was absent. They have given me tremendous support and deserve so much more than a simple 'thank you'. I owe them a lot and will be grateful to them all my life.

Finally, to my daughters, Asal and Aysan, my sincere apologies for not being able to be the full-time mom you deserve. Although from time to time I had to travel for my work, I always did my best to fulfill your desires, wishes and needs. Thank you for being two tolerant angels and bringing so much happiness and joy into my life.

Last but not least, to my husband, Ali, I say thank you for your presence, support and encouragement. You left your job to join me and support me here in the Netherlands. However, I realized that you had so much to do over the past two years that I even had to support you! I am sincerely grateful to you for your patience, appreciation, trust and most of all for your love.

*To my family*

# Chapter One

## General Introduction

## 1.1. Remote sensing of vegetation biophysical and biochemical characteristics

Vegetation is a fundamental element of the earth's surface and has a major influence on the exchange of energy between the atmosphere and the earth's surface (Bacour et al., 2002). Accurate quantitative estimation of vegetation biochemical and biophysical characteristics is necessary for a large variety of agricultural, ecological, and meteorological applications (Asner, 1998; Hansen and Schjoerring, 2003; Houborg et al., 2007). Likewise, the mapping and monitoring of vegetation biochemical and biophysical variables is important for the spatially distributed modeling of vegetation productivity, evapotranspiration, and surface energy balance (Turner et al., 1999). The direct measurement of these characteristics is labor-intensive and costly, and is thus only practical on experimental plots of limited size (Pu et al., 2003a). Remote sensing, because of its global coverage, repetitiveness, and non-destructive and relatively cheap characterization of land surfaces, has been recognized as a reliable method and a practical means of estimating various biophysical and biochemical vegetation variables (Cohen et al., 2003; Curran et al., 2001; Hansen and Schjoerring, 2003; Hinzman et al., 1986; McMurtrey et al., 1994; Weiss and Baret, 1999). However, a major drawback of traditional remote sensing products is that they use average spectral information over broad-band widths, which results in the loss of crucial information available in specific narrow bands (Blackburn, 1998; Thenkabail et al., 2000). In this regard, the advent of hyperspectral remote sensing (section 1.2) has offered possibilities to overcome this limitation.

## 1.2. Hyperspectral remote sensing and vegetation characteristics

The tools for vegetation remote sensing have developed considerably in the past decades (Asner, 1998). Optical remote sensing has expanded from the use of multi-spectral sensors to that of imaging spectrometers. Imaging spectrometry or hyperspectral remote sensing, with sensors that typically have hundreds of narrow, contiguous spectral bands between 400 nm and 2500 nm, has the potential to measure specific vegetation variables that are difficult to measure using conventional multi-spectral sensors. For example, Zarco-Tejada et al. (2002) assessed vegetation stress from a derivative chlorophyll index using CASI (Compact Airborne Spectrographic Imager) airborne data; Mutanga and Skidmore (2004) overcame the saturation problem in estimating biomass by using narrow-band vegetation indices; Ferwerda et al. (2005) demonstrated that across multiple plant species nitrogen could be detected by using hyperspectral indices; and Cho (2007) used hyperspectral indices to discriminate species at leaf and canopy scales. Previous studies have shown that hyperspectral data are crucial in providing essential information for quantifying the biochemical (Broge and Leblanc, 2001;

Ferwerda et al., 2005; Gamon et al., 1992; Gitelson and Merzlyak, 1997; Mutanga et al., 2005; Peterson et al., 1988) and the biophysical (Blackburn, 1998; Elvidge and Chen, 1995; Gong et al., 1992; Lee et al., 2004; Mutanga and Skidmore, 2004; Schlerf et al., 2005) characteristics of vegetation.

In general, current remote sensing approaches to estimating vegetation biochemical and biophysical parameters include statistical (also called inductive) (section 1.3) and physically based models (also called deductive) (section 1.4) (Skidmore, 2002), each having advantages and disadvantages. Both models (statistical/physical) have been used widely for estimating biochemical and biophysical parameters in agricultural and forestry environments (these are typically homogenous areas in terms of species type) with multi-spectral remote sensing data (e.g., Atzberger, 1997). Nevertheless, the estimation of vegetation characteristics for structurally different vegetation canopies and heterogeneous fields with different vegetation communities using either approach has not been widely addressed in the literature. Using both statistical and physically based models, this research has addressed the estimation of leaf area index (LAI), leaf chlorophyll content (LCC) and canopy chlorophyll content (CCC), which are of prime importance among the many vegetation biochemical and biophysical characteristics.

## 1.3. Statistical approach

One of the most common approaches to estimating vegetation parameters from remotely sensed data is the statistical approach. It involves univariate (computation of spectral vegetation indices) or multivariate (e.g., stepwise linear regression/partial least square regression) models. In this approach, statistical techniques are used to find a relation between the target parameter (parameter measured *in situ,* such as LAI) and its spectral reflectance or some transformation of reflectance (e.g., a vegetation index). Originally, the purpose of spectral vegetation indices was to minimize variability due to external factors such as illumination and atmosphere conditions and internal factors such as the underlying soil and leaf angle distribution.

Developments in the field of hyperspectral remote sensing have promoted a new group of vegetation indices that includes narrow-band indices and the red edge of the vegetation spectrum. The importance of hyperspectral indices for quantifying the biochemical and biophysical characteristics of vegetation have been demonstrated by many studies (Blackburn, 1998; Broge and Leblanc, 2001; Ferwerda et al., 2005; Gamon et al., 1992; Gitelson and Merzlyak, 1997; Lee et al., 2004; Mutanga and Skidmore, 2004; Mutanga et al., 2005; Schlerf et al., 2005). In this case, a limited number of spectral wavelengths from the massive spectral contents of hyperspectral data are used.

In contrast, several studies have addressed statistical techniques such as stepwise multiple linear regression (SMLR) and partial least square regression (PLSR) that integrate spectral information of several spectral wavelengths for estimating vegetation biochemical and biophysical properties (Atzberger et al., 2003b; Cho et al., 2007; Curran, 1989; Curran et al., 2001; De Jong et al., 2003; El Masry et al., 2007; Grossman et al., 1996; Hansen and Schjoerring, 2003; Huang et al., 2004; Kokaly and Clark, 1999; Lefsky et al., 1999; Lefsky et al., 2001; Naesset et al., 2005; Nguyen and Lee, 2006). Statistical approaches lack generalization and transferability as the derived statistical relationships are recognized as being sensor-specific and dependent on site and sampling conditions, and are expected to change in space and time (Colombo et al., 2003; Gobron et al., 1997; Meroni et al., 2004). Much of the present research using statistical models to link vegetation parameters such as LAI to spectral data has been conducted on typically homogenous vegetation, for example on conifer stands (Running et al., 1986), agricultural crops (Colombo et al., 2003; Hansen and Schjoerring, 2003; Walter-Shea et al., 1997), tropical moist forest (Kalacska et al., 2004), broad-leaf forests (Chen et al., 1997; White et al., 1997), and mangrove forest (Kovacs et al., 2004). However, to our knowledge, the estimation of canopy characteristics such as LAI and canopy/leaf chlorophyll content for structurally different vegetation canopies and heterogeneous Mediterranean grassland has not been addressed by researchers, and remains to be examined.

## 1.4. Physically based models

The second approach (physical approach; here also called deductive, biophysical, physical and physically based) to estimating vegetation parameters involves radiative transfer models, which describe the spectral variation of canopy reflectance as a function of canopy, leaf and soil background characteristics based on physical laws (Atzberger, 1995; Goel, 1989; Meroni et al., 2004; Verhoef, 1984). As radiative transfer models are able to explain the transfer and interaction of radiation inside the canopy based on physical laws, they offer an explicit connection between the vegetation biophysical and biochemical variables and the canopy reflectance (Houborg et al., 2007). Depending on the canopy structures, different models ranging from 1D (Gastellu-Etchegorry et al., 1996a; Verhoef, 1984) to 3D (Gastellu-Etchegorry et al., 1996b; Kimes and Kirchner, 1982) have been developed. In 1D radiative transfer models, the vegetation canopy is presumed to be a turbid medium with randomly distributed canopy elements (Liang, 2004). While 1D radiative transfer models are used for horizontally homogeneous canopies, 3D models are applicable to horizontally heterogeneous or discontinuous canopies (such as orchards with isolated tree crowns).

To actually use physically based models for retrieving vegetation characteristics from observed reflectance data, they must be inverted (Kimes et al., 1998). Different inversion algorithms exist for the inversion of physical models, including

numerical optimization methods (e.g., Atzberger, 1997; Bicheron and Leroy, 1999; Jacquemoud et al., 2000; Jacquemoud et al., 1995; Meroni et al., 2004), look-up table (LUT) approaches (e.g., Combal et al., 2002; Combal et al., 2003; Gastellu-Etchegorry et al., 2003; Knyazikhin et al., 1998; Weiss et al., 2000), and artificial neural network methods (e.g., Fang and Liang, 2005; Gopal and Woodcock, 1996; Schlerf and Atzberger, 2006; Walthall et al., 2004; Weiss and Baret, 1999), each having advantages and disadvantages (Kimes et al., 2000; Liang, 2004). A drawback in using physically based models is the ill-posed nature of model inversion (Atzberger, 2004; Combal et al., 2002), meaning that the inverse solution is not always unique as various combinations of canopy parameters may yield almost similar spectra (Weiss and Baret, 1999) (Figure 1.1). Possible solutions to the ill-posed inverse problem involve the use of prior knowledge about model parameters (Combal et al., 2002), the use of information provided by the temporal course of key canopy parameters (CROMA, 2000), and/or the analysis of color textures and object signatures (Atzberger, 2004).

Generally, these models are known to be computationally more demanding and need a number of leaf and canopy input variables. Significant efforts to estimate and quantify vegetation properties using radiative transfer models have been carried out in the last two decades. Several studies have been successfully conducted covering different vegetation types and remote sensing data: on global data sets (Bacour et al., 2006; Baret et al., 2007; Bicheron and Leroy, 1999; Fang and Liang, 2005), on agricultural crops (Atzberger, 2004; Atzberger et al., 2003a; Danson et al., 2003; Jacquemoud et al., 2000; Jacquemoud et al., 1995; Weiss et al., 2001; Zarco-Tejada et al., 2004b), in semiarid regions (Qi et al., 2000), and on forests (Disney et al., 2006; Eklundh et al., 2001; Fang et al., 2003; Fernandes et al., 2002; Gemmell et al., 2002; Kötz et al., 2004; Meroni et al., 2004; Schlerf and Atzberger, 2006; Zarco-Tejada et al., 2004a; Zarco-Tejada et al., 2004b). Many other studies have analyzed simulated data (Gong et al., 1999; Weiss et al., 2000). Despite the efforts undertaken, a review of the literature reveals that there is a gap in estimating vegetation biophysical and biochemical variables for heterogeneous grasslands, such as Mediterranean grasslands with combinations of different grass species. Furthermore, studies that use hyperspectral measurements and include validation with large numbers of ground truth data for heterogeneous grasslands are rare.

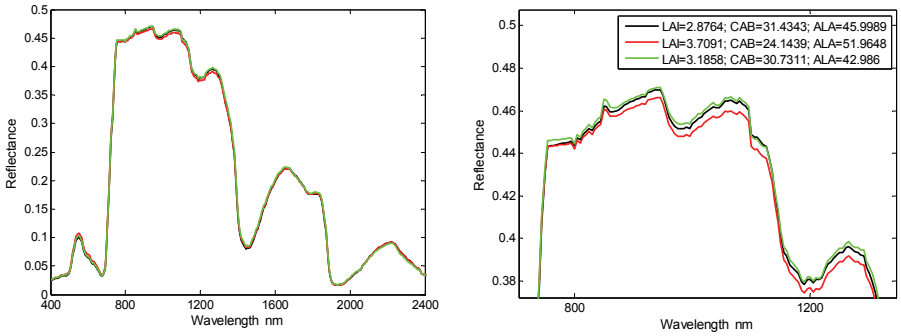


Figure 1.1. The ill-posed problem. Simulated reflectances using the PROSAIL model for a subplot in Majella National Park, Italy. Various combinations of canopy parameters have yielded almost similar spectra. LAI is the leaf area index, CAB is the leaf chlorophyll content and ALA is the mean leaf angle.

## 1.5. Objectives and scope of the thesis

The main objectives of this study were to (1) investigate the potential of hyperspectral remote sensing for estimating biophysical and biochemical vegetation characteristics such as LAI and chlorophyll content at canopy level, (2) investigate the performance of different statistical techniques, such as univariate versus multivariate techniques, to predict biophysical and biochemical vegetation characteristics, and (3) test the performance of the statistical versus the physical approach to mapping and prediction of biophysical and biochemical vegetation characteristics.

Although two important biochemical characteristics (leaf chlorophyll content and canopy chlorophyll content) were investigated at field and airborne levels (i.e., HyMap (Hyperspectral Mapping imaging spectrometer)), more emphasis was placed on the estimation and prediction of biophysical vegetation characteristics (LAI) from laboratory level up to airborne level when utilizing statistical and physical models.

The potential of hyperspectral remote sensing to predict vegetation LAI at canopy level was investigated (1) under controlled laboratory conditions, (2) at field level using a field spectrometer, and (3) at airborne platform level (i.e., HyMap). Majella National Park in Italy was used as a test site for both field and airborne spectrometry.

## 1.6. The study area

Majella National Park, Italy, is located at latitude 41°52' to 42°14'N and longitude 13°14' to 13°50'E. The park covers an area of 74.1 ha and extends into

the southern part of the Abruzzo region, at a distance of 40 km from the Adriatic Sea (Figure 1.2). The region is situated in the mountain massifs of the Apennines. The park is characterized by several mountain peaks, the highest being Mount Amaro (2794 m). Geologically, the region is made up of calcareous rocks, which date back to the Jurassic period. The flora of the park includes more than 1800 plant species, which approximately constitute one third of the entire flora in Italy (Cimini, 2005).

Abandoned agricultural areas and settlements in Majella are returning to oak (*Quercus pubescens*) woodlands at the lower altitude (400 m to 600 m) and beech (*Fagus sylvatica*) forests at higher altitudes (1200 m to 1800 m). Between these two formations is a landscape composed of shrubby bushes, patches of grass/herb vegetation, and bare rock outcrops. The dominant grass and herb species include *Brachypodium genuense, Briza media, Bromus erectus, Festuca sp, Helichrysum italicum, Galium verum, Trifolium pratense, Plantago lanceolata, Sanguisorba officinalis* and *Ononis spinosa* (Cho, 2007).

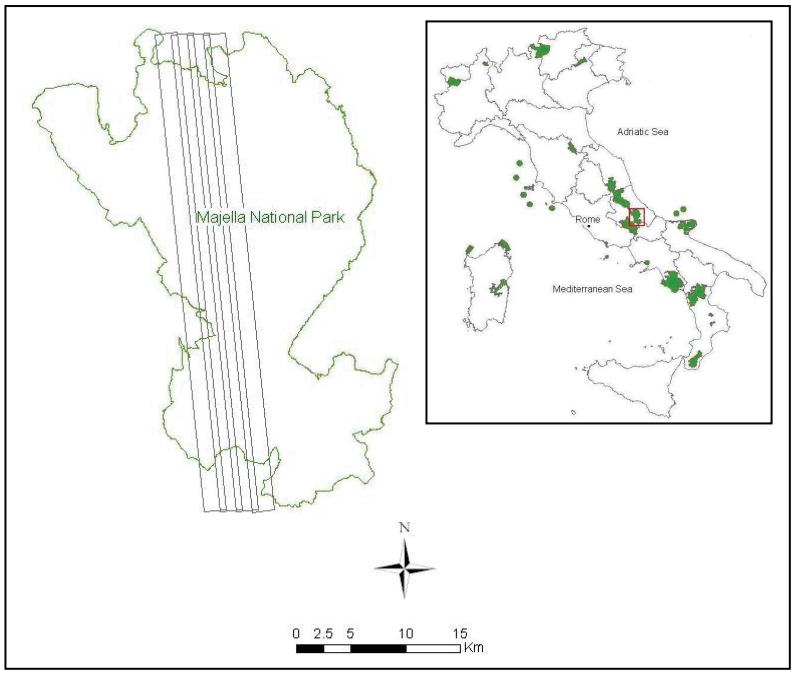


Figure 1.2. Flight lines of HyMap and the location of Majella National Park in Italy (red box).

## 1.7. Thesis outline

This thesis comprises five main chapters, which are presented under three different levels of investigation.

### 1.7.1. Laboratory level

Chapters 2 and 3 utilize greenhouse experimental data to estimate LAI, using hyperspectral measurements. In brief, chapter 2 investigates the relationship between LAI and narrow-band indices, including the red edge inflection point (REIP). The investigation involves plant species differing widely in structure and with varying leaf chlorophyll contents, which have been measured above contrasting soil backgrounds. Chapter 3 examines whether the estimation of LAI from hyperspectral reflectance measurements is significantly affected by soil type and/or plant architecture (e.g., leaf shape and size). The effects of these factors both on the characterization of canopy reflectance behavior in the visible to mid-infrared bands and on the stability of linear LAI-VI relationships are analyzed. The observations in these chapters permitted further development of the next chapters at field and airborne imaging spectrometry levels.

### 1.7.2. Field level

Chapters 4 and 5 use canopy spectral measurements that were acquired using a GER 3700 spectroradiometer (Geophysical and Environmental Research Corporation, Buffalo, New York) in the heterogeneous grasslands of Majella National Park during fieldwork in Italy. Chapter 4 examines the utility of different univariate and multivariate methods in predicting canopy characteristics such as LAI and canopy/leaf chlorophyll content. Partial least squares regression and stepwise multiple linear regression, two important linear statistical methods known to be well suited to dealing with highly multicollinear data sets, are used to compare narrow-band vegetation indices, including red edge inflection point. Chapter 5 investigates the estimation and prediction of prime canopy characteristics such as LAI and chlorophyll content by inverting the canopy radiative transfer model PROSAIL (Jacquemoud and Baret, 1990; Verhoef, 1984; Verhoef, 1985). A LUT-based inversion algorithm has been used to account for available prior information relating to the distribution (probable range) of several vegetation characteristics.

### 1.7.3. Airborne platform level

Chapter 6 is based on the airborne hyperspectral imagery (i.e., HyMap) data acquired at the same time as the field campaign. It uses observations and conclusions from previous chapters and evaluates the mapping of LAI and canopy chlorophyll content using statistical and physical models.

Finally, in chapter 7 the findings of this study are summarized and the contribution of the thesis within the context of vegetation biophysical and biochemical parameter estimation is discussed.

# Chapter Two

## Laboratory level

# Leaf area index derivation from hyperspectral vegetation indices and the red edge position

*This chapter is based on:*

Darvishzadeh, R., Atzberger, C. and Skidmore, A.K., 2008. Leaf area index derivation from hyperspectral vegetation indices and the red edge position. *International Journal of Remote Sensing,* **In Press**.

## Abstract

The aim of this study was to compare the performance of various narrow band vegetation indices in estimating the leaf area index (LAI) of structurally different plant species having different soil backgrounds and leaf optical properties. The study takes advantage of using a dataset collected during a controlled laboratory experiment. Leaf area indices were destructively acquired for four species with different leaf size and shape. Six widely used vegetation indices were investigated. Narrow band vegetation indices involved all possible two band combinations which were used for calculating RVI, NDVI, PVI, TSAVI, and SAVI2. The red edge inflection point (REIP) was computed using three different techniques. Linear regression models as well as an exponential model were used to establish relationships. REIP determined using any of the three methods was generally not sensitive to variations in LAI ($R^2 < 0.1$). On the contrary, LAI was estimated with reasonable accuracy from red/near infrared based narrow band indices. We observed a significant relationship between LAI and SAVI2 ($R^2_{cv}$ =0.77, $RMSE_{cv}$=0.59). Our results confirmed that bands from the SWIR region contain relevant information for LAI estimation. The study verified that within the range of LAI studied ($0.3 \leq LAI \leq 6.1$); linear relationships exist between LAI and the selected narrow band indices.

## 2.1. Introduction

Leaf area index (LAI) measures one half of the total leaf area of the vegetation per unit area of soil (background) surface. It can be used to infer processes such as photosynthesis, transpiration and evapotranspiration and is closely related to net primary production of terrestrial ecosystems (Running et al. 1989; Bonan 1993). Measuring LAI on the ground is difficult and requires a great amount of labor and hence cost (Gower et al. 1999). Therefore, many studies have sought to discover relationships between LAI and remote sensing data for its cost-effective, rapid, reliable and objective estimation. To minimize the variability due to external factors such as underlying soil brightness, leaf angle distribution and leaf optical properties, remote sensing data have been transformed and combined into various vegetation indices (VIs).

Spectral vegetation indices are usually calculated as combinations of near infrared and red reflectance. In many studies, these broad-band VIs have shown to be well correlated with canopy parameters related to chlorophyll and biomass abundance such as green leaf area index and absorbed photosynthetically active radiation (e.g., Elvidge and Chen 1995). Two common classes of indices have been the subject of considerable research: (1) ratio based indices such as the ratio vegetation index (RVI) (Pearson and Miller 1972) and the normalized difference vegetation index (NDVI) (Rouse et al. 1974), (2) soil line related indices such as the perpendicular vegetation index (PVI) (Richardson and Wiegand 1977) and the

transformed soil adjusted vegetation index (TSAVI) (Baret et al. 1989). A large number of relationships have been discovered between these vegetation indices and canopy variables including LAI (Elvidge and Chen 1995; Rondeaux and Steven 1995; Broge and Leblanc 2001; Schlerf et al. 2005; Wang et al. 2005).

Developments in the field of hyperspectral remote sensing and imaging spectrometry have opened new ways for monitoring plant growth and estimating biophysical properties of vegetation. It has promoted a new group of vegetation indices based on the shape and relative position of the spectral reflectance curve. These include the red edge of the vegetation spectrum, which is the sharp slope between the low reflectance in the visible region and the higher reflectance in the near infrared region, around 670-780 nm. The red edge inflection point (REIP), that is the wavelength which has maximal slope in the red edge, and the shape of the red edge have been investigated in several studies and have demonstrated a good correlation with biophysical parameters such as LAI, while simultaneously being less sensitive to spectral noise due to soil background and/or atmospheric effects (Demetriades-Shah et al. 1990; Baret et al. 1992). The blue and red shift of the red edge inflection point (REIP) has been related to plant growth conditions in many studies (Horler et al. 1983; Gilabert et al. 1996; Blackburn 1998). REIP depends on the amount of chlorophyll seen by the sensor and is strongly correlated with foliar chlorophyll content and presents a very sensitive indicator of vegetation stress (Dawson and Curran 1998; Rossini et al. 2007). The chlorophyll amount present in a vegetation canopy is characterized by the chlorophyll concentration of the leaves and the leaf area index (Schlerf et al. 2005).

Danson and Plummer (1995) found a strong correlation between LAI and REIP in coniferous forests and suggested complementary use of REIP with NDVI. Kodani et al. (2002) concluded that the red edge position was strongly correlated with LAI in a deciduous beech forest, thus being a good estimator of LAI as well as canopy chlorophyll content. In the study of Hansen and Schjoerring (2003) using winter wheat, the red edge responded linearly to LAI and chlorophyll content. Lee et al. (2004) concluded that spectral channels in the red edge and shortwave infrared (SWIR) regions are generally very important for predicting LAI in four different biomes of row-crop agriculture, tall grass prairie and mixed conifer forest. Pu et al. (2003b) studied the relationship between forest LAI and two red edge parameters: red edge position (REP) and red well position (RWP) and found good correlations between forest LAI and red edge parameters calculated from four point interpolation methods. Clevers (1994) showed that leaf area index and leaf chlorophyll concentration of crops are the main parameters determining the value of the red edge index.

In contrast, Broge and Leblanc (2001) indicated that REIP measures relate poorly to LAI according to a simulation analysis using a combined PROSPECT and SAIL (*Scattering by Arbitrarily Inclined Leaves*) radiative transfer model. Gong et al. (1992) used imaging spectrometer data to investigate the relationship between

the LAI of ponderosa pine stands and their spectral response. They found that the magnitude of the red edge slope was not strongly correlated with LAI. Schlerf et al. (2005) used HyMap (Hyperspectral Mapping imaging spectrometer) data for highly managed conifer stands and discovered a relatively close linear relationship between forest LAI and REIP only for a subset of their data. Imanishi et al. (2004) found that REIP was neither a good indicator of drought status nor of LAI for two tree species, *Quercus glauca* and *Quercus serrata*. Blackburn (2002) found no relationship between REIP and LAI using CASI (Compact Airborne Spectrographic Imager) data in coniferous forests.

From the above literature it is evident that many of the conclusions drawn for similar vegetation types are contradictory. Moreover, many studies focus on single plant species and/or structurally similar plant types. Hence, there is a need to further investigate the relationship between LAI and narrow band indices including the REIP. The investigation should involve structurally widely different plant species with varying leaf chlorophyll concentration and should be measured above contrasting backgrounds. The objectives of this study were to examine the relationship between the LAI of structurally different vegetation canopies and the hyperspectral reflectance data, narrow band VI and REIP. The laboratory study was designed to test two hypotheses: (i) REIP is controlled primarily by canopy LAI and is a good predictor for LAI, and (ii) the narrow band VI is more responsive than REIP and broad-band VI for estimation of canopy LAI. The study is based on canopy spectral reflectances measured during a laboratory experiment using canopy species with different leaf sizes and leaf shapes.

## 2.2. Materials and methods

### *2.2.1. Experimental setup*

Four different plant species with different leaf shapes and sizes were selected for sampling: *'Asplenium nidus'*: an epiphytic fern which has apple green leaves of about 50 cm length and 20 cm width, *'Halimium umbellatum'*: a Mediterranean procumbent shrub which has crowded leaves at the apex of branchlets, the leaves being linear and about 25 mm in length, *'Schefflera arboricola Nora'*: a shrub with palm shaped leaves, dark green in color and palmately compound with 7-9 leaflets each about 5 to 7 cm long, and *'Chrysalidocarpus decipiens'*: a single trunked or clustering palm with slightly plumose leaves, each about 25 cm long with a width of 2 to 3 cm. A total of 24 plants were used for the study, 6 plants per species. The plants were maintained in a green house with a day temperature of 25º C and night temperature of 21º C. Photos taken from nadir (Figure 2.1) show the four plant species and illustrate their variability in leaf size and shape.

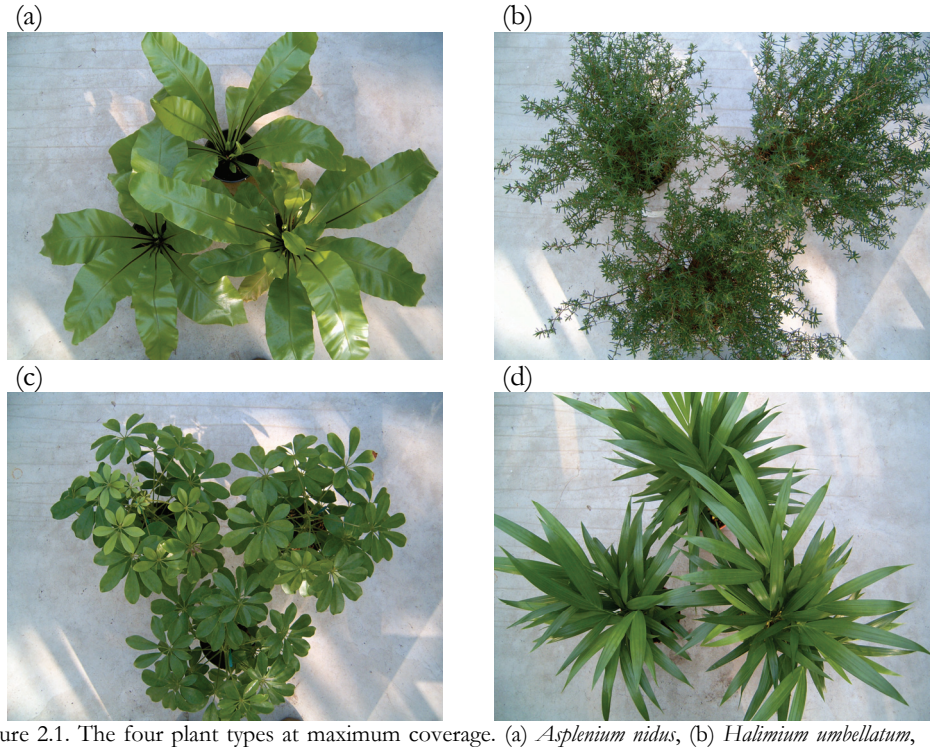


Figure 2.1. The four plant types at maximum coverage. (a) *Asplenium nidus*, (b) *Halimium umbellatum*, (c) *Schefflera arboricola Nora* and (d) *Chrysalidocarpus decipiens*.

Canopy spectral reflectance in visible and mid infrared regions, is affected by many factors such as LAI, pigment concentration, canopy architecture and soil brightness (Jackson and Pinter 1986; Gitelson et al. 2003). In order to artificially generate a wide variability within each species, we artificially induced variations in LAI and canopy chlorophyll content as well as variations in background brightness. To obtain differences in leaf optical properties (e.g. leaf chlorophyll concentration), the plants (from each species) were randomly divided into two equal groups (3 plants per species in each group) on 8th March 2005. One group (12 plants) was placed in a nutrient rich soil (soil enriched with ammonium nitrate) and the other group (12 plants) was placed in a very poor soil (soil mainly consist of peat) to induce nutrient shortage and thus to reduce the amount of chlorophyll in the leaves. After four weeks, a SPAD-502 Leaf Chlorophyll Meter (MINOLTA, Inc.) was used to measure relative chlorophyll concentration in the leaves and to verify that the goal of creating differences in leaf chlorophyll concentration was achieved.

### *2.2.2. Spectral measurements*

Spectra were measured in a remote sensing laboratory with all walls and the ceiling coated with black material in order to avoid any ambient light or reflection, therefore minimizing the effect of diffuse radiation and lateral flux. A GER 3700 spectroradiometer (Geophysical and Environmental Research Corporation, Buffalo, New York) was used for the spectral measurements. The wavelength range is 350 nm to 2500 nm, with a spectral sampling of 1.5 nm in the 350 nm to 1050 nm range, 6.2 nm in the 1050 nm to 1900 nm range, and 9.5 nm in the 1900 nm to 2500 nm range. The fiber optic, with a field of view of 25°, was placed in a pistol and mounted on an arm of a tripod and positioned 90 centimeters above a 50 cm x 50 cm soil bed at nadir position. In the setting, the spectrometer had a field of view with a diameter of 40 centimeters on the soil surface with the nadir point being the centre of the circle. We prepared two beds with two different soil types. One bed was filled with dark soil (peat) and one with light soil (sand silica). Three empty pots were fixed in each soil bed such that their centers were positioned on the border of the field of view and a line drawn from centre to centre would form an equal-distance triangle. Figure 2.2 shows the arrangement of the pots in the experiment.

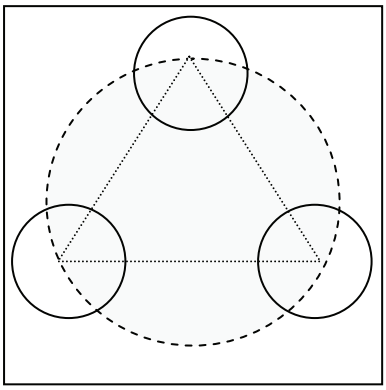

Figure 2.2. Schematic representation of the position of the pots in our field of view (dashed circle).

Spectral measurements of bare (and air-dried) soils were acquired each time before starting the canopy reflectance measurements of one group of species. Mean reflectance spectra associated with the two soil types are shown in Figure 2.3. Further the spectral measurements continued by placing three plants (with the same species and treatment) in their predefined positions in one of the soil beds directly under the sensor and the halogen lamp (235W) positioned next to it, while the centre of the soil bed was made to coincide with the centers of the light and the sensor's field of view (FOV). We made sure that the FOV of the sensor was fully covered by the plants. In this manner we achieved a constant illumination, but a variable reflectance as determined by leaf area and differences in leaf shape of the

various species. The soil beds were rotated by 45° after every spectral measurement in order to average out differences in canopy orientation and hence minimize any BRDF effect. Next the plants were moved to the other soil bed to repeat the measurements in the other soil type. The readings were calibrated by means of a white ($BaSO_4$) reference panel (50 cm x 50 cm) of known reflectivity. Reference measurements were taken after every eight target measurements. As the halogen lamp was relatively close to the plants and was not fully collimated, the incoming flux density of the various leaf layers depended on the distance to the light source. However, care was given in the selection of the plants, so that the investigated plants had more or less the same height (about 45 cm). Our main objective was to compare the performance of different VIs in estimating LAI of structurally different plant types having different soil backgrounds. Hence, the absolutely correct canopy reflectance (with a fully collimated light source) was not of primary importance.

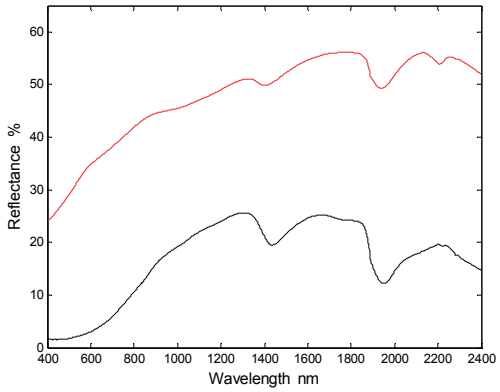


Figure 2.3. Spectral reflectance characteristics of the light (red) and dark (black) soils. Each curve represents the average of 64 bare soil reflectance measurements.

To create variations in LAI, the leaves on the inner side of the plants were harvested in 6 steps. At each step, approximately 1/6 of the total canopy (total leaves) was harvested. The leaves for removal were selected from different layers of the canopy. Each time we separated a leaf or a portion of the leaves we measured its surface area with a LI-3100 scanning planimeter. The LI-3100 (LICOR, NE, USA) is a commercial leaf area meter which makes use of a fluorescent light source and a solid-state scanning camera to 'sense' the area of leaves as they move through the instrument. The calibration of the instrument was checked each time with a metal circle of known surface. The measured surface area of the leaves was then divided by the ground area ($r^2*\pi$) to calculate the leaf area index (LAI, $m^2\ m^{-2}$).

## *2.2.3. Method*

### 2.2.3.1. Pre-processing of spectra

An average spectrum was calculated from every eight replicated measurements. A moving Savitzky-Golay filter (Savitzky and Golay 1964) with a frame size of 15 (2nd degree polynomial) was applied to the reflectance spectra to eliminate sensor noise.

### 2.2.3.2. Hyperspectral vegetation indices

Narrow band vegetation indices were computed from the averaged, smoothed spectra using all possible two wavelength combinations involving 584 wavelengths between 400 nm and 2400 nm. Additionally the red edge inflection point (REIP) was calculated using three different methods, i.e. first derivative, linear interpolation and inverted gaussian model.

#### *2.2.3.2.1. The narrow band indices*

The most common indices are generally ratio indices and soil based indices which are based on discrete red and NIR bands. This is due to the fact that vegetation reveals distinctive reflectance properties in these bands. Ratio based vegetation indices are often preferred over soil based indices as the required soil line parameters are often unavailable or influenced by soil variability (Broge and Mortensen 2002). The soil line originally defined by Richardson and Wiegand (1977) is a linear relationship between the NIR and red reflectance of bare soils and is defined by the slope and intercept of this line. In this study, the soil line parameters (slope 'a' and intercept 'b') were calculated from spectral measurements of the two soils. We assumed that the soil line concept, originally defined for the red-NIR feature space can be transferred into other spectral domains (Thenkabail et al. 2000; Schlerf et al. 2005). The narrow band indices were systematically calculated for all possible 584*584 = 341056 wavelength combinations. The narrow band RVI, NDVI, PVI, TSAVI and SAVI2 were computed according to Table 2.1.

#### *2.2.3.2.2. Red edge inflection point*

In the literature, several techniques are proposed to calculate the REIP. For this study, the REIP was calculated using three different approaches which are widely used in the literature, namely first derivative (Dawson and Curran 1998), linear interpolation (Guyot and Baret 1988) and inverted gaussian model (Bonham-Carter 1988).

Table 2.1. Vegetation indices formulas used in the study. $\rho$ denotes reflectance, $\lambda_1$ and $\lambda_2$ are wavelengths and *a* and *b* are the soil line coefficients for $\lambda_1$ and $\lambda_2$ respectively.

| ***Acronym*** | ***Name*** | ***VI*** | ***Eq.*** | ***Reference*** |
|---|---|---|---|---|
| ***RVI*** | Ratio vegetation index | $RVI = \rho_{\lambda 1} / \rho_{\lambda 2}$ | (1) | (Pearson and Miller, 1972) |
| ***NDVI*** | Normalized difference vegetation index | $NDVI = \frac{\rho_{\lambda 1} - \rho_{\lambda 2}}{\rho_{\lambda 1} + \rho_{\lambda 2}}$ | (2) | (Rouse et al., 1974) |
| ***TSAVI*** | Transformed soil- adjusted vegetation index | $TSAVI = \frac{a(\rho_{\lambda 1} - a\rho_{\lambda 2} - b)}{a\rho_{\lambda 1} + \rho_{\lambda 2} - ab}$ | (3) | (Baret et al., 1989) |
| ***SAVI2*** | Second soil-adjusted vegetation index | $SAVI2 = \frac{\rho_{\lambda 1}}{\rho_{\lambda 2} + (b/a)}$ | (4) | (Major et al., 1990) |
| ***PVI*** | Perpendicular vegetation index | $PVI = \frac{\rho_{\lambda 1} - a\rho_{\lambda 2} - b}{\sqrt{1 + a^2}}$ | (5) | (Richardson and Wiegand, 1977) |

*A first difference transformation* of the reflectance spectrum was derived according to equation 6 (Eq. 6) (Dawson and Curran 1998):

$$FDiff_{\lambda(i)} = \left(R_{\lambda(j+1)} - R_{\lambda(j)}\right) / \Delta_{\lambda} \quad \text{(Eq. 6)}$$

$$REIP_{FDiff} = \lambda_{\max(FDiff)} \quad \text{(Eq. 7)}$$

where *FDiff* is the first difference transformation at a wavelength *i* midpoint between wavebands *j* and *j*+1. $R_{\lambda(j)}$ is the reflectance at the *j* waveband, $R_{\lambda(j+1)}$ is the reflectance at the *j*+1 waveband and $\Delta_{\lambda}$ is the difference in wavelengths between *j* and *j*+1. The REIP is simply the wavelength where the first difference is greatest.

*The linear interpolation,* as described by Guyot and Baret (1988), assumes that the spectral reflectance at the red edge can be simplified to a straight line centered around a midpoint between a) the reflectance in the near infrared shoulder at about 780 nm and b) the reflectance minimum of the chlorophyll absorption feature at about 670 nm. The reflectance value is estimated at the inflection point. It applies a linear interpolation procedure for the measurements at 700 nm and 740 nm estimating the wavelength corresponding to the estimated reflectance value at the inflection point. The REP is determined using the following equations:

$$R_{red-edge} = \left(R_{670} - R_{780}\right) / 2 \quad \text{(Eq. 8)}$$

$$REIP_{linear} = 700 + 40\left[\frac{R_{red-edge} - R_{700}}{R_{740} - R_{700}}\right] \quad \text{(Eq. 9)}$$

where the constants 700 and 40 result from interpolation between the 700 -740 nm intervals, and $R_{670}$, $R_{700}$, $R_{740}$ and $R_{780}$ are, respectively, the reflectance values at 670, 700, 740 and 780 nm.

*The inverted gaussian method* (Bonham-Carter 1988) fits a gaussian normal function to the measured reflectance data points between 670 and 800 nm to determine the REIP. The fitting involves iterative techniques to determine the parameters of interest:

$$R_{estimated}(\lambda) = R_s - (R_s - R_O)\exp\left(\frac{-(\lambda_o - \lambda)^2}{(2\sigma)^2}\right) \quad \text{(Eq. 10)}$$

$$REIP_{IGM} = \lambda_O + \sigma \quad \text{(Eq. 11)}$$

Where σ is the gaussian shape parameter, measured in nanometers, $R_s$ is the (maximum) shoulder reflectance usually between 780-800 nm, $R_o$ is the minimum reflectance usually at about 670-690 nm and $\lambda_o$ is the wavelength at the point of minimum reflectance. The measured reflectance data points are fitted by adjusting the values of $R_s$, $R_o$, $\lambda_o$ and σ in such a way that the RMSE is minimized (Mathworks 2007).

### *2.2.4. Regression models*

We used two approaches for modeling the relationship between LAI and predictor variables (i.e., narrow band vegetation indices and REIP): (i) simple linear regression models, and (ii) a more flexible exponential model, initially suggested by Baret and Guyot (1991). The latter is a modified version of Beer's law expressing the variation in vegetation index as a function of the LAI measurements (Equation (12)).

$$VI = VI_\infty + (VI_g - VI_\infty)\exp^{(-K_{VI}LAI)} \quad \text{(Eq. 12)}$$

The exponential model assumes the canopy to be a homogenous body of green plant material with an optical thickness given by the *LAI*. The dynamic range of the vegetation index is expressed as the difference between the bulk vegetation index ($VI_\infty$) and the index value corresponding to bare soil ($VI_g$). The $K_{VI}$ parameter is equivalent to the extinction coefficient in Beer's law and characterizes the relative increase in vegetation index due to an increase in LAI. Previous studies (Wiegand et al. 1992; Atzberger 1995, 1997; Broge and Mortensen 2002) have confirmed the effectiveness of this model to relate vegetation indices to biophysical variables particularly to leaf area index. Thus we also used this model to evaluate the relationships between narrow band vegetation indices/REIP and LAI.

### *2.2.5. Validation*

To validate the regression models, a cross validation procedure (also called the leave-one-out method) was used. In cross validation, each sample is estimated by the remaining samples. Benefits of the cross validation method are its aptitude to detect outliers (Schlerf et al. 2005) and its capability for providing nearly unbiased estimations of the prediction error (Efron and Gong 1983). This implied that for each regression variant we developed 95 individual models, each time with data from 94 observations. The calibration model was then used to predict the observation that was left out. As the predicted samples are not the same as the samples used to build the models, the cross validated RMSE is a good indicator for the accuracy of the model in predicting unknown samples.

## 2.3. Results and discussion

### *2.3.1. Variation in LAI and spectral reflectance*

The experimental protocol ensured a wide range of variation in LAI (Table 2.2). LAI ($m^2$ $m^{-2}$) varied between 0.3 and 6.1 with an average of 1.69. Due to the different leaf sizes and shapes, and different canopy architectures, as well as variations caused by nutrient stress and differences in soil brightness, canopy reflectance measurements showed a large variability (Figure 2.4).

Table 2.2. Description of the data acquired during the experiment (n=95). * indicates the samples placed in poor soils to reduce the leaf chlorophyll content. *SPAD* is the average SPAD (relative chlorophyll measure) reading for 30 randomly selected leaves in each canopy species.

| *Canopy species* | *Min LAI $m^2$ $m^{-2}$* | *Mean LAI $m^2$ $m^{-2}$* | *Max LAI $m^2$ $m^{-2}$* | *StDev LAI* | *SPAD* | *StDev SPAD* | *No. of Obs.* |
|---|---|---|---|---|---|---|---|
| ***Asplenium nidus*** | 0.87 | 3.28 | 6.11 | 1.93 | 34.7 | 4.6 | 11 |
| ***Asplenium nidus**** | 0.34 | 2.02 | 3.70 | 1.26 | 31.7 | 6.3 | 12 |
| ***Halimium umbellatum*** | 0.49 | 1.11 | 1.63 | 0.43 | 44.2 | 3.6 | 12 |
| ***Halimium umbellatum**** | 0.42 | 1.09 | 1.73 | 0.48 | 40.0 | 4.6 | 12 |
| ***Schefflera arboricola Nora*** | 0.41 | 1.15 | 1.78 | 0.53 | 59.1 | 2.8 | 12 |
| ***Schefflera arboricola Nora**** | 0.54 | 1.75 | 2.92 | 0.92 | 49.2 | 6.7 | 12 |
| ***Chrysalidocarpus decipiens*** | 0.30 | 0.85 | 1.64 | 0.50 | 41.5 | 5.9 | 12 |
| ***Chrysalidocarpus decipiens**** | 0.62 | 2.27 | 3.66 | 1.11 | 33.5 | 8.8 | 12 |
| ***All combined*** | 0.30 | 1.69 | 6.11 | 1.19 | 41.7 | 10.2 | 95 |

Canopy reflectances of all plant types with an approximate LAI of 1.5 are shown in Figure 2.4(a) to illustrate the influence of canopy architecture and leaf

optical properties; like any other green vegetation spectrum, they all have a high reflectance in the near infrared and low reflectance in the visible regions. However, their red and near infrared reflectance values vary significantly. This variability can be attributed to variations in optical properties of the foliage (i.e. canopy chlorophyll contents) and differences in canopy architecture (Jackson and Pinter 1986; Gitelson et al. 2003). The canopy reflectance of *Asplenium nidus* with an approximate LAI of 1.5 is shown in Figures 2.4(b) and 2.4(c). Spectral reflectance of canopy with nutrient stress shows lower absorption peaks in the visible region but along the red edge (~700 nm) it stayed relatively stable (Figure 2.4(b)).

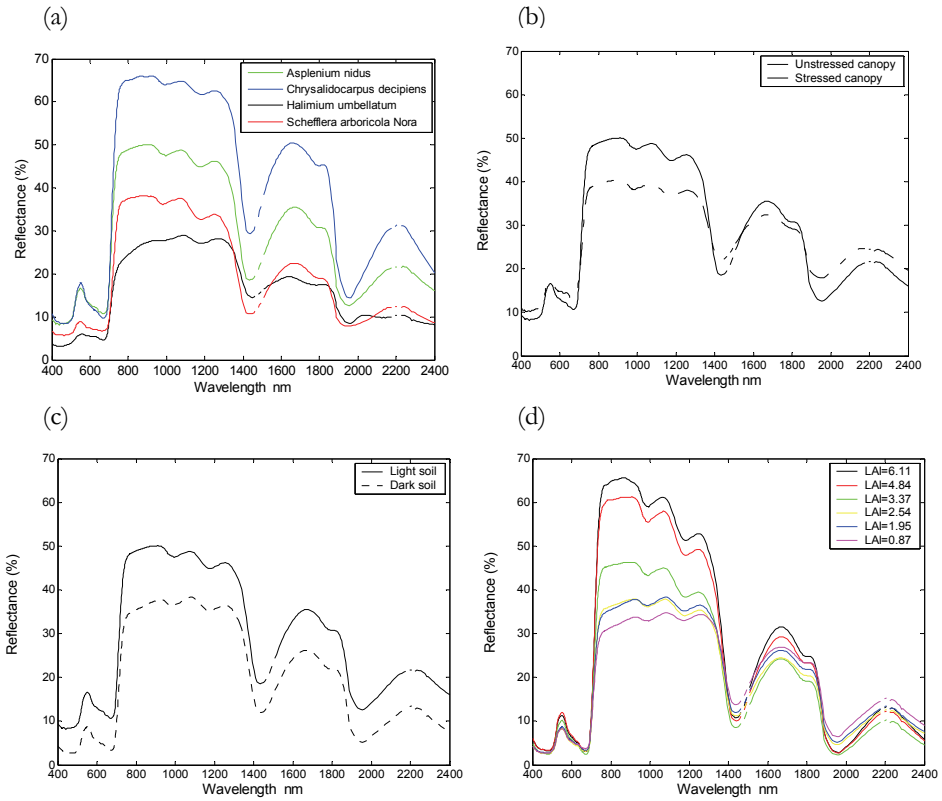


Figure 2.4. (a) Spectral reflectance of different canopy species with an LAI of 1.5. (b) Spectral reflectance of *Asplenium nidus,* with an LAI of 1.5, stressed and unstressed. (c) Spectral reflectance of *Asplenium nidus,* with an LAI of 1.5, in dark and light soil. (d) Spectral reflectance of *Asplenium nidus* corresponding to LAI between 0.87 and 6.11.

Our two investigated soils mainly differed in overall albedo. Consequently, for a given LAI and plant species (Figure 2.4(c)), soil background variations translated into simple reflectance offsets in the measured canopy reflectance spectra. As expected, canopy LAI variation had a strong influence on the reflectance spectra (Figure 2.4(d)). The most distinct effects were found in the NIR and the smallest

effects in the VIS region. As LAI increased within a canopy, a clear deepening of the two water absorption features within the NIR (~1000 nm and 1200 nm) were observed in the reflectance spectra (Asner 1998).

### *2.3.2. REIP and LAI*

Figure 2.5 shows box plots of the red edge positions calculated using the three methods. The red edge positions calculated using the inverted gaussian model and the first derivative show a (too) wide dynamic range and have a tendency toward shorter wavelengths while the REIP calculated using the linear interpolation varies only between 715 nm and 726 nm. It is apparent from Figure 2.5 that the result of REIP calculations from the three methods yield very dissimilar results and are highly dependent on the choice of methodology (Broge and Leblanc 2001; Cho and Skidmore 2006). In the case of the first derivative method, part of the outliers is probably due to the remaining noise in reflectance measurements (Broge and Leblanc 2001). In a recent study, Cho and Skidmore (2006) have demonstrated that double peaks in the first derivative reflectance could cause discontinuities in the data and hence lead to poor relationships between LAI and REIP.

REIP calculated via any of the three methods did not show a close relation to variations in LAI. The coefficient of determination ($R^2$) calculated between LAI and REIP was very low ($R^2 < 0.1$) when measurements of the different plant species were pooled together.

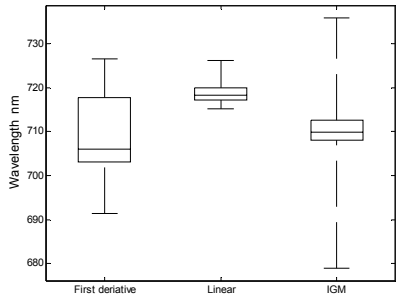


Figure 2.5. Box plots showing the median, lower and upper quartile values, and extent of the rest of the red edge position (REIP) calculated using three different methods (first derivative, linear interpolation, and an inverted gaussian model).

Examples of these confusing relationships are shown in Figure 2.6 for REIP determined using the first derivative. As is evident from Figure 2.6, REIP was not sensitive to variations in LAI.

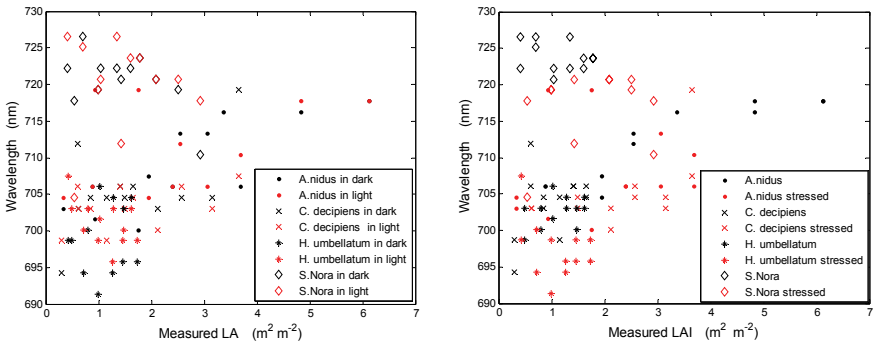


Figure 2.6. The relationship between LAI of different canopies and REIP calculated using first derivative. Different symbols indicate different plant species and different colors show different soil backgrounds (left) and different nutrient status (right).

We also evaluated the correlation between REIP derived from different methods and LAI of each individual canopy (not shown). The results varied somewhat, but confirmed that REIP is not a good variable to estimate LAI. Consequently, we had to reject our first hypothesis that 'REIP is controlled primarily by canopy LAI and is a good predictor of LAI'.

Our findings are supported by results obtained from other studies. Blackburn (2002) found no relation between REIP and LAI for coniferous stands using CASI data, while Broge and Leblanc (2001) indicated a poor relationship between REIP and LAI. Attempts by Schlerf et al. (2005), to relate LAI to REIP for Norway spruce forest stands, were only successful for a subset of their data. Further, our results are confirmed by the findings of Imanishi et al. (2004), who verified that there is no significant relationship between REIP and LAI for two deciduous and evergreen tree species. However, our results contradict the results of Broge et al. (1997) as well as Hansen and Schjoerring (2003) and Kodani et al. (2002), who showed REIP to be better than NDVI for estimation of LAI for a single species. Also, Danson and Plummer (1995) found a strong, non linear correlation between LAI and REIP for Sitka spruce using a helicopter borne spectroradiometer. We conclude that at canopy level, REIP is not an appropriate variable to be considered for LAI estimations if several contrasting species are pooled together, though it may be appropriate for single species. Note that successful studies with REIP did not use destructive sampling for LAI retrieval, as was the case in this study. Many studies have found relationships between REIP and vegetation characteristics at leaf level. As such, REIP has been used as a means to estimate changes in foliar chlorophyll concentration and also as an indicator of vegetation stress (Horler et al. 1983; Curran et al. 1995; Lamb et al. 2002; Rossini et al. 2007).

### *2.3.3. Narrow band indices*

For both types of indices (ratio and soil based indices), the optimal narrow band vegetation index was determined using two approaches. First, the coefficients of determination ($R^2$) of all possible two band combinations of vegetation index and LAI were computed. An illustration of these results is shown in the 2-D correlation plot in Figure 2.7 (Left). The meeting point of each pair of wavelengths corresponds to the $R^2$ value of LAI and the vegetation index calculated from the reflectance values in those two wavelengths. In the second approach (Figure 2.7 (Right)), all possible two band combinations of vegetation indices were calculated and used to estimate the LAI using an exponential model. The 2-D plot shows the coefficients of determination ($R^2$) between measured and estimated LAI.

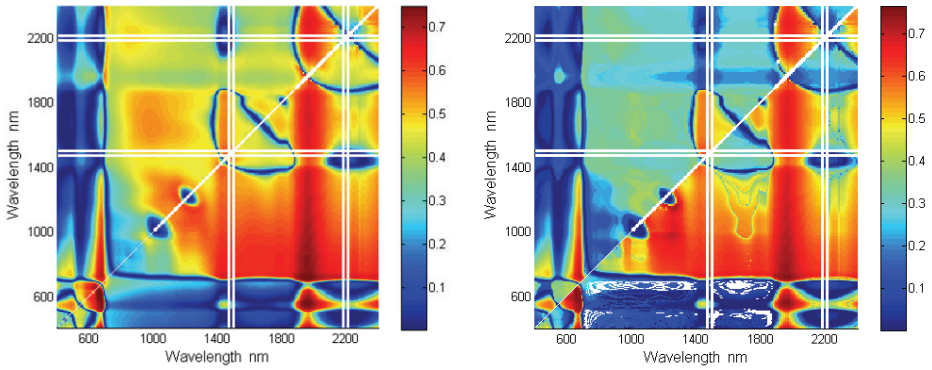


Figure 2.7. (Left): 2-D correlation plot representing the coefficient of determination ($R^2$) of narrow band RVI values and LAI. (Right): 2-D correlation plot that illustrates the coefficient of determination ($R^2$) of estimated LAI (using an exponential model) and measured LAI for narrow band RVI. Please note that the plots are not symmetrical. Y axis is the nominator and X axis is the denominator, respectively.

For both approaches, band combinations that formed the best indices for estimating LAI were recognized based on the $R^2$ values in the 2-D correlation plots. The coefficient of determination ($R^2$) and the band positions of the best performing indices are tabulated in Table 2.3 ((a) and (b)). In Figure 2.8, 'hot spot' regions with relatively high $R^2$ values ($R^2$>0.7), are highlighted for all vegetation indices.

Although the near infrared region has been the keystone of the omnipresent vegetation indices (NDVI, RVI), our results show that for most indices, bands from the SWIR region contain most information relevant to canopy LAI (Figure 2.8). As it is clear from Figure 2.8 the "hot spots" with high $R^2$ values mostly occur in this region. These results support findings from studies by Brown et al. (2000), Cohen and Goward (2004), Lee et al. (2004), Nemani et al. (1993) and Schlerf et al. (2005), that suggest a strong contribution by SWIR bands to the strength of relationships between spectral reflectance and LAI. Considering that the SWIR

bands were important for most vegetation indices in this study, vegetation indices that do not include this spectral region may be less satisfactory for LAI estimation (Lee et al. 2004). A number of other studies have recognized this region of the reflectance spectrum as potentially important for tracking vegetation properties (Asner 1998; Eklundh et al. 2001; Cohen et al. 2003).

Table 2.3(a). The wavelength positions and the coefficient of determination ($R^2$) of the best performing narrow band indices and LAI (linear model).

| *VI* | $\lambda_1$ *(nm)* | $\lambda_2$ *(nm)* | $R^2$ |
|---|---|---|---|
| ***RVI*** | 718 | 1943 | 0.749 |
| ***NDVI*** | 651 | 653 | 0.745 |
| ***PVI*** | 1132 | 1238 | 0.741 |
| ***TSAVI*** | 700 | 1966 | 0.707 |
| ***SAVI2*** | 718 | 1966 | 0.775 |

Table 2.3(b). The wavelength positions and the coefficient of determination ($R^2$) of the best estimated LAI and measured LAI (exponential model).

| *VI* | $\lambda_1$ *(nm)* | $\lambda_2$ *(nm)* | $R^2$ |
|---|---|---|---|
| ***RVI*** | 651 | 653 | 0.765 |
| ***NDVI*** | 650 | 658 | 0.755 |
| ***PVI*** | 731 | 1717 | 0.768 |
| ***TSAVI*** | 703 | 1955 | 0.751 |
| ***SAVI2*** | 719 | 1966 | 0.775 |

In the next step of the analysis, for the best performing narrow band index of all vegetation indices, cross validated $R^2$ and RMSE were computed using linear regression and the exponential model of Baret and Guyot (1991). The results are reported in Table 2.4. As can be observed from the table, the linear model gave relatively lower RMSE values for all indices compared to the exponential model. This is probably due to the fact that in the exponential model, at high LAI values, small reflectance variations cause (too) large variations in the estimated LAI and hence lead to increased RMSE.

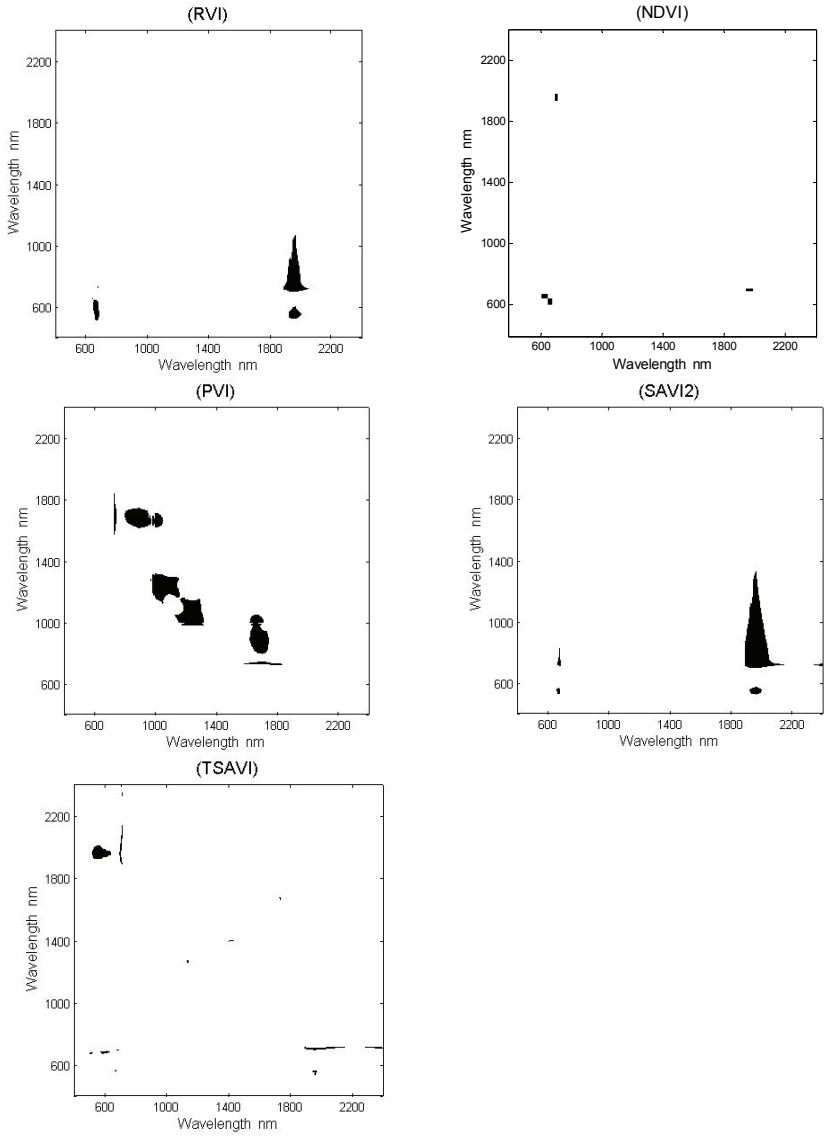


Figure 2.8. 'Hot spot' regions with relatively high values of the coefficient of determination ($R^2 > 0.7$) between narrow band vegetation index (VI) and LAI. Note that for TSAVI, black regions correspond to $R^2$ values greater than 0.6 ($R^2 > 0.6$).

The best narrow band indices for predicting LAI were identified from their RMSE values (Table 2.4). Comparison between different narrow band vegetation indices revealed that the narrow band SAVI2 (Major et al. 1990) followed by the narrow band RVI (Pearson and Miller 1972) were the best overall choices as estimator of LAI based on $R^2$ and RMSE values if the reflectance measurements of the plant species were pooled together. This result is in agreement with those of

Broge and Mortensen (2002), who defined SAVI2 as the best estimator for green canopy area index. Further, SAVI2 has been proven to be relatively insensitive to external factors such as background reflectance and atmospheric effects (Broge and Leblanc 2001).

Table 2.4. Cross validated $R^2$ & RMSE for estimation of LAI using a linear and an exponential model. $NDVI_{typical}$ is the typical NDVI (680 nm, 833 nm) vegetation index.

| ***Narrow band VI*** | ***$R^2_{CV}$ & $RMSE_{CV}$*** | ***Linear model*** | ***Exponential model*** |
|---|---|---|---|
| ***RVI*** | $R^2$ | 0.729 | 0.754 |
| | RMSE | 0.625 | 0.686 |
| | | (718 nm , 1943 nm) | (651 nm , 653 nm) |
| ***NDVI*** | $R^2$ | 0.728 | 0.71 |
| | RMSE | 0.628 | 0.74 |
| | | (651 nm , 653 nm) | (650 nm , 658 nm) |
| ***PVI*** | $R^2$ | 0.725 | 0.714 |
| | RMSE | 0.629 | 0.757 |
| | | (1132 nm ,1238 nm) | (731 nm , 1717 nm) |
| ***TSAVI*** | $R^2$ | 0.686 | 0.684 |
| | RMSE | 0.672 | 0.806 |
| | | (700 nm , 1966 nm) | (703 nm , 1955 nm) |
| ***SAVI2*** | $R^2$ | 0.768 | 0.766 |
| | RMSE | 0.590 | 0.672 |
| | | (718 nm , 1966 nm) | (719 nm , 1966 nm) |
| ***$NDVI_{typical}$*** | $R^2$ | 0.354 | 0.586 |
| | RMSE | 0.965 | 0.988 |

Vegetation indices have been frequently correlated with LAI through linear or exponential models, depending on the existence of the saturation effect. VIs exhibit decreasing sensitivity to LAI at increasing greenness measurements (LAI values). To overcome the saturation problem, previous studies have confirmed the effectiveness of the exponential model developed by Baret and Guyot (1991) to relate vegetation indices to biophysical variables particularly to leaf area index (Wiegand et al. 1992; Atzberger 1995; Broge and Mortensen 2002). However, in some studies vegetation indices tend to be almost linearly related to canopy greenness without saturation (Hinzman et al. 1986; Goel 1989; Broge and Mortensen 2002; Chen et al. 2002; Schlerf et al. 2005). The scatter plots between best band combinations of SAVI2 and LAI illustrate a linear relationship (Figure 2.9). Also evident from the scatter plot is that even at relatively high values of LAI (LAI=6) saturation did not yet occur.

In the next step of the analysis, the best narrow band NDVI (651 nm, 653 nm, $R^2$= 0.745) was compared to a typical NDVI (680 nm, 833 nm) (Hurcom and Harrison 1998; Mutanga and Skidmore 2004), to see if narrow band vegetation

indices would improve the prediction accuracy of LAI. The analysis of the LAI-NDVI in linear and exponential relationships showed that the best selected narrow band NDVI more accurately predicted LAI (Table 2.4).

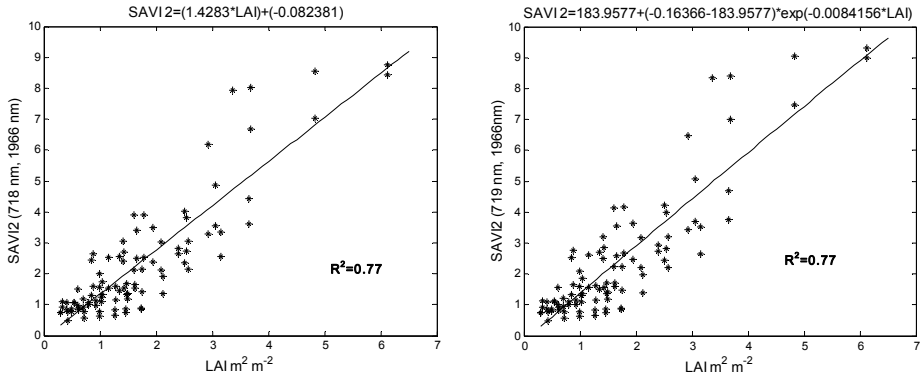


Figure 2.9. Relationships between best narrow band SAVI2 and LAI. (Left) using a simple linear model, (Right) using an exponential relationship (Baret and Guyot, 1991).

Cross validated RMSE and $R^2$ values revealed that best narrow band NDVI (651 nm, 653 nm) is a better predictor for LAI than typical NDVI (680 nm, 833 nm). Figure 2.10 illustrates the relationship between measured and estimated LAI for typical NDVI and best narrow band NDVI using the linear regression model. It can be observed that LAI saturates very early (around 4) for the typical NDVI. Using the best narrow band NDVI, saturation occurs later (around a LAI of 6). This confirms previous findings by Lee et al. (2004) and Schlerf et al. (2005), who showed that narrow band vegetation indices are better predictors of vegetation biophysical variables, such as LAI, compared to broad band vegetation indices.

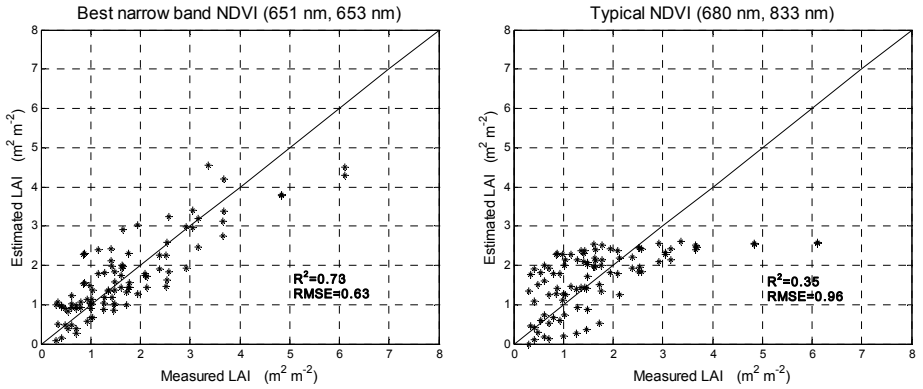


Figure 2.10. The relationship between measured and estimated LAI for best narrow band NDVI (left) and typical NDVI (right) using a linear regression model. Note that the values of $R^2$ and RMSE are cross validated.

## 2.4. Conclusions

This chapter has investigated the relationship between LAI and narrow band spectral indices, based on a laboratory experiment. Three types of narrow band vegetation indices, namely ratio based, soil based and REIP, were compared for their effectiveness in estimating LAI. The following conclusions were drawn from this study:

- REIP determined using any of the three investigated methods, had a very poor relationship with LAI, in particular when the plant species were pooled together.
- LAI of vegetation canopies was estimated with reasonable accuracy from red/near infrared based narrow band indices.
- Narrow band SAVI2 based on wavelengths in the near infrared and SWIR proved to be the best index, in both exponential and linear models, for estimating LAI.
- Spectral channels in the SWIR region (and those in the near infrared) were important for predicting LAI.
- Linear model gave a better estimation of LAI than the exponential model.
- Narrow band vegetation indices were better predictors of LAI, than broad band typical vegetation indices.

Although in our pooled dataset we used a relatively wide range of canopy spectral reflectances, we recommend that further studies should investigate on data sets covering more species to show the relationships between biophysical variables and narrow band vegetation indices more clearly. Furthermore the number of plants within the scene should be increased to ensure that the reflected flux is representative of an infinitely extended canopy. Likewise, more care should be taken to uniformly illuminate the target by using fully collimated light sources. The latter two points will be particularly important, if physically based canopy reflectance models are investigated in similar laboratory settings.

This study investigated laboratory measured reflectance data. Of course, in case that finding should be applicable to real-world measurements, representative band widths and band settings of existing airborne or satellite based hyperspectral sensors should be used.

## Acknowledgements

We thank the UNIFARM experimental station in Wageningen University for providing facilities for the experiment. Many thanks to Dr. Sip van Wieren for his help and support in setting up the experiment. We would also like to extend our gratitude to Mr. Jelger Kooistra for his assistance in facilitating the execution of the experiment.

# Chapter Three

# Estimation of vegetation LAI from hyperspectral reflectance data: effects of soil type and plant architecture

*This chapter is based on*:

Darvishzadeh, R., Skidmore, A., Atzberger, C. and van Wieren, S., 2008. Estimation of vegetation LAI from hyperspectral reflectance data: effects of soil type and plant architecture. *International Journal of Applied Earth Observation and Geoinformation,* **In Press**, DOI: 10.1016/j.jag.2008.02.005

## Abstract

The retrieval of canopy biophysical variables is known to be affected by confounding factors such as plant type and background reflectance. The effects of soil type and plant architecture on the retrieval of vegetation leaf area index (LAI) from hyperspectral data were assessed in this study. *In situ* measurements of LAI were related to reflectances in the red and near-infrared and also to five widely used spectral vegetation indices (VIs). The study confirmed that the spectral contrast between leaves and soil background determines the strength of the LAI-reflectance relationship. It was shown that within a given vegetation species, the optimum spectral regions for LAI estimation were similar across the investigated VIs, indicating that the various VIs are basically summarizing the same spectral information for a given vegetation species. Cross-validated results revealed that, narrow-band PVI was less influenced by soil background effects ($0.15 \leq RMSE_{cv} \leq 0.56$). The results suggest that, when using remote sensing VIs for LAI estimation, not only is the choice of VI of importance but also prior knowledge of plant architecture and soil background. Hence, some kind of landscape stratification is required before using hyperspectral imagery for large-scale mapping of vegetation biophysical variables.

## 3.1. Introduction

Over the past decades, the tools for vegetation remote sensing have evolved significantly. Optical remote sensing has expanded from the use of multispectral sensors to the use of imaging spectrometers. Imaging spectrometry is a unique type of optical remote sensing, because the surface radiance is sampled in many contiguous narrow spectral bands with bandwidths of a few nanometers (nm). Imaging spectrometers typically acquire radiance information between 400 nm and 2500 nm, ideal for monitoring plant growth and estimating the biophysical properties of vegetation.

A large number of relationships have been discovered between remote sensing data and the biophysical properties of vegetation (e.g. Baret et al., 1987; Broge and Leblanc, 2001; Elvidge and Chen, 1995; Gilabert et al., 1996; Jackson and Pinter, 1986; Rondeaux and Steven, 1995; Schlerf et al., 2005; Wang et al., 2005). To minimize the variability due to external factors such as underlying soil, leaf angle distribution and leaf optical properties, remote sensing data have been transformed and combined into various spectral vegetation indices (VIs). Broadband VIs calculated as combinations of near-infrared and red reflectance have been found to be well correlated with biophysical properties of vegetation such as canopy cover, leaf area index (LAI), and absorbed photosynthetically active radiation (Baret and Guyot, 1991; Elvidge and Chen, 1995; Turner et al., 1999). However, it has been suggested that most VIs are sensitive to soil background, particularly when the LAI is low (Huete, 1989; Huete et al., 1985).

Here LAI is defined as the one sided surface area of leaves per unit ground area, and it is the key biophysical variable influencing land surface photosynthesis, transpiration, and energy balance (Bonan, 1995; Running et al., 1989). Previous studies have shown that VIs have considerable sensitivity to LAI, but more so at relatively low LAI values (Asrar et al., 1984; Chen and Cihlar, 1996; Fassnacht et al., 1997; Friedl et al., 1994; Turner et al., 1999). VIs typically increase over an LAI range from 0 to about 3 to 5 before an asymptote is reached. The upper limit of this sensitivity apparently differs among vegetation types (Turner et al., 1999). Simulation studies involving radiative transfer models suggest that saturation is more pronounced for planophile canopies (Atzberger, 2004; Baret and Guyot, 1991). On the other hand, compared with erectophile canopies of the same LAI, planophile canopies are less influenced by soil brightness variations.

Although VIs resulting from remote sensing data have been successfully used for estimating vegetation LAI, previous studies have demonstrated that variations in biophysical and biochemical features affecting plant canopy reflectance, such as vegetation type and related optical properties, background soil reflectance, and atmospheric quality, are bounding the generality and significance of their relationships with LAI (Baret and Guyot, 1991; Colombo et al., 2003; Huete, 1989; Nagler et al., 2004; Ridao et al., 1998; Turner et al., 1999; Wang et al., 2005).

Researchers have shown that, in comparison with broad-band VIs, narrow-band VIs may be crucial for providing additional information for quantifying the biophysical characteristics of vegetation (Blackburn, 1998; Elvidge and Chen, 1995; Gong et al., 1992; Lee et al., 2004; Mutanga and Skidmore, 2004). However, only a few studies deal with the effect of exterior features on the estimation and prediction of vegetation LAI using hyperspectral reflectance data. The study of Broge and Leblanc (2001) relied exclusively on simulated data from reflectance models rather than on actual imagery and field data. Using AVIRIS (Airborne Visible Infrared Imaging Spectrometer) data, Lee et al. (2004) studied LAI estimation for four different biomes. However, their main objective was to compare hyperspectral data with multispectral data. Hence, considering confounding effects such as plant architecture and soil types, it is difficult to infer from existing studies whether, compared with broad-band indices, narrow-band VIs (combination of wavelengths that are not available with a limited number of broad bands) offer an improved sensitivity to LAI.

Our study aims to address this knowledge gap by investigating whether the estimation of LAI from hyperspectral reflectance measurements is significantly affected by soil type and/or plant architecture (e.g., leaf shape and size). We analyzed the effects of these factors (i) on the characterization of canopy reflectance behavior in visible to near-infrared bands, and (ii) on the stability of linear LAI-VI relationships. The study is based on canopy spectral reflectances measured during a controlled laboratory experiment using four types of plants,

with two different soil backgrounds and destructive LAI measurements. The plants differed widely in leaf size and shape.

## 3.2. Materials and methods

### *3.2.1. Experimental setup*

Four different plant species with different leaf shapes and sizes were selected for sampling: *Asplenium nidus*, an epiphytic fern that has apple-green leaves about 50 cm in length and 20 cm in width; *Halimium umbellatum*, a Mediterranean procumbent shrub that has crowded leaves at the apex of branchlets, the leaves being linear and about 25 mm in length; *Schefflera arboricola Nora*, a shrub with palm-shaped leaves, dark green in color, and palmately compound, with seven to nine leaflets, each about 5 cm to 7 cm in length; and *Chrysalidocarpus decipiens*, a single trunked or clustering palm with slightly plumose leaves, each about 25 cm in length and 2 cm to 3 cm in width. A total of 24 plants were used for the study, six plants per species. The plants were kept in a greenhouse. Photos taken from nadir (Figure 3.1) show the four plant species and illustrate their variability in leaf size and shape.

Canopy spectral reflectance in visible to mid-infrared regions has been revealed to be affected by many factors, such as LAI, pigment concentration, canopy architecture and soil brightness (Gitelson et al., 2003; Jackson and Pinter, 1986). In order to generate a wide variability within each species, we artificially induced variations in LAI and canopy chlorophyll content, as well as in background brightness. To obtain differences in leaf optical properties (e.g., leaf chlorophyll content), the plants (from each species) were randomly divided into two equal groups (three plants per species in each group) on 8th March 2005. One group (12 plants) was placed in a nutrient-rich soil, and the other group (12 plants) was placed in a very poor soil to induce nutrient shortage and thereby reduce the amount of chlorophyll in the leaves. After four weeks, a SPAD-502 Leaf Chlorophyll Meter (MINOLTA, Inc.) was used to measure the relative chlorophyll content in the leaves and to verify that the goal of creating differences in leaf chlorophyll content had been achieved.

### *3.2.2. LAI*

To vary LAI and the corresponding canopy reflectance measurements, the leaves on the inner side of the plants were harvested in six steps. At each step, approximately one-sixth of the total canopy (total leaves) was harvested. Each time we separated a leaf (or a portion of the leaves); we measured its surface area with an LI-3100 scanning planimeter. The LI-3100 (LICOR, NE, USA) is a commercial leaf area meter that makes use of a fluorescent light source and a solid-state scanning camera to 'sense' the area of leaves as they move through the instrument. The calibration of the instrument was checked each time with a metal circle of

known surface. By tracking the respective areas of the clipped leaf surfaces, the canopy LAI ($m^2$ $m^{-2}$) at each stage (i.e., from full canopy to bare soil) was calculated.

We were able to artificially create large variations in LAI. LAI ($m^2$ $m^{-2}$) varied between 0.3 and a maximum of 6.11 (Table 3.1). Among the four vegetation species, *Halimium umbellatum* (with tiny linear leaves) had the lowest (1.73) and *Asplenium nidus* (with leaves of about 50 cm by 20 cm) had the highest (6.11) maximum LAI values.

Table 3.1. Summary statistics of the measured plants during the experiment (n=95). SPAD is the average SPAD reading for 30 randomly selected leaves in each canopy species.

| Canopy species | No. of Obs. | Min LAI $m^2$ $m^{-2}$ | Mean LAI $m^2$ $m^{-2}$ | Max LAI $m^2$ $m^{-2}$ | StDev LAI | SPAD (unstressed /stressed) | StDev SPAD |
|---|---|---|---|---|---|---|---|
| **Asplenium nidus** | 23 | 0.34 | 2.62 | 6.11 | 1.68 | 34.7/31.7 | 5.7 |
| **Halimium umbellatum** | 24 | 0.42 | 1.10 | 1.73 | 0.43 | 44.2/40.0 | 4.58 |
| **Schefflera arboricola Nora** | 24 | 0.41 | 1.44 | 2.92 | 0.76 | 59.1/49.2 | 7.09 |
| **Chrysalidocarpus decipiens** | 24 | 0.30 | 1.63 | 3.66 | 1.03 | 41.5/33.5 | 8.47 |
| **All combined** | 95 | 0.30 | 1.69 | 6.11 | 1.19 | 41.7 | 10.2 |

## *3.2.3. Spectral measurements*

### 3.2.3.1. Canopy

Canopy spectra corresponding to the different LAI levels were measured in a remote sensing laboratory where the walls and ceiling were coated with black material in order to avoid any ambient light or reflection, thereby minimizing the effect of diffuse radiation and lateral flux. A GER 3700 spectroradiometer (Geophysical and Environmental Research Corporation, Buffalo, New York) was used for the spectral measurements. The wavelength range is 350 nm to 2500 nm, with a spectral sampling of 1.5 nm in the 350 nm to 1050 nm range, 6.2 nm in the 1050 nm to 1900 nm range, and 9.5 nm in the 1900 nm to 2500 nm range.

The fiber optic, with a field of view (FOV) of 25°, was placed in a pistol and mounted on an arm of a tripod and positioned 90 cm above a 50 cm x 50 cm soil bed at nadir position. In the setting, the spectrometer had a FOV with a diameter of 40 cm on the soil surface, with the nadir point being the center of the circle. We prepared two beds with two different real soil types. One bed was filled with dark soil (peat; which is lighter, softer, and more crumbly than ordinary garden soil) and

one with light soil (sand silica). Three empty pots were fixed in each soil bed such that their centers were positioned on the border of the FOV and a line drawn from center to center would form an equal-distance triangle (Figure 3.1).

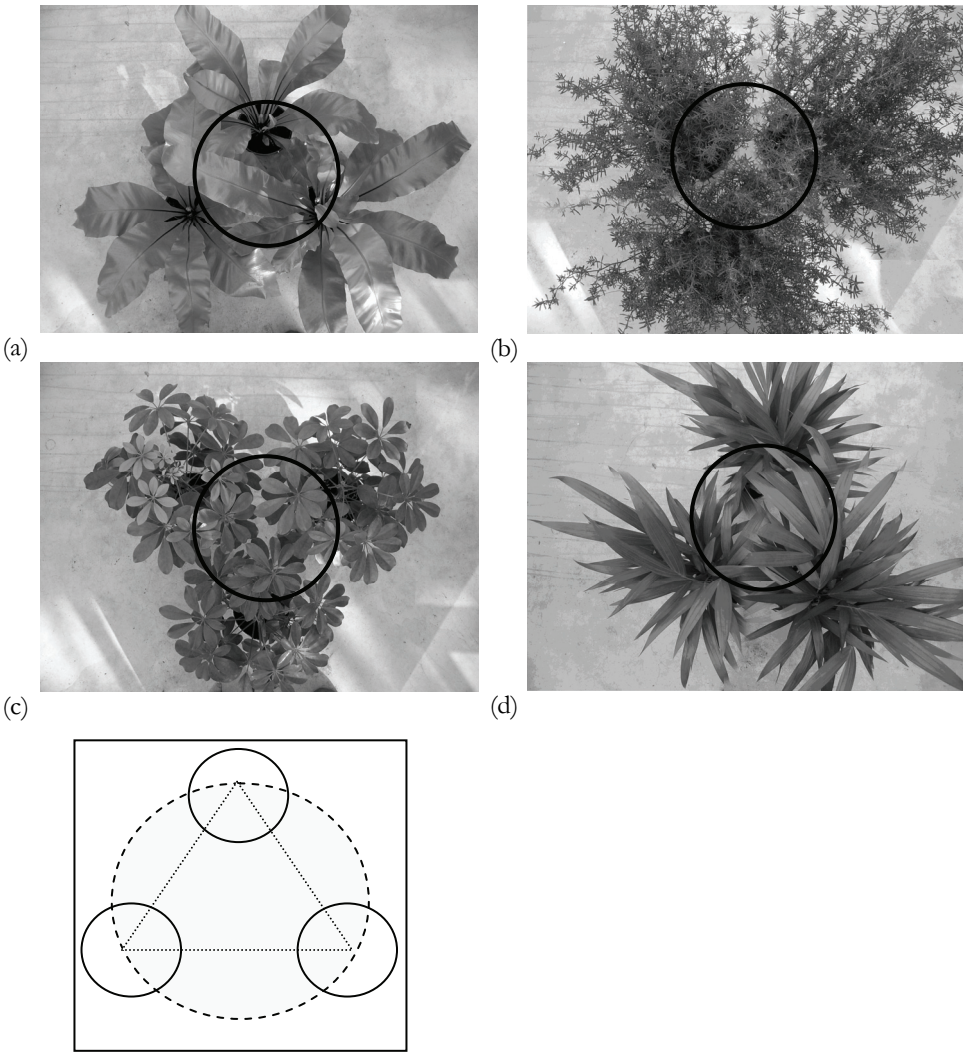

Figure 3.1. The four plant types at maximum coverage: (a) *Asplenium nidus*, (b) *Halimium umbellatum*, (c) *Schefflera arboricola Nora* and (d) *Chrysalidocarpus decipiens*. Black circles indicate approximate FOV at soil level. (e) Schematic representation of the position of the pots in our FOV (dashed circle).

For each LAI level, the spectral measurement began by placing three plants (with the same species and treatment) in their predefined positions in one of the soil beds directly under the sensor and the halogen lamp (235W) positioned at a distance of 90 cm (zenith angle of 30°). The center of the soil bed was made to

coincide with the centers of the light and the sensor's FOV. We made sure that the sensor's FOV was fully covered by the plants. In this manner, we achieved a constant illumination but a variable reflectance as determined by leaf area and differences in leaf shape of the various species. The soil beds were rotated 45° after every spectral measurement in order to average out differences in canopy orientation (BRDF). Next, the plants were moved to the other soil bed to repeat the measurements in the other soil type. The readings were calibrated by means of a white ($BaSO_4$) reference panel (50 cm x 50 cm) of known reflectivity. Reference measurements were taken after every eight target measurements. As the halogen lamp was relatively close to the plants and was not fully collimated, the incoming flux density of the various leaf layers depended on the distance to the light source. Care was given to plant selection, however, so that the investigated plants had more or less the same height (about 45 cm).

#### 3.2.3.2. Leaf

Leaf reflectance spectra were measured on freshly harvested leaves (10 samples from each species having the same chlorophyll treatment). Leaf samples were placed in a non-reflective, black-coated surface (20 cm x 20 cm). The fiber optic, with a FOV of 25°, was placed in a pistol and mounted on an arm of a tripod and placed above the leaf sample at nadir position so that only leaf material was visible. For *Halimium umbellatum* (with tiny linear leaves), the spectral measurements were taken from a thick stacked layer (>8 leaf layers). The spectral measurements were repeated four times and were calibrated against a spectralon reflectance target of known reflectivity. The individual measurements were averaged, resulting in 10 averaged spectra per species with the same chlorophyll treatment. The leaf reflectance measurements were used mainly for illustration purposes.

#### 3.2.3.3. Soil

Spectral measurements of bare (and air-dried) soils were acquired each time before starting the canopy reflectance measurements of one group of species. Mean reflectance spectra associated with the two soil types are shown in Figure 3.2. Soil spectral reflectance varies owing to differences in brightness as well as differences in the absorption features of minerals and organic soil constituents (Baumgardner et al., 1985; Huete, 1989). Figure 3.2 reveals the contrasting overall shapes and brightness levels of the two soils. The two contrasting soils were therefore used as background when measuring each canopy species in order to examine the relative importance of soil background. At the same time, the bare soil reflectance measurements were used to derive the soil line coefficients required for SAVI2, TSAVI and PVI.

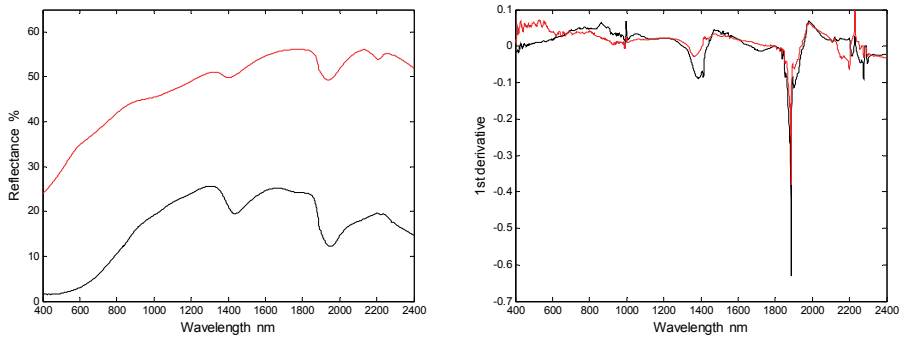


Figure 3.2. Spectral reflectance characteristics of the light (red) and dark (black) soils (left: soil reflectance spectra; right: first derivative of soil reflectance). Each curve represents the average of 64 bare soil reflectance measurements.

## *3.2.4. Methods*

### 3.2.4.1. Preprocessing of spectra

For each canopy realization (plant type x LAI x leaf chlorophyll content x soil type), eight replicate measurements were acquired. These eight replicate measurements were averaged. A moving Savitzky-Golay filter (Savitzky and Golay, 1964) with a frame size of 15 (2nd degree polynomial) was applied to the averaged reflectance spectra to eliminate sensor noise. In total, 95 canopy reflectance measurements were obtained (one outlier had to be removed), of which 48 were made in dark soil and 47 in light soil. For each of the four species, 24 spectral measurements were available (23 for *Asplenium nidus*).

### 3.2.4.2. The narrow-band indices

Narrow-band VIs were computed from the canopy spectra, using all possible two-band wavelength combinations, involving 584 wavelengths between 400 nm and 2400 nm. The most common indices are generally ratio- and soil-based indices that are based on discrete red and near-infrared bands. This is because vegetation reveals distinctive reflectance properties in these bands. Ratio-based VIs are often preferred to soil-based indices as the soil spectral characteristics needed to establish the soil line are often unavailable or are influenced by soil variability (Broge and Mortensen, 2002). The soil line originally defined by Richardson and Wiegand (1977) is a linear relationship between the near-infrared and red reflectance of bare soils and is defined by the slope and intercept of this line. Consequently, the soil line parameters (slope '*a*' and intercept '*b*') were calculated from the pooled soil spectral measurements. We assumed that the soil line concept originally defined for the red and near-infrared feature space could be transferred into other spectral domains (Atzberger, 1997; Schlerf et al., 2005; Thenkabail et al., 2000). The narrow-band indices were systematically calculated for all possible

584x584=341056 wavelength combinations between 400 nm and 2400 nm. Formulas for the various narrow-band vegetation indices (e.g., RVI, NDVI, PVI, TSAVI and SAVI2) are reported in Table 3.2.

Table 3.2. VI formulas used in the study, where $\rho$ denotes reflectance, $\lambda_1$ and $\lambda_2$ are wavelengths, and *a* and *b* are the soil line coefficients between $\lambda_1$ and $\lambda_2$ respectively.

| *Acronym* | *Name* | *VI* | *Eq.* | *Reference* |
|---|---|---|---|---|
| ***RVI*** | Ratio vegetation index | $RVI = \rho_{\lambda 1} / \rho_{\lambda 2}$ | (1) | (Pearson and Miller, 1972) |
| ***NDVI*** | Normalized difference vegetation index | $NDVI = \frac{\rho_{\lambda 1} - \rho_{\lambda 2}}{\rho_{\lambda 1} + \rho_{\lambda 2}}$ | (2) | (Rouse et al., 1974) |
| ***TSAVI*** | Transformed soil- adjusted vegetation index | $TSAVI = \frac{a(\rho_{\lambda 1} - a\rho_{\lambda 2} - b)}{a\rho_{\lambda 1} + \rho_{\lambda 2} - ab}$ | (3) | (Baret et al., 1989) |
| ***SAVI2*** | Second soil-adjusted vegetation index | $SAVI2 = \frac{\rho_{\lambda 1}}{\rho_{\lambda 2} + (b/a)}$ | (4) | (Major et al., 1990) |
| ***PVI*** | Perpendicular vegetation index | $PVI = \frac{\rho_{\lambda 1} - a\rho_{\lambda 2} - b}{\sqrt{1 + a^2}}$ | (5) | (Richardson and Wiegand, 1977) |

### *3.2.5. Regression models*

Regression analysis has been a popular empirical method of linking biophysical variables (such as LAI) to remote sensing data to provide continuous estimates for these variables (Cohen et al., 2003). In most studies, VIs are related to LAI through linear or exponential regression models. Under favorable conditions (i.e., relatively low LAI), VIs can be related to LAI by using linear regression models (Broge and Mortensen, 2002; Chen et al., 2002; Darvishzadeh et al., 2008a; Goel, 1989; Schlerf et al., 2005). At increasing greenness (e.g., higher LAI), however, VIs exhibit decreasing sensitivity to LAI. Studies have shown that this decrease in sensitivity (saturation) may happen at different LAI values, even for the same species (Chen and Cihlar, 1996; Chen et al., 2002; Peterson et al., 1987; Turner et al., 1999). This may indicate that the saturation of VIs by increasing LAI values depends not only on the VI but also on the vegetation species and their associated canopy structures, leaf sizes, etc.

Since in a recent study by Darvishzadeh et al., (2008a), linear regression and exponential relationships have shown to give the same accuracy for LAI estimation (see chapter 2), we chose linear regression to model the relationships between LAI and narrow-band VIs for this study.

### *3.2.6. Validation*

To validate the regression models, a cross-validation procedure (also called the leave-one-out method) was used. In cross-validation, each sample is estimated by the remaining samples. The benefits of the cross-validation method are its aptitude to detect outliers and its ability to provide nearly unbiased estimations of the prediction error (Efron and Gong, 1983; Schlerf et al., 2005). This meant that for each regression variant we developed 48 (analysis based on soil type) and 24 (analysis based on vegetation type) individual models, each time with data from 47 and 23 observations, respectively. The calibration model was then used to predict the observation that was left out. As the predicted samples are not the same as the samples used to build the models, the cross-validated RMSE ($RMSE_{cv}$) was selected as the accuracy indicator of the model in predicting unknown samples.

## 3.3. Results and discussion

### *3.3.1. Variation in spectral reflectance*

Thanks to the experimental setup (i.e., four different plant types, stressed/unstressed plants, dark/light soil and six LAI levels), a wide range of spectral measurements were collected.

At leaf level, reflectance variability at a given wavelength is mainly a function of leaf structure, concentration of biochemicals, and water content (Curran et al., 1992; Fourty et al., 1996; Gates et al., 1965). The measured leaf reflectance spectra and the first derivative of leaf reflectance of the four species are shown in Figures 3.3(a) and 3.3(b) respectively. Their contrasting spectra suppose large differences in their internal leaf structure, concentration of biochemicals, and water content. While their variability in the visible results mainly from differences in absorbing leaf pigments, their variability in the near-infrared results mainly from differences in internal leaf structure (Running et al., 1986).

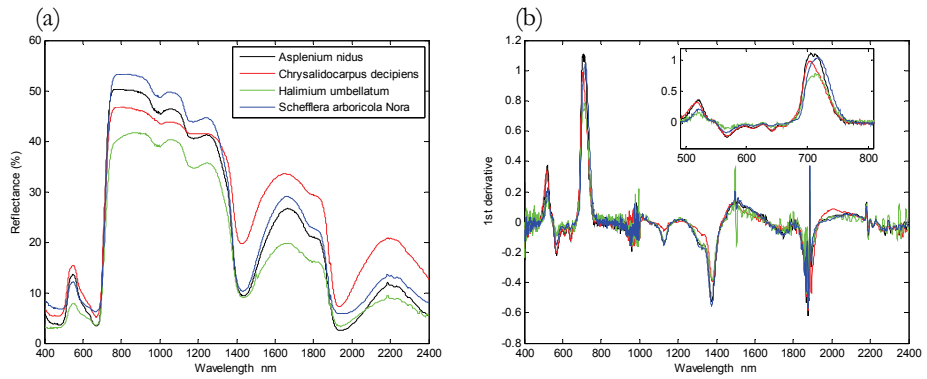


Figure 3.3. Leaf spectral reflectance characteristics of the four species: (a) average spectral reflectance, (b) first derivative of reflectance.

At the canopy level, reflectance variability is due to additional factors such as LAI, canopy architecture and background soil (Gitelson et al., 2003; Jackson and Pinter, 1986). Even with identical soil backgrounds and similar LAI, the four plant species show highly variable reflectance characteristics (Figure 3.4). Plant-specific differences can be seen throughout the investigated spectral range (400 nm to 2400 nm). The observed differences highlight the importance of leaf optical properties, leaf size/shape and leaf angle distribution.

First derivative reflectances of all plant types with an approximate LAI of 1.5 are shown in Figure 3.4(b). The figure clearly shows the variations in the strength and position of major absorption features. As measurements were performed at similar LAI levels and with identical soil backgrounds, the observed variability can be attributed to variations in the optical properties of the foliage (i.e., canopy chlorophyll contents) and differences in canopy architecture (Gitelson et al., 2003).

Comparing Figure 3.3(a) with Figure 3.4(a) reveals that at a low LAI value (LAI=1.5) the leaf properties only partly explain differences in the observed canopy reflectances and are hence underrepresented at a canopy scale (Asner, 1998). The variation that is observed in canopy reflectances in Figure 3.4(a), especially in near-infrared and short wavelength infrared regions, may be explained by differences in canopy architecture (leaf angle distribution and foliage clumping) and their resulting impacts on soil reflectance contribution.

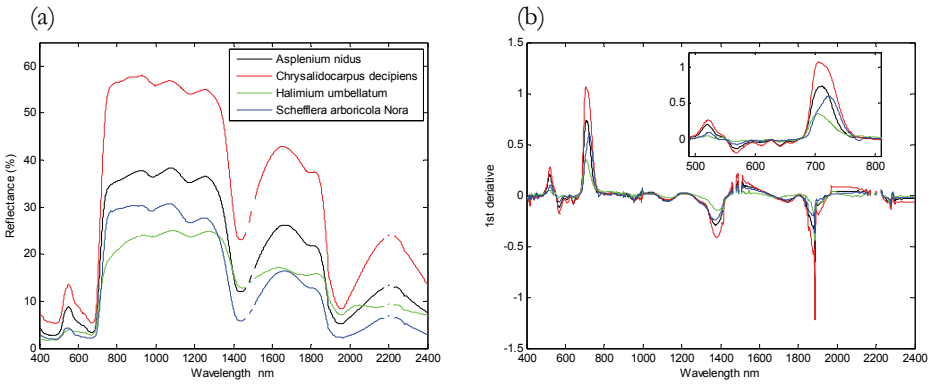


Figure 3.4. Canopy spectral reflectance characteristics of the four plant species over dark soil with an LAI of 1.5: (a) canopy reflectance, (b) the first derivative.

This can be more clearly shown by plotting leaf reflectance against canopy reflectance (Figure 3.5). The scatter plot shows that canopy reflectance is not a simple linear translation of its leaf spectra, but that the relation between leaf and canopy reflectance is modulated by differences in plant architecture/leaf size and leaf transmittance.

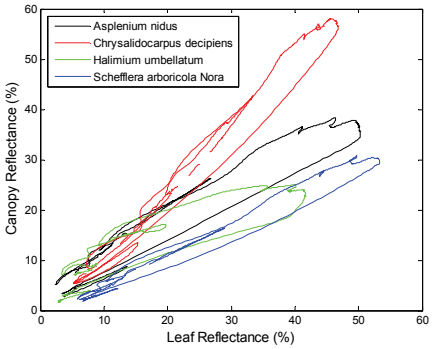


Figure 3.5. Leaf reflectance versus canopy reflectance (LAI=1.5) measured over dark soil. Different (line) colors represent different species.

Figures 3.6(a) and 3.6(b) show the spectral reflectance and the first derivative reflectance of *Asplenium nidus* with an approximate LAI of 1.5 in dark and light soils. In these figures, the observed variation can be explained only by the effect of soil brightness, as all other variables were kept constant. It can be observed from the figure that the highest variations occur in the near-infrared (around 700 nm) and in water-absorption bands (around 1400 nm). Comparison of the first derivatives shows how the difference in reflectance between light and dark soils changes with wavelength. However, soil brightness variations lead essentially to reflectance offsets.

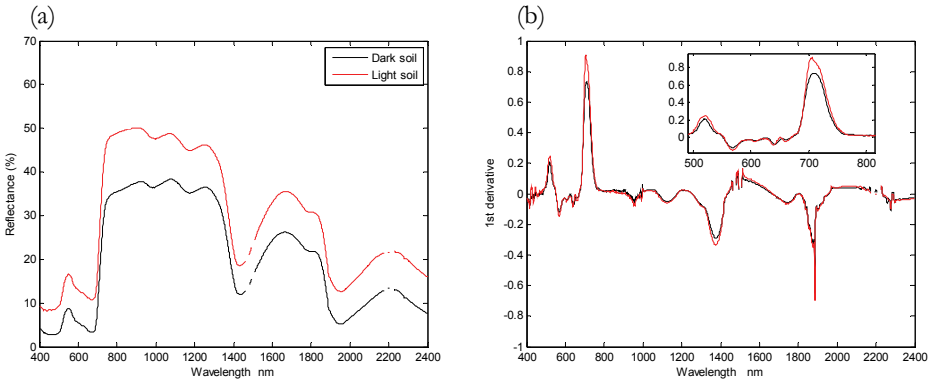


Figure 3.6. Spectral reflectance (a) and first derivative reflectance (b) of *Asplenium nidus* with an LAI of 1.5 in dark and light soils.

### *3.3.2. Relation between LAI and red/near-infrared reflectances*

The influence of LAI of different species on red (680 nm) and near-infrared reflectances (833 nm) (Hurcom and Harrison, 1998; Mutanga and Skidmore, 2004)

is shown in Figures 3.7(a) and 3.7(b) for the four species. Black and red colors are used to distinguish between dark and light soils. In these figures, the sampled species were further separated according to their background soil to evaluate if they behave in the same manner. For the light soil (Figure 3.7(a), red symbols), red reflectance of all species decreases exponentially with LAI. The correlation coefficients are highly significant ($-0.73<r<-0.86$) ($p<0.006$ with a 95% confidence interval), but the predictive ability of these relations is limited to LAI values ≤4 because of the signal saturation for higher LAI values. For the dark soil, canopy reflectance in the red band shows more scattering, and there are no significant relationships between reflectance in this wavelength and LAI for the four species ($-0.11<r<-0.65$) ($p>0.05$). These findings confirm that the spectral contrast between leaves and soil background determines the strength of the LAI-reflectance relationship. The higher the contrast between soil and leaves, the stronger the relationship between LAI and canopy reflectance (Atzberger, 1997).

In the near-infrared band (Figure 3.7(b)), the species show inconsistent behavior. Reflectance is more scattered in light soil than in dark soil. We found a significant correlation between LAI and reflectance for all species ($0.7<r<0.94$) ($p<0.009$), except for *Chrysalidocarpus decipiens*, with correlation coefficients of 0.2 and -0.4 for dark and light soil, respectively.

It is well known that red reflectance decreases with increasing LAI, whereas near-infrared reflectance increases (Huete, 1989). Our findings (Figure 3.7) show that soil brightness strongly affects these relations.

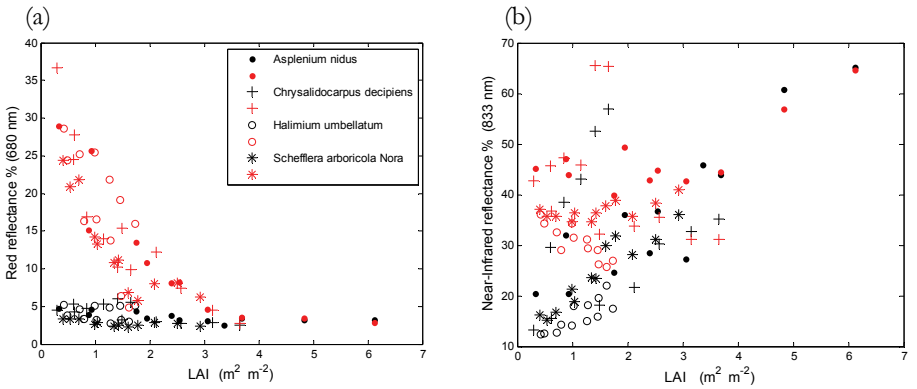


Figure 3.7. Scatter plots showing canopy reflectance and LAI of four plant species measured over two contrasting soil backgrounds: (a) in the red (680 nm) spectral band and (b) in the near-infrared (833 nm) spectral band. The two colors (black and red) correspond to dark and light soil, respectively. Four symbols are used to distinguish between the plant species.

### *3.3.3. LAI versus narrow-band indices*

Narrow-band indices were calculated for the measured canopy reflectance spectra with data sets stratified according to (1) soil type and (2) vegetation species. For all indices (ratio- and soil-based), the optimal narrow-band VI was determined. First, the coefficient of determination ($R^2$) was computed for all possible two-band combinations of VI and LAI. An illustration of these results is shown in the 2-D correlation plots in Figure 3.8. The meeting point of each pair of wavelengths in the 2-D plots corresponds to the $R^2$ value of LAI and the VI calculated from the reflectance values in those two wavelengths.

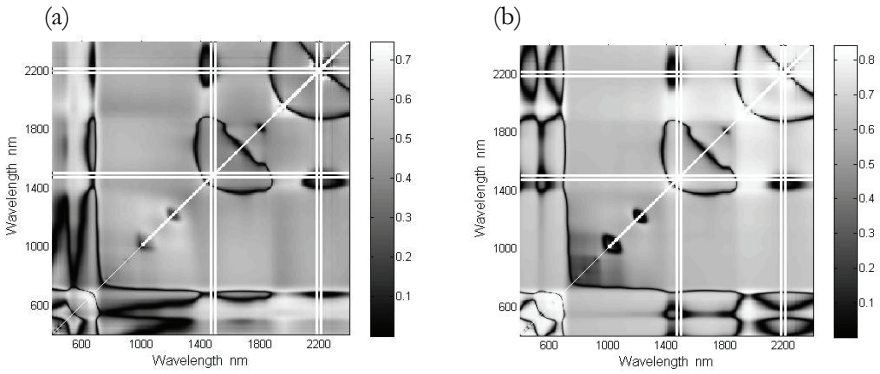


Figure 3.8. 2-D correlation plots illustrating the coefficient of determination ($R^2$) between LAI and narrow-band NDVI in (a) dark soil (n=48) and (b) light soil (n=47). The data for the four plant species have been pooled. The straight (white) lines correspond to wavelengths that have not been measured.

Based on the $R^2$ values in the 2-D correlation plots, the band combinations that formed the best indices for determining LAI were identified. The coefficient of determination ($R^2$) and the band positions of the best performing indices based on the soil types and vegetation species are indicated in Tables 3.3 and 3.4, respectively.

Table 3.3. Band positions and $R^2$ values between LAI and the best narrow-band VI in dark and light soils, with data for the four plant species being pooled.

| ***VI*** | ***Dark soil (n=48)*** | | | ***Light soil (n=47)*** | | |
|---|---|---|---|---|---|---|
| | $R^2$ | $\lambda_1$ | $\lambda_2$ | $R^2$ | $\lambda_1$ | $\lambda_2$ |
| ***RVI*** | 0.77 | 721 | 674 | 0.87 | 741 | 492 |
| ***NDVI*** | 0.75 | 2225 | 2135 | 0.84 | 1955 | 699 |
| ***TSAVI*** | 0.72 | 1955 | 1966 | 0.89 | 1977 | 1955 |
| ***SAVI2*** | 0.77 | 728 | 1966 | 0.89 | 1955 | 1977 |
| ***PVI*** | 0.76 | 1238 | 1041 | 0.73 | 1246 | 1132 |

For the two soil types, all of the five best performing VIs revealed strong correlations ($R^2$>0.7) with LAI (Table 3.3). In general, the correlations were deemed to be stronger for vegetation over light soil than over dark soil. As light soils, compared to dark soils, reflect more radiation attenuated by the leaf layers, the asymptotic reflectance is reached at higher LAI. This may explain the higher sensitivity of light soils compared with that of dark soils, and hence the higher $R^2$ values observed in Table 3.3. As an example, Figure 3.9 shows the relation between narrow-band SAVI2 and LAI for dark and light soils.

Although other studies, such as those of Chen and Cihlar (1996) and Myneni et al. (1997) have shown the nonlinearity of the relationship between VIs and LAI, the relation between SAVI2 and LAI plotted in Figure 3.9 illustrates an almost linear relationship. Even at relatively high LAI values (LAI~6), saturation had not yet occurred. Hence, it appears that by carefully selecting appropriate wavelengths, a relatively high sensitivity of VIs to LAI variations can be maintained, even for high LAI values.

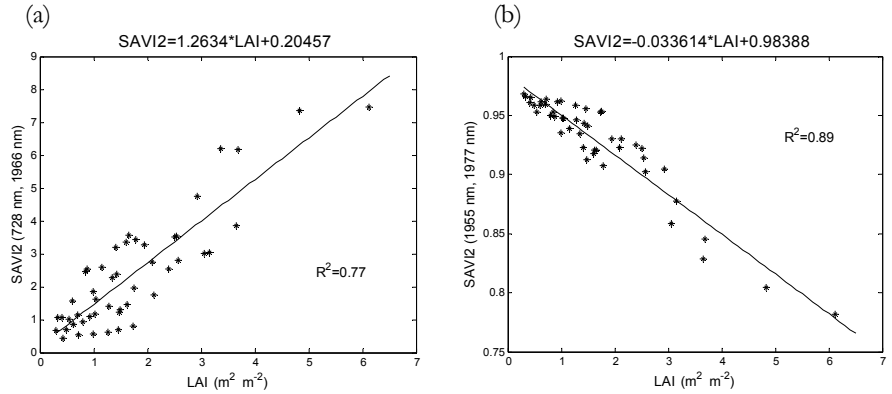


Figure 3.9. Relationships between LAI and best narrow-band SAVI2: (a) in dark soil, (b) in light soil. For the analysis, measurements of the four plant species have been pooled.

The optimal narrow bands forming the best VIs for each soil type are located in different spectral regions. This indicates that the most relevant information for LAI estimation varies with soil type. We also observed that for all VIs (except PVI) larger spectral regions of high correlation between LAI and VI exist in light soil. As the soil surface contributes to the radiation scattered back to the sensor, a higher soil brightness increases VI sensitivity to LAI variations.

In the dark soil, among the five VIs investigated, the narrow-band RVI and SAVI2 showed the highest correlation with LAI, followed by PVI, NDVI and TSAVI. Although many studies have demonstrated that ratio indices such as RVI and NDVI have close relationships with LAI (Broge and Leblanc, 2001; Ridao et al., 1998; Wang et al., 2005), they are known to be sensitive to soil background

effects (Baret and Guyot, 1991; Huete et al., 1985). In the dark soil, however, the effect of the soil is minimized (and its variability reduced), resulting in the ratio indices performing better than the soil line indices under these conditions. However, it also has to be noted that the $R^2$ of all VIs were very close to one another. In the light soil, the narrow-band SAVI2 and TSAVI were the indices with the highest correlation. High correlations were also observed for NDVI and RVI, whereas the PVI performance was much lower. The low PVI performance can be attributed to the small variability that exists in the background reflectance.

Table 3.4. Band positions and maximum $R^2$ values between LAI and narrow-band VIs for different vegetation species. The data for the two contrasting soils have been pooled.

| ***VI*** | ***Asplenium nidus (n=23)*** | | | ***Chrysalidocarpus decipiens (n=24)*** | | | ***Halimium umbellatum (n=24)*** | | | ***Schefflera arboricola Nora (n=24)*** | | |
|---|---|---|---|---|---|---|---|---|---|---|---|---|
| | $R^2$ | $\lambda_1$ | $\lambda_2$ | $R^2$ | $\lambda_1$ | $\lambda_2$ | $R^2$ | $\lambda_1$ | $\lambda_2$ | $R^2$ | $\lambda_1$ | $\lambda_2$ |
| ***RVI*** | 0.90 | 846 | 1410 | 0.77 | 1314 | 1322 | 0.76 | 2205 | 1885 | 0.89 | 727 | 1410 |
| ***NDVI*** | 0.89 | 1487 | 1410 | 0.77 | 1322 | 1314 | 0.74 | 2205 | 1885 | 0.85 | 1114 | 1105 |
| ***TSAVI*** | 0.88 | 1487 | 1410 | 0.78 | 1322 | 1314 | 0.75 | 2196 | 1885 | 0.87 | 1955 | 709 |
| ***SAVI2*** | 0.91 | 875 | 1418 | 0.78 | 1314 | 1322 | 0.75 | 1885 | 2196 | 0.89 | 719 | 2020 |
| ***PVI*** | 0.91 | 1280 | 1255 | 0.89 | 716 | 1723 | 0.90 | 2205 | 1875 | 0.96 | 713 | 1723 |

With data stratified according to plant species, $R^2$ values between narrow-band VI and LAI show high variability (Table 3.4). In general, the highest correlations were observed for *Asplenium nidus* and *Schefflera arboricola* ($R^2$~0.9), whereas *Chrysalidocarpus decipiens* and *Halimium umbellatum* gave poorer correlations ($R^2$~0.8). The leaf orientation of the first two species is more planophile than that of the last two species, which would explain the observed differences. Under otherwise identical conditions, a more planophile leaf displacement reduces soil background influences. However, it should also be noted that the range in LAI (between minimum and maximum LAI; see Table 3.1) differs among plant species. Under such circumstances, the $R^2$ may be biased by the larger range of *Asplenium nidus* and *Schefflera arboricola* compared with that of *Chrysalidocarpus decipiens* and *Halimium umbellatum*.

For most plant species, the selected optimum narrow bands are identical or very close to one another. This was further investigated by studying the 2-D correlation plots. For each species, regions with high correlations ($R^2 \geq 0.7$) between narrow-band VI and LAI are highlighted (Figure 3.10). We found that for

each plant species the optimum spectral region (band combinations) were similar across the investigated VIs. This confirms that the different VIs are closely related to one another (Lawrence and Ripple, 1998; Perry and Lautenschlager, 1984) and do not really provide independent information. Only PVI shows a distinctly different behavior, with generally higher $R^2$ values and wavelengths different from those of the four other VIs (Table 3.4 and Figure 3.10). As the data have been pooled across the two soil backgrounds, PVI seems best adapted to minimize soil background influences.

### *3.3.4. Cross-validated LAI estimates from narrow-band VI*

The accuracy with which the LAI can be estimated from the various VIs (see Tables 3.3 and 3.4) was assessed in a cross-validation procedure. The results are recorded in Tables 3.5 and 3.6.

Table 3.5. Cross-validated $R^2$ and RMSE for estimating LAI in dark and light soils. The $RMSE_{cv}$ is in units of LAI [$m^2\ m^{-2}$]. For each soil background, the data for the four plant species have been pooled. Refer to Table 3.3 for the wavelengths of the so-called optimum bands.

| *VI* | *Dark soil (n=48)* | | *Light soil (n=47)* | |
|---|---|---|---|---|
| | $R^2_{cv}$ | $RMSE_{cv}$ | $R^2_{cv}$ | $RMSE_{cv}$ |
| ***RVI*** | 0.73 | 0.63 | 0.86 | 0.45 |
| ***NDVI*** | 0.71 | 0.65 | 0.81 | 0.52 |
| ***SAVI2*** | 0.74 | 0.62 | 0.88 | 0.42 |
| ***TSAVI*** | 0.68 | 0.69 | 0.88 | 0.42 |
| ***PVI*** | 0.73 | 0.63 | 0.69 | 0.67 |

Compared with canopy reflectance measurements over dark soil, LAI over light soil was generally estimated with higher accuracy (Table 3.5). For light soil, the cross-validated RMSE varies around 0.45 ($m^2\ m^{-2}$) (except PVI), whereas the same indicator is around 0.60 for dark soil. This confirms the findings of §3.3.3, where VIs showed a better correlation with LAI over light soil than over dark soil (e.g., Table 3.3). Within each soil type, differences among the five VIs are generally quite small, except for PVI measured over light soil. This clearly confirms the findings of Baret et al. (1989), Huete (1989) and Roujean and Breon (1995), who noticed that not only ratio-based indices but also soil-based VIs are sensitive to soil brightness effects. It also confirms previous studies by Baret and Guyot (1991) and Broge and Leblanc (2001), who showed that these indices are sensitive to soil brightness effects.

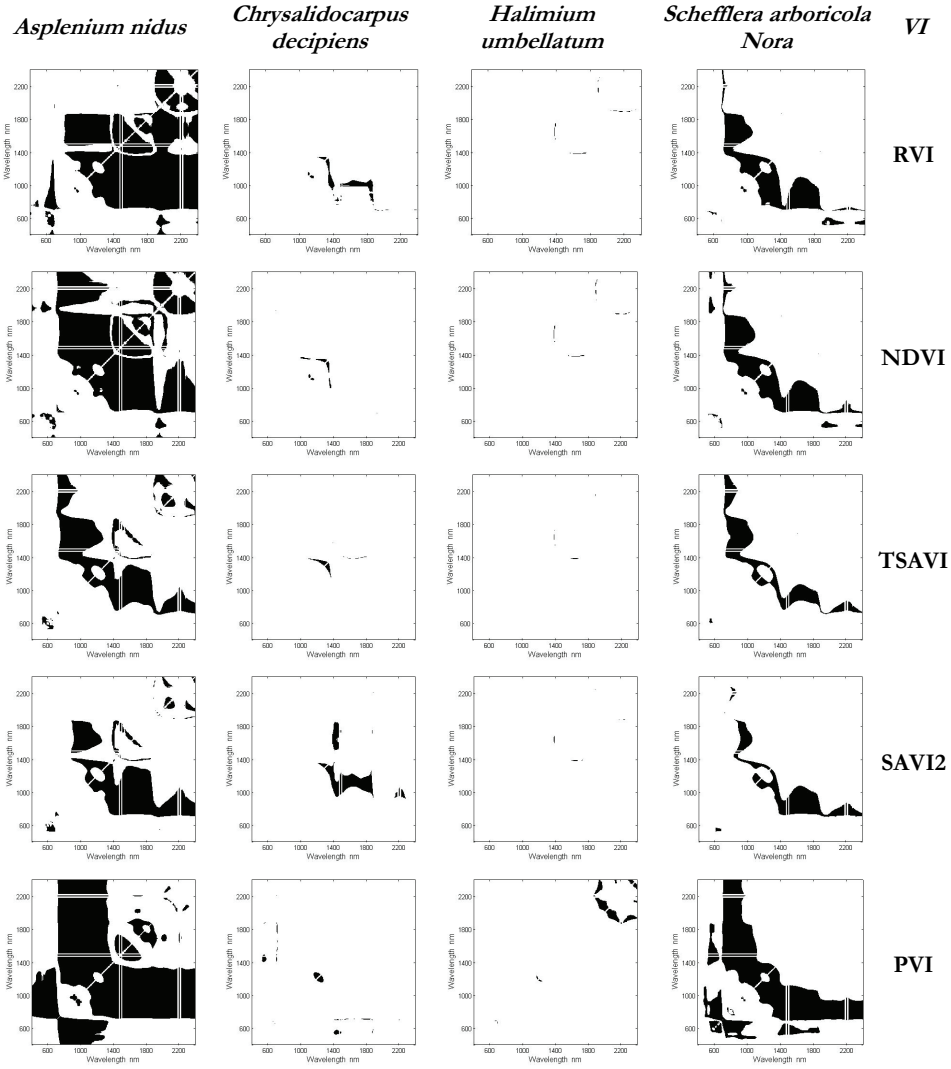


Figure 3.10. Regions with high correlation ($R^2 \geq 0.7$) between narrow-band vegetation indices (VIs) and LAI for each vegetation species.

For this reason, it seems difficult to define the most appropriate VI for estimating LAI in each soil type. Given the cross-validated results reported in Table 3.5, we conclude that for data analyzed by soil type, the narrow-band RVI (Pearson and Miller, 1972) and SAVI2 (Major et al., 1990) are the best overall choices as LAI estimators. This result is in agreement with those of Broge and Leblanc (2001), who used simulated data and found that SAVI2 is relatively insensitive to external factors such as background effects, and RVI is marginally the best VI at low LAI values.

For data stratified according to plant species, Table 3.6 demonstrates relatively accurate estimations of LAI. Cross-validated RMSE were in the range 0.15 to 0.60 $m^2$ $m^{-2}$. These relationships were observed to be dependent on plant species and their associated architectures. This is in agreement with other studies by Colombo et al. (2003), Lee et al. (2004) and Turner et al. (1999), who found that the strength of the relationships between VI and LAI differs for different vegetation species.

The highest accuracies are found for *Halimium umbellatum* and *Schefflera arboricola* ($RMSE_{cv}$~0.25), whereas *Asplenium nidus* and *Chrysalidocarpus decipiens* showed lower accuracies ($RMSE_{cv}$~0.55). This indicates that LAI estimates of plants with small and more randomly distributed leaves produce higher estimation accuracies, probably an effect of reduced mutual shading of leaf elements.

Analysis of Table 3.6 reveals that the variation among the narrow-band VIs, except narrow-band PVI, is only small. Among the five narrow-band VIs studied here, PVI (Richardson and Wiegand, 1977) shows the most significant relationship with LAI for all vegetation species ($0.15 \leq RMSE_{cv} \leq 0.56$). PVI appears to be adaptable to different plant species with different plant architectures, leaf sizes, etc., while effectively reducing soil brightness effects. According to Table 3.6, we rank narrow-band PVI as the most appropriate VI for LAI estimation. However this result contradict with the result of a study by Wu et al., (2007), who found that PVI is not as effective as other indices such as SAVI (soil adjusted vegetation index) and MSAVI (modified soil adjusted vegetation index) in estimating leaf area index of corn and potato canopies because of its narrow dynamic range. In our study, however, the SAVI and MSAVI returned a similar results as SAVI2 with LAI (e.g. for SAVI, $R^2$= 0.73 and 0.87 for dark and light soil, respectively) (not shown).

Table 3.6. Cross-validated $R^2$ and RMSE for estimating LAI of different vegetation species. The $RMSE_{cv}$ are in units of LAI [$m^2$ $m^{-2}$]. For each plant species, data for the two soil backgrounds have been pooled. Refer to Table 3.4 for the corresponding wavelengths.

| ***VI*** | ***Asplenium nidus (n=23)*** | | ***Chrysalidocarpus decipiens (n=24)*** | | ***Halimium umbellatum (n=24)*** | | ***Schefflera arboricola Nora (n=24)*** | |
|---|---|---|---|---|---|---|---|---|
| | $R^2_{cv}$ | $RMSE_{cv}$ | $R^2_{cv}$ | $RMSE_{cv}$ | $R^2_{cv}$ | $RMSE_{cv}$ | $R^2_{cv}$ | $RMSE_{cv}$ |
| ***RVI*** | 0.88 | 0.60 | 0.74 | 0.53 | 0.72 | 0.23 | 0.87 | 0.28 |
| ***NDVI*** | 0.87 | 0.62 | 0.74 | 0.54 | 0.70 | 0.24 | 0.82 | 0.33 |
| ***SAVI2*** | 0.89 | 0.57 | 0.76 | 0.51 | 0.70 | 0.24 | 0.87 | 0.29 |
| ***TSAVI*** | 0.86 | 0.65 | 0.76 | 0.51 | 0.70 | 0.24 | 0.85 | 0.30 |
| ***PVI*** | 0.89 | 0.56 | 0.88 | 0.35 | 0.88 | 0.15 | 0.95 | 0.17 |

Figure 3.11 illustrates the relationship between estimated and measured LAI for the four plant species when using PVI. The relations seem highly linear, except in the case of *Chrysalidocarpus decipiens*, where we observe a slight saturation tendency.

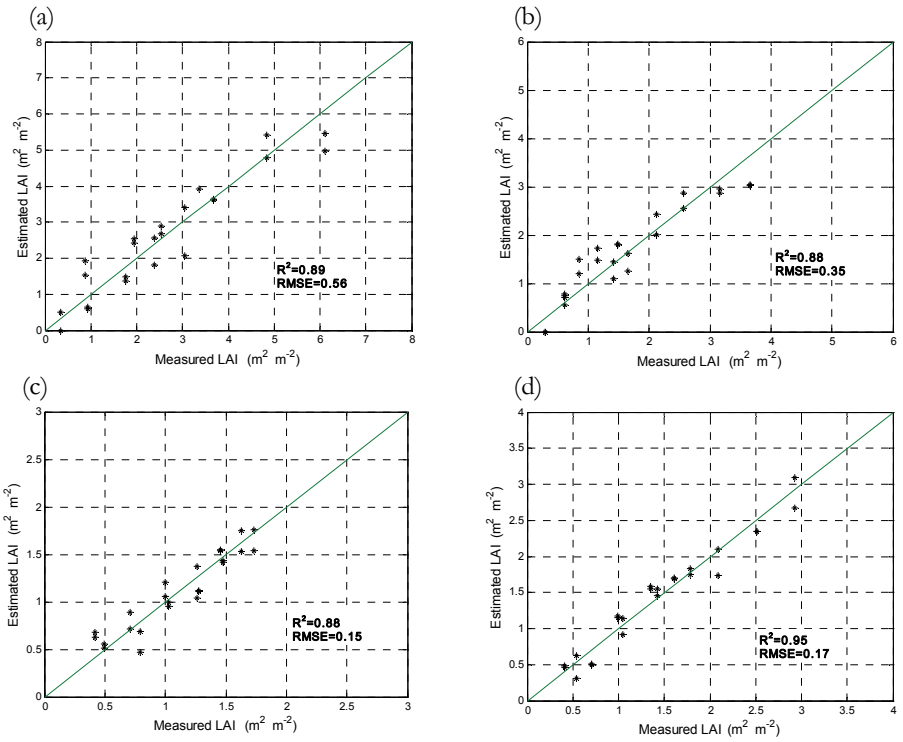


Figure 3.11. Cross-validated estimated LAI versus measured LAI using narrow-band PVI: (a) *Asplenium nidus,* (b) *Chrysalidocarpus decipiens*, (c) *Halimium umbellatum*, and (d) *Schefflera arboricola Nora.* For the analysis, measurements performed over dark and light soils have been pooled. The optimum wavebands are reported in Table 3.4.

The results reported in this paper are derived from measurements in a controlled laboratory experiment. Usually, the methods developed in the laboratory for the estimation of vegetation parameters from remote sensing have had limited success when applied under outside or field conditions. This is mainly caused by scale effects and by additional difficulties for example related to the presence of atmospheric absorption and scattering effects. Despite our efforts, however, the measured data are not completely free of noise (e.g., related to the sensor and illumination system). Likewise, we are aware that the not fully collimated light source limits the applicability of our data set as the different leaf layers received different amounts of energy. However, care was taken to ensure identical plant heights and hence to provide a certain comparability among species. The laboratory experiment did not allow us to create extended canopies. Hence, lateral fluxes can not be ignored, although measurements have been performed in a completely dark (and black-painted) environment. In future work, the number of

plants in the scenario should be increased to ensure that the reflected flux fully represents an infinitely extended canopy. Likewise, a more extensive range of vegetation species and soil types should be studied in order to further confirm the effects of these factors on the relationship between biophysical variables and narrow-band VIs. Replicate measurements may be required to generalize the obtained relationships.

## 3.4. Conclusions

Based on a laboratory experiment, this paper examined whether the estimation of LAI from hyperspectral (narrow-band) VIs is significantly affected by soil type and/or plant species with different leaf sizes and architectures.

The LAI data were compared with red and near-infrared reflectance in dark and light soils, and this confirmed that the spectral contrast between leaves and soil background determines the strength of the LAI-reflectance relationship. In general, the relationship between LAI and VIs was deemed to be stronger in light soil than in dark. It seemed difficult to define the most appropriate VI for estimating LAI in each soil type. However, the cross-validated results revealed that for data analyzed by soil type the narrow-band RVI and SAVI2 were the best overall choices as LAI estimators. In other words, these two indices were the least affected by differences related to the four plant species. The study confirmed that the strength of the relationships between VIs and LAI differs for different vegetation species. PVI appears to be less sensitive to brightness variations in the soil background and adapts well to different plant species with different plant architectures, leaf sizes, etc. This index was thus recognized as the most appropriate VI for LAI estimation under conditions of unknown soil reflectance. Furthermore, the study verified that, for all plant species and the soil types studied, linear relationships exist between LAI and the selected narrow-band indices; however, this should be understood as valid only within the LAI range and conditions measured in the present study.

Our results suggest that, when using remote sensing VIs for estimating vegetation LAI, not only the choice of VIs but also prior knowledge of plant architecture and the background soil of the investigated vegetation is of particular importance.

## Acknowledgements

We would like to thank the UNIFARM experimental station at Wageningen University for providing facilities for the experiment. We appreciate the help of Mr. Jelger Kooistra and Mr. Boudewijn de Smeth for providing laboratory facilities. Furthermore, we would like to acknowledge the assistance of Dr. Martin Schlerf for reading an early version of the manuscript and providing valuable

comments. We extend our gratitude to Prof. Alfred Stein for his valuable comments on the final form of the manuscript.

# Chapter Four

# Field level

## LAI and chlorophyll estimated for a heterogeneous grassland using hyperspectral measurements

*This chapter is based on:*

Darvishzadeh, R., Skidmore, A.K., Schlerf, M., Atzberger, C., Corsi, F. and Cho, M.A., 2008. LAI and chlorophyll estimated for a heterogeneous grassland using hyperspectral measurements. *ISPRS Journal of Photogrammetry and Remote Sensing*, **In Press,** DOI: 10.1016/j.isprsjprs.2008.01.001.

## Abstract

The study shows that leaf area index (LAI), leaf chlorophyll content and canopy chlorophyll content can be mapped in a heterogeneous Mediterranean grassland from canopy spectral reflectance measurements. Canopy spectral measurements were made in the field using a GER 3700 spectroradiometer, along with concomitant *in situ* measurements of LAI and leaf chlorophyll content. We tested the utility of univariate techniques, involving narrow band vegetation indices and the red edge inflection point, as well as multivariate calibration techniques, including stepwise multiple linear regression and partial least squares regression. Among the various investigated models, canopy chlorophyll content was estimated with the highest accuracy ($R^2_{cv}$ = 0.74, relative $RMSE_{cv}$ = 0.35). All methods failed to estimate leaf chlorophyll content ($R^2_{cv}$ <= 0.40), while LAI was estimated with intermediate accuracy ($R^2_{cv}$ = 0.67). Compared with narrow band indices and red edge inflection point, stepwise multiple linear regression generally improved the estimation of LAI. The estimations were further improved when partial least squares regression was used. When a subset of wavelengths was analyzed, it was found that partial least squares regression had reduced the error in the retrieved parameters. The results of the study highlight the significance of using multivariate techniques such as partial least squares regression rather than univariate methods such as vegetation indices for providing enhanced estimates of heterogeneous grass canopy characteristics. To date, partial least squares regression has seldom been applied for studying heterogeneous grassland canopies. However, it can provide a useful exploratory and predictive tool for mapping and monitoring heterogeneous grasslands.

## 4.1. Introduction

Owing to its fast, non-destructive and relatively cheap characterization of land surfaces, remote sensing has been recognized as a reliable method for estimating various biophysical and biochemical vegetation variables (Cohen et al., 2003; Curran et al., 2001; Hansen and Schjoerring, 2003; Hinzman et al., 1986; McMurtrey et al., 1994; Weiss and Baret, 1999). Hyperspectral remote sensing with narrow and continuous spectral bands that provide an almost continuous spectrum is considered more sensitive to specific vegetation variables such as leaf area index (LAI) (Hansen and Schjoerring, 2003). Because of the role of green leaves in controlling many biological and physical processes of plant canopies, LAI (the total one-sided leaf area per ground surface area) is a key structural characteristic of vegetation and thus widely used as an indicator of vegetation status.

LAI has been estimated in numerous studies by using remote sensing in either statistical approaches or physically based (canopy reflectance) models. Many of the previous studies, however, are based on simulated data (Atzberger, 2004; Broge and Leblanc, 2001; Chaurasia and Dadhwal, 2004; Haboudane et al., 2004;

Udelhoven et al., 2000), on agricultural crops (Atzberger, 1995; Atzberger, 1997; Baret et al., 1987; Broge and Mortensen, 2002; Colombo et al., 2003; Danson et al., 2003; Jacquemoud et al., 2000; Walter-Shea et al., 1997; Weiss et al., 2001) or on forest (Chen et al., 1997; Fang et al., 2003; Gemmell et al., 2002; Kalacska et al., 2004; Kovacs et al., 2004; Running et al., 1986; Schlerf and Atzberger, 2006; White et al., 1997), where single species was investigated. Therefore, investigation is required to assess the capability of remote sensing models when it comes to natural heterogeneous canopies with a combination of different plant species in varying proportions. Mediterranean grasslands are characterized by highly heterogeneous canopies, and present a challenge for remote sensing applications because the reflectance is often a mixture of different surface materials (Fisher, 1997; Roder et al., 2007).

On the other hand, researchers have shown that narrow band vegetation indices can be crucial in providing essential information for quantifying the biochemical (Broge and Leblanc, 2001; Ferwerda et al., 2005; Gamon et al., 1992; Gitelson and Merzlyak, 1997; Mutanga et al., 2005) and biophysical characteristics of vegetation (Blackburn, 1998; Elvidge and Chen, 1995; Gong et al., 1992; Lee et al., 2004; Mutanga and Skidmore, 2004; Schlerf et al., 2005). In this case, a limited number of spectral wavelengths from the massive spectral contents of hyperspectral data are used. On the contrary, several studies have focused on statistical techniques such as stepwise multiple linear regression (SMLR), which make use of the spectral information of several spectral wavelengths to estimate vegetation biochemical properties (e.g. Curran, 1989; Curran et al., 2001; Grossman et al., 1996; Huang et al., 2004; Kokaly and Clark, 1999) and biophysical properties (e.g. Atzberger et al., 2003b; De Jong et al., 2003; Lefsky et al., 1999; Lefsky et al., 2001). In either case, the use of hyperspectral data sets is influenced by multicollinearity (De Jong et al., 2003), which mostly occurs when the number of observations is smaller than the number of wavelengths studied and when input (reflectance) data show high correlation (Curran, 1989; Curran et al., 2001; Nguyen and Lee, 2006). Partial least squares regression (PLSR) is widely used in chemometrics (Feudale and Brown, 2005; Geladi and Kowalski, 1986). The method is known to be suitable for analyzing multicollinear spectral data sets (Atzberger et al., 2003b). PLSR is a "full spectrum" method and, unlike SMLR, it uses all available spectral wavelengths simultaneously. There are a few studies that have investigated the potential of PLSR for estimating vegetation biochemical properties (El Masry et al., 2007; Hansen and Schjoerring, 2003; Huang et al., 2004; Nguyen and Lee, 2006) and biophysical properties (Atzberger et al., 2003b; Cho et al., 2007; Hansen and Schjoerring, 2003; Naesset et al., 2005). However, the estimation of canopy characteristics such as LAI and canopy/leaf chlorophyll content for heterogeneous grass canopies has not to our knowledge been addressed by researchers, and still remains to be examined.

For the above noted reasons, the aim of this study was to examine the utility of hyperspectral remote sensing in predicting canopy characteristics such as LAI and

canopy/leaf chlorophyll content in a heterogeneous Mediterranean grassland by means of different univariate and multivariate methods. We compared narrow band vegetation indices, including red edge inflection point (REIP), with two important linear statistical methods known to be well suited for dealing with highly multicollinear data sets: partial least squares regression and stepwise multiple linear regression. The suitability of these different methods will be analyzed in terms of their prediction accuracy. Naturally, the significance of the results is valid only for Mediterranean grasslands and the biophysical variables considered. The study is based on canopy spectral reflectance measured in a heterogeneous grassland during a field campaign in the summer of 2005 in Majella National Park, Italy.

## 4.2. Methods

### *4.2.1. Study area and sampling*

The study site is located in Majella National Park, Italy (latitude 41°52' to 42°14' N, longitude 13°14' to 13° 50'E). The park covers an area of 74,095 ha and extends into the southern part of Abruzzo, at a distance of 40 km from the Adriatic Sea (Figure 4.1). The region is situated in the massifs of the Apennines. The park is characterized by several mountain peaks, the highest being Mount Amaro (2794 m).

Abandoned settlement and agricultural areas in Majella are returning to oak (*Quercus pubescens*) woodlands at the lower altitudes (400 m to 600 m) and beech (*Fagus sylvatica*) forests at the higher altitudes (1200 m to 1800 m). Between these two formations is a landscape composed of shrubby bushes, patches of grass/herb vegetation, and bare rock outcrops. The dominant grass and herb species include *Brachypodium genuense, Briza media, Bromus erectus, Festuca sp, Helichrysum italicum, Galium verum, Trifolium pratense, Plantago lanceolata, Sanguisorba officinalis* and *Ononis spinosa* (Cho, 2007).

Stratified random sampling with clustering was adopted in this study. For this purpose, the area was stratified into grassland, forest, shrubland and bare rock outcrops, using the land cover map provided by the management of Majella National Park. We can distinguish four main phytosociological classes of varying area within the grasslands: semi-natural/farmlands, grazed/periodically flooded areas, open garrigues and abandoned farmlands. Coordinates (x y) were randomly generated in a grassland stratum to select plots. A total of 45 plots (30 m x 30 m) were generated and a GPS (Global Positioning System) was used to locate them in the field. To increase the number of samples in the time available, four to five randomly selected subplots were clustered within each plot. This resulted in a total of 191 subplots being sampled. The 1 m x 1 m subplots differed in species composition and relative abundance while the within-subplot variability was small.

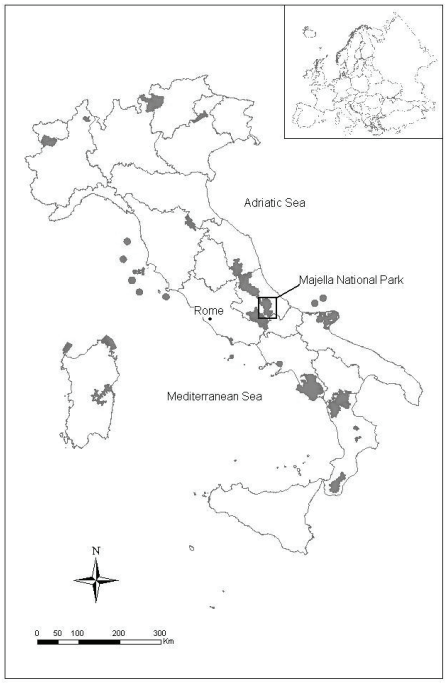


Figure 4.1. The study area, Majella National Park, Italy.

### *4.2.2. Canopy spectral measurements*

Fifteen replicates of canopy spectral measurements were taken from each subplot, using a GER 3700 spectroradiometer (Geophysical and Environmental Research Corporation, Buffalo, New York). The wavelength range is 350 nm to 2500 nm, with a spectral sampling of 1.5 nm in the 350 nm to 1050 nm range, 6.2 nm in the 1050 nm to 1900 nm range, and 9.5 nm in the 1900 nm to 2500 nm range.

The fiber optic, with a field view of 25°, was handheld approximately 1 m above the ground at nadir position. The ground area observed by the sensor of GER had a diameter of 45 cm and was large enough to cover the center of the subplots without being influenced by the surroundings. The 15 replicate spectral measurements taken from each subplot enabled to suppress much of the measurement noise by averaging the replicate measurements. Prior to each reflectance measurement, the radiance of a white standard panel coated with $BaSO_4$ and of known reflectivity was recorded for normalization of the target measurements. The fieldwork was conducted between June 15 and July 15 in 2005. To minimize atmospheric perturbations and BRDF effects, spectral measurements were made on clear sunny days between 11:30 a.m. and 2:00 p.m. The measurement set-up ensured that the ratio of direct to diffuse incoming solar

radiation was approximately constant. Hence, no correction for this possibly perturbing factor has been applied.

### *4.2.3. LAI measurements*

In each subplot, LAI was non-destructively measured using a widely used optical instrument, the Plant Canopy Analyzer LAI-2000 (LICOR Inc., Lincoln, NE, USA). A detailed description of this instrument is given by LI-COR (1992) and Welles and Norman (1991). The LAI-2000 measures the gap fraction in five zenith angles (0° to 13°, 16° to 28°, 32° to 43°, 47° to 58° and 61° to 74°), using measurements of incoming (diffuse) solar radiation above and below the canopy. The measured gap fraction data are inverted to obtain the effective LAI, under the assumption of a random spatial distribution of leaves (Chen et al., 2002). Effective LAI signifies the equivalent leaf area of a canopy with a random leaf distribution to generate the same light interception as the true LAI (Fernandes et al., 2002). However, some factors such as foliage clumping, sky conditions and plant phenology affect LAI estimates (Fournier et al., 2003). In this study, measurements were taken either under clear skies with low solar elevation (i.e., within the two hours following sunrise or preceding sunset) or under overcast conditions. The LAI measurements were taken on the same day that the canopy spectral measurements were made. To prevent direct sunlight on the sensor of LAI-2000, samples of below- and above-canopy radiation were made in the direction facing away from the sun (i.e., with the sun behind the operator), using a view restrictor of 45°. For each subplot, reference samples of above-canopy radiation were determined by measuring incoming radiation above the grass subplot (in an open area). Next, five below-canopy samples were collected and used to calculate the average LAI (Table 4.1).

LAI measured using the LAI-2000 corresponds to plant area index (PAI), including the photosynthetic and non-photosynthetic components (Chen et al., 1997). In our study, non-photosynthetic components were almost non-existent. Despite the non-random distribution of grass leaves, no corrections for clumping were applied. Therefore, the LAI used here corresponds to the effective PAI, and in the following sections these measurements are abbreviated as LAI.

### *4.2.4. Chlorophyll measurements*

A SPAD-502 Leaf Chlorophyll Meter (Minolta, Inc.) was used to assess the leaf chlorophyll content (LCC) in each 1 m x 1 m subplot. The chlorophyll meter (SPAD) provides a simple, quick, non-destructive method for estimating leaf chlorophyll content (Watanabe et al., 1980). SPAD values express relative amounts of chlorophyll in leaves by measuring transmittance in the red (650 nm) and NIR (920 nm) wavelength regions (Minolta, 2003). The ability to predict chlorophyll content from SPAD readings has been demonstrated in several studies (Dwyer et

al., 1991; Markwell et al., 1995; Takebe et al., 1990; Vos and Bom, 1993; Yang et al., 2003). SPAD measurements give a unit-less but highly reproducible measure that is well correlated with leaf chlorophyll concentration and is commonly used to characterize chlorophyll concentration in many plant species (Atzberger et al., 2003a; Atzberger et al., 2003b; Campbell et al., 1990; Dingkuhn et al., 1998; Haboudane et al., 2002; Jongschaap and Booij, 2004; Nakano et al., 2006). A total of 30 leaves representing the dominant species were randomly selected in each subplot, and their SPAD readings were recorded. From the 30 individual SPAD measurements, the average was calculated (Table 4.1). These averaged SPAD readings were converted into leaf chlorophyll content (units: $\mu g\ cm^{-2}$) by means of an empirical calibration function provided by Markwell et al. (1995). The total canopy chlorophyll content (CCC; units: $g\ m^{-2}$) for each subplot was obtained by multiplying the leaf chlorophyll content by the corresponding LAI (CCC = LAI * LCC).

Table 4.1. Summary statistics of the measured biophysical and biochemical variables of grassland sample subplots (n=191). SPAD is the average SPAD reading for 30 randomly selected leaves in each subplot; LCC is the leaf chlorophyll content; and CCC is the canopy chlorophyll content.

| *Measured variables* | *No. of Obs.* | *Min* | *Mean* | *Max* | *StDev* | *Range* | *Variation coefficient* |
|---|---|---|---|---|---|---|---|
| ***LAI ($m^2\ m^{-2}$)*** | 191 | 0.39 | 2.76 | 7.34 | 1.50 | 6.95 | 0.54 |
| ***SPAD (unit-less)*** | 185* | 22.4 | 32.70 | 45 | 4.35 | 22.6 | 0.13 |
| ***LCC ($\mu g\ cm^{-2}$)*** | 185 | 17.1 | 30.07 | 49.66 | 6.12 | 32.55 | 0.20 |
| ***CCC ($g\ m^{-2}$)*** | 185 | 0.1 | 0.87 | 2.7 | 0.55 | 2.56 | 0.63 |

* Six measurements were recognized as outliers and were excluded.

## *4.2.5. Data analysis*

### 4.2.5.1. Preprocessing of spectra

To minimize noise in the measured reflectance spectra, the 15 spectra of each sample subplot were averaged. Bands below 400 nm and above 2400 nm displayed very high levels of noise and were excluded. The resulting 584 wavebands were used for analysis. A moving Savitzky-Golay filter (Savitzky and Golay, 1964) with a frame size of 15 data points (2nd degree polynomial) was applied to the averaged reflectance spectra to further smooth the spectra. The analysis and processing were carried out using MATLAB 7.1 (Mathwork, Inc). In total, 191 canopy reflectance measurements were obtained. The average reflectance spectra of all grass subplots and the spectral variability of the measurements are shown in Figure 4.2.

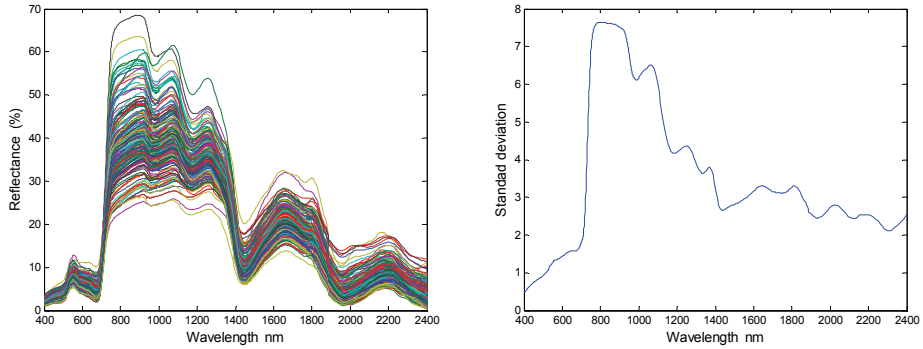


Figure 4.2. The averaged canopy reflectance spectra of all sample subplots (n=191) (left), and their spectral variability (n=191) (right) in Majella National Park, Italy.

#### 4.2.5.2. The narrow band indices

Narrow band vegetation indices were computed from the canopy spectra using all possible two-band combinations, involving 584 wavelengths between 400 nm and 2400 nm. The most common indices are ratio indices and soil-based indices based on discrete red and NIR bands where vegetation reveals distinctive reflectance properties. Ratio-based vegetation indices are often preferred to soil-based indices as the soil spectral characteristics needed to establish the soil line are often unavailable or are influenced by soil variability (Broge and Mortensen, 2002). The soil line originally defined by Richardson and Wiegand (1977) is a linear relationship between the NIR and red reflectance of bare soils, and is defined by the slope and intercept of this line.

We selected the normalized difference vegetation index (NDVI) (Rouse et al., 1974) as a representative of ratio indices, and the second soil-adjusted vegetation index (SAVI2) (Major et al., 1990) as a representative of soil-based indices, for the analysis in this study. The narrow band NDVI and SAVI2 indices were systematically calculated for all possible (584 x 584 = 341,056) band combinations between 400 nm and 2400 nm. The NDVI was computed according to:

$$NDVI_{narrow} = \frac{\rho_{\lambda 1} - \rho_{\lambda 2}}{\rho_{\lambda 1} + \rho_{\lambda 2}} \qquad \text{(Eq. 1)}$$

Where $\rho_{\lambda 1}$ is the reflectance at wavelength $\lambda 1$ and $\rho_{\lambda 2}$ is the reflectance at wavelength $\lambda 2$ with $\lambda 1 \neq \lambda 2$.

The narrow band SAVI2 was calculated according to the following formula:

$$SAVI2_{narrow} = \frac{\rho_{\lambda 1}}{\rho_{\lambda 2} + (b/a)} \qquad \text{(Eq. 2)}$$

Where $\rho_{\lambda 1}$ is the reflectance at wavelength $\lambda 1$, $\rho_{\lambda 2}$ is the reflectance at wavelength $\lambda 2$ with $\lambda 1 \neq \lambda 2$; *a.* is the slope and *b* is the intercept of the soil line.

The soil line parameters were calculated from soil spectral measurement of bare soils which were acquired from few subplots with no vegetation. We assumed that the measured soil optical properties were representative for the study area. Consequently, the soil line parameters were considered constant for all 191 subplots. Implicitly, we assumed that the soil line concept, originally defined for the red-NIR feature space, could be transferred to other spectral domains (Schlerf et al., 2005; Thenkabail et al., 2000). Hence the soil line parameters (*a* and *b*) were systematically calculated for all possible band combinations (584 * 584) between 400 nm and 2400 nm.

#### 4.2.5.3. Red edge inflection point

In many studies (Blackburn, 1998; Gilabert et al., 1996; Horler et al., 1983), the blue and red shift of the red edge inflection point (REIP) has been related to plant growth conditions. The REIP depends on the amount of chlorophyll seen by the sensor. It is strongly correlated with foliar chlorophyll content and presents a very sensitive indicator of vegetation stress (Dawson and Curran, 1998). The chlorophyll amount present in a vegetation canopy can be a product of the chlorophyll content of the leaves and the LAI. For this study, we used three methods to calculate the REIP.

*The inverted Gaussian method (IGM)* (Bonham-Carter, 1988) explains the variations in reflectance $R_{estimated}$ as a function of wavelength (λ) at the REIP as follows:

$$R_{estimated}(\lambda) = R_s - (R_s - R_O)\exp\left(\frac{-(\lambda_o - \lambda)^2}{(2\sigma)^2}\right) \quad \text{(Eq. 3)}$$

$$REIP_{IGM} = \lambda_O + \sigma \quad \text{(Eq. 4)}$$

where σ is the Gaussian shape parameter measured in nanometers; $R_s$ is the (maximum) shoulder reflectance, usually between 780 nm and 800 nm; $R_0$ is the minimum reflectance, usually around 670 nm to 690 nm; and $\lambda_0$ is the wavelength at the point of minimum reflectance. The IGM method fits a Gaussian normal function to the reflectance at the red edge, and the estimated REIP is then the midpoint on the ascending part of the modeled curve. The function is fitted through the measured reflectance data points ($R_{measured}(\lambda)$) by adjusting the values of $R_s$, $R_0$, $\lambda_0$ and σ in such a way that the root mean square error (RMSE) is minimized (Mathworks, 2007).

*The linear interpolation method* (Guyot and Baret, 1988) assumes that the spectral reflectance at the red edge can be simplified to a straight line centered around a midpoint between (i) the reflectance in the NIR shoulder at about 780 nm, and (ii) the reflectance minimum of the chlorophyll absorption feature at about 670 nm. First, the reflectance value is estimated at the inflection point. Then, a linear interpolation procedure for the measurements at 700 nm and 740 nm is applied to estimate the wavelength corresponding to the estimated reflectance value at the inflection point:

$$R_{red\text{-}edge} = (R_{670} - R_{780})/2 \quad \text{(Eq. 5)}$$

$$REIP_{linear} = 700 + 40\left[\frac{R_{red-edge} - R_{700}}{R_{740} - R_{700}}\right] \quad \text{(Eq. 6)}$$

where the constants 700 and 40 result from interpolation between the 700 nm to 740 nm intervals, and $R_{670}$, $R_{700}$, $R_{740}$ and $R_{780}$ are, respectively, the reflectance values at 670 nm, 700 nm, 740 nm and 780 nm.

*The linear extrapolation method (LEM)* (Cho and Skidmore, 2006) is based on the linear extrapolation of two straight lines (Eqs. 7 and 8) through two points on the far-red (680 nm to 700 nm) and two points on the NIR (725 nm to 760 nm) flanks of the first derivative reflectance spectrum (D) of the red edge region. The REIP is then defined by the wavelength value at the intersection of the straight lines (Eq. 9).

*Far-red line*: $D = m_1.\lambda + c_1$ (Eq. 7)

*NIR line*: $D = m_2.\lambda + c_2$ (Eq. 8)

where $m$ and $c$ represent the slope and intercept of the straight lines, respectively. At the intersection, the two lines have equal wavelengths and D values. Therefore, the REIP, which is the wavelength at the intersection, is given by:

$$RIEP_{LEM} = \frac{-(c_1 - c_2)}{(m_1 - m_2)} \quad \text{(Eq. 9)}$$

#### 4.2.5.4. Stepwise multiple linear regression

In stepwise multiple linear regression (SMLR), a primary hypothesis is that only a subset of all available predictor wavelengths have a significant explanatory effect on the studied response variable (Mathworks, 2007). Stepwise multiple regression was used to relate spectral reflectance with grass canopy biophysical and biochemical characteristics. SMLR starts with no predictors (wavelengths) in the

regression equation, and at each step it adds the most statistically significant wavelength (highest F-value or lowest p-value). At the same time, the procedure computes the removal statistic for each wavelength, and removes it (lowest F-value or highest p-value) if possible, until no further entry or removal of wavelengths can be carried out. Stepwise multiple regression was run on reflectance spectra (584 wavelengths between 400 nm and 2400 nm). P-values to enter and remove wavelengths were set at 0.01 and 0.02, respectively, in order to have simple calibration models.

The high number of narrow spectral bands results in a high inter-correlation between them and introduces redundancy into the regression equation (Dunagan et al., 2007). This is a common problem in multiple regression analysis and is called multicollinearity. It is often reflected by high $R^2$ values in the calibration analysis which substantially degrade in the validation analysis (Giacomelli et al., 1998; Hamilton, 1993). We used the variance inflation factor (VIF) to assess the magnitude of multicollinearity (Olyvia, 2000). The variance inflation factor is a measure that can identify the multicollinearity between one independent variable and other independent variables and is given by:

$$VIF_i=(1-R^2_i)^{-1} \quad \text{(Eq. 10)}$$

where $R^2_i$ is the coefficient of determination of the multiple regression produced by regressing the $i^{th}$ narrow spectral predictor band against the other predictor bands. However, there is no universally acceptable level considered to be a "large" variance inflation factor. Some authors have suggested that a variance inflation factor in excess of 10 is an indication that multicollinearity may be causing problems in estimation (Chatterjee and Price, 1977; Myers, 1986). Other authors consider 7 as the maximum value (Sergent et al., 1995), while yet others even consider VIF≥3 as the benchmark for their values (Olyvia, 2000).

#### 4.2.5.5. Partial least squares regression

Partial least squares regression (PLSR) is a technique that reduces the large number of measured collinear spectral variables to a few non-correlated latent variables or factors while maximizing co-variability to the variable(s) of interest (Atzberger et al., 2003b; Cho et al., 2007; Geladi and Kowalski, 1986; Hansen and Schjoerring, 2003; Williams and Norris, 1987). The latent variables represent the relevant information present in the measured reflectance spectra and are used to predict the dependent variables (here, biophysical and biochemical grass characteristics). As with other linear calibration methods, the aim is to build a linear model:

$$Y=X\beta+\varepsilon \quad \text{(Eq. 11)}$$

where Y is the mean-centered vector of the response variable (grass characteristics), X is the mean-centered matrix of the predictor (spectral reflectance), β is the matrix of coefficients, and ε is the matrix of residuals.

PLSR is closely related to principal component regression (Geladi and Kowalski, 1986). Whereas principal component regression performs the decomposition on the spectral data alone, PLSR uses the response variable information during the decomposition process and performs the decomposition on both the spectral and the response simultaneously (Schlerf et al., 2003). The basic PLSR algorithm will not be described in this paper. The interested reader can refer to Ehsani et al. (1999), Geladi and Kowalski (1986), and Williams and Norris (1987).

In conditions where highly correlated input variables (wavelengths) are included in the model, an appropriate variable selection is known to improve PLSR models (Cho et al., 2007; Davies, 2001; Kubinyi, 1996; Martens and Martens, 2000; Schmidtlein and Sassin, 2004). In our study, before running the PLSR, the data were mean-centered. The PLSR was performed using the entire reflectance spectra (400 nm to 2400 nm), first derivative spectra, and a subset of wavelengths (Cho et al., 2007) specifically related to vegetation parameters (Table 4.2). The optimum number of factors was estimated by leave-one-out cross-validation. A common way of using cross-validation for this estimation is to select the number of factors that minimizes the RMSE (Geladi and Kowalski, 1986). To prevent collinearity and to preserve model parsimony, the condition for adding an extra factor to the model was that it had to reduce the root mean square error of cross-validation ($RMSE_{CV}$) by >2% (Cho et al., 2007; Kooistra et al., 2004). In addition, coefficients of determination ($R^2$) between measured and predicted values in the cross-validation were used to evaluate the relationships found. The PLSR analysis was performed using the TOMCAT toolbox 1.01 within MATLAB (Daszykowski et al., 2007).

### *4.2.6. Validation*

Two types of validation were used for the studied models: (i) validation based on an independent test data set, and (ii) a cross-validation procedure (also called the leave-one-out method). The common way of assessing statistical indicators such as $R^2$ and RMSE is to divide the data set into training and test sets and predict the response variable from the test data set (in this study n=64), using models developed from the training data set (in this study n=127). Using a completely different and independent test data set to test the model's performance is important in determining a model's long-term stability (Duckworth, 1998). However, it should also be noted that an arbitrary division of data sets into calibration and validation samples may possibly lead to strongly biased results (Atzberger et al., 2003b). In contrast, cross-validation indicates the overall accuracy

of the different methods. In cross-validation, each sample is estimated by the remaining samples. This meant that for each variant we developed 191 individual models, each time with data from 190 observations. The calibration model was then used to predict the observation that was left out. As the predicted samples were not the same as the samples used to build the models, the cross-validated RMSE ($RMSE_{cv}$) was selected as the accuracy indicator of the model in predicting unknown samples. Benefits of the cross-validation method are its aptitude to detect outliers and its capability of providing nearly unbiased estimations of the prediction error (Efron and Gong, 1983; Schlerf et al., 2005).

Table 4.2. Selected wavelengths for estimating grass characteristics using partial least squares regression.

| ***Wavelength (nm)*** | ***Vegetation parameters*** | ***Reference*** |
|---|---|---|
| 466 | Chlorophyll b | Curran (1989) |
| 695 | Total chlorophyll | Gitelson and Merzlyak (1997), Carter (1994) |
| 725 | Total chlorophyll, leaf mass | Horler et al. (1983) |
| 740 | Leaf mass, LAI | Horler et al. (1983) |
| 786 | Leaf mass | Guyot and Baret (1988) |
| 845 | Leaf mass, total chlorophyll | Thenkabail et al. (2004) |
| 895 | Leaf mass, LAI | Schlerf et al. (2005), Thenkabail et al. (2004) |
| 1114 | Leaf mass, LAI | Thenkabail et al. (2004) |
| 1215 | Plant moisture, cellulose, starch | Curran (1989), Thenkabail et al. (2004) |
| 1659 | Lignin, leaf mass, starch | Thenkabail et al. (2004) |
| 2173 | Protein, nitrogen | Curran (1989) |
| 2359 | Cellulose, protein, nitrogen | Curran (1989) |

## 4.3. Results

### *4.3.1. Grass characteristics*

The spectral reflectance measurements showed considerable variability (Figure 4.2). Table 4.3 lists the linear correlation coefficients between the canopy characteristics. A low correlation was observed between leaf chlorophyll content and LAI. LAI and canopy chlorophyll content were highly correlated. The reason that canopy chlorophyll content is more correlated to LAI than leaf chlorophyll content, for this particular case, is because LAI has a much larger coefficient of variation than leaf chlorophyll content (Table 4.1).

Table 4.3. Linear correlation between grass canopy characteristics (n=185). LCC is the leaf chlorophyll content; and CCC is the canopy chlorophyll content.

| ***Grass canopy characteristic*** | ***LAI*** | ***LCC*** | ***CCC*** |
|---|---|---|---|
| ***LAI ($m^2$ $m^{-2}$)*** | 1.00 | | |
| ***LCC ($\mu g$ $cm^{-2}$)*** | 0.24* | 1.00 | |
| ***CCC (g $m^{-2}$)*** | 0.94* | 0.50* | 1.00 |

* Correlation coefficient significant at P≤0.001

### *4.3.2. Hyperspectral vegetation indices*

NDVI and SAVI2 narrow band vegetation indices were calculated from the measured canopy reflectance spectra, using all possible two-band combinations. The coefficients of determination ($R^2$) between these narrow band vegetation indices and the grass canopy characteristics were computed. An illustration of these results is shown for LAI in the 2-D correlation plot in Figure 4.3. The meeting point of each pair of wavelengths in a 2-D plot corresponds to the $R^2$ value of LAI and the vegetation index calculated from the reflectance values in those two wavelengths. Similar correlation plots were computed for all other variables (not shown). Based on the $R^2$ values in the 2-D correlation plots, band combinations that formed the best indices were determined for LAI, leaf chlorophyll content and canopy chlorophyll content. The best performing indices and the band positions are tabulated in Table 4.4.

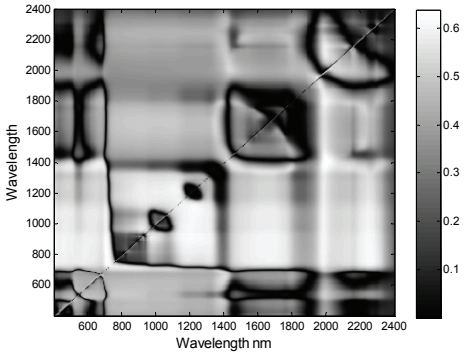


Figure 4.3. 2-D correlation plots illustrating the coefficient of determination ($R^2$) between narrow band SAVI2 and LAI. The data of the 191 sample subplots have been pooled together. Note that the 2-D correlation plot is not symmetrical. The Y axis is the nominator and the X axis is the denominator.

It can be observed from Table 4.4 that narrow band SAVI2 had somewhat higher correlations than narrow band NDVI with the studied variables. However, the coefficients of determination between the grass characteristics and the indices were relatively low, in particular for leaf chlorophyll content. Figure 4.4 highlights

regions where $R^2 \geq 0.6$ for LAI and canopy chlorophyll content (CCC). As can be seen in the figure, LAI had a strong influence on the selection of suitable bands for estimating canopy chlorophyll content. The similarity in the observed patterns is obviously due to the high correlation between the two variables (Table 4.3).

Table 4.4. Band positions and $R^2$ values between the best narrow band NDVI and SAVI2 (derived from 2-D correlation plots of different data sets) and grass variables. LCC is the leaf chlorophyll content; and CCC is the canopy chlorophyll content.

| | ***Narrow band VI*** | ***Pooled data set (n=191)**** | | ***Training set (n=127)**** | |
|---|---|---|---|---|---|
| | | ***λ[nm]*** | ***$R^2$*** | ***λ[nm]*** | ***$R^2$*** |
| ***LAI*** | NDVI | 1105/1229 | 0.61 | 728/745 | 0.61 |
| | SAVI2 | 1998/1402 | 0.64 | 1987/1402 | 0.64 |
| ***CCC*** | NDVI | 1141/1150 | 0.68 | 1123/1132 | 0.67 |
| | SAVI2 | 1211/1086 | 0.69 | 1987/1410 | 0.69 |
| ***LCC*** | NDVI | 547/554 | 0.25 | 547/554 | 0.26 |
| | SAVI2 | 547/554 | 0.29 | 547/554 | 0.28 |

Except for CCC and LCC (n=185); ** Except for CCC and LCC (n=125)

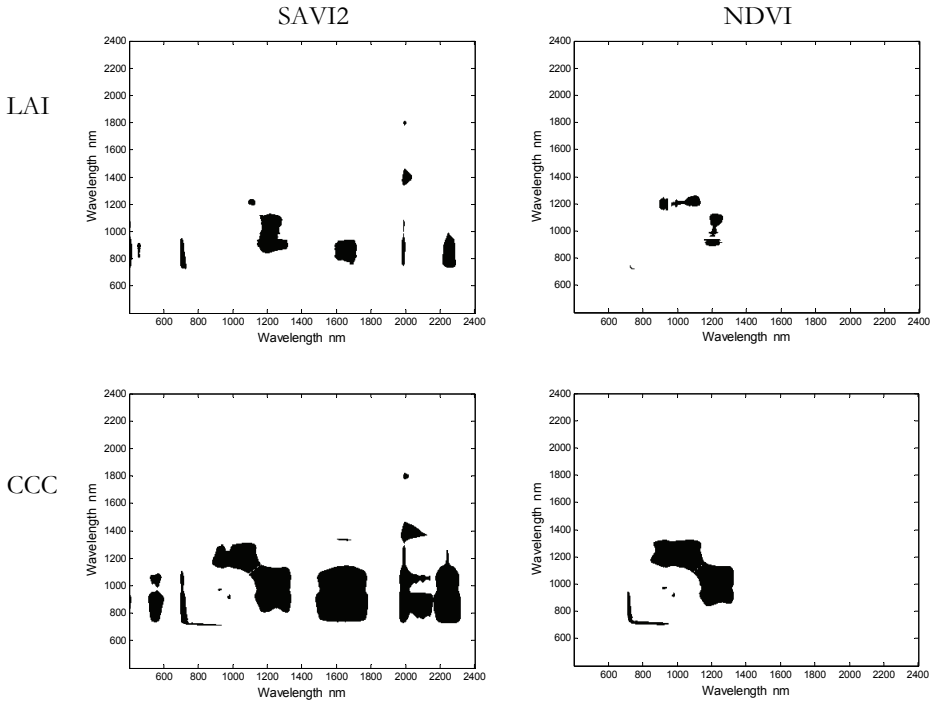


Figure 4.4. Regions with high correlation ($R^2 \geq 0.6$) between narrow band vegetation indices (left: SAVI2, right: NDVI) and LAI and canopy chlorophyll content.

For the best performing narrow band index, cross-validated $R^2$ and relative RMSE (RRMSE = RMSE/mean) were computed from linear regression models (Table 4.5). Further, the best band combinations for the training data set (see Table 4.4) were assessed using the test data set. A comparative analysis of the predictive performance of the narrow band vegetation indices is presented in Table 4.5. As can be observed from this table, compared with narrow band NDVI, narrow band SAVI2 gave slightly higher $R^2$ and lower RMSE values for LAI and canopy chlorophyll content. The better performance of SAVI2 compared with NDVI is probably due to the fact that SAVI2 is less sensitive to external factors such as soil background effects.

Table 4.5. Performance of narrow band vegetation indices for predicting grass variables in Majella National Park, Italy. $R^2_{cv}$ is the cross-validated coefficient of determination between estimated and predicted variables; $RRMSE_{cv}$ is the relative cross-validated root mean square error; $RRMSE_t$ is the relative root mean square error for training data; and $RRMSE_p$ is the relative root mean square error for the test data set. LCC is the leaf chlorophyll content; and CCC is the canopy chlorophyll content.

| | ***Narrow band VI*** | ***Cross-validation for pooled data sets (n=191)**** | | ***Training data set (n=127)**** | | ***Independent test set (n=64)***** | |
|---|---|---|---|---|---|---|---|
| | | $R^2_{cv}$ | $RRMSE_{cv}$ | $R^2_t$ | $RRMSE_t$ | $R^2_p$ | $RRMSE_p$ |
| ***LAI*** | NDVI | 0.60 | 0.34 | 0.61 | 0.34 | 0.58 | 0.36 |
| | SAVI2 | 0.63 | 0.33 | 0.64 | 0.33 | 0.64 | 0.33 |
| ***CCC*** | NDVI | 0.67 | 0.36 | 0.67 | 0.35 | 0.70 | 0.36 |
| | SAVI2 | 0.68 | 0.35 | 0.68 | 0.35 | 0.60 | 0.41 |
| ***LCC*** | NDVI | 0.22 | 0.18 | 0.26 | 0.18 | 0.19 | 0.18 |
| | SAVI2 | 0.26 | 0.17 | 0.27 | 0.17 | 0.29 | 0.17 |

* Except for CCC and LCC (n=185); ** Except for CCC and LCC (n=125); *** Except for CCC and LCC (n=60)

Figure 4.5 shows the relationships between the estimated and measured LAI and canopy chlorophyll content using narrow band SAVI2 and narrow band NDVI. From the figure, it seems that saturation starts to occur for canopy chlorophyll content greater than 2 (g $m^{-2}$) and for LAI greater than 7($m^2$ $m^{-2}$).

### *4.3.3. Red edge inflection point*

The red edge inflection point (REIP) was calculated using three methods. As can be observed from the results reported in Table 4.6, the relationships between measured and estimated grass variables were not reliable using any of the methods. The $R^2$ and relative RMSE of the grass variables obtained from the three methods were relatively similar.

Among the studied variables, estimation of canopy chlorophyll content again yielded the highest $R^2$ values (cross-validated $R^2_{cv}$ = 0.58) and the lowest relative RMSE ($RRMSE_{cv}$ = 0.40) (values for the Gaussian approach). Very low $R^2$ were again observed for the leaf chlorophyll content. Compared with regression models developed using the optimum narrow band indices, the REIP methods produced somewhat lower accuracies.

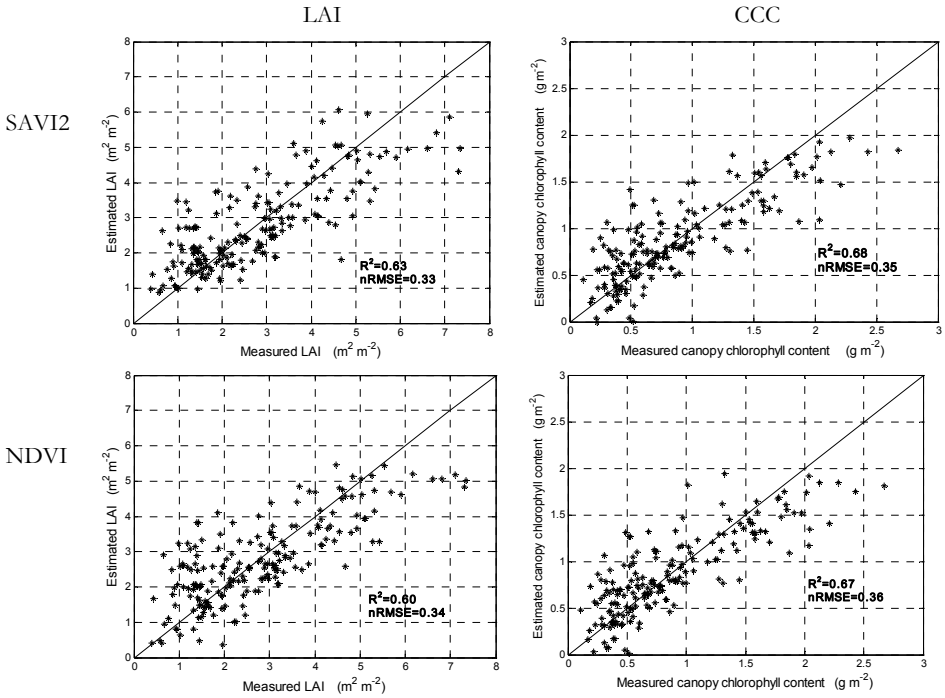


Figure 4.5. Cross-validated prediction of grass variables in Majella National Park, Italy, using narrow band NDVI and SAVI2. Lefts: estimated LAI versus measured LAI; rights: canopy chlorophyll content. The optimum wavebands are those reported in Table 4.4.

### *4.3.4. Stepwise multiple linear regression*

Stepwise multiple linear regression (SMLR) was evaluated for estimating grass biophysical and biochemical variables from measured reflectance spectra. First, stepwise regression was run with the entire data sets to select the wavelengths to be included in the linear model. Next, the selected bands were used to calculate the cross-validated statistics. Cross-validated predictions are shown in Figure 4.6. Compared with narrow band vegetation indices and REIP, the prediction of grass variables was generally improved using SMLR, as indicated by higher $R^2$ and lower relative root mean square values (Table 4.7). The number of narrow spectral bands selected for grass variables ranges from two (for leaf chlorophyll content) to five (canopy chlorophyll content). When the variance inflation factor (VIF) was used to

assess the magnitude of multicollinearity, we observed that even where VIF≥10 none of the bands could be considered collinear, as eliminating any of the selected predictor bands caused considerably higher RMSE and lower $R^2$ values when multiple regression analysis was conducted for either training or test data sets.

Table 4.6. Performance of red edge inflection point calculated using different methods for predicting grass variables in Majella National Park, Italy. $R^2_{cv}$ is the cross-validated coefficient of determination between estimated and predicted variables; $RRMSE_{cv}$ is the relative cross-validated root mean square error; $RRMSE_t$ is the relative root mean square error for training data; and $RRMSE_p$ is the relative root mean square error for the test data sets. LCC is the leaf chlorophyll content; and CCC is the canopy chlorophyll content.

| | | ***Cross-validation for pooled data sets (n=191)**** | | ***Training data set (n=127)**** | | ***Independent test set (n=64)***** | |
|---|---|---|---|---|---|---|---|
| ***REIP method*** | | ***$R^2_{cv}$*** | ***$RRMSE_{cv}$*** | ***$R^2_t$*** | ***$RRMSE_t$*** | ***$R^2_p$*** | ***$RRMSE_p$*** |
| ***Linear interpolation*** | LAI | 0.49 | 0.39 | 0.52 | 0.37 | 0.45 | 0.41 |
| | CCC | 0.56 | 0.41 | 0.6 | 0.39 | 0.51 | 0.46 |
| | LCC | 0.21 | 0.18 | 0.20 | 0.18 | 0.30 | 0.17 |
| ***Gaussian*** | LAI | 0.52 | 0.38 | 0.54 | 0.36 | 0.49 | 0.39 |
| | CCC | 0.58 | 0.40 | 0.61 | 0.39 | 0.54 | 0.44 |
| | LCC | 0.19 | 0.18 | 0.19 | 0.19 | 0.26 | 0.17 |
| ***Linear extrapolation*** | LAI | 0.51 | 0.38 | 0.55 | 0.36 | 0.44 | 0.41 |
| | CCC | 0.57 | 0.41 | 0.63 | 0.37 | 0.45 | 0.49 |
| | LCC | 0.17 | 0.19 | 0.19 | 0.19 | 0.19 | 0.18 |

* Except for CCC and LCC (n=185); ** Except for CCC and LCC (n=125); *** Except for CCC and LCC (n=60)

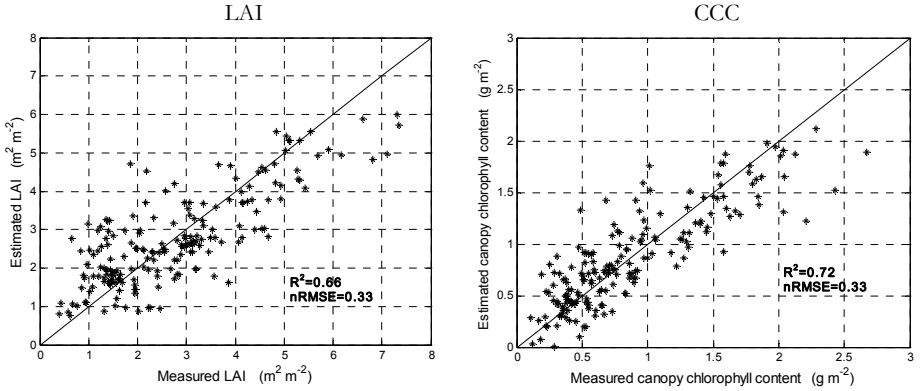


Figure 4.6. Cross-validated prediction of grass variables in Majella National Park, Italy, using stepwise multiple linear regression. Left: estimated LAI versus measured LAI; right: for canopy chlorophyll content. The optimum wavebands are reported in Table 4.7.

Table 4.7. Performance of stepwise multiple linear regression for predicting grass variables in Majella National Park, Italy. $R^2_{cv}$ is the cross-validated coefficient of determination between estimated and predicted variables; $RRMSE_{cv}$ is the relative cross-validated root mean square error; $RRMSE_t$ is the relative root mean square error for training data; and $RRMSE_p$ is the relative root mean square error for the test data sets. º P-values to enter and remove wavelengths were set at 0.001 and 0.002. LCC is the leaf chlorophyll content; and CCC is the canopy chlorophyll content.

| | ***Cross-validation for pooled data sets (n=191)**** | | | ***Training data set (n=127)**** | | | ***Independent test set (n=64)***** | |
|---|---|---|---|---|---|---|---|---|
| | ***Wavelengths (nm)*** | ***$R^2_{cv}$*** | ***$RRMSE_{cv}$*** | ***Wavelengths (nm)*** | ***$R^2_t$*** | ***$RRMSE_t$*** | ***$R^2_p$*** | ***$RRMSE_p$*** |
| **LAI** | 440, 738, 1394, 1402, 1607 | 0.66 | 0.33 | 728, 761, 1394, 1660 | 0.68 | 0.31 | 0.64 | 0.34 |
| **CCC º** | 747, 749, 1425, 1660, 2391 | 0.72 | 0.33 | 657, 690, 707, 902 | 0.69 | 0.35 | 0.59 | 0.43 |
| **LCC** | 529, 564 | 0.25 | 0.18 | 523, 570 | 0.24 | 0.18 | 0.29 | 0.17 |

* Except for CCC and LCC (n=185); ** Except for CCC and LCC (n=125); *** Except for CCC and LCC (n=60)

### *4.3.5. Partial least squares regression*

The relationships between grass variables and reflectance spectra were modeled using PLSR. Cross-validated results using the entire reflectance spectra as inputs are shown in Figure 4.7.

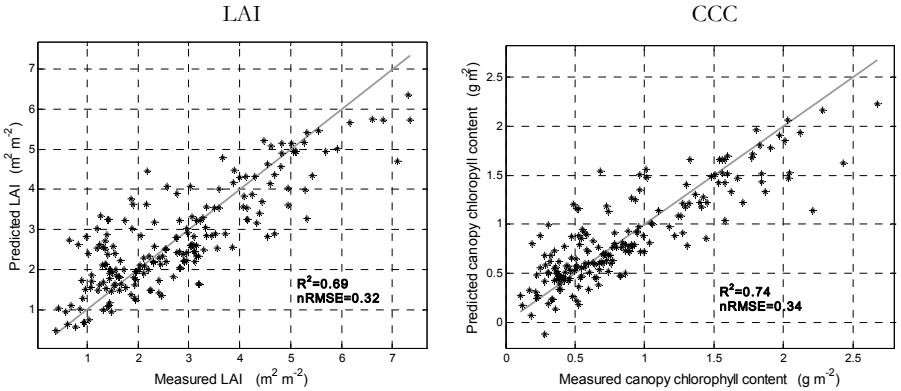


Figure 4.7. Cross-validated prediction of grass variables in Majella National Park, Italy, using the entire reflectance spectra in partial least squares regression models. Left: estimated LAI versus measured LAI; right: for canopy chlorophyll content.

The optimal number of PLSR factors preventing over-fitting was selected in two ways: (i) through visual inspection of cross-validated RMSE versus the number of factors plots (not shown), and (ii) by setting the condition that adding

an extra factor must reduce the RMSE ($RMSE_{CV}$) by >2%. The number of factors in the final model ranged from two in LAI to six in leaf chlorophyll content models (Table 4.8). Compared with other methods (Table 4.7), PLSR using entire reflectance spectra increased all $R^2$ values in the independent test data set by 0.01 to 0.14, whereas the transformation of the reflectance spectra in derivative spectra did not improve the results.

We simplified the full-spectrum PLSR models by selecting a subset of wavelengths closely related to vegetation parameters (Cho et al., 2007) (see Table 4.2). Selection of spectral subsets further improved the prediction of all grass variables. The most significant improvement was observed for leaf chlorophyll content, where $R^2$ increased from 0.39 to 0.45 when testing the models with the independent test data set. Assessed on the basis of the RMSE of the independent data set ($RMSE_p$), and compared with narrow band vegetation indices, REIP and stepwise multiple regression, selection of spectral subsets in PLSR improved the models related to LAI by 0.01, 0.07 and 0.02, to canopy chlorophyll content by 0.03, 0.11 and 0.10, and to leaf chlorophyll content by 0.02, 0.02 and 0.02, respectively.

Table 4.8. Performance of partial least squares regression for predicting grass variables in Majella National Park, Italy. $R^2_{cv}$ is the cross-validated coefficient of determination between estimated and predicted variables; $RRMSE_{cv}$ is the relative cross-validated root mean square error; $RRMSE_t$ is the relative root mean square error for training data; and $RRMSE_p$ is the relative root mean square error for the test data sets. LCC is the leaf chlorophyll content; and CCC is the canopy chlorophyll content.

| | | ***Cross-validation for pooled data sets (191)**** | | | ***Training data set (127)**** | | | ***Independent test set(64)***** | |
|---|---|---|---|---|---|---|---|---|---|
| | | ***No. of factors*** | ***$R^2_{cv}$*** | ***$RRMSE_{cv}$*** | ***No. of factors*** | ***$R^2_t$*** | ***$RRMSE_t$*** | ***$R^2_p$*** | ***$RRMSE_p$*** |
| ***Original reflectance*** | LAI | 4 | 0.69 | 0.32 | 4 | 0.69 | 0.30 | 0.65 | 0.32 |
| | CCC | 5 | 0.74 | 0.34 | 5 | 0.74 | 0.31 | 0.73 | 0.34 |
| | LCC | 4 | 0.38 | 0.17 | 6 | 0.47 | 0.15 | 0.39 | 0.17 |
| ***First derivative reflectance*** | LAI | 2 | 0.64 | 0.33 | 2 | 0.66 | 0.31 | 0.59 | 0.35 |
| | CCC | 2 | 0.66 | 0.37 | 2 | 0.68 | 0.34 | 0.61 | 0.40 |
| | LCC | 3 | 0.31 | 0.18 | 3 | 0.27 | 0.18 | 0.35 | 0.16 |
| ***Selected bands*** | LAI | 4 | 0.67 | 0.32 | 4 | 0.66 | 0.31 | 0.66 | 0.32 |
| | CCC | 6 | 0.74 | 0.35 | 4 | 0.70 | 0.33 | 0.74 | 0.33 |
| | LCC | 6 | 0.40 | 0.17 | 6 | 0.35 | 0.16 | 0.45 | 0.15 |

* Except for CCC and LCC (n=185); ** Except for CCC and LCC (n=125); *** Except for CCC and LCC (n=60)

## 4.4. Discussion

The field experiment led to a large number of sample subplots (191) with high variations in LAI and low variations in leaf chlorophyll content (Table 4.1). The two variables were only slightly related to each other ($r = 0.2$; Table 4.3), allowing an assessment of the utility of different mapping techniques to predict these variables. The canopy integrated chlorophyll content (LAI x leaf chlorophyll content) strongly reflects the variability of LAI and (to a lesser extent) leaf chlorophyll content, expressed by the high inter-correlation between LAI and canopy chlorophyll content (Table 4.3). Among the grass characteristics studied, canopy chlorophyll content was most accurately estimated by nearly all of the applied methods. The canopy chlorophyll content contains both the structure and chlorophyll information of vegetation and can be accurately estimated by canopy spectral reflectance.

In general, the relationships between measured and estimated leaf chlorophyll content were poor for all methods. This indicates poor relationship between the canopy spectra and leaf chlorophyll content. This is in line with previous studies that have demonstrated poor signal propagation from leaf to canopy scale (Asner, 1998; Jacquemoud et al., 1996; Verhoef, 1984; Yoder and Pettigrew-Crosby, 1995).

Although the "optimum" bands for leaf chlorophyll content were found in the visible region, surprisingly this was not the case for the canopy chlorophyll content (NIR and SWIR regions). This artifact is explained by the fact that most of the variation in canopy chlorophyll content stems from the LAI variability; the variability of leaf chlorophyll content was too low to have a noticeable influence on canopy chlorophyll content.

The relationship between measured and estimated LAI was better explained by multivariate calibration methods such as SMLR and PLSR than by univariate methods such as narrow band vegetation indices and REIP. This is because a two-wavelength index utilizes only a limited amount of the total spectral information available in hyperspectral data (Lee et al., 2004).

The bands selected as the best combination of the vegetation indices for LAI were found in the NIR to SWIR regions. This confirmed previous studies by researchers who suggested a strong contribution by SWIR bands to the strength of relationships between spectral reflectance and LAI (Brown et al., 2000; Cohen and Goward, 2004; Lee et al., 2004; Nemani et al., 1993; Schlerf et al., 2005). Compared with the narrow band NDVI, the narrow band SAVI2 gave somewhat higher $R^2$ and lower relative RMSE values for LAI. This result is in agreement with that of Broge and Leblanc (2001), who used simulated data and found SAVI2 to be the best vegetation index for LAI estimation. Moreover, the narrow band SAVI2 performed relatively well for canopy chlorophyll content. This is due to the major

influence of LAI in canopy chlorophyll content and also to the fact that SAVI2 is relatively insensitive to external factors such as soil background effects.

Although red edge has proved to respond more linearly to LAI and chlorophyll when compared with the classical NDVI, which often suffers from saturation problems (Danson and Plummer, 1995), in our study wavelengths within the red edge region were almost absent for leaf chlorophyll content. The "optimum" bands for this variable were found mostly in the visible spectral range, mainly in the green and blue regions characterized by a strong light absorption due to chlorophylls a and b (Hansen and Schjoerring, 2003). Likewise, when the relationships between grass variables and reflectance spectra were examined using SMLR, at least one wavelength was selected from the visible regions for all grass variables. This highlights the importance of visible wavelengths for indices related to leaf pigments.

The PLSR model appears to be a powerful alternative to univariate statistical methods. Compared to the other investigated methods, it achieved relatively better results (Table 4.8). In the present work, the highest number of (latent) factors was six for canopy and leaf chlorophyll contents. At the same time, these two variables were those for which the highest improvement was found. Therefore, important information will be lost by selecting only two wavelengths for narrow band vegetation indices. By selecting a subset of wavelengths related to vegetation parameters and removing unrelated wavelengths, the results of PLSR were further improved when testing the independent data set (Cho et al., 2007; Davies, 2001; Kubinyi, 1996; Martens and Martens, 2000; Schmidtlein and Sassin, 2004). Although our variable selection method was somewhat simplistic, it worked well, because we considered wavelengths related to both biophysical and biochemical properties of vegetation, thus maximizing the information content in the input variables.

When the predicted grass variables were validated using the two validation procedures (i.e., using independent test data sets and cross-validation, respectively), the results concerning the coefficients of determination and the relative RMSE were almost similar. The very small differences confirmed the general applicability of both validation techniques (Selige et al., 2006).

Estimation of biochemical and biophysical characteristics of heterogonous grassland with mixtures of different grass species is challenging in remote sensing (Roder et al., 2007), as the measured signal correspond to different grass species. In our study, an indicator of this was the observed high variations in the SPAD readings within a given subplot (not shown). Nevertheless, by using hyperspectral remote sensing with a large number of narrow spectral bands and powerful multivariate regression techniques, the biophysical and (to a less extent) biochemical grass characteristics could be retrieved with acceptable accuracy.

## 4.5. Conclusion

This study has applied several statistical methods to predict canopy characteristics in heterogeneous Mediterranean grasslands. Narrow band vegetation indices, red edge inflection point (REIP) and two multivariate regression techniques, namely stepwise regression and partial least squares regression, were used in the analysis. Validation of the models was done by comparing differences in the coefficient of determination ($R^2$) and relative root mean square error (RRMSE) of the independent test data sets, as well as through cross-validation. The most important conclusions that can be drawn from this study are as follows:

- Compared with LAI and leaf chlorophyll content, canopy chlorophyll content was estimated with higher accuracy in all models.
- The relationship between estimated and measured leaf chlorophyll content was poor ($R^2 \leq 0.45$).
- LAI was best estimated by stepwise multiple linear regression and partial least square regression. Both methods utilize more than two wavelengths from the entire spectral region (400 nm to 2500 nm) to estimate the variable of interest.
- SAVI2 is a potentially useful vegetation index for extracting canopy variables such as LAI. However, the selection of appropriate wavelengths and bandwidths is important.
- Compared with univariate techniques, multivariate regressions improved the estimation of different grass characteristics.
- Partial least squares regression provided the most useful explorative tool for unraveling the relationship between canopy spectral reflectance and grass characteristics at canopy scale.
- The validation of data based on the independent data sets generally gave results similar to those of the leave-one-out cross-validation as regards to the coefficient of determination ($R^2$) and relative root mean square error. The small differences confirm the general applicability of the two validation techniques.

In summary, multivariate calibration methods, which until now have only been used in a few cases concerning the remote sensing of grasslands, can enhance estimates of different grass variables, and thus present new prospects for mapping and monitoring heterogeneous grass canopies from air- and space-borne platforms.

## Acknowledgements

We would like to acknowledge the assistance of the park management of Majella National Park, Italy, and in particular of Dr. Teodoro Andrisano. We

extend our gratitude to Mr. Istiak Sobhan for his assistance during the field campaign. Special thanks go to Dr. Michal Daszykowski for his assistance in applying the TOMCAT toolbox and for his valuable comments. Further we would like to appreciate the helpful suggestions of two anonymous reviewers.

# Chapter Five

# Inversion of a radiative transfer model for estimating vegetation LAI and chlorophyll in a heterogeneous grassland

*This chapter is based on:*

Darvishzadeh, R., Skidmore, A.K., Schlerf, M. and Atzberger, C., 2008. Inversion of a radiative transfer model for estimating vegetation LAI and chlorophyll in a heterogeneous grassland. *Remote Sensing of Environment*, 112(5): 2592-2604.

## Abstract

Radiative transfer models have seldom been applied for studying heterogeneous grassland canopies. Here, the potential of radiative transfer modeling to predict LAI and leaf and canopy chlorophyll contents in a heterogeneous Mediterranean grassland is investigated. The widely used PROSAIL model was inverted with canopy spectral reflectance measurements by means of a look-up table (LUT). Canopy spectral measurements were acquired in the field using a GER 3700 spectroradiometer, along with simultaneous *in situ* measurements of LAI and leaf chlorophyll content. We tested the impact of using multiple solutions, stratification (according to species richness), and spectral subsetting on parameter retrieval. To assess the performance of the model inversion, the normalized RMSE and $R^2$ between independent *in situ* measurements and estimated parameters were used. Of the three investigated plant characteristics, canopy chlorophyll content was estimated with the highest accuracy ($R^2$ = 0.70, normalized RMSE = 0.18). Leaf chlorophyll content, on the other hand, could not be estimated with acceptable accuracy, while LAI was estimated with intermediate accuracy ($R^2$ = 0.59, normalized RMSE = 0.18). When only sample plots with up to two species were considered (n=107), the estimation accuracy for all investigated variables (LAI, canopy chlorophyll content and leaf chlorophyll content) increased (normalized RMSE = 0.14, 0.16, 0.19, respectively). This shows the limits of the PROSAIL radiative transfer model in the case of very heterogeneous conditions. We also found that a carefully selected spectral subset contains sufficient information for a successful model inversion. Our results confirm the potential of model inversion for estimating vegetation biophysical parameters at the canopy scale in (moderately) heterogeneous grasslands using hyperspectral measurements.

## 5.1. Introduction

Accurate quantitative estimation of vegetation biochemical and biophysical variables is useful for a large variety of agricultural, ecological, and meteorological applications (Asner, 1998; Houborg et al., 2007). The spatial and temporal distribution of vegetation biochemical and biophysical variables are important inputs into models quantifying the exchange of energy and matter between the land surface and the atmosphere. Among the many vegetation characteristics, leaf area index (LAI), leaf chlorophyll content (LCC) and canopy chlorophyll content (CCC) are of prime importance (Bacour et al., 2006; Houborg et al., 2007). LAI, defined here as one-sided leaf area divided by unit of horizontal surface area, is a key structural characteristic of vegetation because of the role of green leaves in controlling many biological and physical processes in plant canopies. Leaf chlorophyll content and canopy chlorophyll content (the latter defined here as the product of LAI and leaf chlorophyll content) contribute to verifying vegetation physiological status and health, and have been found useful for detecting

vegetation stress, photosynthetic capacity, and productivity (Boegh et al., 2002; Carter, 1994).

There are two common approaches to estimating vegetation parameters (including LAI and chlorophyll) from remotely sensed data. In the statistical approach, statistical techniques are used to obtain a correlation between the target variable (e.g., LAI measured *in situ*) and its spectral reflectance or some vegetation indices. The derived statistical relationships are recognized as being sensor-specific and dependent on site and sampling condition, and are expected to change in space and time (Colombo et al., 2003; Meroni et al., 2004). The physical approach, on the other hand, involves using radiative transfer models. This approach assumes that the radiative transfer model accurately describes the spectral variation of canopy reflectance, as a function of canopy, leaf and soil background characteristics, using physical laws (Goel, 1989; Meroni et al., 2004). As radiative transfer models are able to explain the transfer and interaction of radiation inside the canopy based on physical laws, they offer an explicit connection between the vegetation biophysical and biochemical variables and the canopy reflectance (Houborg et al., 2007).

To actually use physically based models for retrieving vegetation characteristics from observed reflectance data, they must be inverted (Kimes et al., 1998). Different inversion techniques have been proposed for physical models, including numerical optimization methods (Jacquemoud et al., 2000; Jacquemoud et al., 1995; Meroni et al., 2004), look-up table (LUT) approaches (Combal et al., 2002; Combal et al., 2003; Gastellu-Etchegorry et al., 2003; Weiss et al., 2000), artificial neural networks (Schlerf and Atzberger, 2006; Walthall et al., 2004; Weiss and Baret, 1999) and, very recently, support vector machines regression (Durbha et al., 2007). In the iterative optimization approach, a stable and optimum inversion is not guaranteed, as the search algorithm may get trapped in local minima before reaching the global minimum. Moreover, the technique is computationally intensive, in particular when using complex radiative transfer models. This makes the retrieval of biophysical variables unfeasible for large geographic areas (Houborg et al., 2007). LUT and neural network approaches reduce the huge computational demand of the traditional optimization approach (Kimes et al., 2000; Liang, 2004). However, for proper training (artificial neural networks) and representation (LUT), they rely on a large database of simulated canopy reflectance spectra to achieve a high degree of accuracy. This increases the computational time for identifying the most appropriate LUT entry (Liang, 2004) and the time required for training the artificial neural network. The interested reader may refer to Kimes et al. (2000) and Liang (2004) for more detailed discussions regarding the advantages and disadvantages of the three inversion methods.

A drawback in using physically based models is the ill-posed nature of model inversion (Atzberger, 2004; Combal et al., 2002), meaning that the inverse solution is not always unique as various combinations of canopy parameters may yield

almost similar spectra (Weiss and Baret, 1999). To overcome this problem, some restriction of the inverse problem may be required to constrain the inversion process. This involves the use of prior knowledge about model parameters (Combal et al., 2002; Lavergne et al., 2007), the use of information provided by the temporal course of key canopy parameters (CROMA, 2000), and/or the analysis of color textures and object signatures (Atzberger, 2004).

Significant efforts to estimate and quantify vegetation properties using radiative transfer models have been carried out in the last two decades. Several studies have been successfully conducted covering different vegetation types and remote sensing data: on global data sets (Bacour et al., 2006; Baret et al., 2007), on agricultural crops (Atzberger, 2004; Jacquemoud et al., 2000; Jacquemoud et al., 1995;), on semiarid regions (Qi et al., 2000), and on forests (Gemmell et al., 2002; Kötz et al., 2004; Meroni et al., 2004; Schlerf and Atzberger, 2006; Zarco-Tejada et al., 2004a; Zarco-Tejada et al., 2004b). Many other studies have analyzed simulated data (Gong et al., 1999; Weiss et al., 2000). Despite these efforts, the review of the literature reveals that there is a gap in estimating vegetation biophysical and biochemical variables for heterogeneous areas such as heterogeneous grasslands with combinations of different grass species. Furthermore, studies that use hyperspectral measurements and that include validation with large numbers of ground truth data for heterogeneous grasslands are extremely rare.

The main objective of this study was to estimate and predict canopy characteristics such as LAI and chlorophyll content in a heterogeneous Mediterranean grassland by inverting the canopy radiative transfer model PROSAIL (Jacquemoud and Baret, 1990; Verhoef, 1984; Verhoef, 1985). The study is based on canopy spectral reflectance measured during a field campaign in the summer of 2005 in Majella National Park in Italy. A LUT-based inversion algorithm has been used, accounting for available prior information relating to the distribution (probable range) of several vegetation characteristics. The suitability of the methods is analyzed in terms of prediction accuracy for estimating LAI, leaf chlorophyll content and canopy chlorophyll content.

## 5.2. Material and methods

### *5.2.1. Study area and sampling*

The study site is located in Majella National Park, Italy (latitude 41°52' to 42°14'N, longitude 13°14' to 13°50'E). The park covers an area of 74,095 ha and extends into the southern part of Abruzzo, at a distance of 40 km from the Adriatic Sea. The region is situated in the massifs of the Apennines. The park is characterized by several mountain peaks, the highest being Mount Amaro (2794 m). Geologically, the region is made up of calcareous rocks, which date back to the

Jurassic period. The flora of the park include more than 1800 plant species, which constitute approximately one third of the entire flora of Italy (Cimini, 2005).

Abandoned agricultural areas and settlements in Majella are returning to oak (*Quercus pubescens*) woodlands at the lower altitude (400 m to 600 m) and beech (*Fagus sylvatica*) forests at higher altitudes (1200 m to 1800 m). Between these two formations is a landscape composed of shrubby bushes, patches of grass/herb vegetation, and bare rock outcrops. The dominant grass and herb species include *Brachypodium genuense, Briza media, Bromus erectus, Festuca* sp*, Helichrysum italicum, Galium verum, Trifolium pratense, Plantago lanceolata, Sanguisorba officinalis* and *Ononis spinosa* (Cho, 2007).

Stratified random sampling was adopted in this study. For this purpose, the area was stratified into grassland, forest, shrubland and bare rock outcrops, using a land cover map provided by the management of Majella National Park. We distinguished four main phytosociological classes of varying areas within the grasslands: semi-natural/farmlands, grazed/periodically flooded areas, open garrigues and abandoned farmlands. Coordinates (x y) were randomly generated in the grassland stratum to select plots. A total of 45 quadratic plots of 30 m side length were generated and a GPS (Global Positioning System) was used to locate their position in the field. To increase the number of samples in the time available, within each plot four to five randomly selected subplots were identified. This resulted in a total of 185 subplots being sampled (from the original 191 subplots, six subplots showed poor quality and had to be discarded). Each subplot covered 1 m x 1 m (average vegetation height, 28 cm), with different species compositions and relative abundances while the within-subplot variability was small. The species varied in terms of leaf shape, leaf size, the amount of leaves and their typical angle distribution. The within-subplot variability of SPAD measurements also indicated some variation in chlorophyll contents, albeit this has not been quantified within the present study.

### *5.2.2. Canopy spectral measurements*

Fifteen replicates of canopy spectral measurements were taken from each subplot, using a GER 3700 (Geophysical and Environmental Research Corporation, Buffalo, New York) spectroradiometer. The wavelength range is 350 nm to 2500 nm, with a spectral sampling of 1.5 nm in the 350 nm to 1050 nm range, 6.2 nm in the 1050 nm to 1900 nm range, and 9.5 nm in the 1900 nm to 2500 nm range. The spectral resolution (band pass) is 3 nm, 11 nm and 16 nm in the 350 nm to 1050 nm range, 1050 nm to 1900 nm range, and 1900 nm to 2500 nm range, respectively.

The fiber optic, with a field of view of 25°, was handheld approximately 1 m above the ground at nadir position. The ground area observed by the sensor had a

diameter of 45 cm and was large enough to cover the center of the subplots without being influenced by the surroundings. The 15 replicate spectral measurements taken from each subplot enabled the measurement noise to be averaged out. Prior to each reflectance measurement, the radiance of a white standard panel coated with $BaSO_4$ and of known reflectivity was recorded for normalization of the target measurements. The fieldwork was conducted between June 15 and July 15 in 2005. To minimize atmospheric perturbations and BRDF effects, spectral measurements were made on clear sunny days between 11:30 a.m. and 2:00 p.m. The measurement set-up ensured that the ratio of direct to diffuse incoming solar radiation was approximately constant. Hence, no correction for this possibly perturbing factor has been applied.

The spectral reflectance of bare soils were acquired from a few subplots with no vegetation and their average was calculated. Mean reflectance spectra are shown in Figure 5.1. We assumed that the measured soil optical properties were representative for the study area.

### *5.2.3. LAI measurements*

In each subplot, LAI was non-destructively measured using a widely used optical instrument, the Plant Canopy Analyzer LAI-2000 (LICOR Inc., Lincoln, NE, USA). A detailed description of this instrument is given by LI-COR (1992) and Welles and Norman (1991). Measurements were taken either under clear skies with low solar elevation (i.e., within the two hours following sunrise or preceding sunset) or under overcast conditions. Care was taken to measure LAI on the same day as the canopy spectral measurements were made. To prevent direct sunlight on the sensor, samples of below- and above-canopy radiation were made with the sun behind the operator and using a view restrictor of 45°. For each subplot, reference sample of above-canopy radiation was taken by measuring incoming radiation above the grass subplot. Next, five below-canopy samples were collected and used to calculate the average LAI.

LAI measured using the LAI-2000 corresponds to plant area index (PAI), including photosynthetic and non-photosynthetic components (Chen et al., 1997). In our study, non-photosynthetic components were almost non-existent. Despite the non-random distribution of grass leaves, no corrections for clumping were applied. Therefore, the LAI used here corresponds to effective PAI, and in the following sections these measurements are abbreviated as LAI.

The statistics of the 185 samples comprising different grass species are summarized in Table 5.1. The table reveals a large range of LAI values, which enables the approach to be validated under contrasting conditions.

### *5.2.4. Chlorophyll measurements*

In each 1 m x 1 m subplot, a SPAD-502 Leaf Chlorophyll Meter (MINOLTA, Inc.) was used to assess leaf chlorophyll content. SPAD values express relative amounts of chlorophyll in leaves by measuring transmittance in the red (650 nm) and near-infrared (920 nm) wavelength regions (Minolta, 2003). SPAD measurements give a unitless but highly reproducible measure, which is well correlated with leaf chlorophyll concentration, and is commonly used to characterize chlorophyll concentration in many plant species (Campbell et al., 1990; Haboudane et al., 2002; Jongschaap and Booij, 2004; Nakano et al., 2006). A total of 30 leaves representing the dominant species were randomly selected in each subplot, and their SPAD readings were recorded. From the 30 individual SPAD measurements, the average was calculated. These averaged SPAD readings (unitless) were converted into leaf chlorophyll content (μg $cm^{-2}$) by means of an empirical calibration function provided by Markwell et al. (1995). Although the Markwell function refers to soybean and corn leaves, the same authors have demonstrated that they can also be applied to other plant species. Hence, we renounced to establish specific calibration functions for the grass species since each sample plot consist of several species. The total canopy chlorophyll content (g $m^{-2}$) for each subplot was obtained by multiplying the leaf chlorophyll content by the corresponding LAI (Table 5.1).

Table 5.1. Summary statistics of the measured biophysical and biochemical variables of grassland sample plots (n=185). SPAD is the average SPAD reading for 30 randomly selected leaves in each subplot; LCC is the leaf chlorophyll content; CCC is the canopy chlorophyll content.

| *Measured variables* | *Min* | *Mean* | *Max* | *StDev* | *Range* | *Variation coefficient* |
|---|---|---|---|---|---|---|
| ***LAI ($m^2$ $m^{-2}$)*** | 0.39 | 2.81 | 7.34 | 1.50 | 6.95 | 0.53 |
| ***SPAD (unitless)*** | 22.4 | 32.70 | 45 | 4.35 | 22.6 | 0.13 |
| ***LCC (μg $cm^{-2}$)*** | 17.1 | 30.07 | 49.66 | 6.12 | 32.55 | 0.20 |
| ***CCC (g $m^{-2}$)*** | 0.1 | 0.87 | 2.7 | 0.55 | 2.56 | 0.63 |
| ***Dominant species number*** | 1 | 2.34 | 4 | 0.87 | 3 | 0.37 |

### *5.2.5. Pre-processing of spectra*

To minimize noise in the measured reflectance spectra, the 15 spectra of each sample plot were averaged. Bands with a wavelength less than 400 nm and more than 2400 nm displayed very high levels of noise and were excluded. The resulting 584 wavebands were used for the analysis. A moving Savitzky-Golay filter (Savitzky and Golay, 1964) with a frame size of 15 data points (2nd degree

polynomial) was applied to the averaged reflectance measurements to further smooth the spectra. The analysis and processing was carried out using MATLAB 7.1 (Mathwork, 2007). In total, 185 canopy reflectance spectra were obtained. The average reflectance spectra of all grass subplots and the spectral variability of the measurements are shown in Figure 5.1.

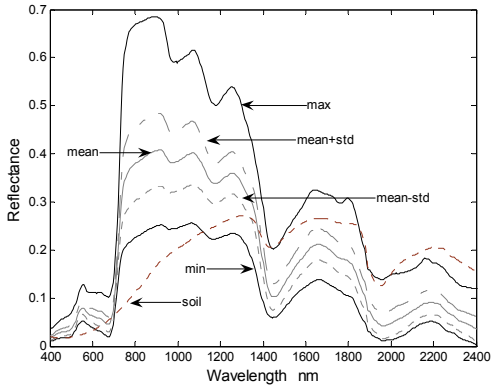


Figure 5.1. Mean and the spectral variability of the canopy reflectance spectra of sample plots (n=185) in Majella National Park, Italy. Also shown is the averaged reflectance spectrum of the bare soil that has been used in the radiative transfer modeling (in bold dashed line).

### *5.2.6. The PROSAIL radiative transfer model*

The widely used PROSAIL radiative transfer model, which is a combination of the SAILH canopy reflectance model (Verhoef, 1984; Verhoef, 1985; Kuusk, 1991) and the PROSPECT leaf optical properties model (Jacquemoud and Baret, 1990), was used to retrieve the LAI and leaf and canopy chlorophyll contents. Both submodels are relatively simple and need only a limited number of input parameters, with reasonable computation time. By inverting the coupled models, both the leaf and canopy parameters can be estimated.

The PROSPECT model (Fourty et al., 1996; Jacquemoud and Baret, 1990; Jacquemoud et al., 1996) calculates the leaf hemispherical transmittance and reflectance as a function of four input parameters, i.e., the leaf structural parameter, $N$ (unitless); the leaf chlorophyll $a + b$ concentration, $LCC$ (μg cm$^{-2}$); the dry matter content, $C_m$ (g cm$^{-2}$); and the equivalent water thickness, $C_w$ (g cm$^{-2}$) (Jacquemoud et al., 2000). The spectral leaf optical properties (reflectance and transmittance) calculated by PROSPECT are inputs into the SAILH canopy reflectance model. This model (Verhoef, 1984; Verhoef, 1985) is a one-dimensional bidirectional turbid medium radiative transfer model that has been later modified to take into account the hot spot effect in plant canopy reflectance (Kuusk, 1991). Turbid medium defines the canopy as a horizontally homogenous and semi-infinite layer that consists of small vegetation elements that act as absorbing and scattering particles of a given geometry and density. Consequently,

the model is best adopted for use in homogeneous vegetation canopies (Meroni et al., 2004; Schlerf and Atzberger, 2006; Verhoef, 1984). Apart from the leaf reflectance and transmittance, the SAILH model requires eight input parameters to produce the top-of-canopy bidirectional reflectance. These are sun zenith angle, $t_s$ (deg); sensor viewing angle, $t_o$ (deg); azimuth angle, *phi* (deg); fraction of diffuse incoming solar radiation, *skyl*; background reflectance (soil reflectance) for each wavelength, *rsl*; *LAI* ($m^2$ $m^{-2}$); mean leaf inclination angle, *ALA* (deg); and hot spot size parameter, *hot* (m $m^{-1}$), defined as the ratio between the average size of the leaves and the canopy height (Verhoef, 1985). To account for the changes induced by moisture and roughness in soil brightness, we used a soil brightness parameter, *scale* (Atzberger et al., 2003). Therefore, when the two models are coupled, 12 input parameters considering the leaf, the canopy and the soil have to be specified. Of the 12 input parameters, four parameters, (sun zenith angle, sensor viewing angle, azimuth angle and fraction of diffuse incoming solar radiation) were fixed. For the eight remaining input parameters (LAI, mean leaf inclination angle, hot spot size parameter, soil brightness parameter, leaf structural parameter, leaf chlorophyll *a* + *b* concentration, dry matter content and the equivalent water thickness), 100,000 sets were generated randomly (Table 5.2).

### *5.2.7. The look-up table (LUT) inversion*

Perhaps the simplest method of solving the inversion of a radiative transfer model is by using a LUT. LUTs offer an interesting alternative to numerical optimization and neural network methods because they permit a global search (avoiding local minima) while showing less unexpected behavior when the spectral characteristics of the targets are not well represented by the modeled spectra (Schlerf and Atzberger, 2006). A LUT is built in advance of the actual inversion through forward calculations using a radiative transfer model. For the inversion, only search operations are needed to identify the parameter combinations that yield the best fit between measured and LUT spectra. However, to achieve high accuracy for the estimated parameters, the dimension of the LUT must be sufficiently large (Combal et al., 2002; Tang et al., 2006; Weiss et al., 2000).

To build the LUT, 100,000 parameter combinations were randomly generated (uniform distributions) and used in the forward calculation of the PROSAIL model. We also tested normally distributed random parameters and found no significant differences (not shown). The ranges (minimum and maximum) for each of the eight "free" model parameters are reported in Table 5.2. To prevent too-wide parameter spaces and to reduce the size of the parameter spacing, the maximum and minimum values of *LAI*, *LCC*, and *ALA* (recorded along with LAI using LAI-2000 instrument) were fixed based on the prior knowledge from the field data collection (Combal et al., 2003). Parameters difficult to measure (e.g., *N*, $C_m$, $C_w$) are often fixed to nominal values (e.g. Chaurasia and Dadhwal, 2004; Haboudane et al., 2004; Houborg et al., 2007; le Maire et al., 2004). For the leaf

structural parameter *N* of PROSPECT, Haboudane et al. (2004) and Houborg et al. (2007) have used a fixed value of 1.55 for various crops, including corn, soybean, wheat and spring barley. Jacquemoud et al. (2000) have used a fixed value of $N = 1.7$ for soybean. Atzberger et al. (2003) have used a range of $N = 2 \pm 0.34$ for wheat crop. Since grasses have relatively thin leaves, we used for the *N* parameter a range from 1.5 to 1.9. The ranges of other input parameters ($C_w$, $C_m$, *hot* and *scale)* were selected similarly in agreement with the existing literature (Atzberger, 2004; Cho, 2007; Combal et al., 2003; Haboudane et al., 2004; le Maire et al., 2004; Schlerf and Atzberger, 2006).

We used the average bare soil reflectance spectrum that was measured in the study area to represent soil optical properties (Figure 5.1). Since the spectral measurements were done around noon with the sensor looking at nadir position, the sensor viewing angle ($t_o$), the relative azimuth angle (*phi*) and the average sun zenith angle ($t_s$) were fixed at 0º, 0º and 30º, respectively, representing the geometry of the measurement setup. With respect to the fraction of diffuse incoming solar radiation, *skyl*, a fixed value of 0.1 across all wavelengths has been used, as in many similar studies (Cho, 2007; Schlerf and Atzberger, 2006). Hence, we neglect that the amount of diffuse sky light depends on atmospheric conditions, solar zenith angle and furthermore is wavelength dependent. This simplification seems justified, however, by the fact that *skyl* has only a very small influence on canopy reflectance (Clevers and Verhoef, 1991) and by the lack of on-site measurements of *skyl*.

Table 5.2. Specific ranges for eight input parameters used for generating the LUT, using forward calculation, of the PROSAIL model. Within the specified ranges, parameter values were drawn randomly (uniform distributions).

| ***Parameter*** | ***Abbreviation in model*** | ***Unit*** | ***Minimum value*** | ***Maximum value*** |
|---|---|---|---|---|
| ***Leaf area index**** | *LAI* | $m^2\ m^{-2}$ | 0.3 | 7.5 |
| ***Mean leaf inclination angle**** | *ALA* | Deg | 40 | 70 |
| ***Leaf chlorophyll content**** | *LCC* | $\mu g\ cm^{-2}$ | 15 | 55 |
| ***Leaf structural parameter*** | *N* | No dimension | 1.5 | 1.9 |
| ***Dry matter content*** | $C_m$ | $g\ cm^{-2}$ | 0.005 | 0.01 |
| ***Equivalent water thickness*** | $C_w$ | $g\ cm^{-2}$ | 0.01 | 0.02 |
| ***Hot spot size parameter*** | *hot* | $m\ m^{-1}$ | 0.05 | 0.1 |
| ***Soil brightness parameter*** | *scale* | No dimension | 0.5 | 1.5 |

* The minimum and maximum values are selected based on the prior knowledge from the field.

To find the solution to the inverse problem for a given canopy spectrum for each modeled reflectance spectrum of the LUT, the RMSE between measured and modeled spectra ($RMSE_r$) is calculated according to:

$$RMSE_r = \sqrt{\frac{\sum_{i=1}^{n}(R_{measured_\lambda} - R_{lut_\lambda})^2}{n}} \qquad \text{(Eq. 1)}$$

where $R_{measured}$ is a measured reflectance at wavelength λ and $R_{lut}$ is a modeled reflectance at wavelength λ in the LUT, and $n$ is the number of wavelengths. Traditionally, the solution is regarded as the set of input parameters corresponding to the reflectance in the LUT that provides the smallest $RMSE_r$. However, this solution is not always the optimal solution since it may not be unique (ill-posed problem). To overcome this problem and to enhance the consistency of the estimated variables, we also investigated the use of some other statistical indicators, such as the mean and median from the best 10, 20, 40 and 100 simulations.

An appropriate band selection – or alternatively, the weighting of different spectral bands – is known to improve radiative transfer model inversion and prevents bias in the estimation of the variables of interest (Bacour et al., 2001; Meroni et al., 2004; Schlerf and Atzberger, 2006; Lavergne et al., 2007). This is particularly the case if hyperspectral data with wavelengths that are either noisy or not well modeled by the radiative transfer model being inverted. Nevertheless, the selection of an optimal spectral subset/weighting of spectral bands is not a trivial problem and is still an open issue within the remote sensing community (Meroni et al., 2004; Lavergne et al., 2007).

To investigate the role of heterogeneity (number of dominant plant species within a subplot) in the estimation of grass variables, we also stratified the data based on dominant species composition.

## 5.3. Results

### *5.3.1. Grass characteristics*

Each subplot varied in species composition and biophysical/biochemical characteristics (Table 5.1). Consequently, spectral reflectance measurements showed considerable variability (Figure 5.1). Linear correlation between the canopy characteristics confirmed independence between leaf chlorophyll content and LAI, while LAI and canopy chlorophyll content were highly correlated (Table 5.3). This is explained by larger coefficient of variation of LAI compared to leaf chlorophyll content (Table 5.1).

Table 5.3. Linear correlation between grass canopy characteristics (n=185). LCC is the leaf chlorophyll content; and CCC is the canopy chlorophyll content.

| **Grass canopy characteristic** | ***LAI ($m^2$ $m^{-2}$)*** | ***LCC ($\mu g$ $cm^{-2}$)*** |
|---|---|---|
| **LCC ($\mu g$ $cm^{-2}$)** | 0.24 | - |
| **CCC ($g$ $m^{-2}$)** | 0.94 | 0.50 |

Correlation coefficients significant at $P \leq 0.001$

### *5.3.2. Inversion results based on the smallest RMSE criterion*

To find the solution to the inverse problem, the LUT is sorted according to the cost function ($RMSE_r$) and the set of variables providing the minimum RMSE is considered as the solution. Figure 5.2 illustrates measured and simulated canopy reflectance spectra found in this way for three subplots with contrasting LAI values.

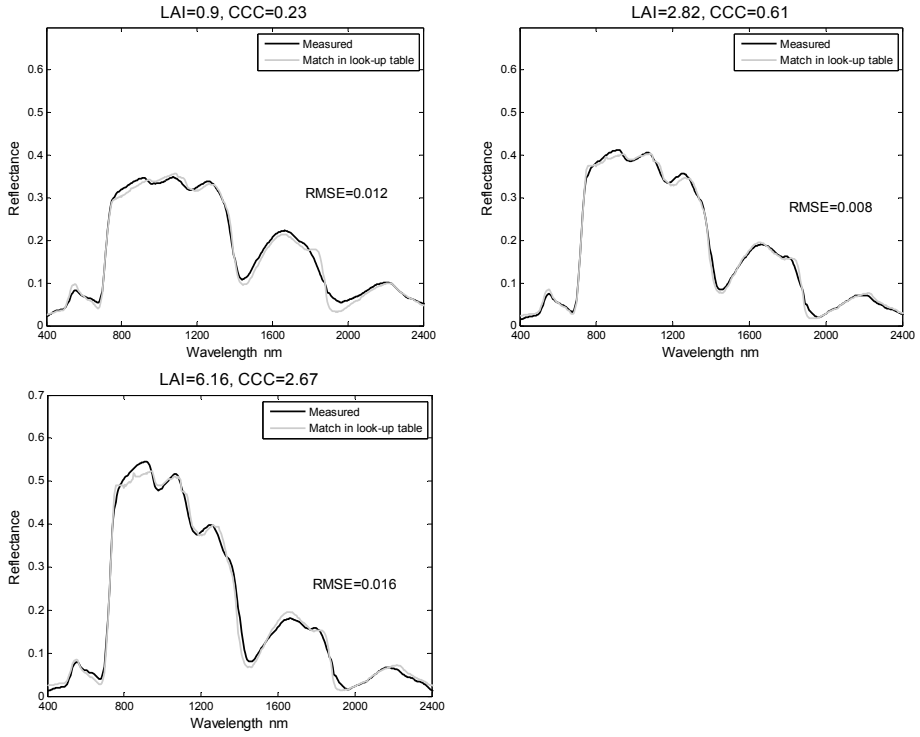


Figure 5.2. Measured and simulated grass canopy reflectance spectra of three sample plots with LAI equal to 0.9 (top left), 2.82 (top right), and 6.16 (bottom), respectively.

In the examples, the simulated reflectances were in relatively good agreement with the measured reflectances for canopies with different LAI values. From analysis of 185 canopy reflectance spectra, we found that medium range LAI sample plots were best modeled by PROSAIL (lowest $RMSE_r$ between measured and modeled spectra). In general, differences between measured and modeled spectral reflectances were inconsistent, even among canopies with a single species. Figure 5.3 demonstrates the average absolute error (AAE) between measured and best-fit spectra as a function of wavelengths. The figure shows that the AAE in some regions is relatively high, especially for the water vapor absorption regions (1135 nm to 1400 nm, and 1820 nm to 1940 nm). The canopy reflectance in these regions is either not well measured or not well modeled by PROSAIL (see section 5.3.5 for spectral subsetting).

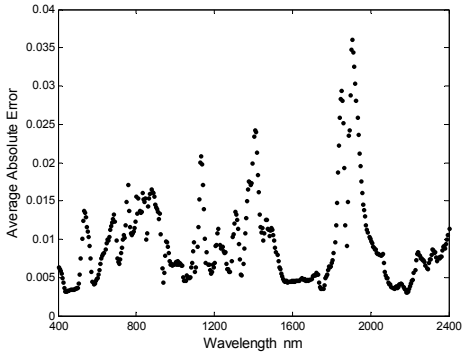


Figure 5.3. The average absolute error (AAE) between measured and best-fit reflectance spectra as a function of wavelengths. The AAE has been calculated from the 185 measured canopy spectra against the best fitting look-up table (LUT) spectra.

The relation between the measured and estimated grass variables based on the smallest RMSE criterion is demonstrated in Figure 5.4. The $R^2$ and the normalized RMSE (NRMSE = RMSE/range) (Atzberger, 1997; Combal et al., 2003) between measured and estimated leaf chlorophyll content indicate poor relationships. LAI and canopy chlorophyll content were estimated with much higher accuracy. As the canopy reflectance is modulated mostly by LAI and the integrated chlorophyll content of the canopy (hence canopy chlorophyll content), which both showed considerable variability (Table 5.1), the poor retrieval of the leaf chlorophyll content was expected (lower variability).

Studying the histograms of the other 6 retrieved parameters ($C_m$, $C_w$, *scale*, *ALA*, *hot* and *N*) revealed that several (160 out of 185) samples plots reached the upper/lower boundary of at least one model parameter. As the parameter ranges were relatively large and consistent with available field observations (Table 5.2), we believe that some wavelengths are either badly measured or not well modeled by

the combined SAILH and PROSPECT canopy reflectance model (Schlerf & Atzberger 2006).

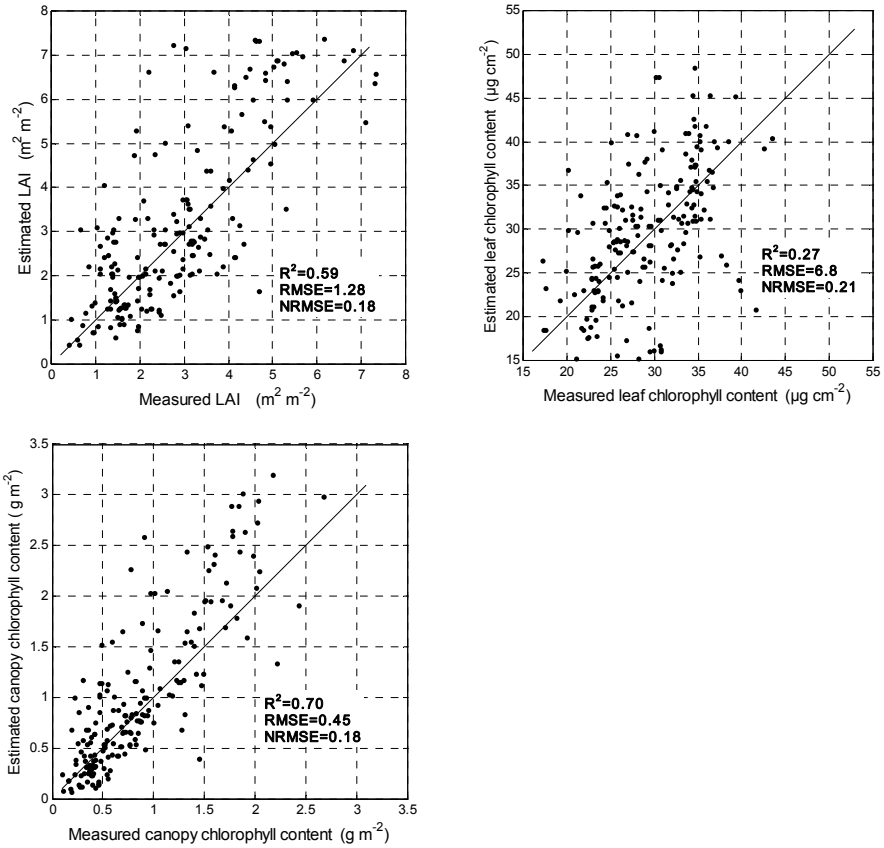


Figure 5.4. Estimated versus measured grass variables in Majella National Park, Italy, using the minimum RMSE criterion (n=185). Top left: LAI; Top right: leaf chlorophyll content (LCC); and bottom: canopy chlorophyll content (CCC).

### *5.3.3. Inversion results based on multiple solutions*

For each measured canopy spectra, the LUT was sorted from minimum to maximum $RMSE_r$ (Eq. 1). Instead of taking simply the PROSAIL parameter corresponding to the lowest $RMSE_r$ (section 5.3.2), we alternatively tested to consider the best 10, 20, 40 and 100 LUT entries as final solution. The importance of considering multiple solutions rather than the single LUT solution with minimum RMSE is seen from Table 5.4. It demonstrates how different solutions affect the accuracy of the estimated variables. We used one-way ANOVA (analysis of variance) to evaluate the existence of significant differences in the mean $R^2$ between the median/mean for the three biophysical grass variables. The test was conducted for the four multiple solutions (i.e., the first 10, the first 20, the first 40

and the first 100 best fits). The results show that, generally, there are no significant differences between the statistical parameters used for any number of solutions ($p>0.05$). Nevertheless, throughout the rest of this study we considered the first 100 solutions as the best measures for estimating the grass variables.

Table 5.4. $R^2$, RMSE and normalized RMSE between measured and estimated grass characteristics (n=185). The standard LUT solution is indicated as "best fitting spectra". The grass characteristics were also retrieved considering the first 10, 20, 40 and 100 solutions. In these cases, the median and mean were investigated. LCC is the leaf chlorophyll content and CCC is the canopy chlorophyll content.

| ***No. of Solution*** | ***Statistical parameter*** | ***LAI ($m^2$ $m^{-2}$)*** | | | ***LCC ($\mu g$ $cm^{-2}$)*** | | | ***CCC (g $m^{-2}$)*** | | |
|---|---|---|---|---|---|---|---|---|---|---|
| | | ***$R^2$*** | ***RMSE*** | ***NRMSE*** | ***$R^2$*** | ***RMSE*** | ***NRMSE*** | ***$R^2$*** | ***RMSE*** | ***NRMSE*** |
| ***Best fitting spectra*** | / | 0.59 | 1.28 | 0.18 | 0.27 | 6.8 | 0.21 | 0.70 | 0.45 | 0.18 |
| ***First 10*** | Median | 0.61 | 1.21 | 0.17 | 0.31 | 5.7 | 0.18 | 0.71 | 0.43 | 0.17 |
| | Mean | 0.62 | 1.18 | 0.17 | 0.30 | 6.0 | 0.18 | 0.71 | 0.43 | 0.17 |
| ***First 20*** | Median | 0.61 | 1.18 | 0.17 | 0.34 | 5.7 | 0.18 | 0.71 | 0.44 | 0.17 |
| | Mean | 0.62 | 1.15 | 0.17 | 0.33 | 5.7 | 0.18 | 0.72 | 0.43 | 0.17 |
| ***First 40*** | Median | 0.60 | 1.21 | 0.17 | 0.24 | 7.5 | 0.23 | 0.70 | 0.45 | 0.18 |
| | Mean | 0.61 | 1.18 | 0.17 | 0.27 | 6.6 | 0.20 | 0.70 | 0.44 | 0.17 |
| ***First 100*** | Median | 0.64 | 1.1 | 0.16 | 0.35 | 5.3 | 0.16 | 0.72 | 0.42 | 0.16 |
| | Mean | 0.63 | 1.1 | 0.16 | 0.35 | 5.4 | 0.17 | 0.72 | 0.42 | 0.16 |

### *5.3.4. Inversion results based on stratification of heterogeneity*

According to the number of dominant species, the subplots were divided into seven data sets (Table 5.5). The statistical analysis was done separately for each of the seven data sets. We considered the "best fitting spectra" and the first 100 solutions for estimating the grass variables (see section 5.3.3). Table 5.5 shows the results of this stratification.

Table 5.5. $R^2$, RMSE and normalized RMSE between measured and estimated grass canopy variables considering stratification based on subplot heterogeneity. LCC is the leaf chlorophyll content and CCC is the canopy chlorophyll content.

| ***Strat. /Domin. species*** | ***Statistical parameter*** | ***LAI ($m^2$ $m^{-2}$)*** | | | ***LCC ($\mu g$ $cm^{-2}$)*** | | | ***CCC (g $m^{-2}$)*** | | |
|---|---|---|---|---|---|---|---|---|---|---|
| | | ***$R^2$*** | ***RMSE*** | ***NRMSE*** | ***$R^2$*** | ***RMSE*** | ***NRMSE*** | ***$R^2$*** | ***RMSE*** | ***NRMSE*** |
| ***One species (n=32)*** | Best fitting spectra | 0.81 | 0.76 | 0.11 | 0.21 | 6.3 | 0.34 | 0.78 | 0.31 | 0.16 |
| | Median of 100 | 0.85 | 0.68 | 0.10 | 0.19 | 6.4 | 0.34 | 0.84 | 0.30 | 0.16 |
| | Mean of 100 | 0.85 | 0.67 | 0.10 | 0.17 | 6.6 | 0.35 | 0.83 | 0.31 | 0.16 |
| ***Two species (n=75)*** | Best fitting spectra | 0.69 | 1.1 | 0.17 | 0.37 | 6.2 | 0.20 | 0.79 | 0.43 | 0.17 |
| | Median of 100 | 0.69 | 1.1 | 0.17 | 0.41 | 5.3 | 0.17 | 0.78 | 0.45 | 0.18 |
| | Mean of 100 | 0.69 | 1.1 | 0.17 | 0.40 | 5.4 | 0.18 | 0.78 | 0.44 | 0.18 |
| ***Three species (n=59)*** | Best fitting spectra | 0.55 | 1.6 | 0.33 | 0.13 | 6.9 | 0.28 | 0.58 | 0.51 | 0.24 |
| | Median of 100 | 0.56 | 1.2 | 0.25 | 0.32 | 5.0 | 0.20 | 0.60 | 0.41 | 0.19 |
| | Mean of 100 | 0.56 | 1.2 | 0.25 | 0.33 | 4.8 | 0.20 | 0.61 | 0.41 | 0.19 |
| ***Four species (n=19)*** | Best fitting spectra | 0.37 | 1.49 | 0.37 | 0.26 | 7.03 | 0.37 | 0.50 | 0.56 | 0.36 |
| | Median of 100 | 0.38 | 1.3 | 0.32 | 0.45 | 4.4 | 0.23 | 0.53 | 0.48 | 0.31 |
| | Mean of 100 | 0.38 | 1.3 | 0.32 | 0.45 | 4.6 | 0.24 | 0.54 | 0.48 | 0.31 |
| ***Up to two species (n=107)*** | Best fitting spectra | 0.71 | 0.99 | 0.14 | 0.40 | 6.2 | 0.19 | 0.80 | 0.40 | 0.16 |
| | Median of 100 | 0.72 | 0.97 | 0.14 | 0.41 | 5.6 | 0.17 | 0.80 | 0.41 | 0.16 |
| | Mean of 100 | 0.71 | 0.97 | 0.14 | 0.40 | 5.8 | 0.18 | 0.80 | 0.41 | 0.16 |
| ***Up to three species (n=166)*** | Best fitting spectra | 0.62 | 1.26 | 0.18 | 0.26 | 6.5 | 0.20 | 0.72 | 0.44 | 0.17 |
| | Median of 100 | 0.66 | 1.1 | 0.16 | 0.34 | 5.4 | 0.17 | 0.74 | 0.41 | 0.16 |
| | Mean of 100 | 0.66 | 1.1 | 0.16 | 0.33 | 5.4 | 0.17 | 0.74 | 0.41 | 0.16 |
| ***Up to four species (n=185)*** | Best fitting spectra | 0.59 | 1.28 | 0.18 | 0.27 | 6.8 | 0.21 | 0.70 | 0.45 | 0.18 |
| | Median of 100 | 0.64 | 1.1 | 0.16 | 0.35 | 5.3 | 0.16 | 0.72 | 0.42 | 0.16 |
| | Mean of 100 | 0.63 | 1.1 | 0.16 | 0.35 | 5.4 | 0.17 | 0.72 | 0.42 | 0.16 |

It can be seen from Table 5.5 that stratification based on the number of species has a strong influence on the estimation accuracy for the grass variables, in particular for LAI and canopy chlorophyll content. For leaf chlorophyll content, on the other hand, no trend could be observed. The estimation accuracy for LAI increased considerably, from $R^2 = 0.59$, NRMSE = 0.18 for up to four species (i.e.,

all subplots) to $R^2$ = 0.81, NRMSE = 0.11 for one species. As regards canopy chlorophyll content, the effect of species reduction was weaker (up to four species: $R^2$ = 0.70, NRMSE = 0.18; one species $R^2$ = 0.78, NRMSE = 0.16). The table also indicates that the inversion of the PROSAIL model enables grass variables to be estimated with relatively good accuracy if only canopies with up to two species are considered (LAI: $R^2$ = 0.71, NRMSE = 0.14; CCC: $R^2$ = 0.80, NRMSE = 0.16). Measured and estimated grass variables of subplots with up to two species are shown in Figure 5.5. The result suggests that the PROSAIL model is not well adapted to multi-species grasslands.

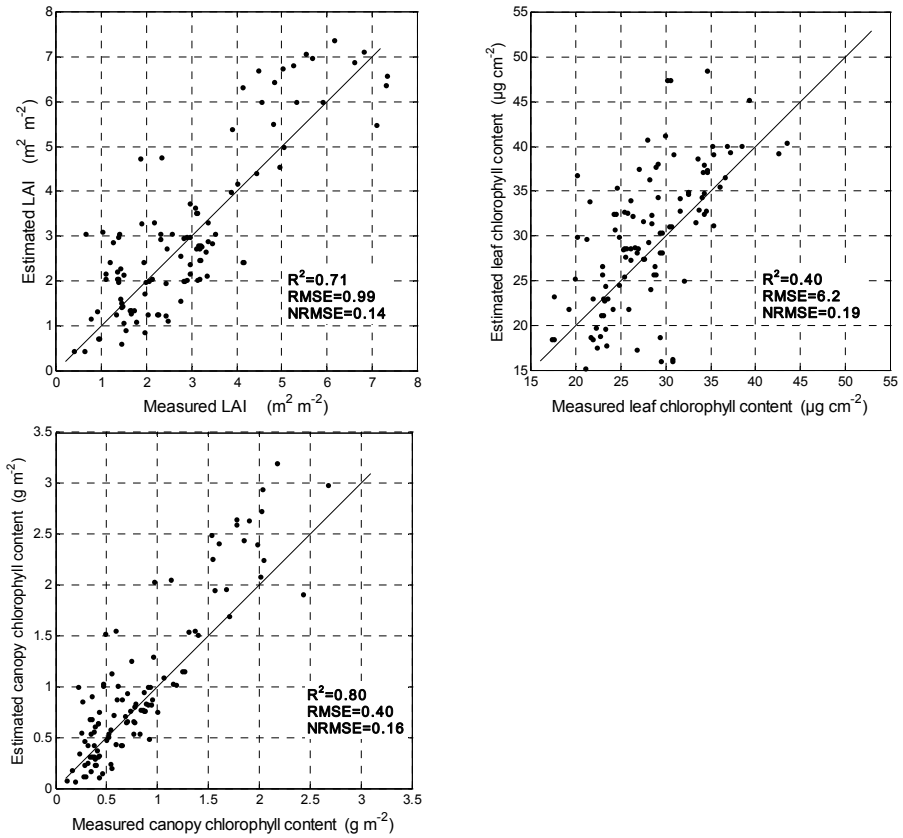


Figure 5.5. Measured versus estimated grass variables based on subplots with up to two species in Majella National Park, Italy (n=107). Top left: LAI, Top right: leaf chlorophyll content, and bottom: canopy chlorophyll content.

Figure 5.5 shows that LAI values up to 4 were better estimated than higher LAI values. It seems that canopies with LAI values greater than 4 were somehow overestimated, whereas canopies with LAI values less than 4 were slightly underestimated. This is seen in the linear relation between measured and retrieved LAI that gave a slope of 0.96 and an intercept of 0.28, and can be considered both

as model error and bias in the reference measurements. Comparison of Figures 4 and 5 reveals that larger scatter was introduced in the estimated grass variables by increasing the number of species. This again confirms that the PROSAIL model is best adapted to canopies with few species (for which it was conceived). No relationships were observed between $RMSE_r$ (best fit) and the residuals of the variables ($R^2$ = 0.008, 0.057 and 0.007 for LAI, leaf chlorophyll content and canopy chlorophyll content, respectively), indicating that the model was properly fitted.

### *5.3.5. Inversion results based on spectral sampling*

In this study, three spectral subsets have been used. Two subsets were prepared based on the results of a previous study by Darvishzadeh et al. (2008c) that included the selection of wavelengths through stepwise multiple linear regression (Table 5.6), as well as the use of a subset of wavelengths closely related to vegetation parameters identified from literature (Cho et al., 2007; Darvishzadeh et al., 2008c) (Table 5.7). The third subset was constructed based on the average absolute error (AAE) between the measured and best-fit reflectance spectra (Figure 5.3). We considered the bands with an AAE greater or equal to 0.02 as wavelengths with high errors. These bands were systematically excluded (one by one) in the inversion process, and each time the AAE between the measured and best-fit reflectance spectra was calculated until the remaining wavelengths were left with an AAE smaller than 0.02. Figure 5.6 shows the distribution of the spectral regions with an AAE greater or equal to 0.02 that were removed from the existing wavelengths. The remaining wavebands (384) were considered as our third spectral subset. Spectral subsets were prepared for the entire field data set (n=185).

The role of the spectral subsets in the estimation of grass variables was again evaluated on the basis of the $R^2$ and the (normalized) RMSE between the measured and estimated grass variables. The results showed that, compared with using all wavebands, employing spectral subset I (Table 5.6) gave significantly larger errors for LAI and leaf chlorophyll content (Table 5.8). In contrast, by employing subset II (Table 5.7) and subset III (Figure 5.6) instead of the full spectral resolution (Table 5.8), the relationships between measured and estimated LAI (and leaf chlorophyll content) were almost similar.

Table 5.6. Selected spectral sampling set (Darvishzadeh et al., 2008c) based on stepwise multiple linear regressions. The 12 wavelengths have been pooled together and are called subset I.

| *Wavelength (nm)* | *Vegetation parameters* |
|---|---|
| 440, 738, 1394, 1402, 1607 | LAI |
| 747, 748, 1425, 1660, 2391 | Canopy chlorophyll content |
| 529, 564 | Leaf chlorophyll content |

Table 5.7. Selected spectral sampling set (Cho et al., 2007; Darvishzadeh et al., 2008c) based on literature. This set of wavelengths is called subset II.

| ***Wavelength (nm)*** | ***Vegetation parameters*** | ***Reference*** |
|---|---|---|
| 466 | Chlorophyll b | Curran (1989) |
| 695 | Total chlorophyll | Gitelson and Merzlyak (1997), Carter (1994) |
| 725 | Total chlorophyll, leaf mass | Horler et al. (1983) |
| 740 | Leaf mass, LAI | Horler et al. (1983) |
| 786 | Leaf mass | Guyot and Baret (1988) |
| 845 | Leaf mass, total chlorophyll | Thenkabail et al. (2004) |
| 895 | Leaf mass, LAI | Schlerf et al. (2005), Thenkabail et al. (2004) |
| 1114 | Leaf mass, LAI | Thenkabail et al. (2004) |
| 1215 | Plant moisture, cellulose, starch | Curran (1989), Thenkabail et al. (2004) |
| 1659 | Lignin, leaf mass, starch | Thenkabail et al. (2004) |
| 2173 | Protein, nitrogen | Curran (1989) |
| 2359 | Cellulose, protein, nitrogen | Curran (1989) |

However, it seemed that the estimation accuracies between measured and estimated canopy chlorophyll content improved using all three subsets (Table 5.8). This shows that the full hyperspectral resolution is not automatically more advantageous than a carefully designed multi-spectral sensor (e.g., Fourty and Baret, 1997). For example, some bands may contain (excessively) high noise levels and therefore damage the results. The same holds for bands that, for various reasons, are not well modeled by the radiative transfer model (see Figure 5.3, the water absorption regions).

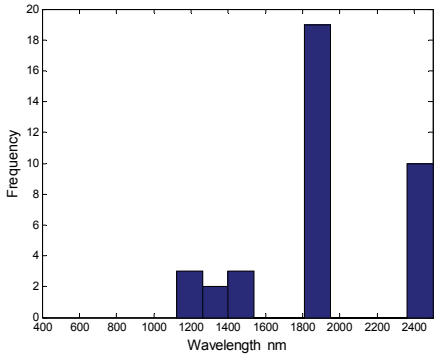


Figure 5.6. The distribution of the spectral regions with average absolute error (AAE) greater or equal to 0.02 that were removed from the existing wavelengths. The remaining 384 wavebands are called subset III.

Table 5.8. $R^2$, RMSE and normalized RMSE between measured and estimated grass canopy variables (n=185) relating to the spectral subsets. LCC is the leaf chlorophyll content, and CCC is the canopy chlorophyll content.

| ***Spectral sampling set*** | ***Statistical parameter*** | ***LAI ($m^2$ $m^{-2}$)*** | | | ***LCC ($\mu g$ $cm^{-2}$)*** | | | ***CCC (g $m^{-2}$)*** | | |
|---|---|---|---|---|---|---|---|---|---|---|
| | | ***$R^2$*** | ***RMSE*** | ***NRMSE*** | ***$R^2$*** | ***RMSE*** | ***NRMSE*** | ***$R^2$*** | ***RMSE*** | ***NRMSE*** |
| ***Using all wavelengths*** | Best fitting spectra | 0.59 | 1.28 | 0.18 | 0.27 | 6.8 | 0.21 | 0.70 | 0.45 | 0.18 |
| | Median of 100 | 0.64 | 1.1 | 0.16 | 0.35 | 5.3 | 0.16 | 0.72 | 0.42 | 0.16 |
| | Mean of 100 | 0.63 | 1.1 | 0.16 | 0.35 | 5.4 | 0.17 | 0.72 | 0.42 | 0.16 |
| ***Subset I (Table 5.6)*** | Best fitting spectra | 0.45 | 1.6 | 0.23 | 0.07 | 12.2 | 0.37 | 0.53 | 0.40 | 0.16 |
| | Median of 100 | 0.50 | 1.35 | 0.19 | 0.25 | 9.1 | 0.28 | 0.64 | 0.34 | 0.13 |
| | Mean of 100 | 0.50 | 1.37 | 0.20 | 0.28 | 8.5 | 0.26 | 0.64 | 0.34 | 0.13 |
| ***Subset II (Table 5. 7)*** | Best fitting spectra | 0.53 | 1.28 | 0.18 | 0.24 | 6.2 | 0.19 | 0.62 | 0.42 | 0.16 |
| | Median of 100 | 0.61 | 1.1 | 0.16 | 0.33 | 5.2 | 0.16 | 0.70 | 0.34 | 0.13 |
| | Mean of 100 | 0.61 | 1.1 | 0.16 | 0.32 | 5.11 | 0.16 | 0.70 | 0.35 | 0.14 |
| ***Subset III (Figure 5.6)*** | Best fitting spectra | 0.56 | 1.29 | 0.19 | 0.24 | 6.6 | 0.20 | 0.68 | 0.44 | 0.17 |
| | Median of 100 | 0.63 | 1.05 | 0.15 | 0.35 | 5.3 | 0.16 | 0.71 | 0.40 | 0.16 |
| | Mean of 100 | 0.63 | 1.05 | 0.15 | 0.34 | 5.4 | 0.17 | 0.71 | 0.40 | 0.16 |

## 5.4. Discussion

The canopy-integrated chlorophyll content (LAI x leaf chlorophyll content) strongly reflects the variability of LAI as the leaf chlorophyll content was relatively stable (Table 5.1). The inclusion of canopy chlorophyll content allows us to assess whether canopy reflectance is a better predictor of leaf or canopy chlorophyll content. Among the grass characteristics studied, canopy chlorophyll content was best retrieved by the inversion algorithm. This is probably due to the information content that exists in this variable (information regarding LAI and leaf chlorophyll content, which are known to conjointly modulate canopy reflectance). The finding is in agreement with the results of a previous study by Darvishzadeh et al. (2008c), who also found that canopy chlorophyll content was estimated with the highest accuracy among all investigated grass variables when empirical regression techniques were used.

According to Meroni et al. (2004), Schlerf and Atzberger (2006) and Verstraete et al. (1996), simple homogeneous targets may require only one-dimensional models for an accurate description of their radiation field, whereas more complex heterogeneous targets require complex three-dimensional models. This may explain the fact that the estimation accuracy in this study increased (heterogeneous grassland) when data were stratified based on the number of species. This is confirmed by the estimation accuracy for LAI in subplots with only one type of species ($R^2$ = 0.81, NRMSE = 0.14). The accuracy systematically decreased each time measurements with more (up to four) species were included in the inversion process, although this was less pronounced for canopy chlorophyll content. From a practical point of view, however, this will be difficult to implement in an operational monitoring program as this would require a mapping/knowledge of species number. The result indicates that the PROSAIL model is not well adapted to multi-species canopies. The inversion of PROSAIL under such conditions leads to a bias in the retrieved biophysical parameters. The higher estimation accuracy that may possibly be obtained through a three-dimensional model (because of its more realistic description of the reflected radiation field) is at the expense of its conceptual/computational complexity and requires a high number of input parameters.

In general, the relationships between measured and estimated leaf chlorophyll content were poor in all inversion processes. This confirms other studies revealing similar difficulties in estimating leaf chlorophyll (Baret and Jacquemoud, 1994; Curran et al., 1992). This is also in line with previous studies that have demonstrated poor signal propagation from leaf to canopy scale (Asner, 1998; Jacquemoud et al., 1996; Yoder and Pettigrew-Crosby, 1995).

According to Combal et al. (2003), three sources of prior information can be distinguished: ancillary data measured on site, knowledge of the type of canopy architecture, and knowledge of the typical distribution of canopy biophysical variables. Combal et al. (2003) as well as Meroni et al. (2004) have shown that utilizing prior information is an efficient way of solving the ill-posed problem and of improving the accuracy of the estimated canopy variables. In the case of spatialized (remote sensing) data, Atzberger (2004) showed that for mono-species canopies the intercorrelation between spectral bands also helps to constrain the ill-posed inverse problem. Extensive field measurement in this study allowed us to identify the maximum and minimum values for the three parameters *LAI, LCC* and *ALA*, which increased the sampling density and facilitated the estimation of grass biophysical characteristics.

For several sample plots at least one of the other 6 retrieved parameters ($C_m$, $C_w$, *scale, ALA, hot* and *N*) reached the upper/lower boundary. We argue that the possible reason is that some wavelengths are either badly measured or not well modeled by the combined SAILH and PROSPECT canopy reflectance model. Similar results have been found by Schlerf & Atzberger (2006) who demonstrated

that the PROSPECT leaf optical properties model is not simulating equally well the leaf optical properties across the 400-2500 nm wavelength range. The possible explanation of too restricted parameter ranges can be excluded as much wider ranges did not ameliorate the results (e.g. LAI: $R^2 = 0.37$, RMSE = 2.46; CCC: $R^2 = 0.56$, RMSE = 1.27).

Selecting subsets of wavelengths derived by Darvishzadeh et al. (2008c) from stepwise linear regression gave significantly higher errors for LAI and leaf chlorophyll content. This was not the case when the selection was based on literature results (subset II) or when only those wavelengths were chosen which were "well" modeled by PROSAIL (subset III). In these cases results similar to those obtained using all wavebands were obtained. The band selection from literature worked well, probably because we only considered wavelengths related to both biophysical and biochemical properties of vegetation, thus maximizing the information content in the input variables while eliminating all other wavelengths that introduce noise and model errors. Similarly, by eliminating wavelength having a high AAE (subset III), we eliminated noisy/badly modeled wavelengths. In the present study, we did not test whether including in the cost function the reflectance uncertainty matrix as shown for example by Lavergne et al. (2007) would improve the results. This would require to run the LUT inversion several times and to use boot-strap techniques to avoid loosing independency between measured and estimated biophysical variables.

It has been demonstrated (Meroni et al., 2004; Schlerf and Atzberger, 2006) that the selection of a few wavebands will give often better results than those achieved using the full spectral resolution. The results in the present study (when using all bands) indicated a relatively good representation of the measured spectra by the PROSAIL model over most spectral regions (see Figures 5.2 and 5.3). Consequently, spectral subsetting did not clearly improve the parameter retrieval.

The results of this study confirm that grass canopy characteristics such as leaf area index and canopy chlorophyll content can be estimated through the inversion of a radiative transfer model using hyperspectral measurements with accuracies comparable to those of statistical approaches (Darvishzadeh et al., 2008c), which is also supported by previous studies (Gemmell et al., 2002; Schlerf and Atzberger, 2006). In contrast to statistical approaches, ground measured biophysical data may be almost entirely used for validating the retrieved model parameters (and to set the LUT ranges) and are not used to calibrate the radiative transfer model (except the soil reflectance spectra which has to be input into the radiative transfer model). Once an appropriate LUT has been built, it can in principle be applied to different remote sensing data acquired over similar vegetation types.

## 5.5. Conclusion

This study selected the widely used PROSAIL model to describe the radiation transfer in a heterogeneous Mediterranean grassland for use with hyperspectral data. For fast model inversion, a LUT approach was used. The LUT was built taking into account prior knowledge regarding *LAI, LCC* and *ALA* measured in the field. The accuracies of the retrieved vegetation variables are discussed on the basis of (i) the role of different ways of selecting the solution from the LUT (i.e., the best fitting spectra against the mean/median of the best 10 to 100 solutions), (ii) the stratification of data based on species heterogeneity, and (iii) the influence of spectral subsetting. We have demonstrated that the retrieval of canopy chlorophyll content and LAI at canopy level is feasible. However, accuracy decreases if the number of species within a subplot increases. This shows that the selected radiative transfer model is not well adapted to multi-species canopies.

Several authors have used the PROSAIL model in homogeneous crop canopies. Its applicability to heterogeneous grasslands requires further experiments and validation work using different hyperspectral data sets. In this way scale and sensor effects as well as phenological influences can be studied. These factors may lead to (partially) different results.

Unfortunately, the turbid medium assumption used in this model does not account for heterogeneities in the canopies (e.g., clumping effects, multiple leaf layers having different optical characteristics). Therefore, when the turbid medium hypotheses are violated, the model cannot realistically simulate the canopy reflectance, and the retrieved biophysical variables are expected to be biased (Meroni et al., 2004). Improvement in parameter retrieval may be expected from models that explicitly take into account canopy heterogeneities such as vertical leaf color gradient and clumping effects (e.g., Verhoef and Bach, 2007). However, heterogeneity is a relative term and is strongly scale dependent. Further studies are required to cope with the ill-posed inverse problem when inverting physically based radiative transfer models (e.g., Durbha et al. 2007).

## Acknowledgements

We would like to acknowledge the assistance of the park management of Majella National Park, Italy, and in particular of Dr. Teodoro Andrisano. Special thanks go to Prof. Herbert Prins, Dr. Fabio Corsi, Dr. Sip van Wieren, Dr. Moses Cho and Dr. Istiak Sobhan for their assistance during the field campaign. The comments of the two anonymous reviewers have been very helpful in improving the manuscript.

# Chapter Six

## Airborne level

# Mapping vegetation biophysical properties in a Mediterranean grassland with airborne hyperspectral imagery: from statistical to physical models

*This chapter is based on:*

Darvishzadeh, R., Atzberger, C., Schlerf, M., Skidmore, A. and Prins, H., 2008. Mapping vegetation biophysical properties in a Mediterranean grassland with airborne hyperspectral imagery: from statistical to physical models. *Remote Sensing of Environment*, **In Review (after revision)**.

## Abstract

Statistical and physical models have seldom been compared in studying grasslands. In this chapter, both modeling approaches are investigated for mapping LAI and canopy chlorophyll contents in a Mediterranean grassland using hyperspectral images. HyMap airborne images were acquired over Majella National Park, Italy, in early July 2005. *In situ* measurements of LAI and leaf chlorophyll content were collected during a field campaign concomitant with the time of image acquisition. We compared inversion of the PROSAIL radiative transfer model with narrow band vegetation indices and partial least squares regression. To assess the performance of the investigated models, the RMSE and $R^2$ between *in situ* measurements and estimated parameters are reported. The results of the study demonstrate that the investigated biophysical grass canopy characteristics can be estimated through the inversion of a radiative transfer model with accuracies comparable to those of statistical approaches. Inversion of the PROSAIL model yielded high accuracies for LAI ($R^2$=0.91, normalized RMSE=0.08) and for canopy chlorophyll content ($R^2$=0.87, normalized RMSE=0.10). We found that a carefully selected spectral subset contains sufficient information for a successful radiative transfer model inversion. The advantage of physical models is that field measurements are not required for model calibration. Our results confirm that biophysical vegetation properties of Mediterranean grasslands can be accurately determined from remote sensing.

## 6.1. Introduction

Hyperspectral remote sensing measurements have enhanced the estimation of vegetation biophysical and biochemical characteristics (Ferwerda et al., 2005; Lee et al., 2004; Mutanga and Skidmore, 2004; Schlerf et al., 2005). Mapping and monitoring these characteristics is important for spatially distributed modeling of vegetation productivity, water and CO2 exchange, and surface energy balance (Pu et al., 2003; Turner et al., 1999). Among the many vegetation characteristics, leaf area index (LAI) and canopy chlorophyll content (CCC) are of prime importance (Bacour et al., 2006; Chen et al., 2002; Hansen and Schjoerring, 2003; Houborg et al., 2007). LAI, defined as one-sided leaf area divided by unit of horizontal surface area, is a key structural characteristic of vegetation because of the role of green leaves in controlling many biological and physical processes in plant canopies. Canopy chlorophyll content (defined as the product of LAI and leaf chlorophyll content) contributes to verifying vegetation physiological status and health, and has been found useful for detecting vegetation stress, photosynthetic capacity, and productivity (e.g., Boegh et al., 2002; Carter, 1994).

In general, there are two common approaches to estimating vegetation biophysical and biochemical characteristics from remotely sensed data (Atzberger, 1997; Liang, 2004). The statistical approach is associated with computation of

spectral vegetation indices or the use of several spectral bands in multiple (linear) regression models. The physical approach involves radiative transfer models (RTM) that describe, based on physical laws, the spectral/directional variation of canopy reflectance as a function of canopy, leaf and soil background characteristics (Goel, 1989; Liang, 2004). Both approaches have advantages and disadvantages. While statistical approaches are fast and easy to implement, the derived relationships are recognized as being sensor-specific and dependent on site and sampling conditions, and are expected to change in space and time (Baret and Guyot, 1991; Colombo et al., 2003; Gobron et al., 1997; Meroni et al., 2004). Conversely, radiative transfer models explaining the transfer and interaction of radiation inside the canopy, and hence offering an explicit connection between the vegetation biophysical and biochemical variables and the canopy reflectance (Houborg et al., 2007), are computationally more complicated and usually require additional input variables. Another drawback in using physically based models is the ill-posed nature of model inversion (Atzberger, 2004; Combal et al., 2002), meaning that the inverse solution is not always unique as various combinations of canopy parameters may yield almost similar spectra (Weiss and Baret, 1999).

Numerous efforts to estimate and quantify vegetation properties by using remote sensing and either statistical or physically based approaches have been carried out in the last decades. Many of the previous studies, however, investigated homogeneous vegetation with typically one type of species, for example, agricultural crops (Atzberger, 2004; Atzberger et al., 2003a; Baret et al., 1987; Broge and Mortensen, 2002; Colombo et al., 2003; Danson et al., 2003; Jacquemoud et al., 2000; Walter-Shea et al., 1997) or forests (Chen et al., 1997; Disney et al., 2006; Fang et al., 2003; Gemmell et al., 2002; Kalacska et al., 2004; Meroni et al., 2004; Schlerf and Atzberger, 2006; White et al., 1997; Zarco-Tejada et al., 2004), or they were based on simulated data (Broge and Leblanc, 2001; Chaurasia and Dadhwal, 2004; Haboudane et al., 2004; Weiss et al., 2000). More research is required to assess the capability of different remote sensing retrieval algorithms in regard to heterogeneous (multiple species) grassland canopies. Mediterranean grasslands are characterized by highly heterogeneous canopies with a combination of different plant species in varying proportions, and appear to be challenging to remote sensing application as the reflectance is often a mixture of different surface materials (Fisher, 1997; Roder et al., 2007).

The main objective of this study was to estimate and predict prime canopy characteristics such as LAI and canopy chlorophyll content in a heterogeneous Mediterranean grassland using both statistical and radiative transfer models. The study is based on airborne HyMap (Hyperspectral Mapping imaging spectrometer) hyperspectral images acquired in parallel with field reference measurements collected during a field campaign in summer 2005 in Majella National Park, Italy. The suitability of the methods is analyzed in terms of their prediction accuracy for estimating of LAI and canopy chlorophyll content.

## 6.2. Material

### 6.2.1. Study area and sampling

The study site is located in Majella National Park, Italy (latitude 41°52' to 42°14'N, longitude 13°14' to 13°50'E). The park covers an area of 74,095 ha and extends into the southern part of Abruzzo, at a distance of 40 km from the Adriatic Sea. The region is situated in the massifs of the Apennines. The park is characterized by several mountain peaks, the highest being Mount Amaro (2794 m). Geologically, the region is made up of calcareous rocks, which date back to the Jurassic period. The flora of the park includes more than 1800 plant species, which approximately constitute one third of the entire flora in Italy (Cimini, 2005).

Abandoned agricultural areas and settlements in Majella are returning to oak (*Quercus pubescens*) woodlands at the lower altitude (400 m to 600 m) and beech (*Fagus sylvatica*) forests at higher altitudes (1200 m to 1800 m). Between these two formations is a landscape composed of shrubby bushes, patches of grass/herb vegetation, and bare rock outcrops. The dominant grass and herb species include *Brachypodium genuense, Briza media, Bromus erectus, Festuca* sp, *Helichrysum italicum, Galium verum, Trifolium pratense, Plantago lanceolata, Sanguisorba officinalis* and *Ononis spinosa* (Cho, 2007).

Stratified random sampling with clustering was adopted in this study. For this purpose, the area was stratified into grassland, forest, shrubland and bare rock outcrops using a land cover map provided by the management of Majella National Park. We distinguish four main phytosociological classes of varying areas within the grasslands: semi-natural/farmlands, grazed/periodically flooded areas, open garrigues and abandoned farmlands. Coordinates (x y) were randomly generated in the grassland stratum to select plots. A total of 45 plots of 30 m x 30 m were generated and a GPS (Global Positioning System) was used to locate them in the field. For each plot, the relevant biophysical and biochemical parameters were measured within four to five randomly selected subplots (1 m x 1 m) and their averages per plot were calculated. The various plots were covered with different species compositions and relative abundances, while the within-plot variability was small. The species varied in terms of leaf shape, leaf size, the number of leaves and their typical angle distribution. The within-plot variability of SPAD measurements also indicated some variation in chlorophyll contents, albeit this has not been quantified within the present study.

### 6.2.2. LAI measurements

In each subplot, LAI was non-destructively measured using a widely used optical instrument, the Plant Canopy Analyzer LAI-2000 (LICOR Inc., Lincoln, NE, USA). A detailed description of this instrument is given by LI-COR (1992) and Welles and Norman (1991). Measurements were taken either under clear skies

with low solar elevation (i.e., within two hours after sunrise or before sunset, respectively) or under overcast conditions. To prevent direct sunlight on the sensor, samples of below- and above-canopy radiation were made with the sun behind the operator and using a view restrictor of 45°. For each subplot, reference samples of above-canopy radiation were taken by measuring incoming radiation above the grass subplot. Next, five below-canopy samples were collected, from which the average subplot LAI was calculated.

LAI measured using LAI-2000 corresponds to plant area index (PAI), including the photosynthetic and non-photosynthetic components (Chen et al., 1997). In our study, non-photosynthetic components were almost non-existent. Despite the non-random distribution of grass leaves, no corrections for clumping were applied. Therefore, LAI used here corresponds to effective PAI, and in the following sections these measurements are abbreviated as LAI.

### *6.2.3. Chlorophyll measurements*

In each 1 m x 1 m subplot, a SPAD-502 Leaf Chlorophyll Meter (Minolta, Inc.) was used to assess leaf chlorophyll content. SPAD values express relative amounts of chlorophyll in leaves by measuring transmittance in the red (650 nm) and NIR (920 nm) wavelength regions (Minolta, 2003). SPAD measurements give a unitless but highly reproducible measure that is well correlated with leaf chlorophyll concentration, and is commonly used to characterize chlorophyll concentration in many plant species (Campbell et al., 1990; Haboudane et al., 2002; Jongschaap and Booij, 2004; Nakano et al., 2006). A total of 30 leaves representing the dominant species were randomly selected in each subplot, and their SPAD readings were recorded. From the 30 individual SPAD measurements, the average was calculated. These averaged SPAD readings (unitless) were converted into leaf chlorophyll contents (μg $cm^{-2}$) by means of an empirical calibration function provided by Markwell et al. (1995). Although the Markwell function refers to soybean and corn leaves, the same authors have demonstrated that it can also be applied to other plant species (Markwell et al., 1995). Hence, we decided not to establish specific calibration functions for the grass species, since each sample plot consists of several species. The total canopy chlorophyll content (g $m^{-2}$) for each subplot was obtained by multiplying the leaf chlorophyll content by the corresponding LAI.

### *6.2.4. Image acquisition and pre-processing*

Airborne HyMap data of the study site were acquired on 4 July 2005. The flight was carried out by DLR, Germany's Aerospace Research Centre and Space Agency. The HyMap sensor contained 126 wavelengths, operating over the spectral range of 436 nm to 2485 nm. The average spectral resolutions were 15 nm for 436 nm to 1313 nm, 13 nm for 1409 nm to 1800 nm, and 17 nm for 1953 nm to 2485 nm. The spatial resolution of the data was 4 m (average flight height 1983

m above ground). The images were taken concomitant with the field campaign. The data were collected in four image strips, each covering an area of about 40 km by 2.3 km. The image acquisition was close to solar noon and the solar zenith and azimuth angles for the four image strips ranged between 30º to 33.7º and 111.5º to 121º, respectively.


Figure 6.1. True color composite of HyMap image acquired on 4 July 2005 (bands 634, 542 and 452 nm) showing part of the study area (Majella National Park, Italy). The red points demonstrate the distribution of sample plots in this part of the study area.

The image strips were atmospherically and geometrically (sub-pixel accuracy) corrected by DLR. The atmospheric correction was performed using ATCOR4-r (Atmospheric and Topographic Correction software, rugged terrain), which is based on the MODTRAN-4 (MODerate spectral resolution atmospheric TRANsmittance) radiative transfer code. However, effects related to the sensor's large field of view in across-track direction (Schiefer et al., 2006) were not accounted for, resulting in some visible artifacts towards the borders of the strips. Conversely, our sample plots were located mainly in the central parts of the images (Figure 6.1).

The corrected strips were used to retrieve the spectra of each sample plot. As the pixel size of the images was 4 m, a 7 x 7 pixel window (i.e., 28 m x 28 m) centered around the central position of a plot was used for collecting grass spectra from each sample plot (30 m x 30 m). By taking only pixels located entirely in the

plot, we avoided border effects. From the 7 x 7 pixel window, the average spectrum was calculated. Owing to cloud coverage in some portions of the strips, the spectra of four of the 45 plots could not be extracted. Hence, only the remaining 41 plots were considered for the analysis. Table 6.1 summarizes the statistics of the measured variables for these plots.

Table 6.1. Summary statistics of the measured biophysical and biochemical variables of grassland sample plots (n=41). SPAD is the average SPAD reading for 120 to 150 randomly selected leaves in each plot. To derive leaf chlorophyll content from SPAD readings, the Markwell et al. (1995) formulas have been used. CCC is the canopy chlorophyll content, being the product of LAI and leaf chlorophyll content.

| *Measured variables* | *Min* | *Mean* | *Max* | *StDev* | *Range* | *Variation coefficient* |
|---|---|---|---|---|---|---|
| ***LAI ($m^2$ $m^{-2}$)*** | 0.72 | 2.87 | 7.54 | 1.59 | 6.8 | 0.55 |
| ***SPAD (unitless)*** | 24.2 | 32.7 | 41.0 | 3.7 | 16.9 | 0.12 |
| ***Leaf chlorophyll (µg $cm^{-2}$)*** | 18.9 | 28.7 | 40.9 | 4.7 | 22.0 | 0.16 |
| ***CCC (g $m^{-2}$)*** | 0.21 | 0.86 | 2.3 | 0.56 | 2.10 | 0.65 |
| ***Dominant species number*** | 1 | 2.34 | 4 | 0.81 | 3 | 0.35 |

## 6.3. Methods

We investigated radiative transfer model inversion and two statistical modeling techniques (narrow band vegetation indices and partial least squares regression) to estimate the LAI and canopy chlorophyll content of the studied grasslands.

### *6.3.1. The narrow band vegetation indices*

Narrow band indices were computed from the extracted HyMap spectra using all possible two-band combinations, involving 126 wavelengths between 436 nm and 2485 nm. The normalized difference vegetation index (NDVI) (Rouse et al., 1974) as a representative of ratio indices, and the second soil-adjusted vegetation index (SAVI2) (Major et al., 1990) as a representative of soil-based indices were selected for analysis. These two vegetation indices have been shown to perform best for estimating vegetation biophysical characteristics computed from field spectra (Darvishzadeh et al., 2008a).

The narrow band NDVI and SAVI2 indices were systematically calculated for all possible 126 x 126 = 15,876 wavelength combinations between 436 nm and 2485 nm. The NDVI was computed according to:

$$NDVI_{narrow} = \frac{\rho_{\lambda 1} - \rho_{\lambda 2}}{\rho_{\lambda 1} + \rho_{\lambda 2}} \quad \text{(Eq. 1)}$$

Where $\rho_{\lambda 1}$ is the reflectance at wavelength $\lambda 1$ and $\rho_{\lambda 2}$ is the reflectance at wavelength $\lambda 2$ with $\lambda 1 \neq \lambda 2$.

The narrow band SAVI2 was calculated according to the following formula:

$$SAVI2_{narrow} = \frac{\rho_{\lambda 1}}{\rho_{\lambda 2} + (b/a)} \quad \text{(Eq. 2)}$$

Where $\rho$ is the reflectance, *a* is the slope and *b* is the intercept of the soil line between bands at wavelengths $\lambda_1$ and $\lambda_2$.

The soil line parameters *a* and *b* were calculated from field spectral measurements of the bare soils of a few plots with no vegetation (Darvishzadeh et al., 2008c). They were systematically calculated for all possible band combinations (126 x 126). We assumed that the measured soil optical properties were representative for the study area. Consequently, the soil line parameters were considered constant for all 41 plots. Implicitly, we assumed that the soil line concept, originally defined for the red-NIR feature space, could be transferred to other spectral domains (Darvishzadeh et al., 2008a; Schlerf et al., 2005; Thenkabail et al., 2000).

### *6.3.2. Partial least squares regression*

Partial least squares regression (PLSR) is a technique that reduces the large number of measured collinear spectral variables to a few non-correlated latent variables or factors while maximizing co-variability to the variable(s) of interest (Atzberger et al., 2003b; Cho et al., 2007; Geladi and Kowalski, 1986; Hansen and Schjoerring, 2003; Williams and Norris, 1987). The latent variables contain the relevant information present in the measured reflectance spectra and are used to predict the dependent variables (here, biophysical and biochemical grass characteristics).

As with other linear calibration methods, in partial least squares regression the aim is to build a linear model:

$$Y = X\beta + \varepsilon \quad \text{(Eq. 3)}$$

where Y is the mean-centered vector of the response variable (grass characteristics), X is the mean-centered matrix of the predictor (spectral reflectance), $\beta$ is the matrix of coefficients, and $\varepsilon$ is the matrix of residuals. Partial

least squares regression is closely related to principal component regression (Geladi and Kowalski, 1986). Whereas principal component regression performs the decomposition on the spectral data alone, partial least squares regression uses the response variable information during the decomposition process and performs the decomposition on both the spectral data and the response variable simultaneously (Schlerf et al., 2003). Valuable descriptions of the partial least squares regression algorithm are given in Ehsani et al. (1999), Geladi and Kowalski (1986), and Williams and Norris (1987).

In conditions where highly correlated input variables (spectral reflectances) are included in the model, an appropriate variable selection is known to improve partial least squares regression models (Cho et al., 2007; Darvishzadeh et al., 2008c; Davies, 2001; Kubinyi, 1996; Martens and Martens, 2000; Schmidtlein and Sassin, 2004), especially if the noisy wavelengths are excluded. Partial least squares regression was applied to the entire reflectance spectra (436 nm to 2485 nm) and to a subset of wavelengths used by Cho et al. (2007) and Darvishzadeh et al. (2008c) specifically related to certain vegetation parameters (Table 6.2).

Table 6.2. Subset of wavelengths for estimating grass characteristics using partial least squares regression and radiative transfer model inversion.

| ***Wavelength (nm)*** | ***Vegetation parameters*** | ***Reference*** |
|---|---|---|
| 466 | Chlorophyll b | Curran (1989) |
| 695 | Total chlorophyll | Gitelson and Merzlyak (1997), Carter (1994) |
| 725 | Total chlorophyll, leaf mass | Horler et al. (1983) |
| 740 | Leaf mass, LAI | Horler et al. (1983) |
| 786 | Leaf mass | Guyot and Baret (1988) |
| 845 | Leaf mass, total chlorophyll | Thenkabail et al. (2004) |
| 895 | Leaf mass, LAI | Schlerf et al. (2005), Thenkabail et al. (2004) |
| 1114 | Leaf mass, LAI | Thenkabail et al. (2004) |
| 1215 | Plant moisture, cellulose, starch | Curran (1989), Thenkabail et al. (2004) |
| 1659 | Lignin, leaf mass, starch | Thenkabail et al. (2004) |
| 2173 | Protein, nitrogen | Curran (1989) |
| 2359 | Cellulose, protein, nitrogen | Curran (1989) |

The optimum number of latent factors was estimated by leave-one-out cross-validation. A common way of using cross-validation for this estimation is to select the number of factors that minimizes the root mean square error (RMSE) between

measured and predicted values (Geladi and Kowalski, 1986). To prevent collinearity and to preserve model parsimony, the condition for adding an extra factor to the model was that it had to reduce the RMSE of cross-validation ($RMSE_{CV}$) by >2% (Cho et al., 2007; Darvishzadeh et al., 2008c; Kooistra et al., 2004). In addition, coefficients of determination ($R^2$) between measured and predicted values in the cross-validation were used to evaluate the relationships found. The partial least squares analysis was performed using the TOMCAT toolbox 1.01 within MATLAB (Daszykowski et al., 2007).

### *6.3.3. Validation of statistical techniques*

Statistical models can be evaluated using two common types of validation procedure: (i) validation based on an independent test data set, and (ii) cross-validation (also called the leave-one-out method). The general applicability of both validation techniques has been analyzed in previous studies and shown to produce similar results (Darvishzadeh et al., 2008c; Selige et al., 2006). In this study we used the cross-validation procedure, which yields reproducible and statistically sound results. In cross-validation, each sample is estimated by the remaining samples. This meant that for each variant we developed 41 individual models, each time with data from 40 observations. The calibration model was then used to predict the observation that was left out. The resulting cross-validated RMSE ($RMSE_{cv}$) was selected as the accuracy indicator of the model in predicting unknown samples.

### *6.3.4. The PROSAIL radiative transfer model*

The widely used PROSAIL radiative transfer model was selected for physically based canopy parameter retrieval. PROSAIL is a combination of the SAILH canopy reflectance model and the PROSPECT leaf optical properties model. Both sub-models are relatively simple and need only a limited number of input parameters with reasonable computation time, which makes model inversion for retrieval of leaf and canopy parameters feasible.

The PROSPECT model (Fourty et al., 1996; Jacquemoud and Baret, 1990; Jacquemoud et al., 1996) calculates the leaf hemispherical transmittance and reflectance as a function of four input parameters: the leaf structural parameter $N$ (unitless); the leaf chlorophyll $a + b$ concentration $LCC$ (μg $cm^{-2}$); the dry matter content $C_m$ (g $cm^{-2}$); and the equivalent water thickness $C_w$ (g $cm^{-2}$). The spectral leaf optical properties (leaf reflectance and transmittance) calculated by PROSPECT are inputs into the SAILH canopy reflectance model. This model (Verhoef, 1984; Verhoef, 1985) is a one-dimensional bidirectional turbid medium radiative transfer model that has been later modified to take into account the hot spot effect in plant canopy reflectance (Kuusk, 1991). Turbid medium defines the canopy as a horizontally homogenous and semi-infinite layer that consists of small

vegetation elements that act as absorbing and scattering particles of a given geometry and density. Consequently, the model is best adopted for use in homogeneous vegetation canopies (Meroni et al., 2004; Schlerf and Atzberger, 2006; Verhoef, 1984). Apart from the leaf reflectance and transmittance, the SAILH model requires eight input parameters to simulate the top-of-canopy bidirectional reflectance. These are sun zenith angle, $t_s$ (deg); sensor viewing angle, $t_o$ (deg); relative azimuth angle between sensor and sun, *phi* (deg); fraction of diffuse incoming solar radiation, *skyl*; background reflectance (soil reflectance) for each wavelength, *rsl*; *LAI* ($m^2$ $m^{-2}$); average leaf inclination angle, *ALA* (deg); and the hot spot size parameter, *hot* (m $m^{-1}$), defined as the ratio between the average size of the leaves and the canopy height (Verhoef, 1985). To account for the changes induced by moisture and roughness in soil brightness, we used a soil brightness parameter, *scale* (Atzberger et al., 2003a). Therefore, in PROSAIL 12 input parameters that characterize the leaf, the canopy and the soil have to be specified. Of the 12 input parameters, four parameters, (sensor viewing angle, azimuth angle, sun zenith angle and fraction of diffuse incoming solar radiation) were fixed. For the eight remaining input parameters (i.e., *LAI, ALA, scale, hot, N, LCC,* $C_m$ and $C_w$), 100,000 parameter sets were generated randomly (Darvishzadeh et al., 2008b) (Table 6.3).

#### 6.3.4.1. The look-up table (LUT) inversion

Perhaps the simplest method of solving the inversion of a radiative transfer model is by using a look-up table (LUT). LUTs offer an interesting alternative to numerical optimization and neural network methods because they permit a global search (avoiding local minima) while showing less unexpected behavior when the spectral characteristics of the targets are not well represented by the modeled spectra (Schlerf and Atzberger, 2006). A LUT is built in advance of the actual inversion through forward calculations using the radiative transfer model. For the inversion, only search operations are needed to identify the parameter combinations that yield the best fit between measured and LUT spectra. However, to achieve high accuracy for the estimated parameters, the dimension of the table must be large enough (Combal et al., 2002; Tang et al., 2006; Weiss et al., 2000).

To build the LUT, 100,000 parameter combinations were randomly generated (uniform distributions) and used in the forward calculation of the PROSAIL model. We also tested normally distributed random parameters and found no significant differences (not shown). The ranges (minimum and maximum) for each of the eight "free" model parameters are reported in Table 6.3. To prevent too-wide parameter spaces and to reduce the size of the parameter spacing, the maximum and minimum values of *LAI, LCC* and *ALA* (recorded along with LAI, using the LAI-2000 instrument) were fixed based on prior knowledge from the field data collection (Combal et al., 2003; Darvishzadeh et al., 2008b). The leaf parameters *N,* $C_m$ and $C_w$ are often fixed at nominal values (e.g., Chaurasia and

Dadhwal, 2004; Haboudane et al., 2004; Houborg et al., 2007; le Maire et al., 2004). For the leaf structural parameter *N* of PROSPECT, Haboudane et al. (2004) and Houborg et al. (2007) used a fixed value of 1.55 for various crops, including corn, soybean, wheat and spring barley. Jacquemoud et al. (2000) used a fixed value of $N$=1.7 for soybean, while Atzberger et al. (2003a) used a range of $N$=2 ± 0.34 for wheat crop. Since grasses have relatively thin leaves, we used a range of 1.5 to 1.9 for the *N* parameter (Darvishzadeh et al., 2008b). The ranges of other input parameters ($C_w$, $C_m$, *hot* and *scale*) were similarly selected in agreement with the existing literature (Cho, 2007; Combal et al., 2003; Darvishzadeh et al., 2008b; Haboudane et al., 2004; le Maire et al., 2004; Schlerf and Atzberger, 2006). We used the measured average bare soil reflectance spectra of the study area to represent soil optical properties. Since most of the plots were located close to the nadir line of the image strips, the sensor viewing angle ($t_o$) and the relative azimuth angle (*phi*) were fixed at 0º. The sun zenith angle was fixed at 31.5º. With respect to the fraction of diffuse incoming solar radiation (*skyl),* a fixed value of 0.1 across all wavelengths was used, as in many similar studies (Cho, 2007; Darvishzadeh et al., 2008b; Schlerf and Atzberger, 2006). Hence, we have neglected the fact that the amount of diffuse sky light depends on atmospheric conditions and solar zenith angle, and, furthermore, is wavelength-dependent. This simplification seems justified, however, by the fact that *skyl* has only a very small influence on canopy reflectance (Clevers and Verhoef, 1991) and by the lack of on-site measurements of *skyl*.

Table 6.3. Specific ranges for nine input parameters used for generating the LUT, using forward calculation of the PROSAIL model. Within the specified ranges, parameter values were drawn randomly (uniform distributions).

| ***Parameter*** | ***Abbreviation in model*** | ***Unit*** | ***Minimum value*** | ***Maximum value*** |
|---|---|---|---|---|
| ***Leaf area index**** | *LAI* | $m^2\ m^{-2}$ | 0 | 8 |
| ***Mean leaf inclination angle**** | *ALA* | deg | 40 | 70 |
| ***Leaf chlorophyll content**** | *LCC* | $\mu g\ cm^{-2}$ | 15 | 45 |
| ***Leaf structural parameter*** | *N* | no dimension | 1.5 | 1.9 |
| ***Dry matter content*** | $C_m$ | $g\ cm^{-2}$ | 0.005 | 0.010 |
| ***Equivalent water thickness*** | $C_w$ | $g\ cm^{-2}$ | 0.01 | 0.02 |
| ***Hot spot size*** | *hot* | $m\ m^{-1}$ | 0.05 | 0.10 |
| ***Soil brightness*** | *scale* | no dimension | 0.5 | 1.5 |

* The minimum and maximum values are selected based on prior knowledge from the field and measurement geometry.

To find the solution to the inverse problem for a given canopy spectra, for each modeled reflectance spectra of the LUT the root mean square error between measured and modeled spectra ($RMSE_r$) is calculated according to:

$$RMSE_r = \sqrt{\frac{\sum_{i=1}^{n}(R_{measured\ \lambda} - R_{lut\ \lambda})^2}{n}} \qquad \text{(Eq. 4)}$$

where $R_{measured}$ is the measured reflectance at wavelength λ, $R_{lut}$ is the modeled reflectance at the same wavelength in the LUT, and $n$ is the number of wavebands. Traditionally, the solution is regarded as the set of input parameters corresponding to the reflectance in the LUT which provides the smallest $RMSE_r$. However, this solution is not always the optimal solution since it may not be unique (ill-posed problem) (Atzberger, 2004). To overcome this problem and to enhance the consistency of the estimated variables, we also investigated the mean and median from the best 10 and 100 simulations, respectively (Combal et al., 2003; Darvishzadeh et al., 2008b).

An appropriate band selection – or alternatively the weighting of different spectral bands – is known to improve radiative transfer model inversion and prevents bias in the estimation of the variables of interest (Bacour et al., 2001; Fang et al., 2003; Lavergne et al., 2007; Meroni et al., 2004; Schlerf and Atzberger, 2006). This is particularly the case if the hyperspectral data set contains wavebands that are either noisy or poorly modeled by the radiative transfer model being inverted. Neither the selection of an optimal spectral subset nor the weighting of spectral bands is a trivial problem, and these are still open issues within the remote sensing community (Lavergne et al., 2007; Meroni et al., 2004). Therefore, to account for band selection the inversion of the model was also tested with a small number of pre-defined bands related to leaf chlorophyll, LAI and leaf mass (Table 6.2) (Cho et al., 2007; Darvishzadeh et al., 2008b; Darvishzadeh et al., 2008c).

The reported values of RMSE and $R^2$ statistics differ. For the statistical models we report the cross-validated $RMSE_{cv}$ and $R^2_{cv}$, and for the radiative transfer model inversion we report values of RMSE and $R^2$ derived from fully independent validation.

## 6.4. Results

### *6.4.1. Narrow band vegetation indices*

NDVI and SAVI2 narrow band indices were calculated from the HyMap reflectance spectra, using all possible two-band combinations. The coefficients of determination ($R^2$) between these narrow band vegetation indices and the grass canopy characteristics were computed. An illustration of these results is shown for

LAI in the 2-D correlation plot in Figure 6.2. The meeting point of each pair of wavelengths in a 2-D plot corresponds to the $R^2$ value of the LAI and the vegetation index calculated from the HyMap reflectance values in those two wavelengths. Similar correlation plots were computed for canopy chlorophyll content (not shown). Based on the $R^2$ values in the 2-D correlation plots, band combinations that formed the best indices were determined for LAI and canopy chlorophyll content. The best performing indices and the band positions are tabulated in Table 6.4.

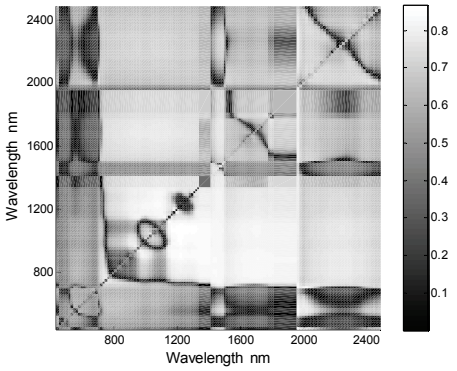


Figure 6.2. 2-D correlation plots illustrating the coefficient of determination ($R^2$) between narrow band SAVI2 and LAI. The 2-D correlation plot is not symmetrical. The Y axis is the nominator and the X axis is the denominator in Eq. 2.

In general, the coefficients of determination between the grass characteristics and the two narrow band indices were relatively high. The narrow band SAVI2 had somewhat higher correlations with the studied variables than did the narrow band NDVI (Table 6.4). This indicates a slight advantage of soil-based indices over ratio indices.

The "optimum" bands for LAI estimation were found in the NIR and SWIR regions. This confirms previous studies that have demonstrated that the bands from these regions are important for LAI estimation (Brown et al., 2000; Cohen and Goward, 2004; Darvishzadeh et al., 2008a; Darvishzadeh et al., 2008c; Lee et al., 2004; Nemani et al., 1993; Schlerf et al., 2005). The "optimum" bands for canopy chlorophyll content were also found mainly in the NIR and SWIR regions, albeit chlorophyll does not absorb outside the visible range. This artifact can be explained by the strong influence of LAI on canopy chlorophyll (LAI x leaf chlorophyll) since, in comparison with the leaf chlorophyll concentration, LAI had a higher coefficient of variation (Table 6.1). Figure 6.3 highlights regions where $R^2 \geq 0.8$ for LAI (top) and canopy chlorophyll content (bottom). Again, the similarity in the observed patterns is obviously due to the high correlation between the two canopy variables ($r=0.97$). The observed patterns are in agreement with a

previous study by Darvishzadeh et al. (2008c), who found similar patterns for these variables when using a different sensor (field spectrometer) and sampling.

Table 6.4. Band positions and $R^2$ values between the best narrow band NDVI and SAVI2 (derived from 2-D correlation plots) and grass variables (n=41). CCC is the canopy chlorophyll content.

| | ***Narrow band VI*** | ***λ (nm)*** | ***$R^2$*** |
|---|---|---|---|
| ***LAI*** | NDVI | 1068/1215 | 0.85 |
| | SAVI2 | 1068/1229 | 0.87 |
| ***CCC*** | NDVI | 1068/1215 | 0.90 |
| | SAVI2 | 1068/1200 | 0.91 |

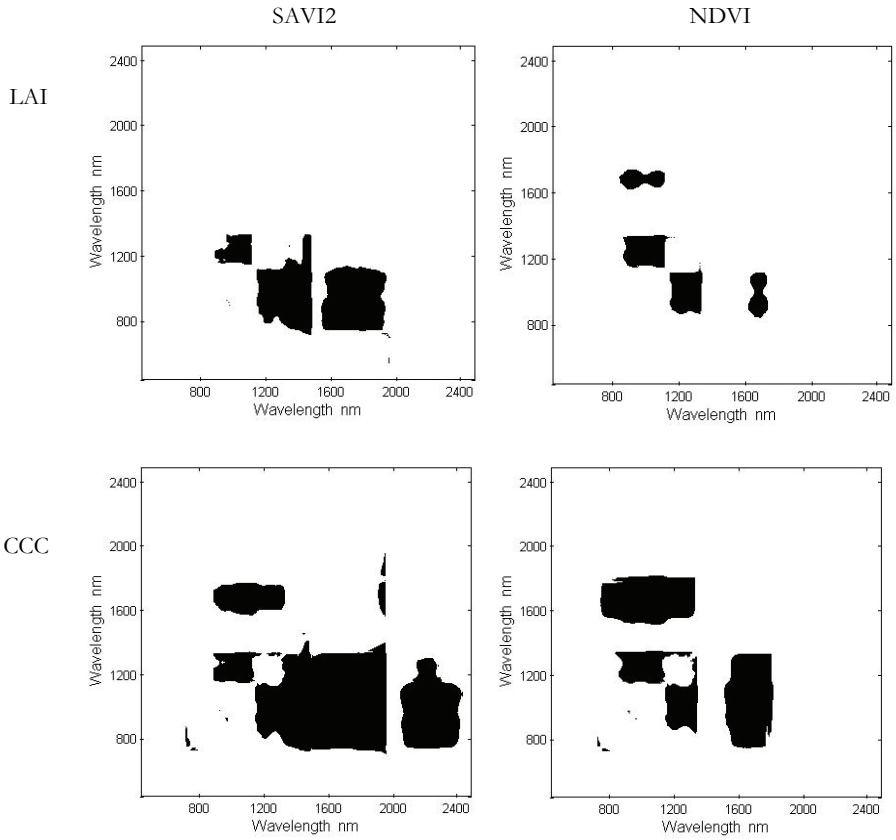


Figure 6.3. Regions with high correlation ($R^2 \geq 0.8$) between narrow band vegetation indices (left: SAVI2, right: NDVI) and LAI and canopy chlorophyll content.

For the best performing narrow band indices (Table 6.4), cross-validated $R^2$, RMSE and the normalized RMSE (NRMSE = RMSE/range) (Atzberger, 1997; Combal et al., 2003; Darvishzadeh et al., 2008b) were computed from linear regression models. A comparative analysis of the predictive performance of the narrow band vegetation indices is presented in Table 6.5. As can be observed from this table, compared with narrow band NDVI, narrow band SAVI2 gave slightly higher $R^2$ and lower RMSE values for both canopy variables. The better performance of SAVI2 compared with NDVI is probably due to the fact that SAVI2 is less sensitive to external factors such as soil background effects.

Table 6.5. Performance of narrow band vegetation indices for predicting grass variables in Majella National Park, Italy, using HyMap data. $R^2_{CV}$ is the cross-validated coefficient of determination between estimated and predicted variables; $RMSE_{cv}$ is the cross-validated root mean square error; and $NRMSE_{cv}$ is the normalized cross-validated root mean square error, i.e., $RMSE_{cv}$ divided by range (n=41).

| | ***Narrow band VI*** | ***$R^2_{cv}$*** | ***$RMSE_{cv}$*** | ***$NRMSE_{cv}$*** |
|---|---|---|---|---|
| ***LAI*** | NDVI | 0.83 | 0.64 | 0.095 |
| | SAVI2 | 0.85 | 0.62 | 0.090 |
| ***CCC*** | NDVI | 0.89 | 0.18 | 0.085 |
| | SAVI2 | 0.90 | 0.17 | 0.080 |

Figure 6.4 shows the relationships between the cross-validated and measured LAI and canopy chlorophyll content when using narrow band SAVI2. From this figure, it seems that no saturation has occurred for the studied variables.

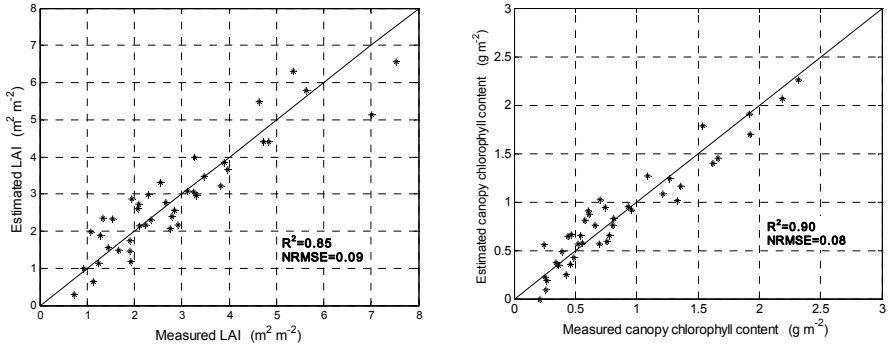


Figure 6.4. Cross-validated prediction of grass variables in Majella National Park, Italy, using narrow band SAVI2. Left: estimated LAI versus measured LAI; right: canopy chlorophyll content. The optimum wavebands are those reported in Table 6.4.

### *6.4.2. Partial least squares regression*

The relationships between grass variables and reflectance spectra were modeled using partial least square regression. Cross-validated results using the entire reflectance spectra as inputs are shown in Figure 6.5. The optimal number of partial least squares regression factors preventing over-fitting was selected in two ways: (i) through visual inspection of cross-validated RMSE versus the number of factors plots, and (ii) by setting the condition that adding an extra factor must reduce the $RMSE_{CV}$ by >2%. The number of factors in the final model was four for both LAI and canopy chlorophyll content. Compared with narrow band vegetation indices (Table 6.5), partial least squares regression using entire reflectance spectra only slightly increased cross-validated $R^2$ values of the estimated and measured LAI and canopy chlorophyll content; however, their $RMSE_{cv}$ were also slightly increased (Table 6.6).

Table 6.6. Performance of partial least squares regression for predicting grass variables in Majella National Park, Italy, using HyMap data. $R^2_{cv}$ is the cross-validated coefficient of determination between estimated and predicted variables; $RMSE_{cv}$ is the cross-validated root mean square error; and $NRMSE_{cv}$ is the normalized cross-validated root mean square error (n=41).

| | | ***No. of factors*** | ***$R^2_{cv}$*** | ***$RMSE_{cv}$*** | ***$NRMSE_{cv}$*** |
|---|---|---|---|---|---|
| **Entire reflectance** | LAI | 4 | 0.87 | 0.68 | 0.10 |
| | CCC | 4 | 0.91 | 0.20 | 0.09 |
| **Spectral subset (Table 6.2)** | LAI | 4 | 0.87 | 0.65 | 0.10 |
| | CCC | 4 | 0.91 | 0.19 | 0.09 |

We formed a spectral subset of the full spectrum to build new partial least squares regression models by selecting a subset of wavelengths closely related to vegetation parameters (see Table 6.2). Waveband selection did not have any effect on the $R^2$ values of the two studied grass variables. It slightly changed the prediction of grass LAI and canopy chlorophyll content by decreasing the $RMSE_{cv}$ ($RMSE_{cv}$ = 0.65 and 0.19 for LAI and canopy chlorophyll content, respectively). This supports the view that in vegetation studies a cautiously selected spectral subset includes almost the entire information of the full spectral resolution (Fourty and Baret, 1997).

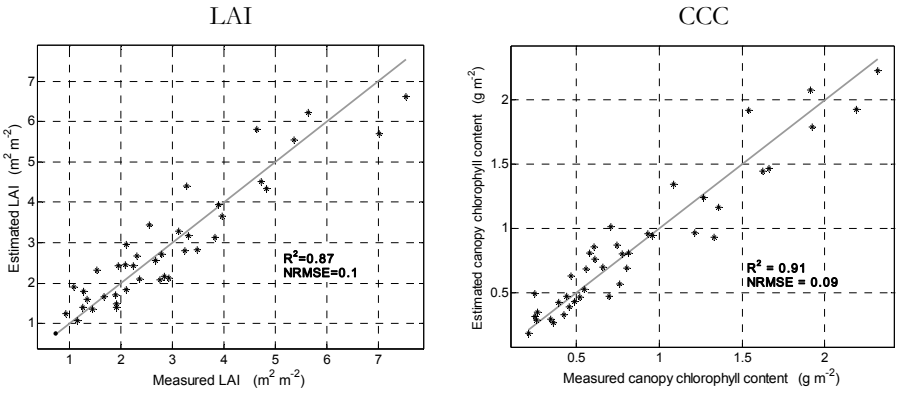


Figure 6.5. Cross-validated prediction of grass variables in Majella National Park, Italy, using the entire reflectance spectra of HyMap in partial least squares regression models. Left: estimated LAI versus measured LAI; right: for canopy chlorophyll content.

### *6.4.3. Inversion of PROSAIL*

To find the solution to the inverse problem, the LUT is sorted according to the cost function ($RMSE_r$) and the set of variables providing the minimum RMSE is considered as the solution. Figure 6.6 illustrates measured and simulated canopy reflectance spectra found in this way for two subplots with contrasting LAI values.

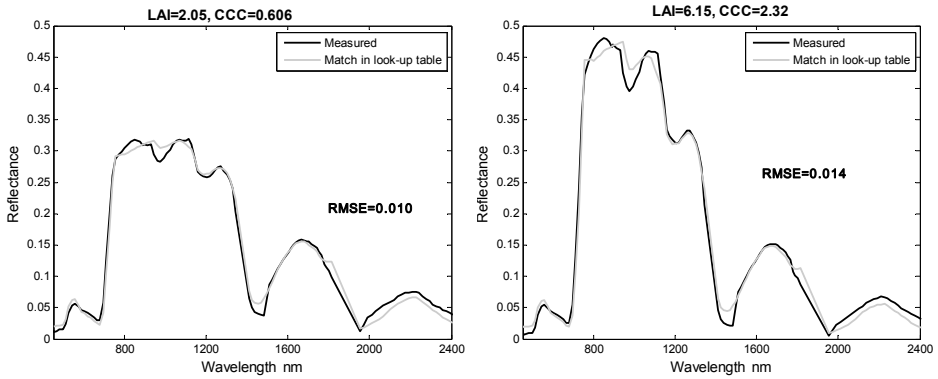


Figure 6.6. Measured and simulated grass canopy reflectance spectra of two sample plots, with LAI equal to 2.1 (left) and 6.2 (right), respectively. Measured and simulated reflectance values are at discrete wavelengths; lines are only drawn to ease interpretation.

As can be observed from Figure 6.6, generally the simulated reflectances were in relatively good agreement with the measured reflectances for canopies with different LAI values. A more concise analysis reveals that most spectral bands were modeled with average absolute error (AAE) (Eq. 5) lower than 0.02 reflectance units (Figure 6.7).

$$AAE_{\lambda} = \frac{1}{q}\left|\sum_{i=1}^{q}(R_{measured\ \lambda} - R_{bestfit_{\lambda}})\right| \qquad \text{(Eq. 5)}$$

where $R_{measured}$ is the measured reflectance at wavelength λ, $R_{bestfit}$ is the best-fit reflectance at the same wavelength, and $q$ is the number of measurements.

Figure 6.7 plots the AAE between measured and best-fit spectra as a function of wavelengths. It shows that the AAE in some regions is relatively high (greater than 0.02), especially close to the water vapor absorption regions (1135 nm to 1400 nm, and 1820 nm to 1940 nm). We considered the bands with an AAE greater or equal to 0.02 as wavelengths being either poorly modeled or poorly measured (Darvishzadeh et al., 2008b). In sub-section 6.4.3.1 we present a spectral subset where these bands have been excluded.

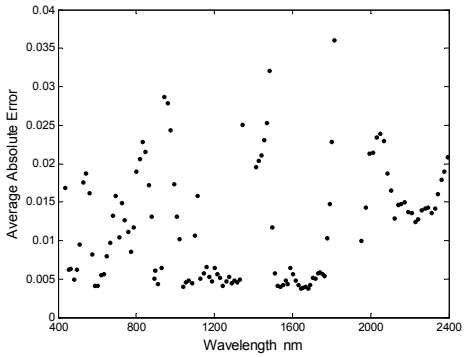


Figure 6.7. The average absolute error (AAE) between best-fit and the measured HyMap reflectance spectra as a function of wavelengths. The AAE has been calculated from the measured HyMap spectra of 41 sample plots against the best fitting LUT spectra (Eq. 5).

The relation between the measured and estimated grass variables based on the smallest RMSE criterion is demonstrated in Figure 6.8. It can be observed that the PROSAIL inversion yielded very similar accuracies for LAI and canopy chlorophyll content, although it seems that LAI was estimated with slightly higher accuracy (NRMSE=0.10 for LAI versus 0.12 for canopy chlorophyll content).

Investigation of the histograms of the other six retrieved parameters (*N, ALA, $C_m$, $C_w$, hot* and *scale*) revealed that several (30 out of 41) sample plots reached the upper/lower boundary of at least one model parameter (not shown). As the parameter ranges were quite large (Table 6.3), the possible reason could be that the reflectance in some wavelengths is either noisy or poorly modeled by the combined SAILH and PROSPECT canopy reflectance model (Darvishzadeh et al., 2008b; Schlerf and Atzberger, 2006).

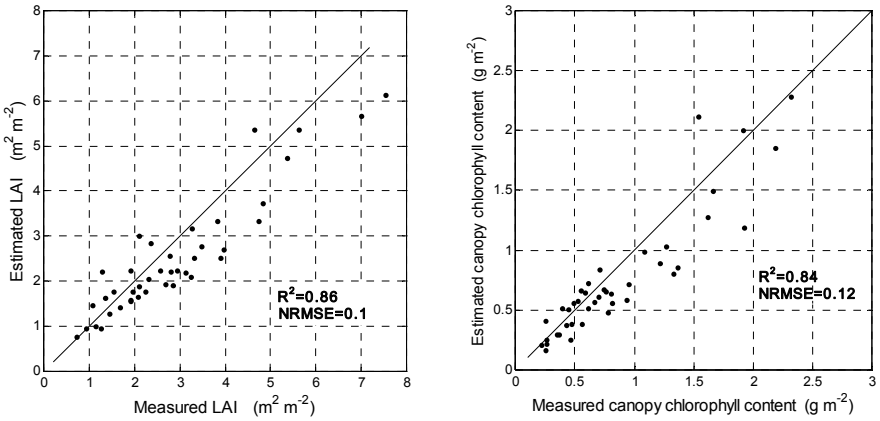


Figure 6.8. Estimated versus measured grass variables in Majella National Park, Italy, using the PROSAIL canopy reflectance model and the minimum RMSE criterion in the LUT search (n=41). Left: LAI; right: canopy chlorophyll content.

We also evaluated the retrieval accuracy if multiple solutions are used (i.e., the first 10 and the first 100 best fits of the LUT) (Combal et al., 2003; Darvishzadeh et al., 2008b). Table 6.7 compares the "multiple solutions" with the "best-fit" LUT solutions. This demonstrates how different solutions affect the accuracy of the estimated variables. We tested for significance of the results and found no significant differences between the statistical parameters used for any number of solutions (one-way ANOVA; $p>0.05$). Throughout the rest of this study, we used the LUT inversion using the first 10 solutions for estimating the grass variables because it gave the highest estimation accuracies (although not significant).

Table 6.7. $R^2$, RMSE and normalized RMSE between measured and estimated grass characteristics (n=41) from PROSAIL inversion. The standard LUT solution is indicated as "best fitting spectra". The grass characteristics were also retrieved considering the first 10 and 100 solutions. In these cases, the median and mean are shown. CCC is the canopy chlorophyll content.

| ***No. of solutions*** | ***Statistical parameter*** | ***LAI ($m^2$ $m^{-2}$)*** | | | ***CCC ($g$ $m^{-2}$)*** | | |
|---|---|---|---|---|---|---|---|
| | | ***$R^2$*** | ***RMSE*** | ***NRMSE*** | ***$R^2$*** | ***RMSE*** | ***NRMSE*** |
| ***Best fitting spectra*** | / | 0.86 | 0.70 | 0.10 | 0.84 | 0.24 | 0.12 |
| ***First 10*** | Median | 089 | 0.65 | 0.09 | 0.84 | 0.24 | 0.12 |
| | Mean | 0.89 | 0.63 | 0.09 | 0.85 | 0.23 | 0.11 |
| ***First 100*** | Median | 0.84 | 0.66 | 0.10 | 0.81 | 0.25 | 0.12 |
| | Mean | 0.85 | 0.62 | 0.09 | 0.82 | 0.24 | 0.11 |

### 6.4.3.1. Use of spectral subsets in the inversion process

We considered bands with an AAE greater or equal to 0.02 as wavelengths with high errors (Darvishzadeh et al., 2008b) (Figure 6.7). These bands were systematically excluded (one by one) in the inversion process, and each time the AAE between the measured and best-fit reflectance spectra was re-calculated until all remaining wavelengths had an AAE smaller than 0.02. The elimination of wavelengths stopped after 19 iterations. The remaining wavebands (n=107) are called subset II. Subset II and the wavelengths identified from literature (Table 6.2) (subset I) were used in the inversion procedure.

The role of the spectral subsets in the estimation of grass variables was again evaluated on the basis of the $R^2$ and the normalized RMSE between the measured and estimated grass variables. The results showed that, after removing the wavelengths with high AAE (AAE≥0.02), the relationships between measured and estimated LAI and between measured and estimated canopy chlorophyll content were considerably improved (Table 6.8). For instance, LAI was estimated with an accuracy of 0.53 $m^2\ m^{-2}$, which represents just 8 percent of the range of LAI. The results obtained by employing subset I (Table 6.2) instead of the full spectral resolution were incoherent. The subsetting gave slightly better results for canopy chlorophyll content, but inferior results for LAI (Table 6.8).

Table 6.8. $R^2$, RMSE and normalized RMSE between measured and estimated grass canopy variables (n=41) from PROSAIL inversion relating to the two spectral subsets. CCC is the canopy chlorophyll content.

| **Spectral sampling set** | ***Statistical parameter*** | ***LAI ($m^2\ m^{-2}$)*** | | | ***CCC ($g\ m^{-2}$)*** | | |
|---|---|---|---|---|---|---|---|
| | | ***$R^2$*** | ***RMSE*** | ***NRMSE*** | ***$R^2$*** | ***RMSE*** | ***NRMSE*** |
| **Using all wavelengths (n=126)** | Best fitting spectra | 0.86 | 0.70 | 0.10 | 0.84 | 0.24 | 0.12 |
| | Median of 10 | 089 | 0.65 | 0.09 | 0.84 | 0.24 | 0.12 |
| | Mean of 10 | 0.89 | 0.63 | 0.09 | 0.85 | 0.23 | 0.11 |
| **Subset I (n=12) (based on literature)** | Best fitting spectra | 0.83 | 0.80 | 0.12 | 0.88 | 0.23 | 0.11 |
| | Median of 10 | 0.85 | 0.74 | 0.11 | 0.89 | 0.22 | 0.10 |
| | Mean of 10 | 0.85 | 0.74 | 0.11 | 0.89 | 0.21 | 0.10 |
| **Subset II (n=107) (based on AAE)** | Best fitting spectra | 0.80 | 0.73 | 0.11 | 0.84 | 0.25 | 0.12 |
| | Median of 10 | 0.90 | 0.57 | 0.08 | 0.87 | 0.23 | 0.11 |
| | Mean of 10 | 0.91 | 0.53 | 0.08 | 0.87 | 0.22 | 0.10 |

Overall, the estimation accuracies between measured and estimated canopy chlorophyll content improved using both spectral subsets (Table 6.8). This reflects

the danger with existing bands that may contain (excessively) high noise levels and/or are poorly modeled by PROSAIL (Darvishzadeh et al., 2008b).

### *6.4.4 Mapping grass variables*

The LAI and canopy chlorophyll content of the Majella grassland were mapped using the PROSAIL model. Before producing the maps, a grassland mask obtained from maximum likelihood classification was used to mask out the non-grass areas from the HyMap image strips, thus eliminating areas occupied by other land cover types (mainly forest and housing areas). The masked HyMap image was used as input to the inversion process and maps of predicted LAI and canopy chlorophyll content were retrieved using the best fitting spectra. They are presented in Figure 6.9.

The means obtained for all image pixels were 2.91 $m^2 m^{-2}$ for LAI and 0.92 $g m^{-2}$ for canopy chlorophyll content, which are very close to the means of the samples measured during the field measurements. We confirm that the spatial distribution of LAI as predicated by inversion of the PROSAIL model is similar to what we observed on the ground during the field campaign.

## 6.5. Discussion

Compared with the statistical models used in this study, inversion of the radiative transfer model gave higher $R^2$ (and lower normalized RMSE values) for LAI, and similar results for canopy chlorophyll content. These findings are also supported by previous studies (Gemmell et al., 2002; Schlerf and Atzberger, 2006), which demonstrated that inversion of a radiative transfer model gave accuracies comparable to those of statistical approaches. The result shows the benefits of using the physical rather than the statistical approach, taking into account that (almost) no calibration work was required for the physical approach. However, inversion of the physically based models is always hampered by the ill-posed inverse problem (Atzberger, 2004; Combal et al., 2002).

We found almost no difference in the accuracies of retrieved LAI and canopy chlorophyll content produced by using the inversion algorithm and the statistical models. This is due to the fact that in our study LAI and canopy chlorophyll content are closely correlated (Darvishzadeh et al., 2008b, 2008c) as leaf chlorophyll contents in the study area were relatively uniform.

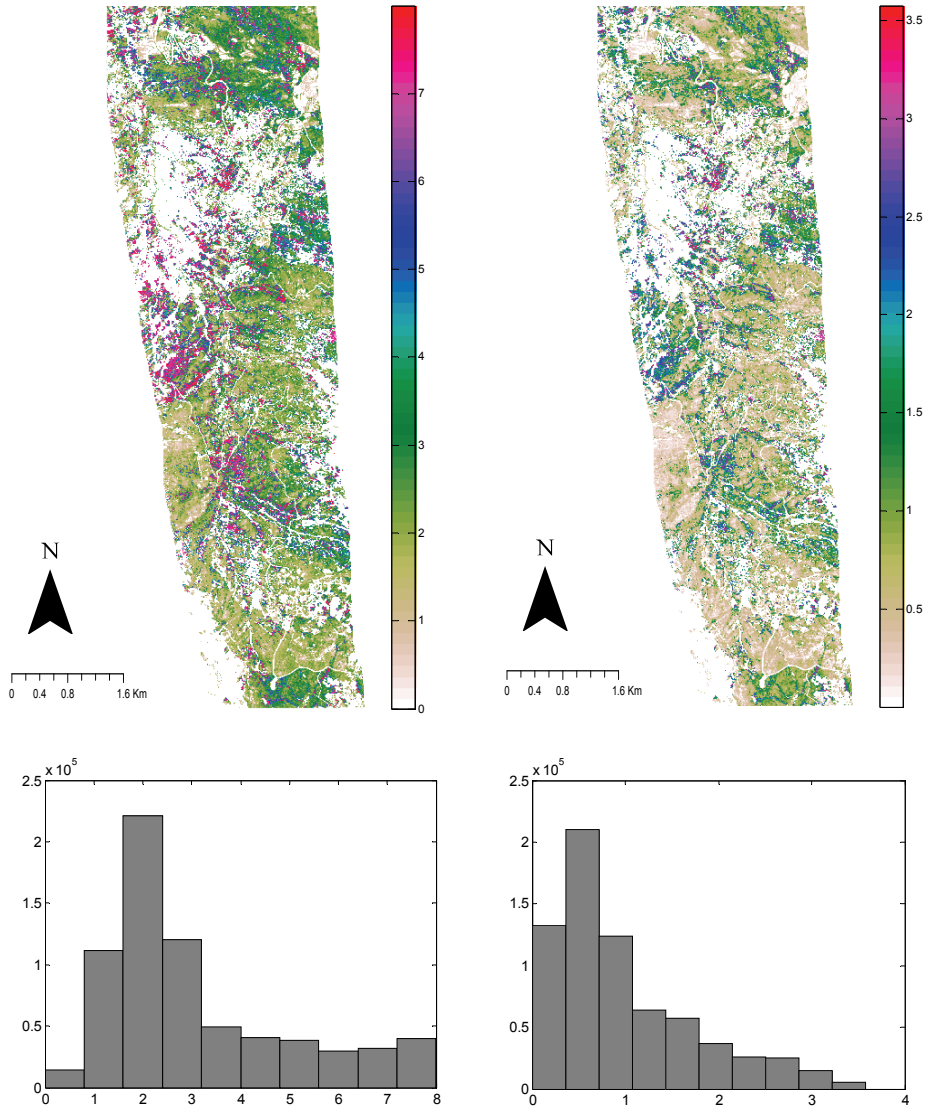


Figure 6.9. Maps (top) and histograms (bottom) of grass variables for a subset area of Majella National Park, Italy, from PROSAIL canopy reflectance model inversion, using the minimum RMSE criterion in the look-up table (LUT) search. Left: LAI ($m^2$ $m^{-2}$); right: canopy chlorophyll content (g $m^{-2}$).

The bands selected as the best combination of the vegetation indices for LAI were found in the NIR to SWIR regions. This confirms previous studies that have suggested a strong contribution by SWIR bands to the strength of relationships between spectral reflectance and LAI (Brown et al., 2000; Cohen and Goward,

2004; Darvishzadeh et al., 2008a; Lee et al., 2004; Nemani et al., 1993; Schlerf et al., 2005).

Compared with the narrow band NDVI, the narrow band SAVI2 gave somewhat higher $R^2$ (and lower normalized RMSE values) for LAI. This result is in agreement with those of Broge and Leblanc (2001) and Darvishzadeh et al. (2008a), who found SAVI2 to be the best vegetation index for LAI estimation. The narrow band SAVI2 performed also relatively well for canopy chlorophyll content. This confirms that SAVI2 is relatively insensitive to external factors such as soil background effects.

Compared with narrow band indices, the partial least squares regression achieved slightly better results (Table 6.6), as important information may lost when only two wavelengths are selected for narrow band vegetation indices from the total spectral information available in hyperspectral data (Darvishzadeh et al., 2008c; Lee et al., 2004). By selecting a subset of wavelengths known to be strongly related to vegetation parameters, the results of partial least squares regression were only slightly improved (Cho et al., 2007; Darvishzadeh et al., 2008c; Davies, 2001; Kubinyi, 1996; Martens and Martens, 2000; Schmidtlein and Sassin, 2004). Although our waveband selection method was somewhat simplistic, it worked well because we considered wavelengths related to both biophysical and biochemical properties of vegetation, thus maximizing the information content in the input variables.

Concerning the physical approach, Combal et al. (2003) and Meroni et al. (2004) have shown that utilizing prior information is an efficient way of solving the ill-posed problem and improving the accuracy of the estimated canopy variables. In the case of spatialized (remote sensing) data, Atzberger (2004) showed that for mono-species canopies the intercorrelation between spectral bands also helps to constrain the ill-posed inverse problem. However, the regularization of the inverse problem was beyond the scope of this study. We simply used the approximate maximum and minimum values from the field measurements for the three parameters *LAI, LCC* and *ALA* as prior information for building the LUT. In this way, we increased the sampling density and constrained the estimated grass biophysical characteristics into their measured ranges (Darvishzadeh et al., 2008b).

The possible reason that in many cases at least one of the other six retrieved parameters ($C_m$, $C_w$, *scale, ALA, hot* and *N*) reached the upper/lower boundary is that some wavelengths are either noisy or poorly modeled by the combined SAILH and PROSPECT canopy reflectance model. Similar results have been found by Darvishzadeh et al. (2008b) and Schlerf & Atzberger (2006), who demonstrated that the radiative transfer models (PROSAIL and PROSPECT, respectively) do not simulate the reflectance equally well across the 400 nm to 2500 nm wavelength range. The possible explanation of too-restricted parameter ranges

can be excluded since much wider ranges, as shown by Darvishzadeh et al. (2008b) did not ameliorate the results (not shown).

The relationships between measured and estimated grass variables were slightly improved when wavelengths either based on low AAE (subset II) or selected from literature (subset I) were used for model inversion. The result is in agreement with those of Fang and Liang (2005), Meroni et al. (2004) and Schlerf and Atzberger (2006). They demonstrated that, when inverting radiative transfer models, the selection of a few wavebands may give better results than those achieved using the full spectral resolution. The results in the present study (when using all bands) indicated good relationships between measured and estimated grass variables and a relatively good representation of the measured spectra by the PROSAIL model over most spectral regions. Consequently, spectral subsetting did not clearly improve the parameter retrieval. Similar results have been obtained at field scale (Darvishzadeh et al., 2008b).

In the present study, we did not evaluate the possible benefits of regularization efforts when inverting the radiative transfer model. Increased retrieval accuracies have, for example, been demonstrated by Lavergne et al. (2007) using the reflectance uncertainty matrix in the cost function. This would require, however, the LUT inversion to be run several times and boot-strap techniques to be used to avoid losing independency between measured and estimated biophysical variables.

## 6.6. Conclusion

The effectiveness of statistical versus physical modeling for mapping LAI and canopy chlorophyll contents in a Mediterranean grassland were investigated in this study. For the retrieval of the grass variables, narrow band vegetation indices, partial least squares regression and the widely used PROSAIL radiative transfer model (Verhoef, 1984; Verhoef, 1985; Jacquemoud and Baret, 1990) were used in the analysis. For radiative transfer model inversion, a LUT approach was used. While constructing the LUT, prior knowledge regarding LAI, leaf chlorophyll content and mean leaf angle measured in the field was taken into account. The models were validated by comparing estimated and field-measured canopy variables ($R^2$ and RMSE).

The results of the study demonstrate that grass canopy characteristics such as LAI and canopy chlorophyll content can be estimated through the inversion of a radiative transfer model with accuracies comparable to (or even better than) those of statistical approaches. In contrast to statistical approaches, ground-measured biophysical data may be almost entirely used for validating the retrieved model parameters (and for setting the LUT ranges) and are not used to calibrate the radiative transfer model (except the soil reflectance spectra that have to be input into the radiative transfer model). Once an appropriate LUT has been built, it can

in principle be applied to different remote sensing data acquired over similar vegetation types (Darvishzadeh et al., 2008b), thereby overcoming the main limitation of statistical models, which are known to be highly site- and sensor-specific.

## Acknowledgements

We would like to acknowledge the assistance of the park management of Majella National Park, Italy, and in particular of Dr. Teodoro Andrisano. Special thanks go to Dr. Fabio Corsi, Dr. Sip van Wieren, Dr. Moses Cho and Dr. Istiak Sobhan for their assistance during the field campaign. Many thanks go to Mr. Willem Nieuwenhuis for helping with the IDL programming. Our appreciation also goes to Dr. Michal Daszykowski for his assistance in applying the TOMCAT toolbox and for his valuable comments.

# Chapter Seven

# Synthesis

## Hyperspectral remote sensing of vegetation parameters using statistical and physical models

## 7.1. Introduction

Accurate quantitative estimation of vegetation biochemical and biophysical characteristics is necessary for a large variety of agricultural, ecological, and meteorological applications (Asner, 1998; Hansen and Schjoerring, 2003; Houborg et al., 2007). Remote sensing, because of its global coverage, repetitiveness, and non-destructive and relatively cheap characterization of land surfaces, has been recognized as a reliable method and a practical means of estimating various biophysical and biochemical vegetation variables (Cohen et al., 2003; Curran et al., 2001; Hansen and Schjoerring, 2003; Hinzman et al., 1986; McMurtrey et al., 1994; Weiss and Baret, 1999). The tools for vegetation remote sensing have developed considerably in the past decades (Asner, 1998). Imaging spectrometry or hyperspectral remote sensing, with sensors that typically have hundreds of narrow, contiguous spectral bands between 400 nm and 2500 nm, has the potential to measure specific vegetation variables that were difficult to measure using conventional multi-spectral sensors. Previous studies have shown that hyperspectral data are crucial in providing essential information for quantifying the biochemical (Broge and Leblanc, 2001; Ferwerda et al., 2005; Gamon et al., 1992; Gitelson and Merzlyak, 1997; Mutanga et al., 2005; Peterson et al., 1988) and biophysical characteristics of vegetation (Blackburn, 1998; Elvidge and Chen, 1995; Gong et al., 1992; Lee et al., 2004; Mutanga and Skidmore, 2004; Schlerf et al., 2005).

In general, current remote sensing approaches for estimating vegetation biochemical and biophysical parameters include statistical (inductive) and physically (deductive) based models (Skidmore, 2002); each having advantages and disadvantages (Kimes et al., 2000; Liang, 2004; Atzberger, 1997; Atzberger, 2003c). Both models (statistical/physical) have been used widely for estimating biochemical and biophysical parameters in agricultural and forestry environments (these are typically homogenous areas in term of species type) (e.g., Atzberger, 1997; Hansen and Schjoerring, 2003; Walter-Shea et al., 1997; Meroni et al., 2004; Schlerf and Atzberger, 2006; Zarco-Tejada et al., 2004a). Nevertheless, the estimation of vegetation characteristics for structurally different vegetation canopies and heterogeneous fields with different vegetation communities using either of the approaches has not been widely addressed in the literature.

The main objectives of this study were (1) to investigate the potential of hyperspectral remote sensing for estimating biophysical and biochemical vegetation characteristics such as leaf area index (LAI) and chlorophyll content at canopy level, (2) to investigate the performance of different statistical techniques such as univariate versus multivariate techniques in predicting biophysical and biochemical vegetation characteristics, and (3) to test the performance of the statistical versus the physical approach for mapping and predicting biophysical and biochemical vegetation characteristics. The study consists of three levels of investigation: under controlled laboratory conditions (7.2), at field level using a

field spectrometer (7.3), and at airborne platform level (i.e., HyMap (Hyperspectral Mapping imaging spectrometer)) (7.4). Majella National Park in Italy was used as a test site for both field and airborne spectrometry.

## 7.2. Laboratory level

Much of the present research linking vegetation parameters such as LAI to spectral data has focused on single plant species (or structurally similar plant types) and background (soil type). Hence, the laboratory study was designed to further investigate the relationship between spectral data and the biophysical parameter (LAI), involving plant species widely different in terms of structure, and with varying leaf chlorophyll concentration and contrasting soil backgrounds. The experimental protocol ensured that a wide range of spectral measurements could be collected. The utility of hyperspectral remote sensing in predicting LAI was then investigated when all data were pooled together (section 7.2.1) and when the data were stratified based on soil type and plant species (section 7.2.2).

### *7.2.1. Estimation of LAI from hyperspectral vegetation indices and the red edge position*

Many studies have investigated the relationships between vegetation indices and canopy variables, including LAI (Elvidge and Chen, 1995; Rondeaux and Steven, 1995; Broge and Leblanc, 2001; Kodani et al., 2002; Pu et al., 2003b; Schlerf et al., 2005; Wang et al., 2005). However, the conclusions drawn are contradictory, even for similar vegetation types. For this reason, we examined the performance of various narrow band vegetation indices, as well as red edge inflection point (REIP), in estimating the LAI of structurally different plant species with different soil backgrounds and leaf optical properties. The laboratory study was designed to test two hypotheses: (1) REIP is controlled primarily by canopy LAI and is a good predictor of LAI, and (2) the narrow band vegetation index is more responsive than REIP and the broad-band vegetation index for estimating canopy LAI. Narrow band vegetation indices involved all possible two-band combinations that are used for calculating ratio vegetation index (RVI) (Pearson and Miller 1972), normalized difference vegetation index (NDVI) (Rouse et al. 1974), perpendicular vegetation index (PVI) (Richardson and Wiegand 1977), second soil adjusted vegetation index (SAVI2) (Major et al. 1990) and the transformed soil adjusted vegetation index (TSAVI) (Baret et al. 1989), whereas the REIP was computed using three different techniques namely first derivative (Dawson and Curran 1998), linear interpolation (Guyot and Baret 1988) and inverted gaussian model (Bonham-Carter 1988).

REIP calculated using any of the three methods did not show a close relation to variations in LAI. The coefficient of determination ($R^2$) calculated between LAI and REIP was very low ($R^2 < 0.1$) when measurements of the different plant

species were pooled together. Consequently, we had to reject our first hypothesis that "REIP is controlled primarily by canopy LAI and is a good predictor of LAI". We note that, as was the case in this study, successful studies with REIP have not used destructive sampling for LAI retrieval. On the contrary, LAI was estimated with reasonable accuracy from red/near infrared-based narrow band indices. Comparison between different narrow band vegetation indices revealed that the narrow band SAVI2 was the best overall choice as estimator of LAI based on cross validated $R^2$ and root mean square error (RMSE) values ($R^2_{cv}$ = 0.77, $RMSE_{cv}$ = 0.59) (Figure 7.1).

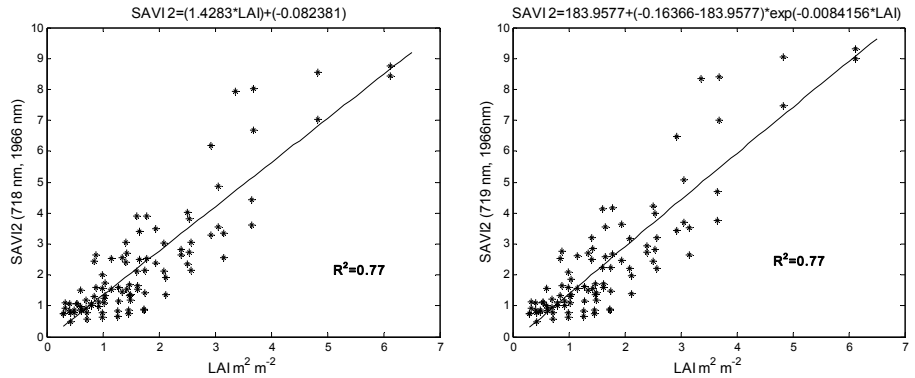


Figure 7.1. Relationships between best narrow band SAVI2 and LAI. Left: using a simple linear model; right: using an exponential relationship (Baret and Guyot, 1991).

Although the near infrared (NIR) region has been the keystone of the omnipresent vegetation indices (NDVI, RVI), our results showed that for most indices bands from the shortwave infrared (SWIR) region contained most information relevant to canopy LAI, and that the "hot spots" (regions with high $R^2$ values) mostly occurred in this region. Considering that the SWIR bands were important for most vegetation indices in this study, vegetation indices that do not include this spectral region may be less satisfactory for LAI estimation (Lee et al., 2004).

### *7.2.2. Effects of soil type and plant architecture in LAI retrieval*

The retrieval of canopy biophysical variables is known to be affected by confounding factors such as plant type and background reflectance. However, only a few studies deal with the effect of exterior features on the estimation and prediction of vegetation LAI using hyperspectral reflectance data. The study aimed to address this knowledge gap by investigating whether estimating LAI from hyperspectral reflectance measurements is significantly affected by soil type and/or plant architecture (e.g., leaf shape and size). *In situ* measurements of LAI were

related to reflectances in the red and NIR and also to five widely used spectral vegetation indices.

The study confirmed that the spectral contrast between leaves and soil background determines the strength of the LAI-reflectance relationship. The higher the contrast between soil and leaves, the stronger the relationship between LAI and canopy reflectance. Figure 7.2 shows an example of this relationship for a red band (680 nm).

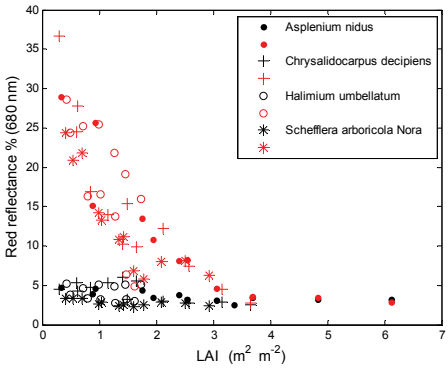


Figure 7.2. Scatter plot showing canopy reflectance and LAI of four plant species measured over two contrasting soil backgrounds in the red (680 nm) spectral band. The two colors (black and red) correspond to dark and light soil, respectively. Four symbols are used to distinguish the plant species.

For the two soil types used in the study, all vegetation indices revealed strong correlations with LAI when the data for the four contrasting species were pooled. In general, the relationship between LAI and vegetation indices was deemed to be stronger in light soil than in dark. The optimal narrow bands forming the best vegetation indices for each soil type were located in different spectral regions. This indicates that relevant information for LAI estimation depends on soil brightness. It seemed difficult to define the most appropriate vegetation indices for estimating LAI in each soil type. However, the cross-validated results revealed that for data analyzed by soil type the narrow band RVI and SAVI2 were the best overall choices as LAI estimators. In other words, these two indices were the least affected by differences related to the four plant species.

By stratifying data according to vegetation type, it was observed that the strength of the relationships between vegetation indices and LAI differs for different vegetation species. We found that for each vegetation species the optimum spectral region for LAI estimation was similar across the investigated vegetation indices, with the exception of PVI. Narrow band PVI showed a distinct behavior, with generally higher $R^2$ values (lower RMSE values) and wavelengths different from those of the four other vegetation indices. PVI appears to be less sensitive to brightness variations in the soil background and adapts well to different plant species with different plant architectures, leaf sizes, etc. This

vegetation index was thus recognized as the most appropriate for LAI estimation under conditions of unknown soil reflectance.

## 7.3. Field level

Heterogeneous (in terms of species diversity) canopies present a challenge for remote sensing applications because the reflectance is often a mixture of different surface materials (Fisher, 1997; Roder et al., 2007). Therefore, more investigation is required to assess the capability of remote sensing models when it comes to natural heterogeneous canopies with a combination of different plant species in varying proportions. Canopy spectral measurements were made in the field using a GER 3700 spectroradiometer (Geophysical and Environmental Research Corporation, Buffalo, New York), along with concomitant *in situ* measurements of LAI and leaf chlorophyll content during a campaign in the summer of 2005. The utility of hyperspectral remote sensing in predicting canopy characteristics such as LAI and canopy/leaf chlorophyll content in a heterogeneous Mediterranean grassland by means of different statistical models (section 7.3.1) and the inversion of a physically based model (section 7.3.2) was investigated.

### *7.3.1. Estimation of LAI and chlorophyll using univariate versus multivariate analysis*

The estimation of canopy characteristics such as LAI and canopy/leaf chlorophyll content, using hyperspectral remote sensing, for heterogeneous grass canopies has not, to our knowledge, been addressed by researchers yet. Therefore, the effectiveness of hyperspectral remote sensing in estimating these characteristics in a heterogeneous Mediterranean grassland by employing different univariate and multivariate methods was examined. We compared narrow band vegetation indices, including REIP, with two important linear statistical methods known to be well suited for dealing with highly multicollinear data sets: partial least squares regression and stepwise multiple linear regression. The suitability of these different methods was analyzed in terms of their prediction accuracy.

Compared with LAI and leaf chlorophyll content, canopy chlorophyll content was estimated with higher accuracy ($R^2_{cv}$ = 0.74, relative $RMSE_{cv}$ = 0.35). The canopy chlorophyll content contains both the structure and chlorophyll information of vegetation and can be accurately estimated by canopy spectral reflectance. However, in our study this can be an artifact, as most of the variation in canopy chlorophyll content stemmed from the LAI variability, and the variability of leaf chlorophyll content was too low to have a noticeable influence on canopy chlorophyll content. On the other hand, the relationships between measured and estimated leaf chlorophyll content were poor for all methods, which indicated poor relationship between the canopy spectra and leaf chlorophyll content, and is in agreement with previous studies that have demonstrated poor

signal propagation from leaf to canopy scale (Asner, 1998; Jacquemoud et al., 1996; Verhoef, 1984; Yoder and Pettigrew-Crosby, 1995).

The bands selected as the best combination of the vegetation indices for LAI were found in the NIR to SWIR regions. This confirmed our earlier results at laboratory level, which suggested a strong contribution by SWIR bands to the strength of relationships between spectral reflectance and LAI. The "optimum" bands for leaf chlorophyll were found mostly in the visible spectral range, mainly in the green and blue regions characterized by a strong light absorption due to chlorophylls *a* and *b* (Hansen and Schjoerring, 2003). Likewise, when the relationships between grass variables and reflectance spectra were examined using stepwise regression, at least one wavelength was selected from the visible regions for all grass variables. This highlighted the importance of visible wavelengths for indices related to leaf pigments.

The REIP methods produced lower prediction accuracies, in particular for LAI. The finding confirmed our earlier result at laboratory level. Furthermore, compared with the narrow band NDVI, the narrow band SAVI2 gave somewhat higher $R^2$ and lower relative RMSE values for LAI. This confirms that SAVI2 is a potentially useful vegetation index for extracting canopy variables such as LAI. However, the selection of appropriate wavelengths and bandwidths is important. The latter results also confirmed our earlier findings at laboratory level.

Overall, multivariate regressions improved the estimation of different grass characteristics (Figure 7.3). The relationship between measured and estimated LAI was better explained by multivariate calibration methods such as stepwise regression and partial least squares regression, respectively, than by univariate methods such as narrow band vegetation indices and REIP. This is probably because a one- or two-wavelength index employs only a limited amount of the total spectral information available in hyperspectral data.

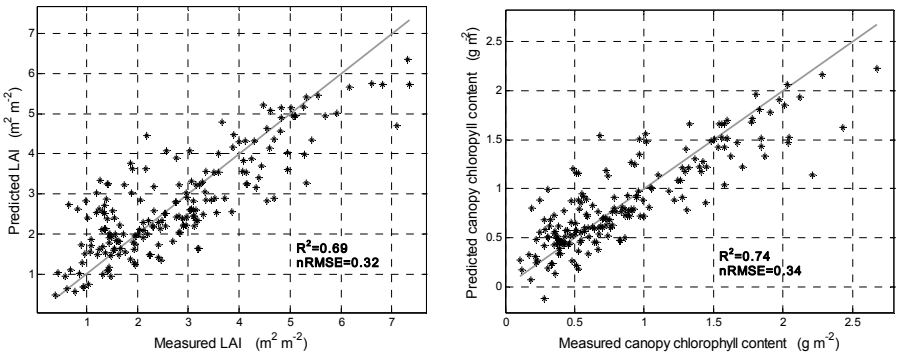


Figure 7.3. Cross-validated prediction of grass variables in Majella National Park, Italy, using the entire reflectance spectra in partial least squares regression models. Left: estimated LAI versus measured LAI; right: for canopy chlorophyll content.

### 7.3.2. Estimation of LAI and chlorophyll by inversion of radiative transfer model

Radiative transfer models have rarely been applied for studying heterogeneous grassland canopies. Therefore, the potential of radiative transfer modeling to predict LAI, leaf and canopy chlorophyll contents in a heterogeneous Mediterranean grassland was investigated. The widely used PROSAIL model was inverted with canopy spectral reflectance measurements by means of a look-up table (LUT). We tested the impact of using multiple solutions, stratification (according to species richness), and spectral subsetting on parameter retrieval.

Of the three investigated parameters, canopy chlorophyll content was estimated with the highest accuracy ($R^2$ = 0.70, normalized RMSE = 0.18). Leaf chlorophyll content, on the other hand, could not be estimated with acceptable accuracy ($R^2$ and RMSE), while LAI was estimated with intermediate accuracy ($R^2$ = 0.59, normalized RMSE = 0.18). The findings are in agreement with the results obtained when statistical regression techniques were used (see section 7.3.1).

The estimation accuracies were increased when data were stratified based on the number of species. This is confirmed by the estimation accuracy for LAI in subplots with only one type of species ($R^2$ = 0.81, normalized RMSE = 0.14). The accuracy systematically decreased each time measurements with more (up to four) species were included in the inversion process, although this was less pronounced for canopy chlorophyll content. This demonstrated the limits of the PROSAIL radiative transfer model when the spectral reflectance stems from a rather heterogeneous condition.

Prior information was incorporated by identifying the maximum and minimum values for three important model parameters (LAI, leaf chlorophyll concentration and mean leaf angle), which increased the sampling density and facilitated the estimation of grass biophysical characteristics. While considering multiple solutions, the accuracy of the estimated variables slightly increased, but differences between the statistical parameters were not statistically significant for any number of solutions.

When a limited selection of wavelengths related to vegetation parameters from literature and wavelengths based on low average absolute error (AAE; Figure 7.4) were used for model inversion, the relationships between measured and estimated grass variables were similar to those obtained using all wavebands. This indicated that a carefully selected spectral subset contains sufficient information for a successful model inversion. Similar results have been reported in the literature (Meroni et al., 2004; Schlerf and Atzberger, 2006).

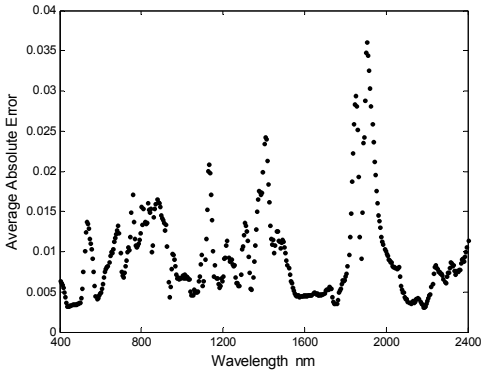


Figure 7.4. The average absolute error (AAE) between measured and best-fit reflectance spectra as a function of wavelengths. The AAE has been calculated from the 185 measured canopy spectra obtained using GER 3700 field spectroradiometer against the best fitting look-up table (LUT) spectra.

## 7.4. Airborne level

Statistical and physical models have seldom been applied simultaneously with hyperspectral data for studying grassland canopies. Consequently, the competence of statistical versus physical modeling for mapping LAI and canopy chlorophyll content in a Mediterranean grassland using hyperspectral HyMap airborne images was investigated. *In situ* measurements of LAI and leaf chlorophyll content were collected during a field campaign concomitant with the time of image acquisition. Based on the results obtained at the laboratory and field levels, we examined the effectiveness of using narrow band vegetation indices as well as partial least square regression via the inversion of the PROSAIL radiative transfer model at airborne level.

Both canopy variables, LAI and canopy chlorophyll content, were retrieved with similar accuracy. The relationship between measured and estimated LAI was better explained by partial least square regression and the inversion of PROSAIL than by using narrow band vegetation indices. The findings confirmed earlier results obtained at field level, since both methods utilize more than two wavelengths from the entire spectral region (400 nm to 2500 nm) to estimate the variable of interest.

The bands selected as the best combination of the vegetation indices for LAI were found in the NIR to SWIR regions. This confirmed previous results obtained at laboratory and field levels and emphasized the strong contribution of SWIR bands to the strength of relationships between spectral reflectance and LAI. Furthermore, the observed patterns (regions with high correlations; hot spots) were similar to those obtained at field level using a different sensor (field spectrometer) and sampling.

Compared with the narrow band NDVI, the narrow band SAVI2 gave somewhat higher $R^2$ and lower normalized RMSE values for LAI. These results were also observed at laboratory and field levels and confirmed that SAVI2 is relatively insensitive to external factors such as soil background effects.

Compared with narrow band indices, the partial least square regression achieved similar results. However, important information may be lost when only two wavelengths for narrow band vegetation indices are selected.

The look-up table (LUT) that was built at field level was used at airborne level. The prior information used for the look-up table (the approximate maximum and minimum values from the field measurements of LAI, leaf chlorophyll content and mean leaf angle) facilitated the estimation of grass biophysical characteristics, and confirmed earlier results obtained at field level, as well as by other studies (Atzberger, 2004; Combal et al., 2003; Meroni et al., 2004), that utilizing prior information is an efficient way of solving the ill-posed problem and of improving the accuracy of the estimated canopy variables.

Comparison between estimated and measured canopy variables indicated that the inversion of a radiative transfer model gave accuracies comparable to those of statistical approaches ($R^2$=0.91 and 0.87, normalized RMSE=0.08 and 0.10; for LAI and canopy chlorophyll content, respectively). Figure 7.5 shows the maps of the leaf chlorophyll and water contents for a part of the Majella grassland that were produced using the PROSAIL model, and underlines the advantage of physical models, since ground-measured data were not required for model calibration and can be used for validating the retrieved model parameters.

It can be observed from this figure that the grasses had a relatively high level of water content. This is in agreement with earlier findings by Cho (2007), who showed that the vegetation was fresher in 2005 than in 2004.

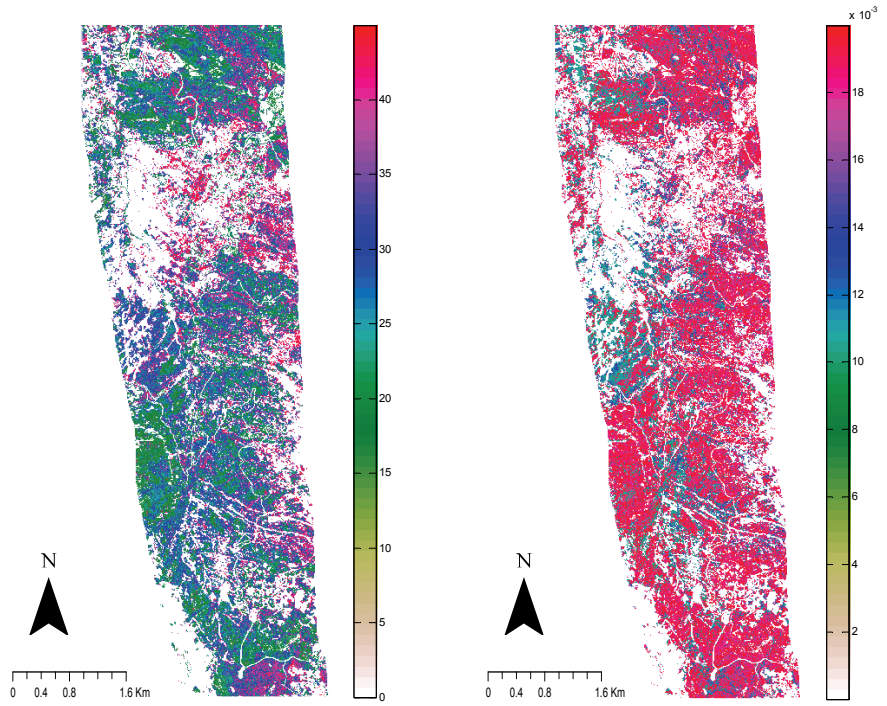


Figure 7.5. Maps of grass variables for a subset area of Majella National Park, Italy, from PROSAIL canopy reflectance model inversion using the minimum RMSE criterion in the look-up table search. Left: leaf chlorophyll content (LCC; μg $cm^{-2}$); right: equivalent water thickness ($C_w$; g $cm^{-2}$).

## 7.5. Conclusion

The intention was to investigate the potential of hyperspectral remote sensing for estimating biophysical and biochemical vegetation characteristics such as leaf area index (LAI) and chlorophyll content with focus on statistical and physical models. We have examined the performance of different statistical techniques such as univariate versus multivariate techniques for predicting biophysical and biochemical vegetation characteristics from laboratory to airborne level. The study further investigated the performance of the statistical versus the physical approach for mapping and predicting biophysical and biochemical vegetation characteristics. We have shown in this thesis that the information contained in hyperspectral data can accomplish these tasks. The main conclusions have been reached from the observations made in this thesis at three levels of investigation.

It has been concluded that at canopy level red edge inflection point (REIP) is not an appropriate variable to be considered for LAI estimations, especially if several contrasting species are pooled together or if a heterogeneous canopy is being investigated. However, it may be appropriate for single species.

Bands in the shortwave infrared (SWIR) region appeared to make a sound contribution regarding the strength of relationships between spectral reflectance and LAI. Since the SWIR bands were important in all three levels investigated and for most vegetation indices in this study, vegetation indices that do not include this spectral region may prove less satisfactory for estimating LAI.

The results suggest that, in addition to the choice of vegetation index, prior knowledge of plant architecture and soil background is important when using remote sensing vegetation indices for LAI estimation. Therefore, before using hyperspectral imagery for large-scale mapping of vegetation biophysical variables, some kind of landscape stratification is required.

The significance of using multivariate techniques such as partial least squares regression rather than univariate methods such as vegetation indices for providing enhanced estimates of heterogeneous grass canopy characteristics is highlighted in the study results, and further use of such techniques is recommended with hyperspectral data.

The utility of the newly introduced subset selection method (wavelengths selection based on low average absolute error; AAE) for model inversion confirmed that a carefully selected spectral subset contains sufficient information for a successful model inversion.

The results of the study demonstrated that grass canopy characteristics such as LAI and canopy chlorophyll content can be estimated through the inversion of a radiative transfer model with accuracies comparable to those of statistical approaches. The advantage of physical models compared to statistical approaches is that (almost) no field measurements are required for model calibration. Instead, ground-measured data are fully useable for validating the retrieved model parameters.

It seemed that the heterogeneity (species diversity) almost disappeared at the airborne level, as the estimation accuracy of the studied variables increased using either the statistical or the physical model. However, heterogeneity is a relative term and is strongly scale dependent.

To summarize, the study not only contributes to the field of information extraction from hyperspectral measurements but also enhances our understanding of vegetation biophysical and biochemical characteristics estimation. A number of achievements have been registered in exploiting spectral information for the retrieval of vegetation parameters using statistical and physical approaches. These concern the derivation of new vegetation indices and the successful implementation of a radiative transfer model inversion (with extensive validation), which involved the development of a new method to subset the spectral data based on average absolute error (AAE).

Since the accuracies obtained through inverting a radiative transfer model were comparable to those of statistical approaches, and taking into account the lack of robustness and transferability of statistical models for varying environmental conditions (Asner et al., 2003; Gobron et al., 1997), the radiative transfer models may be considered viable alternatives.

## 7.6. The future

The future lies in further extending the methods used and developed in this study to hyperspectral spaceborne sensors such as MERIS, MODIS and HYPERION for the prediction and mapping of vegetation biophysical and biochemical characteristics of large areas.

Research such as studying vegetation through the use of remote sensing and biophysical modeling is usually confronted with the problem of unknown input parameters. On the other hand, statistical modeling requires extensive field survey to collect sufficient field data. In an operational project, however, a compromise can be made that includes achieving the research aim and meeting the constraints of time and data availability.

The research presented here illustrates some of the possibilities for estimating and mapping LAI and chlorophyll under controlled laboratory conditions and in a relatively heterogeneous grassland. However, the application of the developed methods to other heterogeneous vegetation types and biophysical/biochemical characteristics not considered in this study needs to be evaluated using different hyperspectral data sets. In this way scale and sensor effects as well as phenological influences can be studied. For this, proper ground sampling measurements for obtaining biophysical variables, in particular leaf chlorophyll content, are required.

Furthermore, a practical extension of the present work would be on the use of information obtained from statistical models to parameterize the physical models. This information may help in choosing the initial parameter values for model inversion and may probably improve the regularization of the model inversion, thus overcoming the ill-posed problem (Atzberger, 2004; Combal et al., 2002). However, the possibility of integrating statistical models with physical models needs to be further explored. A more accurate estimation of the biophysical and biochemical parameters for a variety of vegetation types can be expected from such an integrated approach, which may meet the requirements of ecological and technology-enhanced decision making processes and policies.

# سنجش از دور فراطیفی پارامترهای گیاهان با استفاده از مدلهای آماری و بیوفیزیکی

روشنک درویش زاده

**رساله دکتری**

گروه منابع طبیعی و مدیریت محیط زیست، مؤسسه بین المللی علوم و مشاهدات زمینی، انسخده

و

گروه منابع اکولوژیکی، دانشگاه واخنینگن، واخنینگن

**هلند – اردیبهشت ۱۳۸۷**

# چکیده

تخمین دقیق کمّی پارامترهای بیوشیمیایی و بیوفیزیکی گیاهان در زمینه های مختلفی چون کشاورزی، اکولوژی و هواشناسی اهمیّت بسزایی دارد. امروزه، سنجش از دور به دلایل زیادی همچون پوشش کامل زمین، قابلیت تکرار، عدم تخریب و مشخص نمودن نسبتاً ارزان سطوح زمینی، به عنوان یک روش مطمئن و کاربردی برای تخمین پارامتر های مختلف بیوفیزیکی و بیوشیمیایی گیاهان شناخته می شود. با پیشرفت دانش سنجش از دور فراطیفی، امکانات جدیدی برای اندازه گیری پارامترهای بخصوصی از گیاهان که با استفاده از سنجنده های مرسوم چند طیفی دشوار بودند، میسّر گردیده است.

بطور کلی روشهای موجود برای محاسبه و تخمین پارامتر های بیوشیمیایی و بیوفیزیکی گیاهان با استفاده از سنجش از دور شامل دو روش کلی استفاده از مدلهای آماری و استفاده از مدلهای فیزیکی می شود که هر یک مزایا و معایب خاصّ خود را دارد. هر دو روش بطور گسترده برای تخمین پارامتر های بیوشیمیایی و بیوفیزیکی گیاهان در کشاورزی و جنگل (مناطقی که عمدتاً پوشش همگون و یک نوع گیاه دارند) مورد بهره برداری قرار گرفته اند. این در حالیست که تخمین پارامتر های گیاهان برای تاج پوش (canopy) گیاهانی با ساختار های مختلف و همچنین برای مناطقی با پوشش های ناهمگون توسط هیچ یک از روشهای مذبور مطالعه نگردیده است.

در این مطالعه، با بهره گیری از اندازه گیری های فراطیفی، عملکرد تکنیکهای مختلف آماری همچون روشهای یک متغیری و چند متغیری برای محاسبه و تخمین پارامتر های بیوشیمیایی و بیوفیزیکی گیاهان، مانند کلروفیل موجود و شاخص سطح برگ (LAI) بررسی گردید. همچنین عملکرد مدلهای آماری و مدلهای فیزیکی برای تخمین و به نقشه در آوردن پارامترهای گیاهی مذبور، با استفاده از داده های فراطیفی مقایسه و بررسی شدند. این مقایسه و بررسی برای تاج پوش (canopy) گیاهانی با ساختار های مختلف و همچنین مراتعی با پوشش های ناهمگون و گیاسازندهای (plant communities) گوناگون در سه سطح مختلف آزمایشگاهی، زمینی و تصاویر هوایی فراطیفی سنجنده HYMAP انجام گردیده است.

**سطح آزمایشگاهی**

در این سطح که شامل فصل دوّم و سوّم میشود، داده های بدست آمده از یک تجربهٔ گلخانه ای برای محاسبهٔ LAI با استفاده از اندازه گیری های فراطیفی استفاده شده اند. بطور خلاصه، فصل دوّم رابطه بین LAI و اندکس های گیاهی مرکّب از طیف های باریک را که شامل نقطهٔ عطف لبه قرمز بازتابش طیفی (Red Edge Inflection Point; REIP) هم می شود را بررسی می کند. در این بررسی، گیاهانی با ساختار های بسیار مختلف و دارای مقادیر گوناگون کلروفیل که در خاکهایی با درجهٔ روشنی متفاوت اندازه گیری شده اند، مورد مطالعه قرار گرفته اند. در فصل سوّم به بررسی پاسخ این سؤال که "آیا تخمین LAI با استفاده از اندازه گیری های فراطیفی تحت تأثیر نوع خاک و یا ساختار فیزیکی گیاه (شامل شکل و یا اندازه برگ) قرار می گیرد" پرداخته شده است. در این مبحث تأثیر این عوامل برتغییر رفتار طیفی تاج پوش در باندهای طیفی مرئی و مادون قرمز نیز موردبررسی قرار گرفته است. مشاهدات و نتایج بدست آمده در این فصول به توسعه فصلهای بعدی در سطوح زمینی و تصاویر هوایی فراطیفی سنجنده HYMAP کمک کرده است.

**سطح زمینی**

فصول چهارم و پنجم، از اندازه گیریهای طیفی تاج پوش که با استفاده از دستگاه طیف سنج (spectroradiometer) GER 3700 در عملیات میدانی مراتع ناهمگون بدست آمده اند، بهره می گیرند. فصل چهارم، عملکرد تکنیکهای مختلف آماری همچون روشهای یک متغیری (شامل اندکسهای گیاهی و نقطه عطف لبه قرمز در بازتابش طیفی) و چند متغیری (partial least squares regression and stepwise multiple linear regression) را برای محاسبه و تخمین LAI و کلروفیل موجود در سطح برگها و تاج پوش گیاهان بررسی می کند. در فصل پنجم محاسبه و تخمین LAI و کلروفیل موجود در تاج پوش، با بکارگیری روش معکوس سازی مدل انتقال تابش تاج پوش PROSAIL (PROSAIL, Radiative transfer model) مورد بررسی قرار گرفته است. در این مطالعه، الگوریتم معکوس سازی مدل look up table انتخاب گردیده و از اطّلاعات پیش فرض (prior) مربوط به توزیع حدّ احتمالی تعدادی از پارامترهای گیاهی برای ساخت آن بهره برده شده است.

**سطح تصاویر هوایی فراطیفی سنجنده HYMAP**

فصل ششم، بر اساس داده های تصاویر هوایی فراطیفی سنجنده HYMAP می باشد که همزمان با عملیات میدانی گرفته شده اند. این فصل، مشاهدات و نتایج بدست آمده از فصلهای قبل را بکار می گیرد و به نقشه در آوردن LAI و کلروفیل موجود در تاج پوش را بر اساس مدلهای آماری و فیزیکی ارزیابی می کند.

خلاصه نتایج بدست آمده از سه سطح مورد مطالعه به شرح ذیل می باشد:

نتایج نشان داد که نقطه عطف لبه قرمز در بازتابش طیفی گیاه، شاخص مناسبی برای اندازه گیری و محاسبه LAI در سطح تاج پوش نمی باشد، خصوصاً اگر چندین نوع گیاه متفاوت (از لحاظ ساختار فیزیکی و بیوشیمیایی) با هم در نظر گرفته شوند و یا تاج پوشهای ناهمگون مورد استفاده قرار بگیرند. در طول این مطالعه به مراتب مشاهده گردید که باندهای طیفی موجود در منطقه مادون قرمز دور (SWIR) تاثیر بسزایی در استحکام رابطه میان LAI و بازتابش طیفی دارند. طبیعتاً پیش بینی می شود که نتایج استفاده از اندکس های گیاهیی که شامل طیفی از این منطقه نمی شوند برای محاسبه و تخمین LAI رضایت بخش نخواهند بود. نتایج بدست آمده نمایانگر این است که در هنگام استفاده از اندکس های گیاهی در علم سنجش از دور به منظور تخمین LAI، نه تنها انتخاب درست اندکس گیاهی، بلکه اطّلاعات پیش فرض (prior) مربوط به ساختارگیاه و نوع خاکی که در آن گیاه روئیده است، اهمّیت ویژه ای دارند. به همین دلیل قبل از استفاده از تصاویر بدست آمده از سنجش از دور فراطیفی، به منظور تهیهٔ نقشه بزرگ مقیاس پارامتر های بیوفیزیکی گیاهان، نوعی طبقه بندی و یا جداسازی سرزمین ضروری به نظر می رسد. علاوه بر این، نتایج مطالعه، اهمیّت استفاده از روشهای چند متغیری (مانند partial least squares regression) نسبت به استفاده از روشهای یک متغیری (مانند نقطه عطف لبه قرمز در بازتابش طیفی) را برای بهبود تخمین پارامتر های تاج پوش گیاهان ناهمگون، روشن می سازد. روش نوین معرفی شده جهت انتخاب باندهای طیفی بر اساس میانگین قدر مطلق خطاها (AAE) تأیید کرد، که انتخاب مناسب و دقیق باندهای طیفی، اطّلاعات کافی را برای معکوس سازی موّفق مدل انتقال تابش فراهم می سازد. همچنین نتایج مطالعه نشان می دهد که با استفاده از معکوس سازی مدل انتقال تابش، پارامتر های تاج پوش گیاهان ناهمگون (مانند LAI و کلروفیل موجود در تاج پوش) می توانند

با دقّتی مشابه به مدلهای آماری تخمین زده شوند. با توّجه به این اصل که دقّت بدست آمده از معکوس سازی مدل انتقال تابش، با دقّت بدست آمده از روشهای آماری یکسان می باشد، و با در نظر گرفتن عدم استحکام و عدم قابلیت انتقال مدلهای آماری برای محیطهای گوناگون، مدلهای انتقال تابش می توانند به عنوان جایگزینی مناسب در نظر گرفته شوند.

در مجموع این مطالعه به علم استخراج اطّلاعات از اندازه گیری های فراطیفی می افزاید و دانش ما را در مورد محاسبه و تخمین پارامتر های بیوشیمیایی و بیوفیزیکی گیاهان بهبود می بخشد. چندین موّفقیت هنگام بهره برداری از اطّلاعات طیفی بازتابش برای دست یابی به پارامتر های بیوشیمیایی و بیوفیزیکی گیاهان با استفاده از مدلهای مذکور به ثبت رسیده اند. این موّفقیتها شامل معرفی اندکس های گیاهی جدید و معکوس سازی موّفق مدل انتقال تابش همراه با معتبر سازی گسترده و توسعه یک الگوی جدید جهت انتخاب باندهای طیفی بر اساس میانگین قدر مطلق خطاها می باشند. در پایان یاد آور می شود که یافته های این مطالعه در قالب پنج مقالهٔ علمی در مجله های مرتبط و معتبر ISI پذیرفته گردیده و در حال چاپ می باشند. (برای اطّلاعات بیشتر به فهرست پیوست مراجعه شود)

## References


Asner, G.P., 1998. Biophysical and biochemical sources of variability in canopy reflectance. Remote Sensing of Environment, 64(3): 234-253.

Asner, G.P., Hicke, J.A. and Lobell, D.B., 2003. Per-pixel analysis of forest structure. In: M.A. Wulder and S.E. Franklin (Eds.), Remote sensing of forest environments : concepts and case studies Kluwer Academic Publishers., Boston, pp. 209-254.

Asrar, G., Hipps, L.E. and Kanemasu, E.T., 1984. Assessing solar energy and water use efficiencies in winter wheat: A case study. Agricultural and Forest Meteorology, 31(1): 47-58.

Atzberger, C., 1995. Accuracy of multitemporal LAI estimates in winter wheat using analytical (PROSPECT+SAIL) and semi-empirical reflectance models. In: Guyot, G. (Eds.), Proc. Photosynthesis and Remote Sensing, EARSeL colloquium, Montpellier, 28-30 August 1995, pp. 423-428.

Atzberger, C., 1997. Estimates of winter wheat production through remote sensing and crop growth modelling. VWF Verlag, Berlin, Germany.

Atzberger, C., 2004. Object-based retrieval of biophysical canopy variables using artificial neural nets and radiative transfer models. Remote Sensing of Environment, 93(1-2): 53-67.

Atzberger, C., Jarmer, T., Schlerf, M., Kötz, B. and Werner, W., 2003a. Retrieval of wheat bio-physical attributes from hyperspectral data and SAILH + PROSPECT radiative transfer model. In: M. Habermeyer, A. Müller and S. Holzwarth (Eds.), 3rd EARSeL Workshop on Imaging Spectroscopy. Herrsching, Germany, 13-16 May 2003, pp. 473-482.

Atzberger, C., Jarmer, T., Schlerf, M., Kötz, B. and Werner, W., 2003b. Spectroradiometric determination of wheat bio-physical variables: comparison of different empirical-statistical approaches. In: Goossens, R. (Eds.), Remote Sensing in Transitions, Proc. 23rd EARSeL symposium, Belgium, 2-5 June 2003, pp. 463-470.

Atzberger, C., 2003c. Moeglichkeiten und Grenzen der fernerkundlichen Bestimmung biophysikalischer Vegetationsparameter mittels physikalisch basierter Reflexionsmodelle.- PFG, 1/2003: 51-61.

Bacour, C., Baret, F., Beal, D., Weiss, M. and Pavageau, K., 2006. Neural network estimation of LAI, fAPAR, fCover and LAIxCab from top of canopy MERIS reflectance data: principles and validation. Remote Sensing of Environment, 105(4): 313-325.

Bacour, C., Jacquemoud, S., Tourbier, Y., Dechambre, M. and Frangi, J.P., 2002. Design and analysis of numerical experiments to compare four canopy reflectance models. Remote Sensing of Environment, 79(1): 72-83.

Bacour, C., Jacquemoud, S., Vogt, P., Hosgood, B., Andreoli, G. and Frangi, J.P., 2001. Optimal sampling configurations for the estimation of canopy properties from BRDF data acquired from the EGO/JRC, 8th International Symposium. Physical Measurements and Signatures in Remote Sensing. CNES, Aussois, France.

Baret, F. and Guyot, G., 1991. Potentials and limits of vegetation indices for LAI and APAR assessment. Remote Sensing of Environment, 35(2-3): 161-173.

Baret, F., Jacquemoud, S., Guyot, G. and Leprieur, C., 1992. Modeled analysis of the biophysical nature of spectral shifts and comparison with information content of broad bands. Remote Sensing of Environment, 41(2-3), pp. 133-142.

Baret, F., Guyot, G. and Major, D.J., 1989. TSAVI: A vegetation index which minimizes soil brightness effects on LAI and APAR estimation, Geoscience and Remote Sensing Symposium, IGARSS'89. 12th Canadian Symposium on Remote Sensing. pp. 1355-1358.

Baret, F., Hagolle, O., Geiger, B., Bicheron, P., Miras, B., Huc, M., Berthelot, B., Nino, F., Weiss, M., Samain, O., Roujean, J.L. and Leroy, M., 2007. LAI, fAPAR and fCover CYCLOPES global products derived from vegetation: Part 1: Principles of the algorithm. Remote Sensing of Environment, 110(3): 275-286.

Baret, F. and Jacquemoud, S., 1994. Modeling canopy spectral properties to retrieve biophysical and biochemical characteristics. In: J. Hill and J. Me´gier (Editors), Imaging Spectrometry: A Tool for Environmental Observations. Luxemburg. ECSC, EEC, EAEC, Brussels and Luxemburg, pp. 145-167.

Baret, F., Champion, I., Guyot, G. and Podaire, A., 1987. Monitoring wheat canopies with a high spectral resolution radiometer. Remote Sensing of Environment, 22(3): 367-378.

Baumgardner, M.F., Silva, L.F., Biehl, L.L. and Stoner, E.R., 1985. Reflectance properties of soils. Advances in Agronomy, 38( ): 2-44.

Bicheron, P. and Leroy, M., 1999. A method of biophysical parameter retrieval at global scale by inversion of a vegetation reflectance model. Remote Sensing of Environment, 67(3): 251-266.

Blackburn, G.A., 1998. Quantifying chlorophylls and caroteniods at leaf and canopy scales: an evaluation of some hyperspectral approaches. Remote Sensing of Environment, 66(3): 273-285.

Blackburn, G.A., 2002. Remote sensing of forest pigments using airborne imaging spectrometer and LIDAR imagery. Remote Sensing of Environment, 82(2-3), pp. 311-321.

Bonan, G.B., 1993. Importance of leaf area index and forest type when estimating photosynthesis in boreal forests. Remote Sensing of Environment, 43(3), pp. 303-314.

Bonan, G.B., 1995. Land-Atmosphere interactions for climate system models: coupling biophysical, biogeochemical, and ecosystem dynamical processes. Remote Sensing of Environment, 51(1): 57-73.

Bonham-Carter, G.F., 1988. Numerical procedures and computer program for fitting an inverted Gaussian model to vegetation reflectance data. Computers and Geosciences, 14(3): 339-356.

Boegh, E., Soegaard, H., Broge, N., Hasager, C.B., Jensen, N.O., Schelde, K. and Thomsen, A., 2002. Airborne multispectral data for quantifying leaf area index, nitrogen concentration, and photosynthetic efficiency in agriculture. Remote Sensing of Environment, 81(2-3): 179-193.

Broge, N., Hvidberg, M., Hansen, B.U., Andersen, H.S. and Nielsen, A.A., 1997. Analysis of spectral- biophysical relationships for a wheat canopy, Third international airborne remote sensing conference and exhibition, Copenhagen, Denmark, pp. 373-379.

Broge, N.H. and Leblanc, E., 2001. Comparing prediction power and stability of broadband and hyperspectral vegetation indices for estimation of green leaf area index and canopy chlorophyll density. Remote Sensing of Environment, 76(2): 156-172.

Broge, N.H. and Mortensen, J.V., 2002. Deriving green crop area index and canopy chlorophyll density of winter wheat from spectral reflectance data. Remote Sensing of Environment, 81(1): 45-57.

Brown, L., Chen, J.M., Leblanc, S.G. and Cihlar, J., 2000. A shortwave infrared modification to the simple ratio for LAI retrieval in boreal forests: an image and model analysis. Remote Sensing of Environment, 71(1): 16-25.

Campbell, R.J., Nobley, K.N., Marini, R.P. and Pfeiffer, D.G., 1990. Growing conditions alter the relationship between SPAD-501 values and apple leaf chlorophyll. HortScience, 25: 330-331.

Carter, G.A., 1994. Ratios of leaf reflectances in narrow wavebands as indicators of plant stress. International Journal of Remote Sensing, 15(3): 697-703.

Chatterjee, S. and Price, B., 1977. Regression Analysis by Example. Wiley, New York.

Chaurasia, S. and Dadhwal, V.K., 2004. Comparison of principal component inversion with VI-empirical approach for LAI estimation using simulated reflectance data. International Journal Remote Sensing, 25(14): 2881-2887.

Chen, J.M. and Cihlar, J., 1996. Retrieving leaf area index of boreal conifer forests using Landsat TM images. Remote Sensing of Environment, 55(2): 153-162.

Chen, J.M., Pavlic, G., Brown, L., Cihlar, J., Leblanc, S.G., White, H.P., Hall, R.J., Peddle, D.R., King, D.J. and Trofymow, J.A., 2002. Derivation and validation of Canada-wide coarse-resolution leaf area index maps using high-resolution satellite imagery and ground measurements. Remote Sensing of Environment, 80(1): 165-184.

Chen, J.M., Rich, P.M., Gower, S.T., Norman, J.M. and Plummer, S., 1997. Leaf area index of boreal forests: theory, techniques, and measurements. Journal of Geophysical Research, 102(D24): 29429-29443.

Cho, M.A., 2007. Hyperspectral remote sensing of biochemical and biophysical parameters: the derivative red-edge "double-peak feature": a nuisance or an opportunity? Wageningen University.

Cho, M.A., Skidmore, A., Corsi, F., van Wieren, S.E. and Sobhan, I., 2007. Estimation of green grass/herb biomass from airborne hyperspectral imagery using spectral indices and partial least squares regression. International Journal of Applied Earth Observation and Geoinformation, 9 (2007-4): 375-391.

Cho, M.A. and Skidmore, A.K., 2006. A new technique for extracting the red edge position from hyperspectral data: The linear extrapolation method. Remote Sensing of Environment, 101(2): 181-193.

Cimini, N., 2005. Parco Nazionale della Majella. Park Corporation, Programming and Planning Office.

Clevers, J.G.P.W., 1994. Imaging spectrometry in agriculture- plant vitality and yield indicators. In: J. Hill and j. Megier (Editors), Imaging Spectrometry- A Tool for Environmental Observations. Kluwer Academic, Dordrecht, pp. 193-219.

Clevers, J.G.P.W. and Verhoef, W., 1991. Modelling and synergetic use of optical and microwave remote sensing. Report 2: LAI Estimation from Canopy Reflectance and WDVI: A Sensitivity Analysis with the SAIL Model. BCRS Report 90-39.

Cohen, W.B. and Goward, S.N., 2004. Landsat's role in ecological application of remote sensing. BioScience, 54(6): 535-545.

Cohen, W.B., Maiersperger, T.K., Gower, S.T. and Turner, D.P., 2003. An improved strategy for regression of biophysical variables and Landsat ETM+ data. Remote Sensing of Environment, 84(4): 561-571.

Colombo, R., Bellingeri, D., Fasolini, D. and Marino, C.M., 2003. Retrieval of leaf area index in different vegetation types using high resolution satellite data. Remote Sensing of Environment, 86(1): 120-131.

Combal, B., Baret, F. and Weiss, M., 2002. Improving canopy variables estimation from remote sensing data by exploiting ancillary information. Case study on sugar beet canopies. Agronomie, 22(2): 205-215.

Combal, B., Baret, F., Weiss, M., Trubuil, A., Mace, D., Pragnere, A., Myneni, R., Knyazikhin, Y. and Wang, L., 2003. Retrieval of canopy biophysical variables from bidirectional reflectance: using prior information to solve the ill-posed inverse problem. Remote Sensing of Environment, 84(1): 1-15.

CROMA, 2000: Crop reflectance operational models for agriculture. Description of work.- Energy, Environment and Sustainable Development work programme, EF5/PhD/0035.00.

Curran, P.J., 1989. Remote sensing of foliar chemistry. Remote Sensing of Environment, 30(3): 271-278.

Curran, P.J., Dungan, J.L., Macler, B.A., Plummer, S.E. and Peterson, D.L., 1992. Reflectance spectroscopy of fresh whole leaves for the estimation of chemical concentration. Remote Sensing of Environment, 39: 153-166.

Curran, P.J., Dungan, J.L. and Peterson, D.L., 2001. Estimating the foliar biochemical concentration of leaves with reflectance spectrometry: testing the Kokaly and Clark methodologies. Remote Sensing of Environment, 76(3): 349-359.

Curran, P.J., Windham, W.R. and Gholz, H.L., 1995. Exploring the relationship between reflectance red edge and chlorophyll concentration in slash pine leaves. Tree Physiology, 15, pp. 203-206.

Danson, F.M. and Plummer, S.E., 1995. Red edge response to forest leaf area index. International Journal of Remote Sensing, 16(1): 183-188.

Danson, F.M., Rowland, C.S. and Baret, F., 2003. Training a neural network with a canopy reflectance model to estimate crop leaf area index. International Journal of Remote Sensing, 24(23): 4891-4905.

Darvishzadeh, R., Atzberger, C. and Skidmore, A.K., 2008a. Leaf area index derivation from hyperspectral vegetation indices and the red edge position. International Journal of Remote Sensing, In press.

Darvishzadeh, R., Skidmore, A.K., Schlerf, M. and Atzberger, C., 2008b. Inversion of a radiative transfer model for estimating vegetation LAI and chlorophyll in a heterogeneous grassland. Remote Sensing of Environment, 112(5): 2592-2604.

Darvishzadeh, R., Skidmore, A.K., Schlerf, M., Atzberger, C., Corsi, F., and Cho, M.A., 2008c. LAI and chlorophyll estimated for a heterogeneous grassland using hyperspectral measurements. ISPRS Journal of Photogrammetry and Remote Sensing, In press, DOI: 10.1016/j.isprsjprs.2008.01.001.

Daszykowski, M., Serneels, S., Kaczmarek, K., Van Espen, P., Croux, C. and Walczak, B., 2007. TOMCAT: a MATLAB toolbox for multivariate calibration techniques. Chemometrics and Intelligent Laboratory Systems, 85(2): 269-277.

Davies, A.M.C., 2001. Uncertainty testing in PLS regression. Spectroscopy Europe, 13(2): 16-19.

Dawson, T.P. and Curran, P.J., 1998. A new technique for interpolating the reflectance red edge position. International Journal of Remote Sensing, 19(11): 2133-2139.

De Jong, S.M., Pebesma, E.J. and Lacaze, B., 2003. Above-ground biomass assessment of Mediterranean forests using airborne imaging spectrometry: the DAIS Peyne experiment. International Journal of Remote Sensing, 24(7): 1505-1520.

Demetriades-Shah, T.H., Steven, M.D. and Clark, J.A., 1990. High resolution derivative spectra in remote sensing. Remote Sensing of Environment, 33(1), pp. 55-64.

Dingkuhn, M., Jones, M.P., Johnson, D.E. and Sow, A., 1998. Growth and yield potential of Oryza sativa and O. glaberrima upland rice cultivars and their interspecific progenies. Field Crops Research, 57(1): 57-69.

Disney, M., Lewis, P. and Saich, P., 2006. 3D modelling of forest canopy structure for remote sensing simulations in the optical and microwave domains. Remote Sensing of Environment, 100(1): 114-132.

Duckworth, J., 1998. Spectroscopic quantitative analysis. In: J. Workman and A. Springsteen (Editors), Applied Spectroscopy: A Compact Reference for Practitioners. Academic Press, San Diego, pp.
93-164.

Dunagan, S.C., Gilmore, M.S. and Varekamp, J.C., 2007. Effects of mercury on visible/near-infrared reflectance spectra of mustard spinach plants (Brassica rapa P.). Environmental Pollution, 148(1): 301-311.

Durbha, S.S., King, R.L. and Younan, N.H., 2007. Support vector machines regression for retrieval of leaf area index from multi-angle imaging spectroradiometer. Remote Sensing of Environment, 107(1-2): 348-361.

Dwyer, L.M., Tollenaar, M. and Houwing, L., 1991. A nondestructive method to monitor leaf greenness in corn. Canadian Journal of Plant Science, 71(2): 505-509.

Efron, B. and Gong, G., 1983. A leisurely look at the bootstrap, the jackknife, and cross-validation. The American Statistician, 37(1): 36-48.

Ehsani, M.R., Upadhyaya, S.K., Slaughter, D., Shafii, S. and Pelletier, M., 1999. A NIR technique for rapid determination of soil mineral nitrogen. Precision Agriculture, 1(2): 219-236..

Eklundh, L., Harrie, L. and Kuusk, A., 2001. Investigating relationships between Landsat ETM+ sensor data and leaf area index in a boreal conifer forest. Remote Sensing of Environment, 78(3): 239-251.

El Masry, G., Wang, N., El-Sayed, A. and Ngadi, M., 2007. Hyperspectral imaging for nondestructive determination of some quality attributes for strawberry. Journal of Food Engineering, 81(1): 98-107.

Elvidge, C.D. and Chen, Z., 1995. Comparison of broad-band and narrow-band red and near-infrared vegetation indices. Remote Sensing of Environment, 54(1): 38-48.

Fang, H. and Liang, S., 2005. A hybrid inversion method for mapping leaf area index from MODIS data: experiments and application to broadleaf and needleleaf canopies. Remote Sensing of Environment, 94(3): 405-424.

Fang, H., Liang, S. and Kuusk, A., 2003. Retrieving leaf area index using a genetic algorithm with a canopy radiative transfer model. Remote Sensing of Environment, 85(3): 257-270.

Fassnacht, K.S., Gower, S.T., MacKenzie, M.D., Nordheim, E.V. and Lillesand, T.M., 1997. Estimating the leaf area index of North Central Wisconsin forests using the Landsat thematic mapper. Remote Sensing of Environment, 61(2): 229-245.

Fernandes, R., Miller, J.R., Hu, B. and Rubinstein, I.G., 2002. A multi-scale approach to mapping effective leaf area index in boreal Picea mariana stands using high spatial resolution CASI imagery. International Journal of Remote Sensing, 23(18): 3547-3568.

Ferwerda, J.G., Skidmore, A.K. and Mutanga, O., 2005. Nitrogen detection with hyperspectral normalized ratio indices across multiple plant species. International Journal of Remote Sensing, 26(18): 4083-4095.

Feudale, R.N. and Brown, S.D., 2005. An inverse model for target detection. Chemometrics and Intelligent Laboratory Systems, 77(1-2): 75-84.

Fisher, P., 1997. The pixel: a snare and a delusion. International Journal of Remote Sensing, 18(3): 679-685.

Fournier, R.A., Mailly, D., Walter, J.-M.N. and Soudani, K., 2003. Indirect measurements of forest canopy structure from *in situ* optical sensors. In: M.A. Wulder and S.E. Franklin (Editors), Remote Sensing of Forest Environments: Concepts and Case Studies. Kluwer Academic, Boston, pp. 77-114.

Fourty, T. and Baret, F., 1997. Vegetation water and dry matter contents estimated from top-of-the-atmosphere reflectance data: a simulation study. Remote Sensing of Environment, 61(1): 34-45.

Fourty, T., Baret, F., Jacquemoud, S., Schmuck, G. and Verdebout, J., 1996. Leaf optical properties with explicit description of its biochemical composition: direct and inverse problems. Remote Sensing of Environment, 56(2): 104-117.

Friedl, M.A., Michaelsen, J., Davis, F.W., Walker, H. and Schimel, D.S., 1994. Estimating grassland biomass and leaf area index using ground and satellite data. International Journal of Remote Sensing, 15(7): 1401-1420.

Gamon, J.A., Penuelas, J. and Field, C.B., 1992. A narrow-waveband spectral index that tracks diurnal changes in photosynthetic efficiency. Remote Sensing of Environment, 41(1): 35-44.

Gastellu-Etchegorry, J.P., Demarez, V., Pinel, V. and Zagolski, F., 1996b. Modeling radiative transfer in heterogeneous 3-D vegetation canopies. Remote Sensing of Environment, 58(2): 131-156.

Gastellu-Etchegorry, J., Zagolski, F. and Romier, J., 1996a. A simple anisotropic reflectance model for homogeneous multilayer canopies. Remote Sensing of Environment, 57: 22-38.

Gastellu-Etchegorry, J.P., Gascon, F. and Esteve, P., 2003. An interpolation procedure for generalizing a look-up table inversion method. Remote Sensing of Environment, 87(1): 55-71.

Gates, D.M., Keegan, H.J., Schleter, J.C. and Wiedner, V.R., 1965. Spectral properties of plants. Applied Optics, 4(11-20).

Geladi, P. and Kowalski, B.R., 1986. Partial least-squares regression: a tutorial. Analytica Chimica Acta, 185: 1-17.

Gemmell, F., Varjo, J., Strandstrom, M. and Kuusk, A., 2002. Comparison of measured boreal forest characteristics with estimates from TM data and limited ancillary information using reflectance model inversion. Remote Sensing of Environment, 81(2-3): 365-377.

Giacomelli, L., Boggetti, H., Agnelli, H., Anunziata, J., Silber, J.J. and Cattana, R., 1998. Relevant physicochemical factors in chromatographic separation of Alternaria alternata mycotoxins. Analytica Chimica Acta, 370(1): 79-89.

Gilabert, M.A., Gandia, S. and Melia, J., 1996. Analyses of spectral-biophysical relationships for a corn canopy. Remote Sensing of Environment, 55(1): 11-20.

Gitelson, A.A. and Merzlyak, M.N., 1997. Remote estimation of chlorophyll content in higher plant leaves. International Journal of Remote Sensing, 18(12): 2691-2697.

Gitelson, A.A., Gritz, Y., and Merzlyak, M.N., 2003. Relationships between leaf chlorophyll content and spectral reflectance and algorithms for non-destructive chlorophyll assessment in higher plant leaves. Journal of Plant Physiology, 160(3): 271-282.

Gobron, N., Pinty, B. and Verstraete, M.M., 1997. Theoretical limits to the estimation of the leaf area index on the basis of visible and near-infrared remote sensing data. IEEE Transactions on Geoscience and Remote Sensing, 35(6): 1438-1445.

Goel, N.S., 1989. Inversion of canopy reflectance models for estimation of biophysical parameters from reflectance data. In: G. Asrar (Editor), Theory and Applications of Optical Remote Sensing. Wiley & Sons, New York etc., pp. 205-251.

Gong, P., Pu, R. and Miller, J.R., 1992. Correlating leaf area index of ponderosa pine with hyperspectral CASI data. Canadian Journal of Remote Sensing, 18(4), 275-282.

Gong, P., Wang, D.X. and Liang, S., 1999. Inverting a canopy reflectance model using a neural network. International Journal of Remote Sensing, 20(1): 111-122.

Gopal, S. and Woodcock, C., 1996. Remote sensing of forest change using artificial neural networks. IEEE Transactions on Geoscience and Remote Sensing, 34(2): 398-404.

Gower, S.T., Kucharik, C.J. and Norman, J.M., 1999. Direct and Indirect Estimation of Leaf Area Index, fAPAR, and Net Primary Production of Terrestrial Ecosystems. Remote Sensing of Environment, 70(1), pp. 29-51.

Grossman, Y.L., Ustin, S.L., Jacquemoud, S., Sanderson, E.W., Schmuck, G. and Verdebout, J., 1996. Critique of stepwise multiple linear regression for the extraction of leaf biochemistry information from leaf reflectance data. Remote Sensing of Environment, 56(3): 182-193.

Guyot, G. and Baret, F., 1988. Utilisation de la haute resolution spectrale pour suivre l'état des couverts végétaux. In: Guyenne, T.D., Hunt, J.J. (Eds.), Proc. 4th international colloquium on spectral signatures of objects in remote sensing. ESA SP-287, Aussois, France, 18-22 January 1988, pp. 279-286.

Haboudane, D., Miller, J.R., Tremblay, N., Zarco-Tejada, P.J. and Dextraze, L., 2002. Integrated narrow-band vegetation indices for prediction of crop chlorophyll content for application to precision agriculture. Remote Sensing of Environment, 81(2-3): 416-426.

Haboudane, D., Miller, J.R., Pattey, E., Zarco-Tejada, P.J. and Strachan, I.B., 2004. Hyperspectral vegetation indices and novel algorithms for predicting green LAI of crop canopies: modeling and validation in the context of precision agriculture. Remote Sensing of Environment, 90(3): 337-352.

Hamilton, L.C., 1993. Statistics with STATA 3. Wadsworth, Belmont, California.

Hansen, P.M. and Schjoerring, J.K., 2003. Reflectance measurement of canopy biomass and nitrogen status in wheat crops using normalized difference vegetation indices and partial least squares regression. Remote Sensing of Environment, 86(4): 542-553.

Hinzman, L.D., Bauer, M.E. and Daughtry, C.S.T., 1986. Effects of nitrogen fertilization on growth and reflectance characteristics of winter wheat. Remote Sensing of Environment, 19(1): 47-61.

Horler, D.N.H., Dockray, M. and Barber, J., 1983. The red edge of plant leaf reflectance. International Journal of Remote Sensing, 4(2): 273-288.

Houborg, R., Soegaard, H. and Boegh, E., 2007. Combining vegetation index and model inversion methods for the extraction of key vegetation biophysical parameters using Terra and Aqua MODIS reflectance data. Remote Sensing of Environment, 106(1): 39-58.

Huang, Z., Turner, B.J., Dury, S.J., Wallis, I.R. and Foley, W.J., 2004. Estimating foliage nitrogen concentration from HYMAP data using continuum removal analysis. Remote Sensing of Environment, 93(1-2): 18-29.

Huete, A.R., 1989. Soil influences in remotely sensed vegetation-canopy spectra. In: G. Asrar (Editor), Theory and Applications of Optical Remote Sensing Wiley New York.

Huete, A.R., Jackson, R.D. and Post, D.F., 1985. Spectral response of a plant canopy with different soil backgrounds. Remote Sensing of Environment, 17(1): 37-54.

Hurcom, S.J. and Harrison, A.R., 1998. The NDVI and spectral decomposition for semi-arid vegetation abundance estimation. International Journal of Remote Sensing, 19(16): 3109-3125.

Imanishi, J., Sugimoto, K. and Morimoto, Y., 2004. Detecting drought status and LAI of two Quercus species canopies using derivative spectra. Computers and Electronics in Agriculture, 43(2), pp. 109-129.

Jackson, R.D. and Pinter, P.J. Jr., 1986. Spectral response of architecturally different wheat canopies. Remote Sensing of Environment, 20(1): 43-56.

Jacquemoud, S., Bacour, C., Poilve, H. and Frangi, J.-P., 2000. Comparison of four radiative transfer models to simulate plant canopies reflectance: direct and inverse mode. Remote Sensing of Environment, 74(3): 471-481.

Jacquemoud, S. and Baret, F., 1990. PROSPECT: a model of leaf optical properties spectra. Remote Sensing of Environment, 34(2): 75-91.

Jacquemoud, S., Baret, F., Andrieu, B., Danson, F.M. and Jaggard, K., 1995. Extraction of vegetation biophysical parameters by inversion of the PROSPECT + SAIL models on sugar beet canopy reflectance data. Application to TM and AVIRIS sensors. Remote Sensing of Environment, 52(3): 163-172.

Jacquemoud, S., Ustin, S.L., Verdebout, J., Schmuck, G., Andreoli, G. and Hosgood, B., 1996. Estimating leaf biochemistry using the PROSPECT leaf optical properties model. Remote Sensing of Environment, 56(3): 194-202.

Jongschaap, R.E.E. and Booij, R., 2004. Spectral measurements at different spatial scales in potato: relating leaf, plant and canopy nitrogen status. International Journal of Applied Earth Observation and Geoinformation, 5(3): 205-218.

Kalacska, M., Sanchez-Azofeifa, G.A., Rivard, B., Calvo-Alvarado, J.C., Journet, A.R.P., Arroyo-Mora, J.P. and Ortiz-Ortiz, D., 2004. Leaf area index measurements in a tropical moist forest: a case study from Costa Rica. Remote Sensing of Environment, 91(2): 134-152.

Kimes, D. and Kirchner, J.A., 1982. Radiative transfer model for heterogeneous 3D scenes. Applied Optics, 21: 4119-4129.

Kimes, D.S., Knyazikhin, Y., Privette, J.L., Abuelgasim, A.A. and Gao, F., 2000. Inversion methods for physically-based models. Remote Sensing Reviews, 18(2-4): 381-439.

Kimes, D.S., Nelson, R.F., Manry, M.T. and Fung, A.K., 1998. Attributes of neural networks for extracting continuous vegetation variables from optical and radar measurements. International Journal of Remote Sensing, 19(14): 2639-2662.

Knyazikhin, Y., Martonchik, J.V., Myneni, R.B., Diner, D.J. and Running, S.W., 1998. Synergistic algorithm for estimating vegetation canopy leaf area index and fraction of absorbed photosynthetically active radiation from MODIS and MISR data. Journal of Geophysical Research D: Atmospheres, 103(24): 32,257-32,275.

Kodani, E., Awaya, Y., Tanaka, K. and Matsumura, N., 2002. Seasonal patterns of canopy structure, biochemistry and spectral reflectance in a broad-leaved deciduous Fagus crenata canopy. Forest Ecology and Management, 167(1-3), pp. 233-249.

Kokaly, R.F. and Clark, R.N., 1999. Spectroscopic determination of leaf biochemistry using band-depth analysis of absorption features and stepwise multiple linear regression. Remote Sensing of Environment, 67(3): 267-287.

Kooistra, L., Salas, E.A.L., Clevers, J.G.P.W., Wehrens, R., Leuven, R.S.E.W., Nienhuis, P.H. and Buydens, L.M.C., 2004. Exploring field vegetation reflectance as an indicator of soil contamination in river floodplains. Environmental Pollution, 127(2): 281-290.

Kötz, B., Schaepman, M., Morsdorf, F., Bowyer, P., Itten, K. and Allgower, B., 2004. Radiative transfer modeling within a heterogeneous canopy for estimation of forest fire fuel properties. Remote Sensing of Environment, 92(3): 332-344.

Kovacs, J.M., Flores-Verdugo, F., Wang, J. and Aspden, L.P., 2004. Estimating leaf area index of a degraded mangrove forest using high spatial resolution satellite data. Aquatic Botany, 80(1): 13-22.

Kubinyi, H., 1996. Evolutionary variable selection in regression and PLS analyses. Journal of Chemometrics, 10(2): 119-133.

Kuusk, A., 1991. The hot-spot effect in plant canopy reflectance. In: R.B. Myneni and J. Ross (Editors), Photon – vegetation interactions. Springer-Verlag, New York, pp. 139– 159.

Lamb, D.W., Steyn-Ross, M., Schaare, P., Hanna, M.M., Silvester, W. and Steyn-Ross, A., 2002. Estimating leaf nitrogen concentration in ryegrass (Lolium spp.) pasture using the chlorophyll red-edge: theoretical modelling and experimental observations. International Journal of Remote Sensing, 23(18), pp. 3619 - 3648.

Lavergne, T., Kaminski, T., Pinty, B., Taberner, M., Gobron, N., Verstraete, M.M., Vossbeck, M., Widlowski, J.-L. and Giering, R., 2007. Application to MISR land products of an RPV model inversion package using adjoint and Hessian codes. Remote Sensing of Environment, 107(1-2): 362-375.

Lawrence, R.L. and Ripple, W.J., 1998. Comparisons among vegetation indices and bandwise regression in a highly disturbed, heterogeneous landscape: Mount st. Helens, Washington. Remote Sensing of Environment, 64(1): 91-102.

Lee, K.-S., Cohen, W.B., Kennedy, R.E., Maiersperger, T.K. and Gower, S.T., 2004. Hyperspectral versus multispectral data for estimating leaf area index in four different biomes. Remote Sensing of Environment, 91(3-4): 508-520.

Lefsky, M.A., Cohen, W.B., Acker, S.A., Parker, G.G., Spies, T.A. and Harding, D., 1999. Lidar remote sensing of the canopy structure and biophysical properties of Douglas Fir western hemlock forests. Remote Sensing of Environment, 70(3): 339-361.

Lefsky, M.A., Cohen, W.B. and Spies, T.A., 2001. An evaluation of alternate remote sensing products for forest inventory, monitoring, and mapping of Douglas-fir forests in western Oregon. Canadian Journal of Forest Research, 31(1): 78-87.

le Maire, G., Francois, C. and Dufrene, E., 2004. Towards universal broad leaf chlorophyll indices using PROSPECT simulated database and hyperspectral reflectance measurements. Remote Sensing of Environment, 89(1): 1-28.

Liang, S., 2004. Quantitative Remote Sensing of Land Surfaces. Wiley Praxis Series in Remote Sensing, Wiley & Sons, Hoboken etc.

LI-COR, 1992. LAI-2000 Plant Canopy Analyzer Instruction Manual. LICOR Inc., Lincoln, NE, USA.

Major, D.J., Baret, F. and Guyot, G., 1990. A ratio vegetation index adjusted for soil brightness. International Journal of Remote Sensing, 11(5): 727-740.

Markwell, J., Osterman, J.C. and Mitchell, J.L., 1995. Calibration of Minolta SPAD-502 leaf chlorophyll meter. Photosynthetic Research, 46(3): 467-472.

Martens, H. and Martens, M., 2000. Modified jack-knife estimation of parameter uncertainty in bilinear modelling by partial least squares regression (PLSR). Food Quality and Preference, 11(1-2): 5-16.

Mathworks, 2007. Matlab, The Language of Technical Computing. Mathworks, INC. USA.

McMurtrey, J.E., Chappelle, E.W., Kim, M.S., Meisinger, J.J. and Corp, L.A., 1994. Distinguishing nitrogen fertilization levels in field corn (Zea mays L.) with actively induced fluorescence and passive reflectance measurements. Remote Sensing of Environment, 47(1): 36-44.

Meroni, M., Colombo, R. and Panigada, C., 2004. Inversion of a radiative transfer model with hyperspectral observations for LAI mapping in poplar plantations. Remote Sensing of Environment, 92(2): 195-206.

Minolta, 2003. Chlorophyll meter SPAD-502. Instruction Manual, Minolta Camera BeNeLux BV, Maarssen, The Netherlands.

Mutanga, O. and Skidmore, A.K., 2004. Narrow band vegetation indices overcome the saturation problem in biomass estimation. International Journal of Remote Sensing, 25(19): 3999-4014.

Mutanga, O., Skidmore, A.K., Kumar, L. and Ferwerda, J., 2005. Estimating tropical pasture quality at canopy level using band depth analysis with continuum removal in the visible domain. International Journal of Remote Sensing, 26(6): 1093-1108.

Myers, R.H., 1986. Classical and Modern Regression with Applications. PWS Publishers, Boston.

Myneni, R.B., Ramakrishna, R., Nemani, R. and Running, S.W., 1997. Estimation of global leaf area index and absorbed par using radiative transfer models. IEEE Transactions on Geoscience and Remote Sensing, 35(6): 1380-1393.

Nagler, P.L., Glenn, E.P., Lewis Thompson, T. and Huete, A., 2004. Leaf area index and normalized difference vegetation index as predictors of canopy characteristics and light interception by riparian species on the Lower Colorado River. Agricultural and Forest Meteorology, 125(1-2): 1-17.

Naesset, E., Bollandsas, O.M. and Gobakken, T., 2005. Comparing regression methods in estimation of biophysical properties of forest stands from two different inventories using laser scanner data. Remote Sensing of Environment, 94(4): 541-553.

Nakano, M., Nomizu, T., Mizunashi, K., Suzuki, M., Mori, S., Kuwayama, S., Hayashi, M., Umehara, H., Oka, E., Kobayashi, H., Asano, M., Sugawara, S., Takagi, H., Saito, H., Nakata, M., Godo, T., Hara, Y. and Amano, J., 2006. Somaclonal variation in Tricyrtis hirta plants regenerated from 1-year-old embryogenic callus cultures. Scientia Horticulturae, 110(4): 366-371.

Nemani, R.R., Pierce, L.L., Running, S.W. and Band, L.E., 1993. Forest ecosystem processes at the watershed scale: sensitivity to remotely sensed leaf area index estimates. International Journal of Remote Sensing, 14(13): 2519-2534.

Nguyen, H.T. and Lee, B.-W., 2006. Assessment of rice leaf growth and nitrogen status by hyperspectral canopy reflectance and partial least square regression. European Journal of Agronomy, 24(4): 349-356.

Pearson, R.L. and Miller, L.D., 1972. Remote mapping of standing crop biomass for estimation of the productivity of the short-grass Prairie, Pawnee National Grassland, Colorado. 8th International Symposium on Remote Sensing of Environment, ERIMA, Ann Arbor, MI, pp. 1357-1381.

Perry, J.C.R. and Lautenschlager, L.F., 1984. Functional equivalence of spectral vegetation indices. Remote Sensing of Environment, 14(1-3): 169-182.

Peterson, D.L., Aber, J.D., Matson, P.L., Card, D.H., Swanberg, N., Wessman, C.A. and Spanner, M., 1988. Remote sensing of forest canopy and leaf biochemical contents. Remote Sensing of Environment, 24: 85-108.

Peterson, D.L., Spanner, M.A., Running, S.W. and Teuber, K.B., 1987. Relationship of thematic mapper simulator data to leaf area index of temperate coniferous forests. Remote Sensing of Environment, 22(3): 323-341.

Pu, R., Gong, P. and Biging, G.S., 2003a. Simple calibration of AVIRIS data and LAI mapping of forest plantation in southern Argentina. International Journal of Remote Sensing, 24(23): 4699-4714.

Pu, R., Gong, P., Biging, G.S. and Larrieu, M.R., 2003b. Extraction of red edge optical parameters from Hyperion data for estimation of forest leaf area index. IEEE Transactions on Geoscience and Remote Sensing, 41(4): 916-921.

Qi, J., Kerr, Y.H., Moran, M.S., Weltz, M., Huete, A.R., Sorooshian, S. and Bryant, R., 2000. Leaf area index estimates using remotely sensed data and BRDF models in a semiarid region. Remote Sensing of Environment, 73(1): 18-30.

Olyvia, P.R., 2000. Data Mining Cookbook. Wiley, New York.

Richardson, A.J. and Wiegand, C.L., 1977. Distinguishing vegetation from soil background information. Photogrammetric Engineering and Remote Sensing, 43: 1541-1552.

Ridao, E., Conde, J.R. and Minguez, M.I., 1998. Estimating fAPAR from nine vegetation indices for irrigated and nonirrigated faba bean and semileafless pea canopies. Remote Sensing of Environment, 66(1): 87-100.

Roder, A., Kuemmerle, T., Hill, J., Papanastasis, V.P. and Tsiourlis, G.M., 2007. Adaptation of a grazing gradient concept to heterogeneous Mediterranean rangelands using cost surface modelling. Ecological Modelling, 204(3-4): 387-398.

Rondeaux, G. and Steven, M.D., 1995. Comparison of vegetation indices to retrieve vegetation cover from remotely sensed data: a simulation study for the ATSR-2 channels. Photosynthesis and remote sensing. Proc. colloquium, Montpellier, 1995, Published by EARSeL, Editors Guyot G.: 237-242.

Rossini, M., Panigada, C., Meroni, M., Busetto, L., Castrovinci, R. And Colombo, R., 2007. Pedunculate oak forests (Quercus robur L.) survey in the Ticino Regional Park (Italy) by remote sensing. Forest@ 4( 2): 194-203.

Roujean, J.L. and Breon, F.M., 1995. Estimating PAR absorbed by vegetation from bidirectional reflectance measurements. Remote Sensing of Environment, 51: 375-384.

Rouse, J.W., Haas, R.H., Schell, J.A., Deering, D.W. and Harlan, J.C., 1974. Monitoring the Vernal Advancement of Retrogradation of Natural Vegetation. NASA/GSFC, Type III, Final Report, Greenbelt, MD.

Running, S.W., Nemani, R., Peterson, D.L., Band, L.E., Potts, D.F., Pierce, L.L. and Spanner, M.A., 1989. Mapping regional forest evapotranspiration and photosynthesis by coupling satellite data with ecosystem simulation. Ecology, 70(4): 1090-1101.

Running, S.W., Peterson, D.L., Spanner, M.A. and Teuber, K.B., 1986. Remote sensing of coniferous forest leaf area. Ecology, 67(1): 273-276.

Savitzky, A. and Golay, M.J.E., 1964. Smoothing and differentation of data by simplified least square procedure. Analytical Chemistry, 36(8): 1627-1638.

Schiefer, S., Hostert, P. and Damm, A., 2006. Correcting brightness gradients in hyperspectral data from urban areas. Remote Sensing of Environment, 101(1): 25-37.

Schlerf, M. and Atzberger, C., 2006. Inversion of a forest reflectance model to estimate structural canopy variables from hyperspectral remote sensing data. Remote Sensing of Environment, 100(3): 281-294.

Schlerf, M., Atzberger, C. and Hill, J., 2005. Remote sensing of forest biophysical variables using HyMap imaging spectrometer data. Remote Sensing of Environment, 95(2): 177-194.

Schlerf, M., Atzberger, C.G., Udelhoven, T., Jarmer, T., Mader, S., Werner, W. and Hill, J., 2003. Spectrometric estimation of leaf pigments in Norway spruce needles using band-depth analysis, partial least-square regression and inversion of a conifer leaf model. In: Habermeyer, M., Müller, A., Holzwarth, S. (Eds.), Proc. 3rd EARSeL workshop on imaging spectroscopy. Herrsching, Germany, 13-16 May 2003, pp. 559-568.

Schmidtlein, S. and Sassin, J., 2004. Mapping of continuous floristic gradients in grasslands using hyperspectral imagery. Remote Sensing of Environment, 92(1): 126-138.

Selige, T., Bohner, J. and Schmidhalter, U., 2006. High resolution topsoil mapping using hyperspectral image and field data in multivariate regression modeling procedures. Geoderma, 136(1-2): 235-244.

Sergent, M., Mathieu, D., Phan-Tan-Luu, R. and Drava, G., 1995. Correct and incorrect use of multilinear regression. Chemometrics and Intelligent Laboratory Systems, 27(2): 153-162.

Skidmore, A.K. (Editor), 2002. Environmental modelling with GIS and remote sensing. Taylor & Francis, London etc., 268 pp.

Takebe, M., Yoneyama, T., Inada, K. and Murakami, T., 1990. Spectral reflectance ratio of rice canopy for estimating crop nitrogen status. Plant and Soil, 122(2): 295-297.

Tang, S., Chen, J.M., Zhu, Q., Li, X., Chen, M., Sun, R., Zhou, Y., Deng, F. and Xie, D., 2006. LAI inversion algorithm based on directional reflectance kernels. Journal of Environmental Management, doi:10.1016/j.jenvman.2006.08.018: 58.

Thenkabail, P.S., Enclona, E.A., Ashton, M.S., Legg, C. and De Dieu, M.J., 2004. Hyperion, IKONOS, ALI, and ETM+ sensors in the study of African rainforests. Remote Sensing of Environment, 90(1): 23-43.

Thenkabail, P.S., Smith, R.B. and De Pauw, E., 2000. Hyperspectral vegetation indices and their relationships with agricultural crop characteristics. Remote Sensing of Environment, 71(2): 158-182.

Turner, D.P., Cohen, W.B., Kennedy, R.E., Fassnacht, K.S. and Briggs, J.M., 1999. Relationships between leaf area index and landsat tm spectral vegetation indices across three temperate zone sites. Remote Sensing of Environment, 70(1): 52-68.

Udelhoven, T., Atzberger, C. and Hill, J., 2000. Retrieving structural and biochemical forest characteristics using artificial neural networks and physically based reflectance models. In: Buchroithner, M. (Eds.), A Decade of Trans-European Remote Sensing Cooperation, Proc. 20th EARSeL Symposium, Dresden, Germany, 14-16 June 2000, pp. 205-211.

Verhoef, W., 1984. Light scattering by leaf layers with application to canopy reflectance modeling: the SAIL model. Remote Sensing of Environment, 16(2): 125-141.

Verhoef, W., 1985. Earth observation modeling based on layer scattering matrices. Remote Sensing of Environment, 17(2): 165-178.

Verhoef, W. and Bach, H., 2007. Coupled soil-leaf-canopy and atmosphere radiative transfer modeling to simulate hyperspectral multi-angular surface reflectance and TOA radiance data. Remote Sensing of Environment, 109: 166-182.

Verstraete, M.M., Pinty, B. and Myneni, R., 1996. Potential and limitations of information extraction on the terrestrial biosphere from satellite remote sensing. Remote Sensing of Environment, 58: 201-214.

Vos, J. and Bom, M., 1993. Hand-held chlorophyll meter: a promising tool to assess the nitrogen status of potato foliage. Potato Research, 36(4): 301-308.

Walter-Shea, E.A., Privette, J., Cornell, D., Mesarch, M.A. and Hays, C.J., 1997. Relations between directional spectral vegetation indices and leaf area and absorbed radiation in Alfalfa. Remote Sensing of Environment, 61(1): 162-177.

Walthall, C., Dulaney, W., Anderson, M., Norman, J., Fang, H. and Liang, S., 2004. A comparison of empirical and neural network approaches for estimating corn and soybean leaf area index from Landsat ETM+ imagery. Remote Sensing of Environment, 92(4): 465-474.

Wang, Q., Adiku, S., Tenhunen, J. and Granier, A., 2005. On the relationship of NDVI with leaf area index in a deciduous forest site. Remote Sensing of Environment, 94(2): 244-255.

Watanabe, S., Hatanaka, Y. and Inada, K., 1980. Development of a digital chlorophyll meter: I. Structure and performance. Japanese Journal of Crop Science, 49(spec. issue): 89-90.

Wiegand, C.L. Maas, S. J., Aase, J. K., Hatfield, J. L., Pinter, Jr., P. J, Jackson, R. D., Kanemasu, E. T., and Lapitan, R. L. 1992. Multisite analyses of spectral-biophysical data for wheat. Remote Sensing of Environment, 42(1), pp. 1-21.

Weiss, M. and Baret, F., 1999. Evaluation of canopy biophysical variable retrieval performances from the accumulation of large swath satellite data. Remote Sensing of Environment, 70(3): 293-306.

Weiss, M., Baret, F., Myneni, R.B., Pragnere, A. and Knyazikhin, Y., 2000. Investigation of a model inversion technique to estimate canopy biophysical variables from spectral and directional reflectance data. Agronomie, 20(1): 3-22.

Weiss, M., Troufleau, D., Baret, F., Chauki, H., Prevot, L., Olioso, A., Bruguier, N. and Brisson, N., 2001. Coupling canopy functioning and radiative transfer models for remote sensing data assimilation. Agricultural and Forest Meteorology, 108(2): 113-128.

White, J.D., Running, S.W., Nemani, R., Keane, R.E. and Ryan, K.C., 1997. Measurement and remote sensing of LAI in rocky mountain montane ecosystems. Canadian Journal of Forest Research, 27(11): 1714-1727.

Welles, J.M. and Norman, J.M., 1991. Instrument for indirect measurement of canopy architecture. Agronomy Journal, 83(5): 818-825.

Williams, P.C. and Norris, K.H. (Editors), 1987. Near-Infrared Technology in the Agricultural and Food Industries. American Association of Cereal Chemists, St. Paul, Minnesota, USA, 288 pp.

Wu, J., Wang, D. and Bauer, M.E., 2007. Assessing broadband vegetation indices and QuickBird data in estimating leaf area index of corn and potato canopies. Field Crops Research, 102(1): 33-42.

Wylie, B.K., Meyer, D.J., Tieszen, L.L. and Mannel, S., 2002. Satellite mapping of surface biophysical parameters at the biome scale over the North American grasslands: a case study. Remote Sensing of Environment, 79(2-3): 266-278.

Yang, W.-H., Peng, S., Huang, J., Sanico, A.L., Buresh, R.J. and Witt, C., 2003. Using leaf color charts to estimate leaf nitrogen status of rice. Agronomy Journal, 95(1): 212-217.

Yoder, B.J. and Pettigrew-Crosby, R.E., 1995. Predicting nitrogen and chlorophyll content and concentration from reflectance spectra (400–2500 nm) at leaf and canopy scales. Remote Sensing of Environment, 53(3): 199-211.

Zarco-Tejada, P.J., Miller, J.R., Harron, J., Hu, B., Noland, T.L., Goel, N., Mohammed, G.H. and Sampson, P., 2004a. Needle chlorophyll content estimation through model inversion using hyperspectral data from boreal conifer forest canopies. Remote Sensing of Environment, 89(2): 189-199.

Zarco-Tejada, P.J., Miller, J.R., Mohammed, G.H., Noland, T.L. and Sampson, P.H., 2002. Vegetation stress detection through chlorophyll a + b estimation and fluorescence effects on hyperspectral imagery. Journal of Environmental Quality, 31(5): 1433-1441.

Zarco-Tejada, P.J., Miller, J.R., Morales, A., Berjon, A. and Aguera, J., 2004b. Hyperspectral indices and model simulation for chlorophyll estimation in open-canopy tree crops. Remote Sensing of Environment, 90(4): 463-476.

## Acronyms

| | |
|---|---|
| 2-D | Two dimensional |
| AAE | Average absolute error |
| ALA | Mean leaf inclination angle |
| ATCOR | Atmospheric and topographic correction software |
| AVIRIS | Airborne visible infrared imaging spectrometer |
| BRDF | Bidirectional reflectance distribution function |
| CASI | Compact airborne spectrographic imager |
| CCC | Canopy chlorophyll content |
| $C_m$ | Dry matter content |
| cv | Cross validated |
| $C_w$ | Equivalent water thickness |
| FOV | Field of view |
| GER | (Geophysical and environmental research corporation, Buffalo, New York) |
| GPS | Global positioning system |
| *hot* | Hot spot size parameter |
| HyMap | Hyperspectral mapping imaging spectrometer |
| LAI | Leaf area index |
| LAI-2000 | Plant canopy analyzer LAI-2000 (LICOR Inc., Lincoln, NE, USA) |
| LCC | Leaf chlorophyll content |
| LI-3100 | LI-3100 leaf area meter (scanning planimeter) (LICOR Inc., NE, USA) |
| LUT | Look-up table |
| MLR | Multiple linear regression |
| MODTRAN | Moderate spectral resolution atmospheric transmittance |
| MSAVI | Modified soil adjusted vegetation index |
| $N$ | Leaf structural parameter |
| NDVI | Normalized difference vegetation index |
| NIR | Near infrared |
| NRMSE | Normalized root mean square error (RMSE/range) |
| PAI | Plant area index |

| | |
|---|---|
| PLSR | Partial least square regression |
| PROSAIL | Combined SAILH and PROSPECT radiative transfer model |
| PVI | Perpendicular vegetation index |
| r | Correlation coefficient |
| $R^2$ | Coefficient of determination |
| REIP | Red edge inflection point |
| RMSE | Root mean square error |
| RRMSE | Relative root mean square error (RMSE/mean) |
| RTM | Radiative transfer model |
| RVI | Ratio vegetation index |
| SAIL | Scattering by arbitrarily inclined leaves |
| SAVI | Soil adjusted vegetation index |
| SAVI2 | Second soil- adjusted vegetation index |
| *scale* | Soil brightness parameter |
| *skyl* | Fraction of diffuse incoming solar radiation |
| SMLR | Stepwise multiple linear regression |
| SPAD | SPAD-502 leaf chlorophyll meter (Minolta, Inc.) |
| SWIR | Shortwave infrared |
| TSAVI | Transformed soil- adjusted vegetation index |
| VI | Vegetation index |

## ITC Dissertation list

A list of ITC dissertation can be found in:
http://www.itc.nl/research/phd/phd_graduates.aspx

## PE&RC PhD Education Certificate

With the educational activities listed below the PhD candidate has complied with the educational requirements set by the C.T. de Wit Graduate School for Production Ecology and Resource Conservation (PE&RC) which comprises of a minimum total of 32 ECTS (= 22 weeks of activities)


**Review of Literature (5.6 ECTS)**
- Review of different method for estimation of leaf area index (2004)

**Writing of Project Proposal (7 ECTS)**
- Monitoring and estimating vegetation biophysical variables using GIS & hyperspectral remote sensing (2004)

**Laboratory Training and Working Visits (4.2 ECTS)**
- Estimation of leaf area index of natural vegetation; WUR (2005)
- Chlorophyll measurements; WUR (2005)

**Post-Graduate Courses (2.8 ECTS)**
- IDL programming course; ITC (2006)
- Spatial statistic; ITC (2008)

**Competence Strengthening / Skills Courses (1.4 ECTS)**
- Scientific writing; ITC (2005)

**Discussion Groups / Local Seminars and Other Meetings (7 ECTS)**
- PhD master class with ESRI representative; Dr. Jack Dangermond (2004)
- Forth-nightly PhD discussion (2004-2008)
- PhD and research seminars (2004-2008)
- PhD master class with Professor Salomon Kroonenberg (2007)

**PE&RC Annual Meetings, Seminars and the PE&RC Weekend (2.4 ECTS)**
- PE&RC Weekend (2005)
- PE&RC days (2005, 2006, and 2007)
- Natural resources day (2005, 2006, and 2007)

**International Symposia, Workshops and Conferences (6.2 ECTS)**

- ISPRS Technical commission VII symposium: remote sensing, from pixels to processes; international conference; oral presentation: "hyperspectral remote sensing indices for estimation of leaf area index"; Enschede, The Netherlands (2006)

- 5th EARSeL SIGIS "Innovation in environmental research"; international conference; presentation on: "response of hyperspectral vegetation indices to vegetation architecture and background soil for estimation of leaf area index"; Bruges, Belgium (2007)

- 10th International symposium on physical measurements and signatures in remote sensing, ISPMSRS'07; Davos, Switzerland (2007)

## Author's Biography

Roshanak Darvishzadeh was born on the 24th of September 1971 in Tehran, Iran. She completed her secondary school in physics and mathematics. In January 1992, she obtained her Technologist degree in Civil Engineering, with a specialization in Cartography, from the College of Surveying and Mapping, Tehran, Iran. She worked as a cartographer at the National Cartographic Center of Iran from 1991 to 1992. In September 1992, she enrolled at the Azad University to study for her Bachelor's degree in English Translation. At the same time, she joined the GIS department of Tehran Municipality (TGIS) and was appointed head of the digital mapping section. In 1994, she was awarded a scholarship by Nuffic to follow the diploma course in Cartography at ITC, where she graduated with distinction. The experience gained at TGIS proved useful, as she later joined the Department of Urban Planning and Management at ITC to obtain a postgraduate diploma. Since she had performed very well at the postgraduate level (distinction), she continued her study toward an MSc degree in the same department. She obtained her MSc in 1997 in GIS for Urban Application, with a thesis focusing on the use of remote sensing and GIS techniques for urban change detection. In 2000, she became a staff fellow at the Soil Conservation and Watershed Management Research Institute (SCWMRI) and joined the JIK joint educational program conducted by ITC and Iran. Following the new experience gained at the research institute, she returned to ITC to read for a PhD at the Department of Natural Resources and Wageningen University, which resulted in this thesis. After her PhD, she will take up her new position as an assistant professor in the Department of Remote Sensing and GIS at Shahid Beheshti University, Tehran, Iran.

## Author's publications

**Journal Articles:**

Darvishzadeh, R., Atzberger, C. and Skidmore, A.K. (2008), Leaf area index derivation from hyperspectral vegetation indices and the red edge position, *International Journal of Remote Sensing*, In press.

Darvishzadeh, R., Skidmore, A.K., Schlerf, M. and Atzberger, C. (2008), Inversion of a radiative transfer model for estimating vegetation LAI and chlorophyll in a heterogeneous grassland, *Remote Sensing of Environment*, 112(5): 2592-2604.

Darvishzadeh, R., Skidmore, A.K., Schlerf, M., Atzberger, C., Corsi, F., and Cho, M.A. (2008), LAI and chlorophyll estimated for a heterogeneous grassland using hyperspectral measurements, *ISPRS Journal of Photogrammetry and Remote Sensing*, In press, DOI: 10.1016/j.isprsjprs.2008.01.001.

Darvishzadeh, R., Skidmore, A.K., Atzberger, C. and van Wieren, S.E. (2008), Estimation of vegetation LAI from hyperspectral reflectance data: effects of soil type and plant architecture, *International Journal of Applied Earth Observation and Geoinformation*, In press, DOI: 10.1016/j.jag.2008.02.005.

Darvishzadeh, R., Atzberger, C., Schlerf, M., Skidmore, A. and Prins, H. (2008), Mapping vegetation biophysical properties in a Mediterranean grassland with airborne hyperspectral imagery: from statistical to physical models, *Remote Sensing of Environment*, In Review (after revision).

**International conferences/ Other scientific publications:**

Darvishzadeh, R., Skidmore, A.K., Schlerf, M., Atzberger, C., Corsi, F., and Cho, M.A. (2008), Estimation of leaf area index and chlorophyll for a Mediterranean grassland using hyperspectral data, ISPRS Congress 2008: Silk road for information from imagery remote sensing, 3-11 July 2008, Beijing, China.

Darvishzadeh, R., Skidmore, A.K. and Atzberger, C. (2007), Response of hyperspectral vegetation indices to vegetation architecture and background soil for estimation of leaf area index, Abstract book 5th EARSeL Workshop on Imaging Spectroscopy: innovation in environmental research. 23-25 April 2007, Bruges, Belgium,

Darvishzadeh, R., Atzberger, C. and Skidmore, A.K. (2006), Hyperspectral vegetation indices for estimation of leaf area index, ISPRS mid-term symposium

2006 remote sensing: from pixels to processes, 8-11 May 2006, Enschede, the Netherlands.

Darvishzadeh, R. (2000), Change detection for urban spatial databases using remote sensing and GIS, ISPRS Congress 2000, Proceeding of International Society for Photogrametry and Remote Sensing (ISPRS), Amsterdam, The Netherlands.

Darvishzadeh, R. (1999), Semi-Automatic Change Detection for Updating of Large Scale Spatial Databases, Proceeding of International Cartographic Conference, Ottawa, Canada, (Recognized as the best young author for young scientist awards).

Darvishzadeh, R. (1997), Semi Automatic Updating of Large Scale Spatial Databases Using GIS And Remote Sensing " A Case Study of an Informal Settlements in Dar Es Salaam, Tanzania", ITC, MSc Thesis.